The Atherosclerotic Environment Accentuates Endochondral Ossification in Vessel-Derived Stem Cells: *In-vitro* and *In-vivo* Assessment

A thesis submitted to the National University of Ireland as fulfilment of the requirement for the degree of

Doctor of Philosophy

By

Aleksandra Leszczynska

Regenerative Medicine Institute (REMEDI),

College of Medicine, Nursing & Health Sciences,

National University of Ireland Galway

Research Supervisor:

Dr. Mary Murphy

Date of Submission: August 2013

TABLE OF CONTENTS

Chapter 1

Chapter 2

Chapter 3

Chapter 5

Chapter 6

Declaration

I declare that all the work in this thesis was performed personally. No part of this work has been submitted for consideration as part of any other degree or award.

LIST OF ABBREVIATIONS

7-AAD	7-aminoactinomycin D
ApoE	Apolipoprotein E
$ApoE^{-/-}$	Apolipoprotein E knockout
Alp	Alkaline phosphatase
APCs	Antigen Presenting Cells
APOBEC-1	Apolipoprotein B mRNA-editing Enzyme Catalytic poly-peptide 1
APS	Ammonium Persulfate
ATCC	American Type Culture Collection
α-SMA	α-Smooth Muscle Actin
α-MEM	Minimum Essential Medium α
BBB	Blood-Brain Barrier
BD	Becton Dickinson
Bio	Biotinylated
BM	Bone Marrow
BMMNC	BM Mononuclear Cell
BMP-2	Bone Morphogenetic Protein 2
bp	base pair
BSA	Bovine Serum Albumin
bFGF	basic Fibroblast Growth Factor
β-Gal	β-galactosidase
ºC	Celsius
CASMC	Coronary Artery Smooth Muscle Cell
CD	Cluster of Differentiation
CCM	Complete Culture Medium
CCR	Chemokine C-C motif Receptor
cDNA	complementary Deoxyribonucleic Acid
CIM	Complete Induction Medium
CM	Culture Medium
cm	centimeter
CO_2	Carbine dioxide

CuZnSOD	Cu/Zn Superoxide Dismutase
Ct	Threshold cycle
ΔCT	Delta threshold cycle
ΔΔCt	Delta-delta threshold cycle
CVCs	Calcifying Vascular Cells
DAB	Diaminobenzidine
DC	Dendritic cell
dH_2O	Distilled water
DMEM	Dulbecco's Modified Eagle Medium
DMEM- HG	Dulbecco's Modified Eagle Medium High Glucose
DMMB	Dimethylmethylene Blue (Buffer)
DMSO	Dimethyl Sulfoxide
dNTPs	Deoxyribonucleotide triphosphates
DPX	Mounting Media (Distyrene Plesticizer/Xylene)
EC	Endothelial Cell
ECL	Enhanced Chemiluminescence
ECM	Extracellular Matrix
EDTA	Ethylenediaminetetraacetic Acid
EGTA	Ethylene Glycol Tetraacetic Acid
eGFP	enhanced Green Fluorescent Protein
eNOS	endothelial Nitric Oxide Synthase
ER	Endoplasmic Reticulum
EPC	Endothelial Progenitor Cells
FACS	Fluorescence Activated Cell Sorting
FBS	Fetal Bovine Serum
FGF	Fibroblast Growth Factor
Fig.	Figure
FISH	Fluorescence In Situ Hybridization
FITC	Fluorescein Isothiocyanate
FMO	Fluorescence Minus One
GAG	Glycosaminoglycan

GAM	Gene Activated Matrix
h	hours
H_2O_2	Hydrogen Peroxide
HBSS	Hank's Balanced Salt Solution
HCl	Hydrochloric acid
HDLs	High Density Lipoproteins
HG	High Glucose
H&E	Hematoxylin and Eosin
HEPES	4-(2-hydroxyethyl)-1-piperazineethanesulfonic acid)
HIF	Hypoxia Inducible Factor
HRP	Horseradish Peroxidase
HS	Horse Serum
HSCs	Hematopoietic Stem Cells
IBMX	Isobutylmethylxanthine
ICC	Immunocytochemistry
IFN- γ	Interferon-γ
IgG	Immunoglobulin G
IgM	Immunoglobulin M
Ihh	Indian Hedgehog
IL	Interleukin
ITS	Insulin Transferrin Selenium
kDa	kilodaltons
kg	kilogram
LCAT	Lecithin Cholesterol Acyltransferase
LDL	Low Density Lipoprotein
$LDLR^{-/-}$	Low Density Lipoprotein Receptor knockout
LTC	Long Term Cultures
M	Molar, (moles/liter)
M-CSF	Multi-Colony Stimulating Factor
MCP	Monocyte Chemoattractant Protein
mg	milligram

MHC	Major Histocompatibility Complex
Mig	Monokine induced by IFN-γ
min	minute
mM	millimolar
mm	millimeter
ml	milliliter
µ (l) or (g)	microliter or (gram)
µm	micron
µM	micromolar
MMPs	Matrix Metalloproteinases
mMSCs	mouse Mesenchymal Stem Cells
MSCs	Mesenchymal Stem Cells
NF-κB	Nuclear Factor κ B
NG2	Nerve/Glial antigen 2
NGS	Normal Goat Serum
NK	Natural Killer
ng	nanogram
nm	nanometer
nM	nanomolar
NO	Nitric Oxide
no.	number
NP-40	Nonidet-P40
ORO	Oil Red O
oxLDL	oxidized LDL
P	Passage
PCR	Polymerase Chain Reaction
PBS	Phosphate Buffered Saline
PBS-T	Phosphate Buffered Saline-Tween 20
PDGF	Platelet Derived Growth Factor
PE	Phycoerythrin
PEG	Polyethylene Glycol

PFA	Paraformaldehyde
PI	Propidium Iodide
PLA	Polylactic Acid
PLGA	Poly (Lactic-*Co*-Glycolic Acid)
pmol	picomol
P/S	Penicillin/Streptomycin
Rag	Recombinant activity gene
RGS	Regulator of G-protein Signaling
RIN	RNA Integrity Number
RNA	Ribonucleic Acid
RNAse	Ribonuclease
RPMI	Roswell Park Memorial Institute Medium
RT	Room Temperature
RT-PCR	Real Time PCR
s	seconds
SA-PE	Streptavidin-phycoerythrin
SCF	Stem Cell Factor
SCID	Severe Combined Immunodeficiency
SD	Standard Deviation
SDS-PAGE	Sodium Dodecyl-Polyacrylamide Gel Electrophoresis
SMC	Smooth Muscle Cell
SMMHC	Smooth Muscle Myosin Heavy Chain
SMPC	Smooth Muscle Progenitor Cells
TEMED	Tetramethylethylenediamine
TGF-β	Transforming Growth Factor- β
TIMP	Tissue Inhibitor of Metalloproteinases
TNF-α	Tumor Necrosis Factor-α
Tris	Tris (hydroxymethyl) aminomethane
Triton X-100	t-octylphenoxypolyethoxyethanol
Tween-20	polyoxyethylene-sorbitan monolaurate
U	Units

UV	Ultraviolet
VC	Vascular Calcification
VCAM	Vascular Cell Adhesion Molecule
VEGF	Vascular Endothelial Growth Factor
VSMCs	Vascular Smooth Muscle Cells
VSCs	Vascular Stem Cells
x g	g-force

LIST OF FIGURES

Chapter 1

Chapter 3

Chapter 4

Chapter 5

Chapter 6

LIST OF TABLES

Chapter 2

Chapter 3

Chapter 5

ACKNOWLEDGEMENTS

I wish to express the deepest appreciation to my supervisor Dr. Mary Murphy for the support and guidance during my PhD and for motivation and patience.

Also I would like to thank to Dr. Aideen O'Doherty for her everyday help and assistance and constructive feedback; to Dr. Eric Farrell for his expertise.

I would like to thank Prof. Timothy O'Brien, Prof. Laurence Egan and Dr. Amjad Hayad for support and help.

I would also like to thank the IRCSET for granting me scholarship and funding this project, without which this project would not have been possible.

I would like to express my special gratitude to the all members of our group for everyday help, especially Miriam, Una, Siobhan, Jana, Xizhe.

To Siva, Sumi, Inniya, Paulina, Madzia, Dimitri, Sreenath, Venkatesh and all house friends and devotees, thanks for support, memories and friendship.

Special thanks to Aditya for all his phenomenal help in thesis submission.

Finally, I want to thank my mom for her patience, teachings and encouragements, to my sister Joanna and her husband Ramin also to my brother Sebastian and his family and all extended family and my in-laws, my heartfelt thanks for the patience, guidance and unconditional love. There are no words to express my gratitude and love for them.

And for my husband, I save my last and best. Your understanding, support and encouragements, have been immense. Words cannot express my appreciation for your generosity, for optimistic thoughts and continuous love.

Dedicated to my wonderful mom

(Dla kochanej mamy)

Abstract

Vascular calcification, far from being a passive degenerative process, is now perceived as an active, highly organized cell-controlled event. The presence of a number of stem progenitor niches and/or lineages in the vasculature has been established and their possible role in vascular calcification is under increasing investigation. Pericytes are purported to be involved in this process and are currently a poorly defined cell population. Although traditionally considered as supporting cells, more recently these cells have been proposed to play a more active role in the repair and pathogenesis of various vascular diseases. Pericytes have been shown to have a mesenchymal origin. Mesenchymal stem cells (MSCs) have been associated with a perivascular niche and have the ability to undergo osteogenic and chondrogenic differentiation. In this study, the hypothesis that a pericyte-like stem cell population, termed vessel-derived stem cells (VSCs) exists in the vessel wall was tested. Furthermore, it was proposed that in the presence of inflammatory cytokines seen in the atherosclerotic environment, these cells, along with circulating MSCs, contribute to the calcification of atherosclerotic plaque via endochondral ossification.

VSCs from aortae of $ApoE^{-/-}$ atherosclerotic mice and background control C57BL/6 mice were isolated and characterized for differentiation potential and by screening for cell surface markers by flow cytometry and immunocytochemistry. MSCs from the bone marrow of these mice were also isolated and characterized in a similar fashion. When these cells were differentiated down the osteogenic lineage, there was an increase in calcium levels which was more pronounced in $ApoE^{-/-}$ VSCs. Differentiation to the chondrogenic lineage suggested that all the isolated cell populations have chondrogenic potential; however, $ApoE^{-/-}$ MSCs and VSCs showed more extensive deposition of glycosaminoglycan. Phenoytpic analysis demonstrated that both $ApoE^{-/-}$ and C57BL/6 VSCs were strongly positive for Sca-1 and CD44, positive for CD146 and negative for CD31 and CD34. Immunocytochemistry for the specific pericyte marker 3G5 revealed that a sub-population of VSCs expressed 3G5, demonstrating that cell populations isolated were of the hypothesized lineage and contained pericyte-like cells.

In order to investigate the effect of proinflammatory cytokines associated with the atherosclerotic niche on chondrogenic differentiation *in vitro,* levels of gene expression for markers of chondrogenesis were monitored. All the cell populations were subjected to chondrogenesis for 21 days in the presence or absence of the pro-inflammatory cytokines IL-6, IL-1β or TNF-α. At 21 days following IL-6 treatment, $ApoE^{-/-}$ VSCs showed increased levels of Sox9, fibromodulin, type II collagen, aggrecan and alkaline phosphatase indicating extensive differentiation along the chondrogenic lineage. On the contrary, IL-6 had a suppressive effect on C57BL/6 VSCs. For IL-β and TNF-α, results indicated that both cytokines suppressed chondrogenic markers in $ApoE^{-/-}$ and C57BL/6 VSCs at 21 days.

To assess the ability of VSCs and MSCs from $ApoE^{-/-}$ and C57BL/6 mice to form bone, cells were seeded onto collagen glycosoaminoglycan scaffolds and chondrogenically primed *in vitro* followed by subcutaneous implantation *in vivo* for 8 weeks. From this study it was clear that endochondral ossification and calcification in atherosclerosis is a complex interplay of a number of factors, each contributing differently to the process. Histomorphological analysis showed that 5 out of 5 $ApoE^{-/-}$ MSCs and VSCs formed bone (with 77.5% and 58.4% overall bone formation, respectively) in C57BL/6 mice suggesting that the major contributing factor is the intrinsic capacity of MSCs and VSCs derived from atherosclerotic mice. In addition, the data indicated that 5 out of 5 $ApoE^{-/-}$ MSCs and 6 out of 6 $ApoE^{-/-}$ VSCs generated more mature bone in $ApoE^{-/-}$ mice (with 68.5% and 83.25% overall bone formation, respectively) than C57BL/6 MSCs (1 of 5) and VSCs (0 of 4). Thus, this study also demonstrated that the environment in which the pre-differentiated, or primed cells, are placed also plays a role; the host environment drives the implanted constructs to form bone or immature bone, bone marrow or calcified cartilage and promotes the infiltration of blood vessels and fat formation. This study supports the hypothesis that a progenitor cell population in the aorta vessel wall may contribute to vascular calcification via endochondral ossification in the atherosclerotic environment. However, recruitment of circulating MSCs derived from bone marrow to atherosclerotic plaque cannot be ruled out.

Chapter 1

Introduction

1.1 Atherosclerosis

Atherosclerosis, a disease primarily affecting large arteries[1,2], is characterized by a chronic insidious pathological progress over decades. Generally, the clinical diagnosis of atherosclerosis becomes overt only through a complication such as plaque rupture and/or a thrombo-embolic episode which takes place years after the appearance of fatty streak, the first pathological manifestation of the disease. The enormous aetiopathological complexity of the disease with multiple factors, both known and yet unknown, playing a role in disease induction and progression, has stymied progress in unraveling characteristic interactions at tissue, cellular and molecular level. Hence, despite being the primary cause of heart disease and stroke, especially in the developed world, the precise roles of various factors in the pathogenesis of atherosclerosis are yet to be revealed.

1.1.1 Normal vessel wall

A blood vessel wall usually contains three morphologically distinct layers, namely the intima, media and adventitia (Fig. 1.1 A). The intima is the innermost layer of the wall which consists of the endothelial layer and internal elastic lamina. The endothelial layer is closest to the blood flow in the vessel lumen. The internal elastic lamina consists of a proteoglycan layer which is closest to the endothelial layer and a musculoelastic layer which lies adjacent to the media[3]. The next layer is media which primarily consists of smooth muscle cells (SMC) and extracelluar matrix made up of elastic fibers and proteoglycans[4]. Media is separated from adventitia by the external elastic lamina. The adventitia contains fibroblasts, sparsely organized SMC, collagen and elastic fibers. Vasa vasora, the blood vessels supplying nutrients and oxygen to the arterial wall are located in the adventitia.

1.1.2 Early atherosclerotic lesion- fatty streak

Although overt atherosclerosis generally develops late, the process of plaque formation starts quite early in life. In fact, fatty streaks, identified as the earliest atherosclerotic lesions, have been spotted as early as during fetal development[5]. Fatty streak (Fig. 1.1B)

is comprised of characteristic cells called foam cells which are lipid laden cells localized underneath the endothelial layer[6]. A majority of these cells are transformed macrophages; nonetheless there are some T cells present in the fatty streak[7].

It takes decades for fatty streak to develop into an advanced lesion; however, it may also disappear. While fatty streaks as such do not have clinical complications; decades after their appearance, the progression to advanced lesions which may rupture results in clinically overt disease [8].

1.1.3 Advanced lesion

The early lesion progresses by recruitment of more inflammatory cells and lipids into the vessel wall (Fig. 1.1 C). The recruited macrophages secrete a number of cytokines, chemokines and growth factors which lead to proliferation and migration of SMC from media into the intima. The core of the lesion is populated by foam cells and lipids while the cap which surrounds the core consists of SMC and matrix rich in collagen[9]. Although mostly macrophages, foam cells can also be formed by SMC which can store lipid droplets[10]. The growth of the plaque primarily takes place at the shoulder regions where most of the immune cells gather and interface between the cap and core[6,11,12]. Necrosis can take place in the core and the lesion becomes more complex with a necrotic core and formation of cholesterol crystals. The thickness of the fibrous cap surrounding the necrotic core varies[13]. Apart from macrophages, mast cells, dendritic cells (DC) and natural killer cells are recruited by the influence of the pro-inflammatory environment[11,12,14,15]. Initially, although the lesion is growing, the external boundaries are adjusted and the lumen remains unaffected. However, as the lesion becomes more fibrous with accumulation of collagen producing SMC, the lumen of the artery starts to narrow. Thus, advancement of the lesion leads to clinically obvious and limiting stenosis.

1.1.4 Plaque rupture

The necrotic core and the lipids in the plaque are thrombogenic and separated from the blood by the fibrous cap[7]. However, the fibrous cap is destabilized by the process of

remodeling of the atheromatous plaque leading to its erosion and eventual rupture[16,17] (Fig. 1.1 D). The shoulder regions of the lesion, which are seats for the majority of activated T cells, macrophages and mast cells, are the most prone areas for rupture[14,16,18,19]. The cap is rendered weak and prone to rupture by two processes happening in parallel; namely inhibition of SMC proliferation and thereby collagen production by inflammatory cytokines such as interferon gamma (INFγ) and tumor necrosis factor alpha (TNFα) and degradation of extracellular matrix (ECM) by matrix metalloproteinases (MMPs)[20-23]. The rupture of the plaque leads to one of the most severe complications. The thrombogenic contents of the plaque are exposed to blood which results in thrombus formation by activation of the extrinsic coagulation pathway. While thrombus formation or its embolic dislodgement in arteries supporting the brain may lead to ischemic stroke, this may take also place in other organs leading to complication such as myocardial infarction, renal impairment, critical limb ischemia or other hypertension or aortic aneurysm[9]. However, the thrombus does not always lead to occlusion and subsequent ischemic symptoms; it may be reabsorbed. Thereafter, the platelets in the thrombus trigger SMC proliferation and collagen synthesis[17], rendering the plaque more fibrotic. With further progression of the lesion, calcification may follow resulting in advanced calcified plaques[24].

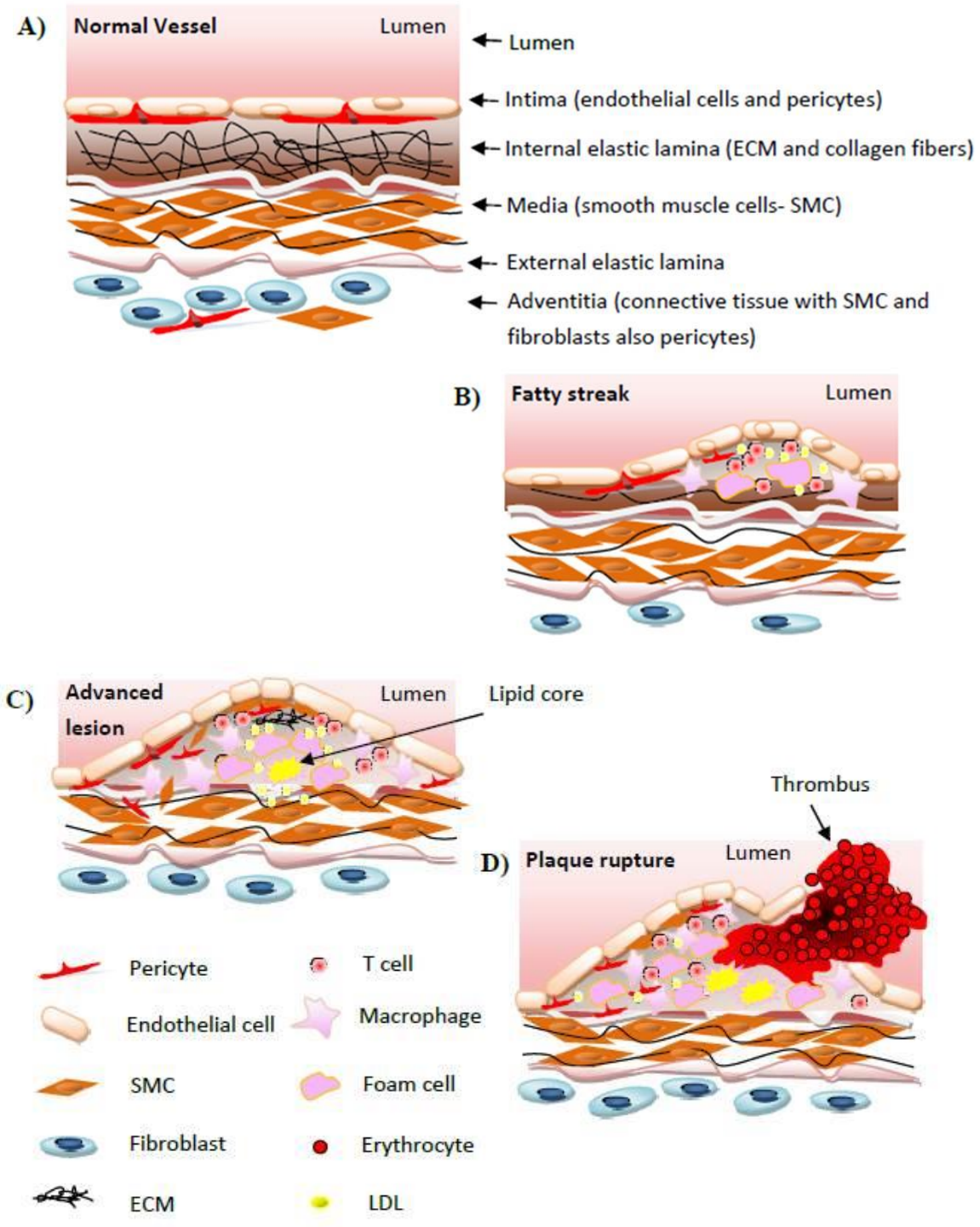

Figure 1.1: Progression and developmental stages of atherosclerotic lesions

1.2 Etiology of atherosclerosis

From 1904 when Felix Marchand introduced the term atherosclerosis and suggested that it was responsible for nearly all obstructive processes in arteries[25], many theories have evolved to try and explain the etiopathology of the disease. This early work by Marchand was followed shortly by A.I. Ignatowski establishing a possible relationship between cholesterol-rich foods and experimental atherosclerosis[25]. Nikolai Anichkov demonstrated in 1913 that it was cholesterol alone that caused these atherosclerotic changes in the rabbit intima[26]. He found early lesions, such as fatty streaks, as well as advanced lesions; by standardizing cholesterol feeding, he discovered that the amount of cholesterol uptake was directly proportional to the degree of atherosclerosis severity[25]. The early atherosclerotic lesions are characterized by intracellular accumulation of cholesterol esters and the subsequent lesions have extracellular cholesterol esters[6].

Following on from Anickov's theory associating cholesterol with atherosclerosis was the hemodynamic theory. This theory addressed the focal nature of lesions. According to this theory, the hydrostatic and shear forces are responsible for the formation of the atherosclerotic lesions. The relation between hypertension and atherosclerosis and lesions having predilection for branched and high turbulent sites go in favor of this theory. Also, it has been shown that the endothelial permeability to low density lipoproteins (LDL) is modified by hemodynamic alterations[27].

The thrombogenic or encrustration theory originally implicated the abnormal deposition of fibrin or blood products on the surface of blood vessels in the development of plaques. The role of fibrin deposition and thrombus organization in the development of atherosclerosis has recently been re-emphasized[28]. The mesenchymal hypothesis believes that a wide range of physical and chemical stimuli induce migration of smooth muscle cells from media to intima of the arterial vessel wall, which then proliferate and produce connective tissue. The response to injury theory hypothesizes that an injury to endothelium might precipitate the atherosclerotic process and the role of infection and inflammation has also been implicated in pathogenesis of atherosclerosis[29,30]. The

oxidation theory suggests that LDL must be oxidized to trigger the pathological events in atherosclerosis[31,32]. The acidity theory of atherosclerosis proposes that most of the risk factors for atherosclerosis might result in altered autonomic nervous system, sympathetic bias, increased lactic acid and an acidic environment. This lowered pH increases perfusion pressure and provokes contractility of coronary arteries, leading to changes in hemodynamic shear stress and consequently, atherosclerosis. Recently, a major focus has been on the role of stem or progenitor cells in the pathogenesis of atherosclerosis[33]. It has been shown that circulating progenitor cells contribute to the formation of atherosclerosis in a variety of animal models[34-36].

1.3 Immune response in atherosclerosis

Atherosclerosis is a chronic disease of the arterial wall where there is imbalance between pro-inflammatory and anti-inflammatory processes. It is characterized by thickening of the intima layer of the arterial wall. The endothelial cells in the intima react to local stimuli, become permeabilized and secrete chemo-attractant mediators which attract leukocytes to migrate inwards and bind to the intima. This migration is facilitated by monocytes. Monocytes-macrophages are not only involved in formation of the foam cells and deposition of lipids, but also contribute to the growth of the plaque via production of inflammatory cytokines, MMPs and reactive oxygen species[37]. Therefore the complex process of plaque progression within the arterial wall involves different cells like macrophages, endothelial cells, smooth muscle cells and the plaque becomes filled with lipids, ECM, immune cells debris and an array of pro-inflammatory cytokines, chemokines and growth factors. There are lot of interactions between the plaque environment and cells involved in the atherosclerotic process. Inflammation is an interaction between soluble factors and cells responding to the stimuli similar to situations where cells respond to infections, post-ischemic and toxic autoimmune injury. The atherosclerotic lesion progresses when the initial protective process acting as scavenger of the debris develops into chronic inflammation.

The immune response in atherosclerosis is twofold: the innate response with monocyte infiltration and macrophage transformation into foam cells and also the adaptive response involving regulatory T cells and B cells.

1.3.1 Innate immune response in atherosclerosis

Under physiological conditions, inflammation, one of the first responses of the immune system, is a self-protective mechanism that defends the host from pathogens. However, in the case of atherosclerosis, the immune system plays an important role in the development, progression and complications of the disease[9,38]. During atherogenesis, inflammation in the arterial wall is initiated as a response to deposition of lipoproteins, especially oxidized LDL (oxLDL)[1,39], however in some cases, infection initiates the process[40,41]. In fact, lipid retention beneath the endothelial layer is an important factor that triggers the cascade of events leading to atherosclerotic disease[38]. Lipids are transported as lipoproteins[38]. Higher plasma LDL levels are directly reflected in higher LDL levels in the intimal region due to an increased rate of entry into the intima[42].

Innate immunity is described as initial activation of cells to respond to a pathogen. Monocyte migration to the tissue is an indispensable feature of host defense. It takes place through a cascade of events namely tethering, rolling, arrest, stable adhesion, and intravascular crawling followed by migration across the endothelium and basement membrane[43]. These events are mediated by complex molecular interactions which are sequentially controlled. Many of these steps are regulated by integrins which are complex molecules involved in adhesion and signaling. For example, monocyte arrest requires increased affinity of integrins to their ligands which is triggered by conformational change in the integrins, a process induced by intracellular signaling initiated by chemokines[43]. Following infiltration, monocytes differentiate into macrophages, an event considered central to atherosclerotic lesion development[44]. Macrophages play a very important role in the innate immune response (Fig. 1.2). The numbers of monocyte-macrophage migrating to the plaque area[45], especially at the sites prone for rupturing, are linked strongly with the disease activity.

In atherosclerosis, two factors keep the immune-inflammatory process activated chronically. One is persistence of pro-inflammatory stimuli and the other is failure of regulatory mechanisms involved in resolution. Both the pro-inflammatory M1 macrophages and regulatory M2 macrophages involved in resolution are present in atherosclerotic plaque[45].

In apolipoprotein-E knock out ($ApoE^{-/-}$) mice, a model of atherosclerosis, the early lesion is infiltrated by M2 macrophages[46]; however, when the lesion progresses, they switch to the M1 phenotype. Following exposure to oxLDL, macrophages exhibit reduced expression of salient genes of both M1 and M2 phenotype coupled with upregulation of a distinctive redox gene signature including hemoxygenase 1[45]. It has been observed that $Ly6C^{+}$ monocytes form a major proportion of macrophages located in the plaque and are thought to be recruited by activated endothelium[45,47]. In advanced atherosclerotic lesions in LDL receptor deficient ($LDLR^{-/-}$) mice[45,48], another accepted model of atherosclerosis, this unique population of macrophages, termed as Mox macrophages, comprises 30% of all macrophages[48]. These alternatively activated macrophages have been described as comprised of a number of subtypes[49,50]. For example, in genetically obese diabetic (db/db) mice, administration of interleukin (IL)-33 leads to a phenotypic switch between adipose tissue macrophages to a $CD206^{+}$ M2 phenotype[51], associated with increased levels of Th2 cytokines[45]. Human lesions are characterized by the presence of different phenotypes, depending on the location in the atherosclerotic plaque. M1 ($CD68^{+}$ $CCL2^{+}$ (CC chemokine ligand-2)) macrophage localization patterns are distinct from those of M2 ($CD68^{+}$, $CD206^{+}$) macrophages which are abundant in stable areas of plaque, away from the necrotic lipid core[52]. This heterogeneity in the macrophage phenotypes is possibly driven by the plaque microenvironment.

Apart from the inflammatory cell recruitment and differentiation, another factor that influences the lesion progression and stability is the differential ability of cell subsets to either degrade ECM by MMPs or inhibit its degradation by tissue inhibitor of metalloproteinases (TIMP)[53].

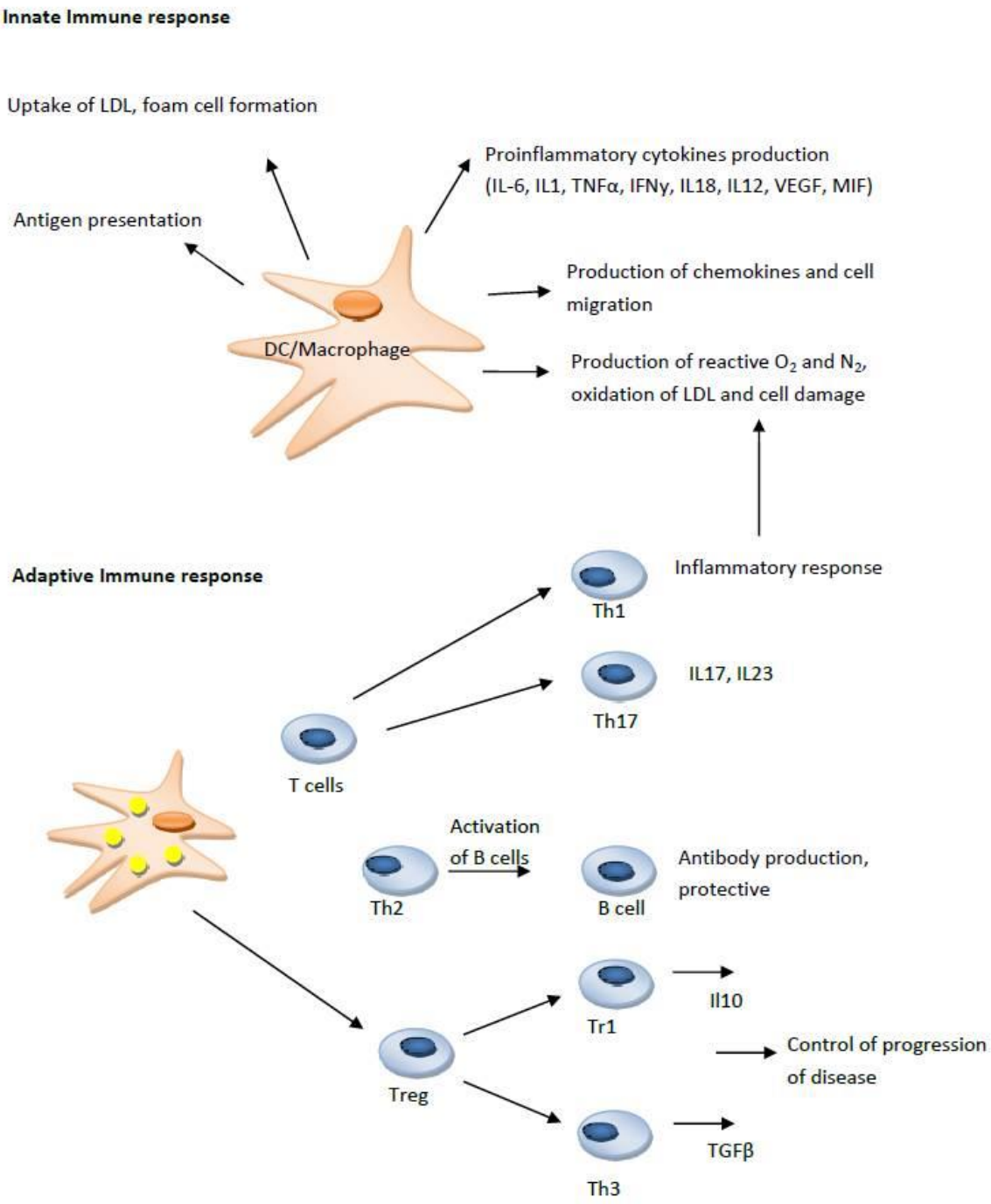

Figure 1.2: Immune response in atherosclerosis (adapted from Samson *et al.*, 2012)[38].

1.3.2 Adaptive immunity in atherosclerosis

Adaptive immunity involves both T and B cells (Fig. 1.2). It comes into play once some specific molecular epitopes on antigens are recognized by highly specific receptors on T cells or B cells with strong affinity[54]. The role of T cells and B cells is evident from the findings that atherosclerotic lesions show a 40-80% reduction following T or B cell deficiency[55]. These results were observed in ApoE$^{-/-}$ and LDLR$^{-/-}$ mice when crossed with either a recombinant activating gene (Rag) deficient background mice[56,57] or severe combined immunodeficiency (SCID) mice[58]. Moreover, replenishing the CD4^{+} T cells from ApoE$^{-/-}$ mice to those crossbred with SCID mice nullifies the reduction in atherosclerotic lesion development, confirming the pro-atherogenic role of T cells[58]. Atherosclerotic lesions usually show abundant T cells and antigen presenting cells (APCs). Natural killer T (NKT) cells have been implicated in development of fatty streak[59,60]. In atherosclerosis, apart from peptide antigens[61], lipid antigens have been considered to be triggers for cell-mediated immune responses and the cluster of differentiation 1 (CD1) molecule can present them to T cells[62]. The lesion size in ApoE$^{-/-}$ mice shows a reduction after crossbreeding with CD1-deficient mice whereas an increase in lesion size is noted following the administration of activator of NKT cells[63]. B cells, on the contrary, appear to play a protective role[64,65]. Upon induction with oxLDL, B1 cells may produce IgM antibodies targeted against oxLDL and reduce the lesion size in ApoE$^{-/-}$ mice[66,67]. IL-5 produced as a part of Th-2 response seems to stimulate these B1 cells[68]. Also, treatment with splenic B cells from ApoE$^{-/-}$ mice abolishes the increase in atherosclerosis resulted from splenectomy in hypercholesterolemic ApoE$^{-/-}$ mice[65]. However, recent studies suggest a dual role of B cells. It has been shown that B2 cells have an atherogenic function performed via a T cell-dependent process[69]. While selective depletion of B2 cells by an anti CD20 monoclonal antibody resulted in attenuation of atherosclerosis in atherosclerosis prone mice[70,71], transfer of B2 cells aggravated atherosclerosis[71]. While the thymus independent antigens lead to IgM via B cell stimulation, antigen presenting cells such as dendritic cells (DC) and macrophages are required for adaptive immunity which act through the antigen specific T cell receptor (TCR). Certain co-stimulatory signals are

also involved. These include interactions between CD80 or CD86 with CD28[72] or interactions of CD40L with CD40[73]. More importantly, both murine and human atherosclerotic plaques show the presence of co-stimulatory molecules[72]. Although the role of these molecules in development of atherosclerotic plaques has been shown in murine models[72,74], their importance is not well established in humans. However, it has been postulated that in humans, co-stimulation may be essential[75].

Antigen presentation by DC needs DC maturation which is coordinated by an array of cytokines and growth factors. DC maturation is affected substantially by the balance between pro- and anti-inflammatory signals[76]. The molecules shown to be involved in the process of maturation include CD40, and the TNF and IL-1 receptors (TNFR and IL-1R). Various T-helper cell responses are finely controlled by unique subsets of DCs[77]. Based on the finding of failure of IL-12$^{-/-}$ mice to induce Th1 responses[78], it is clear that IL-12 production by DCs is critically involved in helper T cell (Th) 1 differentiation[79] whereas, molecules like Il-6, IL-13 and TNFSF4 are involved in Th2 differentiation[77]. Interestingly, anti-inflammatory cytokines such as IL-10 and TGF-β have a unique effect on DCs revealing the plasticity of these cells. Under the influence of these anti-inflammatory cytokines, DCs, instead of inducing a Th1 response, induce a Th2 response[79]. DCs have been observed to cluster with T cells in atherosclerotic lesions[80] and oxLDL has been shown to have an inhibitory effect on the migration of DCs in hypercholesterolemic mice[81].

Most of the T cells involved in the plaque are CD4$^+$ cells[82] which express αβ-TCR and interact with the MHC (major histocompatibility complex) class II molecules[72,83]. Although, among the T cells in the plaque, CD4$^+$ cells are the major source of cytokines, cytotoxic CD8$^+$ killer cells may also act as source of cytokines such as IFN-γ[84,85]. Th1 and Th2 responses have been classified based on the cytokine profile of the T cells involved. The Th1 cell response typically involves secretion of IFN-γ and IL-2 and is responsible for cell-mediated immunity. Th2 response, on the other hand, helps B cells in antibody production through secretion of IL-4, IL-5, IL-10 and IL-13[86]. The cell lineage development from a common precursor depends on the

microenvironment created by cytokines. IL-12 and TCR induce Th1 response whereas IL-4 is important for induction of antigen specific Th2 cells[86].

The Th1 response predominates in the initial stages of plaque development while in the chronic stage, the Th2 response takes over[87]. Thus, although occurrence of atherosclerosis involves Th1 predominance, in a given patient Th1 and/or Th2 responses contribute to development and progression of disease. The prevailing hypothesis is that an imbalance between pathogenic T cells (Th1 and Th2) and regulatory T cells leads to amplification of innate and adaptive immunity, which in turn lead to plaque development and progression[88].

1.3.3 Causes of cytokine production

Cytokines are important mediators of the immune response. They are clustered in several classes and are secreted factors of the innate and adaptive immunity[86]. Based on their structure, they are classified into different families such as interleukins (IL), interferons, tumor necrosis factors (TNF), chemokines, transforming growth factors (TGF), IL-10 and IL-17 families[89].

For a number of years, atherosclerosis was considered to be a disease causes by lipid accumulation[38]. Recently, apart from high LDL levels, the role of chronic inflammation has been emphasized[9]. Currently, from an inflammation perspective, atherosclerosis is described as a multifactorial and multiphasic chronic inflammatory disease.

In general, the cytokines are produced in response to infections and immune responses. Immune-inflammatory processes are involved in each step of atherosclerotic plaque progression, right from appearance of fatty streak to vessel occlusion[90].

Immune-inflammatory processes modulating the inflammation in the vasculature are regulated through production of a number of cytokines which influence key processes such as proliferation, differentiation and function in a variety of cells. As described earlier, the stability of plaque depends on the balance between collagen production and degradation. The relative proportions of pro- and anti-inflammatory cytokines influence

both processes, thereby controlling the structure of the fibrous cap. Thus, cytokines are closely related with atherogenesis and plaque stability.

Although, there have been many attempts to ascertain the relationship between infection and atherosclerosis[91], experimental evidence suggests that infection is not essential for initiation or progression of atherosclerosis[92].

The dominant role of cholesterol in atherosclerosis, both in preclinical models and humans, cannot be overemphasized. The link between cholesterol and cytokine production is more than likely.

Of the atherogenic lipoproteins, namely very low density lipoprotein (VLDL), intermediate density lipoprotein (IDL) and LDL, oxidation of LDL accentuates its atherogenicity[38]. In fact, oxidized lipids, especially oxLDL, have been suggested to be primary triggers for cytokine production[86]. OxLDL is potent inflammatory agent and induces many atherogenic processes through a variety of mechanisms such as modulation of oxidative stress, accentuation of foam cell formation, chemo-attraction for monocytes, maturation of DC and phenotypic switch in macrophages[93]. In $ApoE^{-/-}$ mice, oxLDL is one of the manifestations of chronic inflammation[94]. In genetically modified C3H/HeJ mice, which do not develop atherosclerosis, EC cells do not respond to oxLDL but are activated by IL-1 and TNF-α[95].

1.3.4. Cellular sources of cytokines

Macrophages

Macrophages are the main source of cytokine production in the plaque[86]. They are important for tissue homeostasis and are derived from circulating monocytes that are recruited to the involved tissue by cellular signals[96]. When they reach the source of inflammation, they act as scavengers and start to become macrophages. Generally, they clear up debris and are also responsible for removing modified LDLs. It is particularly important to note that the macrophage-derived foam cells express scavenger receptors which are important in atherogenesis[96].

Macrophages are also known to play prominent role in remodeling during both development and wound healing. Their repertoire, which includes a number of cytokines, growth factors and proteases, perform multiple functions such as recruiting other cells types involved in the healing process including fibroblasts and SMC, and facilitating remodeling of ECM[96].

Both pro- and anti-inflammatory cytokines are produced by macrophages. The pro-inflammatory cytokines include TNF-α[97], IL-1[98], IL-6[99], IL-12[72,86], IL-15[100] and IL-18[101]. The anti-inflammatory cytokines include IL-10[54], IL-32[102] and TGF-β[103], all of which play important roles in the pathology of atherosclerosis. They also produce IFN-γ following stimulation by IL-12 and IL-18[104]. Apart from these cytokines, macrophages produce a variety of chemokines and growth factors which are mediators of smooth muscle cell growth, migration and differentiation; for macrophage differentiation for example, FGFs (fibroblast growth factors), platelet derived growth factor (PDGF) and M-CSF (multi-colony stimulating factor)[96]. All of these cytokines are critical players in the pathology of the atherosclerosis. They also take part in the NF-κb pathway cascade involved in atherosclerosis[105]. Proteases secreted by macrophages, especially in atherosclerosis, play important roles in plaque stability. The important ones are MMPs[106]. Macrophages have also scavenger receptors to endocytose oxidized LDLs as described above.

T cells

Apart from macrophages, T cells affect the immune response in atherosclerosis. Their importance is supported by reports of reduction in atherosclerotic lesion development following depletion of T cells, a phenomenon which also holds true for B cell depletion[55,56,107]. In the atherosclerotic lesion, the predominantly found T cells are $CD4^+$ T cells[108,109]. $CD4^+$ T cells are known to induce either Th1 or Th2 responses. Intracellular pathogens normally lead to a Th1 type of response while the Th2 response supports allergic inflammation. Similar, a response involving activation of macrophages and initiation of an inflammatory response is primarily seen in atherosclerotic lesions[7,9]. The cytokine profile mainly includes IFN-γ, IL-12, IL-15, IL-18 and TNF-α. Furthermore,

interactions between cytokines are important; for example IFN-γ stimulates production of IL-1 and TNF-α which in turn stimulate macrophages and vascular cells to produce a number of pro-inflammatory molecules[61,110].

Other cells like platelets and mast cells are also sources of cytokines, chemokines and growth factors. Platelets are the main source of CD40L and are involved in the cellular inflammatory response[111]. The mast cells, which are also part of the atherosclerotic plaque, produce TNF-α[112].

Mast cells

The precursors of mast cells respond to chemokine signals such as stem cell factor (SCF) and extravasate into the tissue[113]. This migration is directed by chemokine receptors such as CCR3 (chemokine C-C motif receptor 3) and 5[114]. The presence of factors such as IL-3, IL-6 and SCF induce their differentiation[115]. Tryptase- and chymase- producing mast cells, called connective tissue type mast cells, and tryptase only producing mucosal type mast cells reside in the arterial wall[116]. The presence of mast cells, the majority of which lie in the basal side of the vessel wall,[117] does not necessarily indicate a diseased state. However, the presence of proliferating mast cells, may be related to disease progression in atherosclerosis[118], substantiated by mast cell localization in ruptured plaques[119]. Although most of the mast cells are in adventitia, it is possible that they influence the inflammatory process occurring in intima[120]. However, apart from the adventitia, mast cells have also been shown to localize in sub-endothelial region of intima[120]. This localization has been attributed to the fact that endothelial cells produce SCF[121]. Mast cells have also been associated with new vessel formation in atherosclerotic plaques[122]. The observation of reduction of atherosclerosis in mast cell deficiency[118,120] and plaque instability by activated mast cells[123] establishes the pathological role of mast cells in atherosclerosis in mice, at least to some extent. However, it should be noted that the mediators in rodents and humans differ substantially[124].

Endothelial cells

Endothelial cells lie most interior of the vessel wall and thus are the first to take the assault and to respond to pathogens and damage. They secrete cytokines which induce migration of number of other cells in order to mop up the debris and/or act as guardian for the host. In inflammation, the endothelial cell permeability alters and facilitates trans-endothelial migration of leukocytes[54]. Although IL-1 receptor antagonist expression by endothelial cells is low[125], they form an important source of SCF, IL-3, GM-CSF[126]. The chemokine expression profile of endothelial cells is wide and includes MCP-1/CCL2 (monocyte chemoattractant protein-1) and I-309/CCL-1 and define, (Mig)/CXCL9 (monokine induced by IFN-γ/chemokine (C-X-C motif) ligand 9)[127].

Smooth muscle cells (SMC)

SMC are an important source of TNF-α, and IL-1α and β. They also secrete IL-6. In terms of chemokines, they produce MCP-1/CCL2, and (Mig)/CXCL9 and also SDF-1/CXCL12 which is the scavenger receptor that binds oxidized lipoproteins[127].

1.3.5. Lesions in atherosclerosis-stable and unstable plaque

Disease progression and plaque stability are strongly correlated. In the early stages, the plaques are stable and are generally asymptomatic. The usual composition of a stable plaque is solid fibrous and fibro-cellular tissue with little or no extracellular lipid deposition. Most coronary artery plaques remain stable and may cause stable angina pectoris ultimately. On the other hand, unstable plaques are vulnerable to rupture and typically form a necrotic lipid core composed of debris and extracellular lipids. This necrotic core is captured within a fibrous cap that provides structural integrity to the plaque. The lipid core does not contain any living cells and is surrounded by macrophages filled with lipids. These lipid filled macrophages called foam cells result from engulfment of oxLDL by macrophages causing further instability of atheroma[11]. Foam cells die leading to further growth of atheroma which is complicated by binding of lipids to ECM components such as collagen fibers and proteoglycans. As plaque

builds up and grows, it leads to narrowing of the inside of the artery and may restrict blood flow.

Plaque rupture is influenced by a number of factors apart from the mechanical forces which mainly include composition and thickness of the fibrous cap. The actual rupture site is the edge of plaque where high circumferential stress lies and the MMPs act on the collagen fibers to render the plaque more unstable. Reports of expression of MMPs by macrophages in the plaques leading to increased breakdown of ECM[128-130] have made the role of active degradation by MMPs more obvious alongside the passive plaque disruption[131]. Reports suggest that overexpression of MMP-9 in atherosclerotic mice leads to enhanced elastin breakdown and consequent induction of plaque rupture[132].

The aftermath of plaque rupture usually includes thrombosis which may result in acute occlusion leading to acute coronary syndromes such as unstable angina. At times, the rupture may be in the form of a small tear which may induce entry to blood into the plaque thus uprooting the plaque. Other times the rupture is big enough to cause a large thrombus occluding the vessel lumen[133]. The large thrombi eventually get replaced by a vascular repair response[134,135] and may give a misleading picture at angiography wherein permeation by several channels may give a partially open appearance to the thrombus.

1.4 Vascular Calcification

Metaplasia is a common occurrence in atherosclerosis. The metaplastic tissues found in atherosclerotic plaque such as bone, cartilage, marrow, and fat undergo a process of remodeling[136]. Vascular calcification (VC) is an important complication of atherosclerosis contributing to cardiovascular morbidity and mortality[137], given the increased risk of heart attack with calcified coronaries and the growing incidence of calcified aortic stenosis[138]. It is increasingly being accepted that VC is far from a passive degenerative process as thought for the last few decades. Rather, the most recent concept is that VC is an active, organized, complex and highly regulated process. In particular, calcification of atherosclerotic plaque recapitulates virtually the same

biologic reactions inherent to normal physiologic bone formation[139]. This recapitulation is evidenced by the presence of bone like structures in the atherosclerotic arteries and valves, which in many cases is structurally complete trabecular bone[140]. This resemblance is not just at the macroscopic level but even at microscopic level showing features such as completely formed marrow cavities with hematopoietic and marrow stromal cells[141,142]. Energy dispersive x-ray analysis has shown that the mineral in vascular lesions is hydroxyapatite[143] the same mineral as in bone, not just amorphous calcium phosphate.

Although the sequence of events leading to normal bone formation is well known, the sequence of events leading to VC is not completely understood. The expression of growth factors, matrix proteins and other bone related proteins that are involved in both the initiation and inhibition of mineralization supports the dogma of VC being a cell controlled event[144]. In the early and mid-90's, it was postulated that VC was a consequence of active bone formation by osteoblast-like cells[145,146]. One of the hypotheses abounding to the origin of these cells is that vascular SMC (VSMC) trans-differentiate to osteoblastic cells[147,148]. Calcifying vascular cells, a subpopulation of VSMC, that form bone like calcifying nodules, have been found[149,150]. In fact, the likelihood for the presence of a number of stem progenitor niches and/or lineages in vasculature has been described [151,152].

Vascular biology, in the field of regenerative medicine, has witnessed a surge of interest. Vasculature is virtually an omnipresent organ and has a notably high capacity for repair throughout embryonic and adult life. The presence of a number of stem progenitor niches and/or lineages in vasculature has been described. Therefore, despite the fact that the understanding of these resident stem progenitor populations is currently at an early stage, tantalizing prospects for their biological and pathological role are being envisaged. Here, we describe a population of progenitor cells isolated from aortae of $ApoE^{-/-}$ mice and control C57BL/6 mice. These cell populations were characterized for surface signature. The differentiation potential of these cells was then investigated to

understand whether these cells could play a role in aberrant tissue formation in the atheromatous plaque.

1.4.1 Molecular basis for calcification

The mechanistic details of calcification are not fully understood; however, it is envisaged that there is some etiological link between calcification and atherosclerosis. This notion is supported by the fact that coronary artery calcification, not seen in the normal physiological state, occurs almost exclusively in atherosclerosis[153]. This at least partially refutes passive absorption of carboxyglutamic acid gamma-carboxyglutamate-containing serum proteins[154] and supports the idea that it is an active, well regulated and controlled process. In fact, many have compared calcification to bone formation due to it being an organized and regulated processing with close resemblance to bone formation in many aspects.

Molecules such as osteopontin, osteonectin, osteocalcin and bone morphogenetic protein-2 (BMP-2) have been in some way implicated in the process of calcification. Fitzpatrick, who described the passive model of arterial calcification, demonstrated very specific and intense osteopontin staining especially in the outer margins of diseased sections[155]. It has been shown by northern blotting that mRNA expression of osteopontin is associated with the severity of atherosclerosis. On the contrary, osteonectin mRNA expression was inversely related with atherosclerosis. Macrophage derived foam cells have been shown to be predominantly involved in the ectopic protein expression[156,157].

The possibility that osteopontin plays a role in the proliferation and migration phases of blood vessel injury was demonstrated by the chronological increase in osteopontin levels at both protein and RNA level following injury to adult rat aorta or carotid artery starting with very low levels in uninjured vessels[158]. Also, osteopontin expression was increased when vascular smooth muscles were treated in vitro with proteins associated with vascular injury response such as bFGF, TGF-β and angiotensin II. BMP-2, which is a potent osteogenic agent involved in osteoblastic differentiation, has been shown to

be expressed in calcified atherosclerotic plaques[146]. Formation of calcified nodules by calcifying vascular cells (CVCs) and the response to TGF-β, similar to bone cultures[150] provide further strong evidence that vascular calcification is similar to bone formation rather than a passive deposition of calcium. Apart from CVCs, SMC have also been shown to form mineralized nodules[159].

1.5 Progenitor stem cells

1.5.1 Smooth muscle progenitor cells and smooth muscle cells in atherosclerosis

SMC play an important role in disease development in atherosclerosis. SMC proliferation and matrix protein synthesis, including collagen, elastin and/or proteoglycans, lead to plaque accretion[36,160] making fibrous tissue a major component of plaque[161] and may contribute significantly to coronary artery stenosis[162]. The risk of plaque rupture and a subsequent thrombotic event increases substantially with scarcity of SMC in the fibrous cap[163]. Thus SMC can be considered to play a major role in plaque stability. They also play a role in healing the ruptured plaque by secretion of ECM[160,164]. However, this healing may result in increased plaque size causing further stenosis[164,165]. SMC found in plaque may be sourced from locally available preexisting SMC which migrate to the outer layer of plaque[166]. The SMC, present in media and intima of vessel wall, more importantly cells from media[167], may form the fibrous component of the plaque while acquiring a synthetic and migrating phenotype through a process called phenotypic modulation[168]. Due to their almost exclusive production of the ECM and fibrous tissue in the plaque, recruitment of SMC to vasculature has been an area of major research in recent decades[169]. The phenotypic differences between the contractile and synthetic phenotype and ability of SMC to undergo such changes in response to external cues were thought to imply phenotypic modulation[170].

This hypothesis that SMC recruitment and phenotypic modulation is being challenged with suggestions that differentiation of progenitors cells such as hematopoietic stem cells (HSC) contributes to pathogenesis of atherosclerosis[33]. Also, another possibility suggests that migration of progenitor cells from adventitia contributes to atherosclerotic

plaque. Bone marrow-derived circulating progenitor cells have been also been recently claimed to be the source of a sizeable proportion of SMC found in the atherosclerotic lesion[171]. According to some researchers, the phenotypical differences between contractile SMC with an abundance of myofilaments and synthetic SMC with plenty of rough ER and golgi complexes do not suggest phenotypic modulation but rather hint towards different sources, such as a subpopulation in the arterial media with synthetic phenotype[172], stem cells in adventitia[166,173] or circulating smooth muscle progenitor cells[174]. A study showed that when bone marrow of mice were transplanted with donor cells from transgenic mice expressing either eGFP (enhanced green fluorescent protein) or β-Gal (β-galactosidase), it was found that roughly 50% of SMC in atherosclerotic lesions were positive for eGFP or β-Gal[33]. HSCs were implied as a possible source. In a human study, using sex mismatched BM transplantation it was shown that ~20% of SMC in the plaque originated from the BM marrow transplant[175]. In the case of plaque rupture, the local SMC have been reported to have short telomeres and other markers of senescence[176,177], thus suggesting that rupture healing SMC are not locally proliferating SMC and may very well be derived from circulating progenitor cells.

This is also suggested by that fact that circulating cells can be induced to express SMC proteins like α-SMA (α-smooth muscle actin) or SMMHC (smooth muscle myosin heavy chain). Furthermore, a recent study showed that MSCs express α-SMA protein and so also do stem cells derived from the arterial wall[178,179]. Additionally, recent reports have revealed a relationship between coronary artery disease and the ability to form colonies resembling SMC from blood[180]. The role of smooth muscle progenitor cells (SMPC) in atherosclerosis is more complicated. The severity of luminal stenosis has been related to SMPC, whereas a decrease in SMPC number may be involved in causing a thinner neointima and unstable plaque.

Thus, over the years, research investigating the origin of SMC in atherosclerotic lesions has swung from an underlying medial origin to circulating progenitor cells of bone marrow origin. However, reports started to pour in recently with detailed studies showing that the contribution of circulating bone marrow-derived cells to intimal tissue

is less likely[181-183]. One report found that the HSC differentiation to SMC in the atherosclerotic plaque is by no means routine, rather very rare. To investigate this possibility, authors transplanted sex-mismatched BM cells from $eGFP^{+}ApoE^{-/-}$ mice to lethally irradiated $ApoE^{-/-}$ and did not find any BM-derived SMC amongst ~10,000 plaque SMC from a number of sites in the vasculature even in presence of confirmed long term engraftment of $eGFP^{+}$ HSCs[36]. Furthermore, fluorescence in situ hybridization (FISH) analysis of Y chromosome confirmed this finding[36]. The authors also confirmed that upon induction of plaque in $ApoE^{-/-}$ vessels grafted into $eGFP^{+}ApoE^{-/-}$ mice, the presence of circulatory derived SMC were not observed[36]. These results strongly prompted researchers to conclude that SMC are recruited from the local vessel wall and the contribution of circulating cells in the blood is minimal. In another study, the authors investigated the origin of SMC at the healed plaque rupture sites; four weeks after microsurgically-induced disruption of plaque and subsequent thrombosis in old $ApoE^{-/-}$ mice BM transplanted with $eGFP^{+}ApoE^{-/-}$ donor cells, and in carotid bifurcations transplanted between $eGFP^{+}ApoE^{-/-}$ mice and $ApoE^{-/-}$ mice, the study showed that SMC healing the plaque ruptures originate from the local vascular wall[160].

1.5.2 Endothelial progenitor stem cells and circulating progenitor stem cells

The functional integrity of the endothelial layer to prevent atherogenic processes is crucial. The known risk factors of coronary artery disease have been shown to induce apoptosis in endothelial cells, leading to disruption of monolayer integrity[184,185]. In atherosclerosis, activation of the damaged endothelial cells triggers the development of the lesions[186]. Increasingly, it is being understood that endothelial progenitor cells (EPC) have a strong role in vascular repair by contributing to regeneration of the injured endothelial layer. A negative correlation between severity of atherosclerosis and number of EPC in patients has been established and an increased number of EPC in the patients has been reported to decrease risk for the stroke.

On account of their ability to proliferate and differentiate *in vitro* to endothelial cells, EPC are promising targets for transplantation for treatment of ischemia. Promotion of

neovascularization and thereby enhancement of perfusion has been achieved by EPC in hind limb ischemia models in mice and rabbits, leading to functional recovery[187,188] with expression of endothelial markers and functional characteristics of endothelial cells[189]. Following isolation from peripheral blood mononuclear cells and *ex vivo* expansion, EPC have been shown to be involved in myocardial neovascularization[190] while the cells isolated from peripheral blood or bone marrow when infused in coronary artery significantly benefit remodeling following myocardial infarction[191,192].

EPC have been described to express CD34, CD133 or VEGFR2 (vascular endothelial growth factor receptor 2). Of the multiple precursors, hemangioblasts, bone marrow-derived monocytic cells or tissue resident stem cells are the prominent ones[186]. When isolated from peripheral blood, two populations can be isolated namely early outgrowth EPCs and late out growth EPC. The early outgrowth EPC, despite exhibiting certain EC characteristics such as eNOS expression, show low proliferation potential and do not form functional vessels *in vivo*. The late out growth EPC, on the other hand, have high proliferative capacity and form vessels in vivo[193]. Cell surface studies show that these cells are CD34 positive and CD45 negative precursors[194]. Further analysis of these two fraction showed that early EPC come from CD14 positive cells while the late fraction develops almost exclusively from CD14 negative cells[195].

Recent studies in mice demonstrated that circulating EPC are directly incorporated in the vessel wall and are involved in re-endothelialization[186]. A study has shown that the newly regenerated ECs in a model of transplant atherosclerosis were derived from circulating blood from the recipient and not from donor vessels[196]. Also, it was observed that circulating endothelial progenitors completely replace the endothelial monolayer in a vein graft within 3 days of surgery[34]. This ability to repair vessel wall remains even when vascular injury continues and EPCs help arrest the disease progression[197]. Disease development can be prevented by treatment with bone marrow-derived progenitor cells from young non-atherosclerotic $ApoE^{-/-}$ mice in aged $ApoE^{-/-}$ mice[198]. In a carotid artery model with endothelial cell injury, spleen homogenate-derived EPCs not only reduced formation of neointima but also augmented restoration

of endothelial layers[199]. In another model of balloon injury, a beneficial effect of circulating EPCs was observed with enhanced endothelial repair coupled with reduced activation of medial SMC and neointima formation[200]. A number of studies have established a direct link between number of EPCs and endothelial repair and reduction in neointima formation[197,201].

However, the new vessel formation supported by these progenitor cells may prove to be detrimental as shown by a study using a hind limb ischemia model in ApoE$^{-/-}$ mice which demonstrated increased plaque size along with improved blood supply to the ischemic areas[202]. Another study observed that EPC treatment led to increased instability of the plaque which can be attributed to their pro-inflammatory effects especially because of the finding of reduced local IL-10 levels. Thus, it seems that EPCs can have opposite effects; impaired mobilization of EPCs may hamper re-endothelialization while excessive mobilization may cause stenosis[203]. However, while evaluating the effects of EPCs, their heterogenicity must be considered as different isolation protocols have been shown to affect the functionality of the cells[204]. The role of microvessels in the vessel wall in atherogenesis has been emphasized[205-207]; however it has also been demonstrated that endothelial cells in these microvessels are derived from progenitor cells[196]. Thus, considering their role in endothelial repair and plaque angiogenesis, it is clear that EPCs play both beneficial and detrimental roles, at least in transplant atherosclerosis.

1.5.3 Hematopoietic stem cells

HSCs reside in the arterial tissue and are believed to be involved in maintaining the vascular system on account of their capacity for self-renewal and differentiation in multiple lineages[208]. Recruitment of circulating blood leukocytes in the vessel wall has been implicated in the development of atherosclerotic plaque[1,209]. The role of HSCs in atherosclerosis was investigated recently by inactivating p27 which resulted in enhanced HSC proliferation in arterial macrophages and inflammatory response and accelerated atherosclerosis[210].

1.5.4 Mesenchymal stem cells

MSCs are multipotent stem cells which have capability to differentiate to cell types and to regenerate damaged tissues and organs[211]. Along with the progenitor cells in vessel wall, bone marrow-derived progenitors play a critical role in the development of cardiovascular diseases[212,213].

MSCs from bone marrow and resident in the vessel wall, have been demonstrated to differentiate into ECs and SMC, respectively[214,215]. In different models of atherosclerosis such as injury-induced, vein graft or transplant atherosclerosis, these cells may be involved either directly or at least indirectly in development of lesions[213].

Circulating MSC can swim through the blood stream and reach the site of injury in the vessel wall[216]. It is now believed that previously described CVCs in the arterial wall are a type of MSC, one generation below in mesenchymal hierarchy as suggested by their self-renewal and pluripotent plasticity with lack of adipogenic lineage[217]. Regarding the differentiation of MSC to smooth muscle cells, the controversy still remains; although, through studies investigating the pathogenesis of transplant arteriosclerosis, the role of MSC or EPC in repair of EC is quite clear along with the apparent role of vascular stem cells in replenishing dead cells[211].

In a recent study with balloon injury in hyperlipidemic rats, bone marrow-derived MSC (BM-MSC) were found to clearly increase the size of atherosclerotic lesion[218]. In this study, transferring BM-MSC resulted in vascular calcification in medial layers detected at 6 weeks after balloon angioplasty[218]. Although the exact mechanism of calcification following BM-MSC transfer is not clear, there was a possible association with upregulation of BMP-2[148,218]. Also, evidence suggests that the regulation of this calcification involves locally expressed bone calcification regulatory factors[147,219,220]. Another study has demonstrated that transfer of bone marrow and EPC not only stimulate disease progression in atherosclerosis but also impacted stability of the plaque[221]. Studies have provided enough evidence to suggest a link between MSC transfer and pathogenesis of atherosclerosis[33,174].

1.5.5 Vascular stem cells

There is evidence that stem or progenitor cells reside in different organs and differentiate to repair the injury. However, it might be that these resident stem/progenitor cells are not only contributing to the repair but play an important role to the pathogenesis of diseases.

1.6 Pericytes

Pericytes were first time described by Ebreth and Rouget more than a century ago. They were initially called Rouget cells. Later by their anatomical localization, abluminal to endothelial cells and luminal to parenchymal cells, they were renamed by Zimnerman in 1923 as peri- around and cyte- cells (vessel)[222]. Pericytes are elongated cells, around 70μm[223-225] long, embedded within the basement membrane adjacent to the EC junctions[226]. Being closely associated with endothelium, they play a crucial function in maintaining vessel wall integrity and contributing to the generation of the venular basement membrane[227-230].

1.6.1 Distribution and function

The cells have been identified in the inner intimal layer and also the outer layer of the media in vasa vasora in adventitia of large, medium or small arteries and veins. Pericyte coverage is highest in the central nervous system. It has been suggested that pericytes also contribute to the blood-brain barrier (BBB)[227,231,232] which is considered to be comprised of EC, pericytes, basal lamina along with neurons, astrocytes and other glial cells forming the neurovascular unit[232].

Pericytes are also observed in retina in high numbers. Although not replicating in the adult retina, they play important functions as suggested by increased vascular permeability and retinal edema following their degeneration in disease states like diabetes[233,234]. It has been postulated that loss of pericytes in the vascular wall of the capillary vessels is an early feature of diabetic retinopathy[235]. The consequences of

pericyte loss include micro-aneurysms or at times EC degeneration and formation of acellular capillaries resulting eventually in foci of non-perfusion[236,237].

Pericytes are also found in kidney where they are called mesangial cells[238], and in BM, where they are termed as reticular or adventitial cells[239]. The physiological and pathological role of these cells in kidney function is poorly understood[240]. They are involved in angiogenesis and vessel integrity, thus they might, in the case of kidney injury, infiltrate to the injury site and participate actively in scar formation by myofibroblast generation[240]. They are also thought to be a source of the myofibroblasts in the fibrotic kidney.

Hepatic satellite cells are similar to pericytes[238]. They regulate EC fate and contribute to remodeling of ECM components[241]. They are also important in the inflammatory response during fibrotic diseases[242,243].

It has been suggested that the cells are relatively undifferentiated with the slender projections that wrap around the capillaries. It has also been suggested that they are MSC associated with the blood vessel walls where they serve as a support to these vessels. These cells can differentiate not only into fibroblasts, SMC but also into different lineages, especially to osteoblasts[178,244-247], chondrocytes[178,239,245,248] or adipocytes[178,248] under appropriate cell culture conditions. Pericytes can also act as macrophage precursors and express macrophage markers such as CD4 class I and class II MHC molecules and perform macrophage-like activities[238,247].

The heterogeneity of pericytes is reflected in their function[239,249]. Their morphology, distribution, frequency and physiology[248] depend on the type of vessel, stage of development, species and also pathological conditions[224]. In large arteries, pericytes are embedded within the endothelial basement membrane. They facilitate and integrate cell communication[227]. Usually, pericytes overlap several endothelial cells and regulate certain functions by secretion of factors[227,250,251]. Pericytes extend long processes exhibiting contractile microfilament bundles which wrap around the blood vessel[222].

They can also form more confined finger like projections and retract them when migrating[222].

Pericyte coverage varies considerably in different organs, implying their varied functions in different tissues[225]. For example, a study from the Proebstl and Nourshagh group investigated the role of pericytes in neutrophil crawling and leukocyte trafficking during inflammation in pathological conditions[225]. These authors investigated the mechanism and dynamics of neutrophil migration through a pericyte sheet and found that pericytes support neutrophil migration actively through the venular wall[225]. The cells were also found to express receptors for inflammatory cytokines like TNF-α and IL-1β[225]. These results are consistent with a role of pericytes in inflammation.

Since they are contractile and respond to environmental changes, pericytes are suggested to play a role in controlling blood flow and pathological conditions. It has been reported that the number of pericytes is increased in hypertensive conditions[252]. It has also been shown that pericytes can inhibit EC proliferation by producing TGF-β in retina[238]. PDGF-β secreted by EC plays a role in recruiting pericytes whereas the receptor for PDGF-β expressed by pericytes plays a crucial role in maturation of blood vessels[238,253]. There is a significant interaction between the cells where EC stimulate pericyte growth by secretion of endothelin-1[238].

1.6.2 Origin

Similar to VSMC, pericytes are thought to have multiple origins. In the axial and lateral plate mesenchyme, the vessel wall cells around the developing trunk vessels have been attributed to a mesodermal origin[254]. In the central nervous system, they might also be derived from neurocrest[238,255], at least partly[256] or mesodermal precursors called angioblasts[257]. On the other hand, coronary vessel wall cells have been thought to develop from epicardial cells which have a splanchnic mesodermal origin[258,259]. Nevertheless, in general, pericytes are considered to be of mesenchymal origin. They are thought to be associated with MSC[227,260,261] since they can differentiate into different cell types. A recent study investigating adult angiogenesis confirmed the bone marrow

origin of mural cells[262]. Also, though pericytes share the common endothelial and smooth muscle markers, they are different from these cells.

Though not a major pathway of pericyte formation in normal physiological development, there has been some evidence of trans-differentiation from endothelial cells[227,262,263], where TGF-β3 can initiate the differentiation. It has been reported that quail embryonic EC in the dorsal aorta of the embryo are able to trans-differentiate into sub-endothelial mesenchymal cells expressing smooth muscle actins in vivo[263].

1.6.3 Characterisation

Pericytes are distinguished from other cell types by their marker expression. They express different markers during the different stages of their growth and also depending on their origin. Pericytes are clearly distinguished from other stromal cells such as SMC and EC; however, they share many similarities with other cells like myofibroblasts[264].

There are several markers which are used to characterize pericytes like α-SMA[265,266], NG2[178,265,267] (nerve/glial antigen 2), PDGFR-β[178,268], aminopeptidase A[269] and RGS5[270](regulator of G-protein signaling 5). It is believed that none of the markers absolutely characterize the pericytes on account of their different origins and stage of development. Some of the markers might be expressed dynamically and vary between different organs. 3G5, considered to be a pericyte-specific marker is found on the surface of the pericytes[271,272]. 3G5 is expressed in pericytes of human and bovine aorta[146,271]. A study has shown that pericyte-like cells from aortic medial cell nodules stain positive for alpha actin, beta actin and the epitope of mAb 3G5 with characteristic patterns on immunofluorescence staining such as filamentous, granular or peripheral patterns, respectively[146]. These characteristics, although different from those of endothelial and smooth muscle cells from human or bovine aorta and human fibroblasts, match with those of microvascular pericytes.

1.7 Animal models for atherosclerosis

1.7.1 Mice models

ApoE$^{-/-}$ mice

ApoE is a major component within lipoprotein metabolic pathways that plays role in preventing development of atherosclerotic lesions[273]. The ApoE polypeptide is important in hepatic clearance of circulating cholesterol[274]. It is a constituent of VLDL synthesized by the liver, and of a subclass of high density lipoproteins (HDLs) involved in cholesterol transport among cells[275]. ApoE is normally expressed predominantly by hepatocytes and macrophage cells of hematopoietic lineage, and transplantation of normal bone marrow cells into ApoE$^{-/-}$ mice results in increased lipoprotein clearance, reversal of hypercholesterolemia, and protection against development of atherosclerosis[273].

When ApoE is dysfunctional or absent, severe hyperlipidemia occurs in humans and in animal models[274]. The presence of osteoblasts and chondrocyte-like cells within calcified atherosclerotic plaques, indicating the formation of structures resembling bone and cartilage, has been reported in humans[276,277] and ApoE$^{-/-}$ mice[278]. The generation of ApoE$^{-/-}$ mice[279] has helped in the study of hyperlipidemia and mechanisms involved in atherosclerotic plaque formation, and in developing therapies for atherosclerosis in humans[280]. In ApoE$^{-/-}$ mice, atherosclerosis develops and progresses spontaneously, with lesions covering over 20% of the proximal aortic wall at 4 months and 50% at 13 months[275]. The transfer of plasma cholesterol in these mice mostly takes place by VLDL as against LDL in humans. Despite the dissimilarities of plasma lipids between ApoE$^{-/-}$ mice and humans, the atherosclerotic lesions in these mice are closest to humans than any other available model. The stages of plaque development such as early influx of inflammatory cytokines, formation of necrotic cores and accumulation of SMC and fibrous tissue are the same in ApoE$^{-/-}$ mice and humans. However, there are differences to be noted. Since, mice have very thin intima consisting of only endothelium and few dendritic cells[281,282], SMC in the plaque are invariably recruited from the media. Humans, on the other hand, can recruit SMC locally as human intima is known to harbor SMC and connective tissue[283]. Another difference is in terms of complications.

Plaque ruptures and subsequent thrombosis seen in human atherosclerosis are very rare in mice models.

There are other less studied mice models involving ApoE. Humans express ApoE in three isoforms namely ApoE-2, -3 and -4, of which ApoE-3 is most common. Transgenic mice have been created with the ApoE-2 isoform. Both ApoE-2 and -3 leiden transgenic mice develop a beta migrating form of VLDL even in presence of normal ApoE[284,285]. When fed with diets rich in saturated fat, cholesterol and cholate, these transgenic mice form atherosclerotic lesions at the aortic root which progress from lesions with abundant foam cells to lesions with fibrous caps[286,287].

ApoB transgenic mice

Transgenic mice expressing human ApoB have lipid levels similar to normal healthy humans[288]. However, it is a diet responsive model; Paigen or western-type diet trigger development of atherosclerosis in these mice[289,290] with lesions consisting mainly of macrophage foam cells[291]. Female mice show a greater extent of atherosclerosis compared to males[292].

LDLR $^{-/-}$ mice

LDLR$^{-/-}$ mice, created in early 1990s[293], develop large lesions on Paigen diet[294] or even on western-type diet[295]. The lipoprotein abnormalities are less prominent in these mice compared to ApoE$^{-/-}$ mice. The lesions are characterized by a predominance of macrophage foam cells[296]; however, after long term feeding with high fat diet, necrotic cores and calcification can be observed in the lesions[295].

Mice models with more complex genetic abnormalities

Severe atherosclerotic disease has been observed in a recently developed model with double knockout of ApoE and LDL receptor[294,297] without feeding atherogenic diet[298]. Another double knockout model was created by knocking out eNOS (endothelial nitric oxide synthase) in ApoE$^{-/-}$ mice which resulted not only in increased atherosclerosis but also various vascular complications not observed in ApoE$^{-/-}$ mice such as heart failure

and ischemia[299]. Combined ApoB100 transgenic mice and LDLR$^{-/-}$ mice have pronounced endogenous hypercholesterolemia and widespread atherosclerosis even when fed with normal diet[300]. Interestingly, when ApoE$^{-/-}$ mice were made homozygous for ApoB100, the resulting model has a lesser degree of hypercholesterolemia[301]. Also, ApoE$^{-/-}$ mice that overexpress ApoA-1 have significantly reduced lesions, probably related to higher HDL levels observed in these mice[302,303].

1.7.2 Rabbit models

Rabbit has been used extensively as a model to study atherosclerosis, especially due to its high sensitivity to develop hypercholesterolemia within days of feeding with high cholesterol diet[304]. The similarity of the lesions in rabbits to the fatty streaks in humans is high and the model is therefore suitable for testing effectiveness of drugs[305]. Development of advanced lesions similar to the human scenario was observed in rabbits fed with intermittent high fat and normal diet[306]. The illustration of pathogenic mechanisms involved in initiation and progression of the disease are being aided by recent developments in transgenic rabbit models.

In NZW rabbits, transgenes for human apoA, apoA-I, apoB, apoE2, apoE3 and lecithin cholesterol acyltransferase (LCAT), as well as for rabbit apolipoprotein B mRNA-editing enzyme catalytic poly-peptide 1 (APOBEC-1), have been developed. However, only the transgenes for human apoA-I and LCAT have been expressed on a WHHL (Watanabe Heritable Hyperlipidemic) background[307].

1.7.4 Guinea pig and hamster models

Atherosclerosis in guinea pigs is affected by gender and hormonal status[308]. One major advantage of guinea pigs as a model is that they use LDL for transporting circulating cholesterol as in humans[309]. Syrian hamsters are becoming popular in recent years due to ease of handling and a striking similarity to humans in regards to response to diet changes[310]. They develop plaques with a complexity level similar to humans when fed on a fatty diet[311].

1.8 Thesis Objectives

Atherosclerosis is a leading cause of morbidity and mortality. Despite the identification of a number of risk factors, all the current theories explaining pathogenesis of atherosclerosis are far from complete. Recent focus on circulating and resident progenitor cells in the vasculature and their role in pathogenesis has been the driving force behind this thesis. The most widely accepted response to injury theory and smooth muscle transdifferentiation to explain the vascular calcification observed in atherosclerosis is being challenged. Recent evidence supports differentiation of progenitor cells and this thesis investigates this alternative. The thesis attempts to investigate the contribution of isolated resident and circulating progenitor cells from diseased and background mice models to vascular calcification by differentiation studies and the effect of atherosclerotic environment on the process. Thus, the thesis can be divided into following phases:

1) **Isolation and surface characterisation of VSCs from aortae and MSCs from bone marrow of ApoE$^{-/-}$ and background C57BL/6 mice**

   In the first phase of the thesis, various protocols for isolation and culture of VSCs and MSCs from both ApoE$^{-/-}$ and C57BL/6 mice were tested and optimised for establishment of long term cultures. Following isolation and in vitro culture, the surface characteristics of these cells were studied for presence of hematopoietic, endothelial, MSC and pericyte-associated markers.

2) ***In vitro*** **differentiation potential of VSCs and MSCs from ApoE$^{-/-}$ and C57BL/6 mice**

   Following surface signature evaluation, it was important to examine the multipotency of all the isolated cell types. This phase of the study investigated the differentiation potential of VSCs and MSCs from ApoE$^{-/-}$ and C57BL/6 mice to osteogenic, chondrogenic, adipogenic and myogenic lineages under appropriate inductive culture conditions *in vitro*.

3) Effect of pro-inflammatory cytokines found in the atherosclerotic environment on *in vitro* differentiation of VSCs from ApoE$^{-/-}$ and C57BL/6 mice at molecular level

The atherosclerotic plaque is known to harbour a number of pro-inflammatory cytokines. This phase of the work was based on the hypothesis that individual cytokines found in the atherosclerotic plaques can alter the differentiation of VSCs from ApoE$^{-/-}$ and C57BL/6 mice. Here, chondrogenic differentiation was supplemented with pro-inflammatory cytokines such as IL-6, IL-1β or TNF-α and the effect was investigated at a molecular level by quantitative PCR for lineage specific markers such as Sox9 (transcription factor)[312] and associated factors such as fibromodulin (early chondrogenesis)[313], Collagen Type II (definitive chondrogenesis)[312], Runx2 (runt-related transcription factor 2) (prehypertrophy in endochondral ossification)[314] and Alp (alkaline phosphatase) (hypertrophy)[315].

4) Investigation of *in vivo* differentiation of VSCs and MSCs from ApoE$^{-/-}$ and C57BL/6 mice when implanted in either ApoE$^{-/-}$ or C57BL/6 mice

Following the investigation of the effect of individual factors, it was important to study the overall effect of the atherosclerotic environment *in vivo* and compare it with the intrinsic capacity of the isolated cells to differentiate to osteogenic and chondrogenic lineages. In this phase, cells seeded into collagen-chondroitin sulphate scaffolds were chondrogenically primed *in vitro* and implanted subcutaneously in atherosclerotic or control mice. Thus, the intrinsic capacity of isolated cells from atherosclerotic mice to form bone and the effect of the atherosclerotic environment on the intrinsic capacity was investigated. The effect of priming was also investigated.

1.9 References

1. Lusis, A.J. Atherosclerosis. *Nature* **407**, 233-241 (2000).
2. Pappalardo, F., Musumeci, S. & Motta, S. Modeling immune system control of atherogenesis. *Bioinformatics* **24**, 1715-1721 (2008).
3. Stary, H.C., *et al*. A definition of the intima of human arteries and of its atherosclerosis-prone regions. A report from the Committee on Vascular Lesions of the Council on Arteriosclerosis, American Heart Association. *Circulation* **85**, 391-405 (1992).
4. Clark, J.M. & Glagov, S. Structural integration of the arterial wall. I. Relationships and attachments of medial smooth muscle cells in normally distended and hyperdistended aortas. *Lab Invest* **40**, 587-602 (1979).
5. Napoli, C., *et al*. Fatty streak formation occurs in human fetal aortas and is greatly enhanced by maternal hypercholesterolemia. Intimal accumulation of low density lipoprotein and its oxidation precede monocyte recruitment into early atherosclerotic lesions. *The Journal of clinical investigation* **100**, 2680-2690 (1997).
6. Stary, H.C., *et al*. A definition of initial, fatty streak, and intermediate lesions of atherosclerosis. A report from the Committee on Vascular Lesions of the Council on Arteriosclerosis, American Heart Association. *Circulation* **89**, 2462-2478 (1994).
7. Hansson, G.K. Inflammation, atherosclerosis, and coronary artery disease. *N Engl J Med* **352**, 1685-1695 (2005).
8. Gutstein, D.E. & Fuster, V. Pathophysiology and clinical significance of atherosclerotic plaque rupture. *Cardiovasc Res* **41**, 323-333 (1999).
9. Hansson, G.K. & Libby, P. The immune response in atherosclerosis: a double-edged sword. *Nature reviews*. *Immunology* **6**, 508-519 (2006).
10. Campbell, J.H., Popadynec, L., Nestel, P.J. & Campbell, G.R. Lipid accumulation in arterial smooth muscle cells. Influence of phenotype. *Atherosclerosis* **47**, 279-295 (1983).
11. van der Wal, A.C. & Becker, A.E. Atherosclerotic plaque rupture--pathologic basis of plaque stability and instability. *Cardiovasc Res* **41**, 334-344 (1999).
12. Pasterkamp, G., *et al*. Inflammation of the atherosclerotic cap and shoulder of the plaque is a common and locally observed feature in unruptured plaques of femoral and coronary arteries. *Arteriosclerosis, thrombosis, and vascular biology* **19**, 54-58 (1999).
13. Aigner, T., Neureiter, D., Campean, V., Soder, S. & Amann, K. Expression of cartilage-specific markers in calcified and non-calcified atherosclerotic lesions. *Atherosclerosis* **196**, 37-41 (2008).
14. Kovanen, P.T., Kaartinen, M. & Paavonen, T. Infiltrates of activated mast cells at the site of coronary atheromatous erosion or rupture in myocardial infarction. *Circulation* **92**, 1084-1088 (1995).
15. Bobryshev, Y.V. & Lord, R.S. Co-accumulation of dendritic cells and natural killer T cells within rupture-prone regions in human atherosclerotic plaques. *The*

journal of histochemistry and cytochemistry : official journal of the Histochemistry Society **53**, 781-785 (2005).
16. Falk, E., Shah, P.K. & Fuster, V. Coronary plaque disruption. *Circulation* **92**, 657-671 (1995).
17. Libby, P. The molecular mechanisms of the thrombotic complications of atherosclerosis. *Journal of internal medicine* **263**, 517-527 (2008).
18. van der Wal, A.C., Becker, A.E., van der Loos, C.M. & Das, P.K. Site of intimal rupture or erosion of thrombosed coronary atherosclerotic plaques is characterized by an inflammatory process irrespective of the dominant plaque morphology. *Circulation* **89**, 36-44 (1994).
19. Kaartinen, M., *et al*. Mast cell infiltration in acute coronary syndromes: implications for plaque rupture. *Journal of the American College of Cardiology* **32**, 606-612 (1998).
20. Mach, F., Schonbeck, U., Bonnefoy, J.Y., Pober, J.S. & Libby, P. Activation of monocyte/macrophage functions related to acute atheroma complication by ligation of CD40: induction of collagenase, stromelysin, and tissue factor. *Circulation* **96**, 396-399 (1997).
21. Hansson, G.K., Hellstrand, M., Rymo, L., Rubbia, L. & Gabbiani, G. Interferon gamma inhibits both proliferation and expression of differentiation-specific alpha-smooth muscle actin in arterial smooth muscle cells. *The Journal of experimental medicine* **170**, 1595-1608 (1989).
22. Saren, P., Welgus, H.G. & Kovanen, P.T. TNF-alpha and IL-1beta selectively induce expression of 92-kDa gelatinase by human macrophages. *J Immunol* **157**, 4159-4165 (1996).
23. Amento, E.P., Ehsani, N., Palmer, H. & Libby, P. Cytokines and growth factors positively and negatively regulate interstitial collagen gene expression in human vascular smooth muscle cells. *Arteriosclerosis and thrombosis : a journal of vascular biology / American Heart Association* **11**, 1223-1230 (1991).
24. Demer, L.L. Vascular calcification and osteoporosis: inflammatory responses to oxidized lipids. *International journal of epidemiology* **31**, 737-741 (2002).
25. Mehta, N.J. & Khan, I.A. Cardiology's 10 greatest discoveries of the 20th century. *Tex Heart Inst J* **29**, 164-171 (2002).
26. Konstantinov, I.E., Mejevoi, N. & Anichkov, N.M. Nikolai N. Anichkov and his theory of atherosclerosis. *Tex Heart Inst J* **33**, 417-423 (2006).
27. Ku, D.N., Giddens, D.P., Zarins, C.K. & Glagov, S. Pulsatile flow and atherosclerosis in the human carotid bifurcation. Positive correlation between plaque location and low oscillating shear stress. *Arteriosclerosis* **5**, 293-302 (1985).
28. Wilcox, J.N. Thrombin and other potential mechanisms underlying restenosis. *Circulation* **84**, 432-435 (1991).
29. Spence, J.D. & Norris, J. Infection, inflammation, and atherosclerosis. *Stroke* **34**, 333-334 (2003).
30. Ross, R. Atherosclerosis--an inflammatory disease. *N Engl J Med* **340**, 115-126 (1999).

31. Heinecke, J.W. Oxidants and antioxidants in the pathogenesis of atherosclerosis: implications for the oxidized low density lipoprotein hypothesis. *Atherosclerosis* **141**, 1-15 (1998).
32. Navab, M., *et al*. The oxidation hypothesis of atherogenesis: the role of oxidized phospholipids and HDL. *J Lipid Res* **45**, 993-1007 (2004).
33. Sata, M., *et al*. Hematopoietic stem cells differentiate into vascular cells that participate in the pathogenesis of atherosclerosis. *Nature medicine* **8**, 403-409 (2002).
34. Xu, Q., Zhang, Z., Davison, F. & Hu, Y. Circulating progenitor cells regenerate endothelium of vein graft atherosclerosis, which is diminished in ApoE-deficient mice. *Circulation research* **93**, e76-86 (2003).
35. Canfield, A.E., *et al*. Role of pericytes in vascular calcification: a review. *Z Kardiol* **89 Suppl 2**, 20-27 (2000).
36. Bentzon, J.F., *et al*. Smooth muscle cells in atherosclerosis originate from the local vessel wall and not circulating progenitor cells in ApoE knockout mice. *Arterioscler Thromb Vasc Biol* **26**, 2696-2702 (2006).
37. Pamukcu, B., Lip, G.Y., Devitt, A., Griffiths, H. & Shantsila, E. The role of monocytes in atherosclerotic coronary artery disease. *Annals of medicine* **42**, 394-403 (2010).
38. Samson, S., Mundkur, L. & Kakkar, V.V. Immune response to lipoproteins in atherosclerosis. *Cholesterol* **2012**, 571846 (2012).
39. Khalil, M.F., Wagner, W.D. & Goldberg, I.J. Molecular interactions leading to lipoprotein retention and the initiation of atherosclerosis. *Arteriosclerosis, thrombosis, and vascular biology* **24**, 2211-2218 (2004).
40. Hendrix, M.G., Salimans, M.M., van Boven, C.P. & Bruggeman, C.A. High prevalence of latently present cytomegalovirus in arterial walls of patients suffering from grade III atherosclerosis. *Am J Pathol* **136**, 23-28 (1990).
41. Thom, D.H., *et al*. Chlamydia pneumoniae strain TWAR antibody and angiographically demonstrated coronary artery disease. *Arteriosclerosis and thrombosis : a journal of vascular biology / American Heart Association* **11**, 547-551 (1991).
42. Schwenke, D.C. & Carew, T.E. Initiation of atherosclerotic lesions in cholesterol-fed rabbits. II. Selective retention of LDL vs. selective increases in LDL permeability in susceptible sites of arteries. *Arteriosclerosis* **9**, 908-918 (1989).
43. Hyduk, S.J. & Cybulsky, M.I. Role of alpha4beta1 integrins in chemokine-induced monocyte arrest under conditions of shear stress. *Microcirculation* **16**, 17-30 (2009).
44. Gleissner, C.A., Shaked, I., Little, K.M. & Ley, K. CXC chemokine ligand 4 induces a unique transcriptome in monocyte-derived macrophages. *J Immunol* **184**, 4810-4818 (2010).
45. Shalhoub, J., Falck-Hansen, M.A., Davies, A.H. & Monaco, C. Innate immunity and monocyte-macrophage activation in atherosclerosis. *Journal of inflammation* **8**, 9 (2011).

46. Khallou-Laschet, J., *et al*. Macrophage plasticity in experimental atherosclerosis. *PLoS One* **5**, e8852 (2010).
47. Swirski, F.K., *et al*. Ly-6Chi monocytes dominate hypercholesterolemia-associated monocytosis and give rise to macrophages in atheromata. *The Journal of clinical investigation* **117**, 195-205 (2007).
48. Kadl, A., *et al*. Identification of a novel macrophage phenotype that develops in response to atherogenic phospholipids via Nrf2. *Circulation research* **107**, 737-746 (2010).
49. Mosser, D.M. & Edwards, J.P. Exploring the full spectrum of macrophage activation. *Nature reviews. Immunology* **8**, 958-969 (2008).
50. Mantovani, A., *et al*. The chemokine system in diverse forms of macrophage activation and polarization. *Trends in immunology* **25**, 677-686 (2004).
51. Miller, A.M., *et al*. Interleukin-33 induces protective effects in adipose tissue inflammation during obesity in mice. *Circulation research* **107**, 650-658 (2010).
52. Bouhlel, M.A., *et al*. PPARgamma activation primes human monocytes into alternative M2 macrophages with anti-inflammatory properties. *Cell metabolism* **6**, 137-143 (2007).
53. Chase, A.J., Bond, M., Crook, M.F. & Newby, A.C. Role of nuclear factor-kappa B activation in metalloproteinase-1, -3, and -9 secretion by human macrophages in vitro and rabbit foam cells produced in vivo. *Arteriosclerosis, thrombosis, and vascular biology* **22**, 765-771 (2002).
54. Tedgui, A. & Mallat, Z. Cytokines in atherosclerosis: pathogenic and regulatory pathways. *Physiological reviews* **86**, 515-581 (2006).
55. Dansky, H.M., Charlton, S.A., Harper, M.M. & Smith, J.D. T and B lymphocytes play a minor role in atherosclerotic plaque formation in the apolipoprotein E-deficient mouse. *Proc Natl Acad Sci U S A* **94**, 4642-4646 (1997).
56. Song, L., Leung, C. & Schindler, C. Lymphocytes are important in early atherosclerosis. *The Journal of clinical investigation* **108**, 251-259 (2001).
57. Reardon, C.A., *et al*. Effect of immune deficiency on lipoproteins and atherosclerosis in male apolipoprotein E-deficient mice. *Arteriosclerosis, thrombosis, and vascular biology* **21**, 1011-1016 (2001).
58. Zhou, X., Nicoletti, A., Elhage, R. & Hansson, G.K. Transfer of CD4(+) T cells aggravates atherosclerosis in immunodeficient apolipoprotein E knockout mice. *Circulation* **102**, 2919-2922 (2000).
59. Aslanian, A.M., Chapman, H.A. & Charo, I.F. Transient role for CD1d-restricted natural killer T cells in the formation of atherosclerotic lesions. *Arteriosclerosis, thrombosis, and vascular biology* **25**, 628-632 (2005).
60. Major, A.S., *et al*. Quantitative and qualitative differences in proatherogenic NKT cells in apolipoprotein E-deficient mice. *Arteriosclerosis, thrombosis, and vascular biology* **24**, 2351-2357 (2004).
61. Hansson, G.K. Immune mechanisms in atherosclerosis. *Arteriosclerosis, thrombosis, and vascular biology* **21**, 1876-1890 (2001).
62. Joyce, S. & Van Kaer, L. CD1-restricted antigen presentation: an oily matter. *Current opinion in immunology* **15**, 95-104 (2003).

63. Tupin, E., *et al*. CD1d-dependent activation of NKT cells aggravates atherosclerosis. *The Journal of experimental medicine* **199**, 417-422 (2004).
64. Major, A.S., Fazio, S. & Linton, M.F. B-lymphocyte deficiency increases atherosclerosis in LDL receptor-null mice. *Arteriosclerosis, thrombosis, and vascular biology* **22**, 1892-1898 (2002).
65. Caligiuri, G., Nicoletti, A., Poirier, B. & Hansson, G.K. Protective immunity against atherosclerosis carried by B cells of hypercholesterolemic mice. *The Journal of clinical investigation* **109**, 745-753 (2002).
66. Zhou, X., Caligiuri, G., Hamsten, A., Lefvert, A.K. & Hansson, G.K. LDL immunization induces T-cell-dependent antibody formation and protection against atherosclerosis. *Arteriosclerosis, thrombosis, and vascular biology* **21**, 108-114 (2001).
67. Kyaw, T., *et al*. B1a B lymphocytes are atheroprotective by secreting natural IgM that increases IgM deposits and reduces necrotic cores in atherosclerotic lesions. *Circulation research* **109**, 830-840 (2011).
68. Vogel, L.A., Lester, T.L., Van Cleave, V.H. & Metzger, D.W. Inhibition of murine B1 lymphocytes by interleukin-12. *European journal of immunology* **26**, 219-223 (1996).
69. Perry, H.M. & McNamara, C.A. Refining the role of B cells in atherosclerosis. *Arteriosclerosis, thrombosis, and vascular biology* **32**, 1548-1549 (2012).
70. Ait-Oufella, H., *et al*. B cell depletion reduces the development of atherosclerosis in mice. *The Journal of experimental medicine* **207**, 1579-1587 (2010).
71. Kyaw, T., *et al*. Conventional B2 B cell depletion ameliorates whereas its adoptive transfer aggravates atherosclerosis. *J Immunol* **185**, 4410-4419 (2010).
72. Robertson, A.K. & Hansson, G.K. T cells in atherogenesis: for better or for worse? *Arteriosclerosis, thrombosis, and vascular biology* **26**, 2421-2432 (2006).
73. Schonbeck, U. & Libby, P. CD40 signaling and plaque instability. *Circulation research* **89**, 1092-1103 (2001).
74. Buono, C., *et al*. T-bet deficiency reduces atherosclerosis and alters plaque antigen-specific immune responses. *Proc Natl Acad Sci U S A* **102**, 1596-1601 (2005).
75. Metz, D.P., Farber, D.L., Taylor, T. & Bottomly, K. Differential role of CTLA-4 in regulation of resting memory versus naive CD4 T cell activation. *J Immunol* **161**, 5855-5861 (1998).
76. Qu, C., *et al*. Role of CCR8 and other chemokine pathways in the migration of monocyte-derived dendritic cells to lymph nodes. *The Journal of experimental medicine* **200**, 1231-1241 (2004).
77. Banchereau, J., *et al*. Immunobiology of dendritic cells. *Annual review of immunology* **18**, 767-811 (2000).
78. Maldonado-Lopez, R., *et al*. CD8alpha+ and CD8alpha- subclasses of dendritic cells direct the development of distinct T helper cells in vivo. *The Journal of experimental medicine* **189**, 587-592 (1999).

79. MacDonald, A.S. & Maizels, R.M. Alarming dendritic cells for Th2 induction. *The Journal of experimental medicine* **205**, 13-17 (2008).
80. Bobryshev, Y.V. Dendritic cells in atherosclerosis: current status of the problem and clinical relevance. *European heart journal* **26**, 1700-1704 (2005).
81. Llodra, J., *et al*. Emigration of monocyte-derived cells from atherosclerotic lesions characterizes regressive, but not progressive, plaques. *Proc Natl Acad Sci U S A* **101**, 11779-11784 (2004).
82. Zhou, X., Stemme, S. & Hansson, G.K. Evidence for a local immune response in atherosclerosis. CD4+ T cells infiltrate lesions of apolipoprotein-E-deficient mice. *Am J Pathol* **149**, 359-366 (1996).
83. Zhou, X., Robertson, A.K., Rudling, M., Parini, P. & Hansson, G.K. Lesion development and response to immunization reveal a complex role for CD4 in atherosclerosis. *Circulation research* **96**, 427-434 (2005).
84. Theodorou, G.L., *et al*. T helper 1 (Th1)/Th2 cytokine expression shift of peripheral blood CD4+ and CD8+ T cells in patients at the post-acute phase of stroke. *Clinical and experimental immunology* **152**, 456-463 (2008).
85. Gupta, S., *et al*. IFN-gamma potentiates atherosclerosis in ApoE knock-out mice. *The Journal of clinical investigation* **99**, 2752-2761 (1997).
86. Ait-Oufella, H., Taleb, S., Mallat, Z. & Tedgui, A. Recent advances on the role of cytokines in atherosclerosis. *Arteriosclerosis, thrombosis, and vascular biology* **31**, 969-979 (2011).
87. Davenport, P. & Tipping, P.G. The role of interleukin-4 and interleukin-12 in the progression of atherosclerosis in apolipoprotein E-deficient mice. *Am J Pathol* **163**, 1117-1125 (2003).
88. Daugherty, A. & Rateri, D.L. T lymphocytes in atherosclerosis: the yin-yang of Th1 and Th2 influence on lesion formation. *Circulation research* **90**, 1039-1040 (2002).
89. von der Thusen, J.H., Kuiper, J., van Berkel, T.J. & Biessen, E.A. Interleukins in atherosclerosis: molecular pathways and therapeutic potential. *Pharmacological reviews* **55**, 133-166 (2003).
90. Libby, P. Inflammation and cardiovascular disease mechanisms. *The American journal of clinical nutrition* **83**, 456S-460S (2006).
91. Libby, P., Egan, D. & Skarlatos, S. Roles of infectious agents in atherosclerosis and restenosis: an assessment of the evidence and need for future research. *Circulation* **96**, 4095-4103 (1997).
92. Wright, B.H., Corton, J.M., El-Nahas, A.M., Wood, R.F. & Pockley, A.G. Elevated levels of circulating heat shock protein 70 (Hsp70) in peripheral and renal vascular disease. *Heart and vessels* **15**, 18-22 (2000).
93. Peluso, I., Morabito, G., Urban, L., Ioannone, F. & Serafini, M. Oxidative stress in atherosclerosis development: the central role of LDL and oxidative burst. *Endocrine, metabolic & immune disorders drug targets* **12**, 351-360 (2012).
94. Kearney, J.F. Immune recognition of OxLDL in atherosclerosis. *The Journal of clinical investigation* **105**, 1683-1685 (2000).
95. Shi, W., *et al*. Determinants of atherosclerosis susceptibility in the C3H and C57BL/6 mouse model: evidence for involvement of endothelial cells but not

blood cells or cholesterol metabolism. *Circulation research* **86**, 1078-1084 (2000).
96. Lucas, A.D. & Greaves, D.R. Atherosclerosis: role of chemokines and macrophages. *Expert Rev Mol Med* **3**, 1-18 (2001).
97. McKellar, G.E., McCarey, D.W., Sattar, N. & McInnes, I.B. Role for TNF in atherosclerosis? Lessons from autoimmune disease. *Nature reviews. Cardiology* **6**, 410-417 (2009).
98. Netea, M.G. & Dinarello, C.A. More than inflammation: interleukin-1beta polymorphisms and the lipid metabolism. *J Clin Endocrinol Metab* **96**, 1279-1281 (2011).
99. Schieffer, B., *et al*. Impact of interleukin-6 on plaque development and morphology in experimental atherosclerosis. *Circulation* **110**, 3493-3500 (2004).
100. Wuttge, D.M., Eriksson, P., Sirsjo, A., Hansson, G.K. & Stemme, S. Expression of interleukin-15 in mouse and human atherosclerotic lesions. *Am J Pathol* **159**, 417-423 (2001).
101. Tenger, C., Sundborger, A., Jawien, J. & Zhou, X. IL-18 accelerates atherosclerosis accompanied by elevation of IFN-gamma and CXCL16 expression independently of T cells. *Arteriosclerosis, thrombosis, and vascular biology* **25**, 791-796 (2005).
102. Nold, M.F., *et al*. Endogenous IL-32 controls cytokine and HIV-1 production. *J Immunol* **181**, 557-565 (2008).
103. McCaffrey, T.A. TGF-betas and TGF-beta receptors in atherosclerosis. *Cytokine Growth Factor Rev* **11**, 103-114 (2000).
104. Gui, T., Shimokado, A., Sun, Y., Akasaka, T. & Muragaki, Y. Diverse roles of macrophages in atherosclerosis: from inflammatory biology to biomarker discovery. *Mediators of inflammation* **2012**, 693083 (2012).
105. Lawrence, T. The nuclear factor NF-kappaB pathway in inflammation. *Cold Spring Harbor perspectives in biology* **1**, a001651 (2009).
106. Virella, G., *et al*. Proatherogenic and proinflammatory properties of immune complexes prepared with purified human oxLDL antibodies and human oxLDL. *Clinical immunology* **105**, 81-92 (2002).
107. Daugherty, A., *et al*. The effects of total lymphocyte deficiency on the extent of atherosclerosis in apolipoprotein E-/- mice. *The Journal of clinical investigation* **100**, 1575-1580 (1997).
108. Mallat, Z., Taleb, S., Ait-Oufella, H. & Tedgui, A. The role of adaptive T cell immunity in atherosclerosis. *J Lipid Res* **50 Suppl**, S364-369 (2009).
109. Gotsman, I., Sharpe, A.H. & Lichtman, A.H. T-cell costimulation and coinhibition in atherosclerosis. *Circulation research* **103**, 1220-1231 (2008).
110. Szabo, S.J., Sullivan, B.M., Peng, S.L. & Glimcher, L.H. Molecular mechanisms regulating Th1 immune responses. *Annual review of immunology* **21**, 713-758 (2003).
111. Prasad, K.S., Andre, P., Yan, Y. & Phillips, D.R. The platelet CD40L/GP IIb-IIIa axis in atherothrombotic disease. *Curr Opin Hematol* **10**, 356-361 (2003).

112. Bacci, S., *et al*. Smooth muscle cells, dendritic cells and mast cells are sources of TNFalpha and nitric oxide in human carotid artery atherosclerosis. *Thrombosis research* **122**, 657-667 (2008).
113. Ito, T., *et al*. Stem cell factor programs the mast cell activation phenotype. *J Immunol* **188**, 5428-5437 (2012).
114. Ochi, H., *et al*. T helper cell type 2 cytokine-mediated comitogenic responses and CCR3 expression during differentiation of human mast cells in vitro. *The Journal of experimental medicine* **190**, 267-280 (1999).
115. Hu, Z.Q., Zhao, W.H. & Shimamura, T. Regulation of mast cell development by inflammatory factors. *Current medicinal chemistry* **14**, 3044-3050 (2007).
116. Kaartinen, M., Penttila, A. & Kovanen, P.T. Mast cells of two types differing in neutral protease composition in the human aortic intima. Demonstration of tryptase- and tryptase/chymase-containing mast cells in normal intimas, fatty streaks, and the shoulder region of atheromas. *Arteriosclerosis and thrombosis : a journal of vascular biology / American Heart Association* **14**, 966-972 (1994).
117. Galli, S.J. & Tsai, M. Mast cells in allergy and infection: versatile effector and regulatory cells in innate and adaptive immunity. *European journal of immunology* **40**, 1843-1851 (2010).
118. Sun, J., *et al*. Mast cells promote atherosclerosis by releasing proinflammatory cytokines. *Nature medicine* **13**, 719-724 (2007).
119. Lindstedt, K.A. & Kovanen, P.T. Mast cells in vulnerable coronary plaques: potential mechanisms linking mast cell activation to plaque erosion and rupture. *Curr Opin Lipidol* **15**, 567-573 (2004).
120. Lindstedt, K.A., Mayranpaa, M.I. & Kovanen, P.T. Mast cells in vulnerable atherosclerotic plaques--a view to a kill. *Journal of cellular and molecular medicine* **11**, 739-758 (2007).
121. Mierke, C.T., *et al*. Human endothelial cells regulate survival and proliferation of human mast cells. *The Journal of experimental medicine* **192**, 801-811 (2000).
122. Lappalainen, H., Laine, P., Pentikainen, M.O., Sajantila, A. & Kovanen, P.T. Mast cells in neovascularized human coronary plaques store and secrete basic fibroblast growth factor, a potent angiogenic mediator. *Arteriosclerosis, thrombosis, and vascular biology* **24**, 1880-1885 (2004).
123. Bot, I., *et al*. Perivascular mast cells promote atherogenesis and induce plaque destabilization in apolipoprotein E-deficient mice. *Circulation* **115**, 2516-2525 (2007).
124. Bischoff, S.C. Role of mast cells in allergic and non-allergic immune responses: comparison of human and murine data. *Nature reviews. Immunology* **7**, 93-104 (2007).
125. Dewberry, R., Holden, H., Crossman, D. & Francis, S. Interleukin-1 receptor antagonist expression in human endothelial cells and atherosclerosis. *Arteriosclerosis, thrombosis, and vascular biology* **20**, 2394-2400 (2000).
126. Mantovani, A., Bussolino, F. & Introna, M. Cytokine regulation of endothelial cell function: from molecular level to the bedside. *Immunology today* **18**, 231-240 (1997).

127. Weber, C., Schober, A. & Zernecke, A. Chemokines: key regulators of mononuclear cell recruitment in atherosclerotic vascular disease. *Arteriosclerosis, thrombosis, and vascular biology* **24**, 1997-2008 (2004).
128. Libby, P. Molecular bases of the acute coronary syndromes. *Circulation* **91**, 2844-2850 (1995).
129. Galis, Z.S., Sukhova, G.K., Lark, M.W. & Libby, P. Increased expression of matrix metalloproteinases and matrix degrading activity in vulnerable regions of human atherosclerotic plaques. *The Journal of clinical investigation* **94**, 2493-2503 (1994).
130. Galis, Z.S., Sukhova, G.K., Kranzhofer, R., Clark, S. & Libby, P. Macrophage foam cells from experimental atheroma constitutively produce matrix-degrading proteinases. *Proc Natl Acad Sci U S A* **92**, 402-406 (1995).
131. Moreno, P.R., *et al*. Macrophage infiltration in acute coronary syndromes. Implications for plaque rupture. *Circulation* **90**, 775-778 (1994).
132. Gough, P.J., Gomez, I.G., Wille, P.T. & Raines, E.W. Macrophage expression of active MMP-9 induces acute plaque disruption in apoE-deficient mice. *The Journal of clinical investigation* **116**, 59-69 (2006).
133. Wu, G., *et al*. Pravastatin inhibits plaque rupture and subsequent thrombus formation in atherosclerotic rabbits with hyperlipidemia. *Chemical & pharmaceutical bulletin* **61**, 121-124 (2013).
134. Denny, M.F., *et al*. Interferon-alpha promotes abnormal vasculogenesis in lupus: a potential pathway for premature atherosclerosis. *Blood* **110**, 2907-2915 (2007).
135. Inoue, T., *et al*. Vascular inflammation and repair: implications for re-endothelialization, restenosis, and stent thrombosis. *JACC. Cardiovascular interventions* **4**, 1057-1066 (2011).
136. Jeziorska, M., McCollum, C. & Wooley, D.E. Observations on bone formation and remodelling in advanced atherosclerotic lesions of human carotid arteries. *Virchows Archiv : an international journal of pathology* **433**, 559-565 (1998).
137. Alexopoulos, N. & Raggi, P. Calcification in atherosclerosis. *Nature reviews. Cardiology* **6**, 681-688 (2009).
138. Rajamannan, N.M., Bonow, R.O. & Rahimtoola, S.H. Calcific aortic stenosis: an update. *Nature clinical practice. Cardiovascular medicine* **4**, 254-262 (2007).
139. Neven, E. & D'Haese, P.C. Vascular calcification in chronic renal failure: what have we learned from animal studies? *Circulation research* **108**, 249-264 (2011).
140. Hunt, J.L., *et al*. Bone formation in carotid plaques: a clinicopathological study. *Stroke; a journal of cerebral circulation* **33**, 1214-1219 (2002).
141. Bunting, C.H. The Formation of True Bone with Cellular (Red) Marrow in a Sclerotic Aorta. *The Journal of experimental medicine* **8**, 365-376 (1906).
142. Soor, G.S., Vukin, I., Leong, S.W., Oreopoulos, G. & Butany, J. Peripheral vascular disease: who gets it and why? A histomorphological analysis of 261 arterial segments from 58 cases. *Pathology* **40**, 385-391 (2008).
143. Ewence, A.E., *et al*. Calcium phosphate crystals induce cell death in human vascular smooth muscle cells: a potential mechanism in atherosclerotic plaque destabilization. *Circulation research* **103**, e28-34 (2008).

144. Dallas, S.L. & Bonewald, L.F. Dynamics of the transition from osteoblast to osteocyte. *Annals of the New York Academy of Sciences* **1192**, 437-443 (2010).
145. Demer, L.L. A skeleton in the atherosclerosis closet. *Circulation* **92**, 2029-2032 (1995).
146. Bostrom, K., *et al*. Bone morphogenetic protein expression in human atherosclerotic lesions. *The Journal of clinical investigation* **91**, 1800-1809 (1993).
147. Johnson, R.C., Leopold, J.A. & Loscalzo, J. Vascular calcification: pathobiological mechanisms and clinical implications. *Circulation research* **99**, 1044-1059 (2006).
148. Nakagawa, Y., *et al*. Paracrine osteogenic signals via bone morphogenetic protein-2 accelerate the atherosclerotic intimal calcification in vivo. *Arteriosclerosis, thrombosis, and vascular biology* **30**, 1908-1915 (2010).
149. Ting, T.C., *et al*. Increased lipogenesis and stearate accelerate vascular calcification in calcifying vascular cells. *The Journal of biological chemistry* **286**, 23938-23949 (2011).
150. Watson, K.E., *et al*. TGF-beta 1 and 25-hydroxycholesterol stimulate osteoblast-like vascular cells to calcify. *The Journal of clinical investigation* **93**, 2106-2113 (1994).
151. Bautch, V.L. Stem cells and the vasculature. *Nature medicine* **17**, 1437-1443 (2011).
152. Martinez-Agosto, J.A., Mikkola, H.K., Hartenstein, V. & Banerjee, U. The hematopoietic stem cell and its niche: a comparative view. *Genes & development* **21**, 3044-3060 (2007).
153. Simons, D.B., *et al*. Noninvasive definition of anatomic coronary artery disease by ultrafast computed tomographic scanning: a quantitative pathologic comparison study. *Journal of the American College of Cardiology* **20**, 1118-1126 (1992).
154. Doherty, T.M., *et al*. Calcification in atherosclerosis: bone biology and chronic inflammation at the arterial crossroads. *Proc Natl Acad Sci U S A* **100**, 11201-11206 (2003).
155. Fitzpatrick, L.A., Severson, A., Edwards, W.D. & Ingram, R.T. Diffuse calcification in human coronary arteries. Association of osteopontin with atherosclerosis. *The Journal of clinical investigation* **94**, 1597-1604 (1994).
156. Shanahan, C.M., Cary, N.R., Metcalfe, J.C. & Weissberg, P.L. High expression of genes for calcification-regulating proteins in human atherosclerotic plaques. *The Journal of clinical investigation* **93**, 2393-2402 (1994).
157. Ikeda, T., Shirasawa, T., Esaki, Y., Yoshiki, S. & Hirokawa, K. Osteopontin mRNA is expressed by smooth muscle-derived foam cells in human atherosclerotic lesions of the aorta. *The Journal of clinical investigation* **92**, 2814-2820 (1993).
158. Giachelli, C.M., *et al*. Osteopontin is elevated during neointima formation in rat arteries and is a novel component of human atherosclerotic plaques. *The Journal of clinical investigation* **92**, 1686-1696 (1993).

159. Trion, A. & van der Laarse, A. Vascular smooth muscle cells and calcification in atherosclerosis. *Am Heart J* **147**, 808-814 (2004).
160. Bentzon, J.F., Sondergaard, C.S., Kassem, M. & Falk, E. Smooth muscle cells healing atherosclerotic plaque disruptions are of local, not blood, origin in apolipoprotein E knockout mice. *Circulation* **116**, 2053-2061 (2007).
161. Cappendijk, V.C., *et al*. Assessment of human atherosclerotic carotid plaque components with multisequence MR imaging: initial experience. *Radiology* **234**, 487-492 (2005).
162. Kataoka, T., *et al*. Association of plaque composition and vessel remodeling in atherosclerotic renal artery stenosis: a comparison with coronary artery disease. *JACC*. *Cardiovascular imaging* **2**, 327-338 (2009).
163. Schwartz, S.M., Virmani, R. & Rosenfeld, M.E. The good smooth muscle cells in atherosclerosis. *Curr Atheroscler Rep* **2**, 422-429 (2000).
164. Mann, J. & Davies, M.J. Mechanisms of progression in native coronary artery disease: role of healed plaque disruption. *Heart* **82**, 265-268 (1999).
165. Burke, A.P., *et al*. Healed plaque ruptures and sudden coronary death: evidence that subclinical rupture has a role in plaque progression. *Circulation* **103**, 934-940 (2001).
166. Hu, Y., *et al*. Abundant progenitor cells in the adventitia contribute to atherosclerosis of vein grafts in ApoE-deficient mice. *The Journal of clinical investigation* **113**, 1258-1265 (2004).
167. Zoll, J., *et al*. Role of human smooth muscle cell progenitors in atherosclerotic plaque development and composition. *Cardiovasc Res* **77**, 471-480 (2008).
168. Hao, H., *et al*. Phenotypic modulation of intima and media smooth muscle cells in fatal cases of coronary artery lesion. *Arteriosclerosis, thrombosis, and vascular biology* **26**, 326-332 (2006).
169. Owens, G.K., Kumar, M.S. & Wamhoff, B.R. Molecular regulation of vascular smooth muscle cell differentiation in development and disease. *Physiological reviews* **84**, 767-801 (2004).
170. Rensen, S.S., Doevendans, P.A. & van Eys, G.J. Regulation and characteristics of vascular smooth muscle cell phenotypic diversity. *Netherlands heart journal : monthly journal of the Netherlands Society of Cardiology and the Netherlands Heart Foundation* **15**, 100-108 (2007).
171. Tanaka, K., *et al*. Circulating progenitor cells contribute to neointimal formation in nonirradiated chimeric mice. *FASEB J* **22**, 428-436 (2008).
172. Frid, M.G., Moiseeva, E.P. & Stenmark, K.R. Multiple phenotypically distinct smooth muscle cell populations exist in the adult and developing bovine pulmonary arterial media in vivo. *Circulation research* **75**, 669-681 (1994).
173. Torsney, E., Mandal, K., Halliday, A., Jahangiri, M. & Xu, Q. Characterisation of progenitor cells in human atherosclerotic vessels. *Atherosclerosis* **191**, 259-264 (2007).
174. Saiura, A., Sata, M., Hirata, Y., Nagai, R. & Makuuchi, M. Circulating smooth muscle progenitor cells contribute to atherosclerosis. *Nature medicine* **7**, 382-383 (2001).

175. Caplice, N.M., *et al*. Smooth muscle cells in human coronary atherosclerosis can originate from cells administered at marrow transplantation. *Proc Natl Acad Sci U S A* **100**, 4754-4759 (2003).
176. Matthews, C., *et al*. Vascular smooth muscle cells undergo telomere-based senescence in human atherosclerosis: effects of telomerase and oxidative stress. *Circulation research* **99**, 156-164 (2006).
177. Minamino, T. & Komuro, I. Vascular aging: insights from studies on cellular senescence, stem cell aging, and progeroid syndromes. *Nature clinical practice. Cardiovascular medicine* **5**, 637-648 (2008).
178. Klein, D., *et al*. Vascular wall-resident CD44+ multipotent stem cells give rise to pericytes and smooth muscle cells and contribute to new vessel maturation. *PLoS One* **6**, e20540 (2011).
179. da Silva Meirelles, L., Chagastelles, P.C. & Nardi, N.B. Mesenchymal stem cells reside in virtually all post-natal organs and tissues. *J Cell Sci* **119**, 2204-2213 (2006).
180. Sugiyama, S., *et al*. Characterization of smooth muscle-like cells in circulating human peripheral blood. *Atherosclerosis* **187**, 351-362 (2006).
181. Hillebrands, J.L., Klatter, F.A. & Rozing, J. Origin of vascular smooth muscle cells and the role of circulating stem cells in transplant arteriosclerosis. *Arteriosclerosis, thrombosis, and vascular biology* **23**, 380-387 (2003).
182. Hu, Y., *et al*. Smooth muscle cells in transplant atherosclerotic lesions are originated from recipients, but not bone marrow progenitor cells. *Circulation* **106**, 1834-1839 (2002).
183. Daniel, J.M., *et al*. Time-course analysis on the differentiation of bone marrow-derived progenitor cells into smooth muscle cells during neointima formation. *Arteriosclerosis, thrombosis, and vascular biology* **30**, 1890-1896 (2010).
184. Urbich, C. & Dimmeler, S. Endothelial progenitor cells: characterization and role in vascular biology. *Circulation research* **95**, 343-353 (2004).
185. Rossig, L., Dimmeler, S. & Zeiher, A.M. Apoptosis in the vascular wall and atherosclerosis. *Basic Res Cardiol* **96**, 11-22 (2001).
186. Zampetaki, A., Kirton, J.P. & Xu, Q. Vascular repair by endothelial progenitor cells. *Cardiovasc Res* **78**, 413-421 (2008).
187. Kalka, C., *et al*. Transplantation of ex vivo expanded endothelial progenitor cells for therapeutic neovascularization. *Proc Natl Acad Sci U S A* **97**, 3422-3427 (2000).
188. Takahashi, T., *et al*. Ischemia- and cytokine-induced mobilization of bone marrow-derived endothelial progenitor cells for neovascularization. *Nature medicine* **5**, 434-438 (1999).
189. Urbich, C., *et al*. Relevance of monocytic features for neovascularization capacity of circulating endothelial progenitor cells. *Circulation* **108**, 2511-2516 (2003).
190. Kawamoto, A., *et al*. Therapeutic potential of ex vivo expanded endothelial progenitor cells for myocardial ischemia. *Circulation* **103**, 634-637 (2001).
191. Britten, M.B., *et al*. Infarct remodeling after intracoronary progenitor cell treatment in patients with acute myocardial infarction (TOPCARE-AMI):

mechanistic insights from serial contrast-enhanced magnetic resonance imaging. *Circulation* **108**, 2212-2218 (2003).
192. Schachinger, V., *et al*. Transplantation of progenitor cells and regeneration enhancement in acute myocardial infarction: final one-year results of the TOPCARE-AMI Trial. *Journal of the American College of Cardiology* **44**, 1690-1699 (2004).
193. Yoder, M.C., *et al*. Redefining endothelial progenitor cells via clonal analysis and hematopoietic stem/progenitor cell principals. *Blood* **109**, 1801-1809 (2007).
194. Timmermans, F., *et al*. Endothelial outgrowth cells are not derived from CD133+ cells or CD45+ hematopoietic precursors. *Arteriosclerosis, thrombosis, and vascular biology* **27**, 1572-1579 (2007).
195. Gulati, R., *et al*. Diverse origin and function of cells with endothelial phenotype obtained from adult human blood. *Circulation research* **93**, 1023-1025 (2003).
196. Hu, Y., Davison, F., Zhang, Z. & Xu, Q. Endothelial replacement and angiogenesis in arteriosclerotic lesions of allografts are contributed by circulating progenitor cells. *Circulation* **108**, 3122-3127 (2003).
197. Wassmann, S., Werner, N., Czech, T. & Nickenig, G. Improvement of endothelial function by systemic transfusion of vascular progenitor cells. *Circulation research* **99**, e74-83 (2006).
198. Rauscher, F.M., *et al*. Aging, progenitor cell exhaustion, and atherosclerosis. *Circulation* **108**, 457-463 (2003).
199. Werner, N., *et al*. Intravenous transfusion of endothelial progenitor cells reduces neointima formation after vascular injury. *Circulation research* **93**, e17-24 (2003).
200. Kong, D., *et al*. Cytokine-induced mobilization of circulating endothelial progenitor cells enhances repair of injured arteries. *Circulation* **110**, 2039-2046 (2004).
201. Griese, D.P., *et al*. Isolation and transplantation of autologous circulating endothelial cells into denuded vessels and prosthetic grafts: implications for cell-based vascular therapy. *Circulation* **108**, 2710-2715 (2003).
202. Silvestre, J.S., *et al*. Transplantation of bone marrow-derived mononuclear cells in ischemic apolipoprotein E-knockout mice accelerates atherosclerosis without altering plaque composition. *Circulation* **108**, 2839-2842 (2003).
203. Inoue, T., *et al*. Mobilization of CD34-positive bone marrow-derived cells after coronary stent implantation: impact on restenosis. *Circulation* **115**, 553-561 (2007).
204. Seeger, F.H., Tonn, T., Krzossok, N., Zeiher, A.M. & Dimmeler, S. Cell isolation procedures matter: a comparison of different isolation protocols of bone marrow mononuclear cells used for cell therapy in patients with acute myocardial infarction. *European heart journal* **28**, 766-772 (2007).
205. Moulton, K.S., *et al*. Angiogenesis inhibitors endostatin or TNP-470 reduce intimal neovascularization and plaque growth in apolipoprotein E-deficient mice. *Circulation* **99**, 1726-1732 (1999).

206. Kahlon, R., Shapero, J. & Gotlieb, A.I. Angiogenesis in atherosclerosis. *The Canadian journal of cardiology* **8**, 60-64 (1992).
207. Ross, J.S., Stagliano, N.E., Donovan, M.J., Breitbart, R.E. & Ginsburg, G.S. Atherosclerosis and cancer: common molecular pathways of disease development and progression. *Annals of the New York Academy of Sciences* **947**, 271-292; discussion 292-273 (2001).
208. Feng, Y., *et al*. Hematopoietic stem/progenitor cell proliferation and differentiation is differentially regulated by high-density and low-density lipoproteins in mice. *PLoS One* **7**, e47286 (2012).
209. Binder, C.J., *et al*. Innate and acquired immunity in atherogenesis. *Nature medicine* **8**, 1218-1226 (2002).
210. Diez-Juan, A., *et al*. Selective inactivation of p27(Kip1) in hematopoietic progenitor cells increases neointimal macrophage proliferation and accelerates atherosclerosis. *Blood* **103**, 158-161 (2004).
211. Xu, Q. Stem cells and transplant arteriosclerosis. *Circulation research* **102**, 1011-1024 (2008).
212. Anversa, P., *et al*. Concise review: stem cells, myocardial regeneration, and methodological artifacts. *Stem Cells* **25**, 589-601 (2007).
213. Xu, Q. The impact of progenitor cells in atherosclerosis. *Nature clinical practice. Cardiovascular medicine* **3**, 94-101 (2006).
214. Urbich, C. & Dimmeler, S. Endothelial progenitor cells functional characterization. *Trends Cardiovasc Med* **14**, 318-322 (2004).
215. Torsney, E., Hu, Y. & Xu, Q. Adventitial progenitor cells contribute to arteriosclerosis. *Trends Cardiovasc Med* **15**, 64-68 (2005).
216. Abedin, M., Tintut, Y. & Demer, L.L. Mesenchymal stem cells and the artery wall. *Circulation research* **95**, 671-676 (2004).
217. Tintut, Y., *et al*. Multilineage potential of cells from the artery wall. *Circulation* **108**, 2505-2510 (2003).
218. Liao, J., *et al*. Transfer of bone-marrow-derived mesenchymal stem cells influences vascular remodeling and calcification after balloon injury in hyperlipidemic rats. *J Biomed Biotechnol* **2012**, 165296 (2012).
219. Hruska, K.A., Mathew, S. & Saab, G. Bone morphogenetic proteins in vascular calcification. *Circulation research* **97**, 105-114 (2005).
220. Ketteler, M., Schlieper, G. & Floege, J. Calcification and cardiovascular health: new insights into an old phenomenon. *Hypertension* **47**, 1027-1034 (2006).
221. George, J., *et al*. Transfer of endothelial progenitor and bone marrow cells influences atherosclerotic plaque size and composition in apolipoprotein E knockout mice. *Arteriosclerosis, thrombosis, and vascular biology* **25**, 2636-2641 (2005).
222. Dore-Duffy, P. & Cleary, K. Morphology and properties of pericytes. *Methods in molecular biology* **686**, 49-68 (2011).
223. Shepro, D. & Morel, N.M. Pericyte physiology. *FASEB J* **7**, 1031-1038 (1993).
224. Hirschi, K.K. & D'Amore, P.A. Pericytes in the microvasculature. *Cardiovasc Res* **32**, 687-698 (1996).

225. Proebstl, D., *et al*. Pericytes support neutrophil subendothelial cell crawling and breaching of venular walls in vivo. *The Journal of experimental medicine* **209**, 1219-1234 (2012).
226. Voisin, M.B., Probstl, D. & Nourshargh, S. Venular basement membranes ubiquitously express matrix protein low-expression regions: characterization in multiple tissues and remodeling during inflammation. *Am J Pathol* **176**, 482-495 (2010).
227. Armulik, A., Abramsson, A. & Betsholtz, C. Endothelial/pericyte interactions. *Circulation research* **97**, 512-523 (2005).
228. Edelman, D.A., Jiang, Y., Tyburski, J., Wilson, R.F. & Steffes, C. Pericytes and their role in microvasculature homeostasis. *J Surg Res* **135**, 305-311 (2006).
229. Cohen, M.P., Frank, R.N. & Khalifa, A.A. Collagen production by cultured retinal capillary pericytes. *Invest Ophthalmol Vis Sci* **19**, 90-94 (1980).
230. Mandarino, L.J., Sundarraj, N., Finlayson, J. & Hassell, H.R. Regulation of fibronectin and laminin synthesis by retinal capillary endothelial cells and pericytes in vitro. *Experimental eye research* **57**, 609-621 (1993).
231. Balabanov, R. & Dore-Duffy, P. Role of the CNS microvascular pericyte in the blood-brain barrier. *J Neurosci Res* **53**, 637-644 (1998).
232. Bonkowski, D., Katyshev, V., Balabanov, R.D., Borisov, A. & Dore-Duffy, P. The CNS microvascular pericyte: pericyte-astrocyte crosstalk in the regulation of tissue survival. *Fluids and barriers of the CNS* **8**, 8 (2011).
233. Oshitari, T., *et al*. Effect of combined antisense oligonucleotides against high-glucose- and diabetes-induced overexpression of extracellular matrix components and increased vascular permeability. *Diabetes* **55**, 86-92 (2006).
234. Dosso, A.A., Leuenberger, P.M. & Rungger-Brandle, E. Remodeling of retinal capillaries in the diabetic hypertensive rat. *Invest Ophthalmol Vis Sci* **40**, 2405-2410 (1999).
235. Behl, Y., Krothapalli, P., Desta, T., Roy, S. & Graves, D.T. FOXO1 plays an important role in enhanced microvascular cell apoptosis and microvascular cell loss in type 1 and type 2 diabetic rats. *Diabetes* **58**, 917-925 (2009).
236. Makita, J., Hosoya, K., Zhang, P. & Kador, P.F. Response of rat retinal capillary pericytes and endothelial cells to glucose. *Journal of ocular pharmacology and therapeutics : the official journal of the Association for Ocular Pharmacology and Therapeutics* **27**, 7-15 (2011).
237. Hammes, H.P., *et al*. Pericytes and the pathogenesis of diabetic retinopathy. *Diabetes* **51**, 3107-3112 (2002).
238. Bergers, G. & Song, S. The role of pericytes in blood-vessel formation and maintenance. *Neuro-oncology* **7**, 452-464 (2005).
239. Schor, A.M., Allen, T.D., Canfield, A.E., Sloan, P. & Schor, S.L. Pericytes derived from the retinal microvasculature undergo calcification in vitro. *J Cell Sci* **97 (Pt 3)**, 449-461 (1990).
240. Kida, Y. & Duffield, J.S. Pivotal role of pericytes in kidney fibrosis. *Clinical and experimental pharmacology & physiology* **38**, 467-473 (2011).
241. Sato, M., Suzuki, S. & Senoo, H. Hepatic stellate cells: unique characteristics in cell biology and phenotype. *Cell structure and function* **28**, 105-112 (2003).

242. Knittel, T., *et al*. Expression and regulation of cell adhesion molecules by hepatic stellate cells (HSC) of rat liver: involvement of HSC in recruitment of inflammatory cells during hepatic tissue repair. *Am J Pathol* **154**, 153-167 (1999).
243. Sims, D.E. Diversity within pericytes. *Clinical and experimental pharmacology & physiology* **27**, 842-846 (2000).
244. Decker, B., Bartels, H. & Decker, S. Relationships between endothelial cells, pericytes, and osteoblasts during bone formation in the sheep femur following implantation of tricalciumphosphate-ceramic. *The Anatomical record* **242**, 310-320 (1995).
245. Collett, G.D. & Canfield, A.E. Angiogenesis and pericytes in the initiation of ectopic calcification. *Circulation research* **96**, 930-938 (2005).
246. Canfield, A.E., Sutton, A.B., Hoyland, J.A. & Schor, A.M. Association of thrombospondin-1 with osteogenic differentiation of retinal pericytes in vitro. *J Cell Sci* **109 (Pt 2)**, 343-353 (1996).
247. Hall, A.P. Review of the pericyte during angiogenesis and its role in cancer and diabetic retinopathy. *Toxicol Pathol* **34**, 763-775 (2006).
248. Farrington-Rock, C., *et al*. Chondrogenic and adipogenic potential of microvascular pericytes. *Circulation* **110**, 2226-2232 (2004).
249. Canfield, A.E., Allen, T.D., Grant, M.E., Schor, S.L. & Schor, A.M. Modulation of extracellular matrix biosynthesis by bovine retinal pericytes in vitro: effects of the substratum and cell density. *J Cell Sci* **96 (Pt 1)**, 159-169 (1990).
250. Thanabalasundaram, G., El-Gindi, J., Lischper, M. & Galla, H.J. Methods to assess pericyte-endothelial cell interactions in a coculture model. *Methods in molecular biology* **686**, 379-399 (2011).
251. Thanabalasundaram, G., Schneidewind, J., Pieper, C. & Galla, H.J. The impact of pericytes on the blood-brain barrier integrity depends critically on the pericyte differentiation stage. *The international journal of biochemistry & cell biology* **43**, 1284-1293 (2011).
252. Allt, G. & Lawrenson, J.G. Pericytes: cell biology and pathology. *Cells Tissues Organs* **169**, 1-11 (2001).
253. Betsholtz, C. Insight into the physiological functions of PDGF through genetic studies in mice. *Cytokine Growth Factor Rev* **15**, 215-228 (2004).
254. Hungerford, J.E. & Little, C.D. Developmental biology of the vascular smooth muscle cell: building a multilayered vessel wall. *J Vasc Res* **36**, 2-27 (1999).
255. Etchevers, H.C., Couly, G. & Le Douarin, N.M. Morphogenesis of the branchial vascular sector. *Trends Cardiovasc Med* **12**, 299-304 (2002).
256. Etchevers, H.C., Vincent, C., Le Douarin, N.M. & Couly, G.F. The cephalic neural crest provides pericytes and smooth muscle cells to all blood vessels of the face and forebrain. *Development* **128**, 1059-1068 (2001).
257. Carmeliet, P. Manipulating angiogenesis in medicine. *Journal of internal medicine* **255**, 538-561 (2004).
258. Gittenberger-de Groot, A.C., DeRuiter, M.C., Bergwerff, M. & Poelmann, R.E. Smooth muscle cell origin and its relation to heterogeneity in development and

disease. *Arteriosclerosis, thrombosis, and vascular biology* **19**, 1589-1594 (1999).
259. Vrancken Peeters, M.P., Gittenberger-de Groot, A.C., Mentink, M.M. & Poelmann, R.E. Smooth muscle cells and fibroblasts of the coronary arteries derive from epithelial-mesenchymal transformation of the epicardium. *Anatomy and embryology* **199**, 367-378 (1999).
260. Lamagna, C. & Bergers, G. The bone marrow constitutes a reservoir of pericyte progenitors. *J Leukoc Biol* **80**, 677-681 (2006).
261. Creazzo, T.L., Godt, R.E., Leatherbury, L., Conway, S.J. & Kirby, M.L. Role of cardiac neural crest cells in cardiovascular development. *Annual review of physiology* **60**, 267-286 (1998).
262. Rajantie, I., *et al*. Adult bone marrow-derived cells recruited during angiogenesis comprise precursors for periendothelial vascular mural cells. *Blood* **104**, 2084-2086 (2004).
263. DeRuiter, M.C., *et al*. Embryonic endothelial cells transdifferentiate into mesenchymal cells expressing smooth muscle actins in vivo and in vitro. *Circulation research* **80**, 444-451 (1997).
264. Alexander, M.Y., *et al*. Identification and characterization of vascular calcification-associated factor, a novel gene upregulated during vascular calcification in vitro and in vivo. *Arteriosclerosis, thrombosis, and vascular biology* **25**, 1851-1857 (2005).
265. Song, S., Ewald, A.J., Stallcup, W., Werb, Z. & Bergers, G. PDGFRbeta+ perivascular progenitor cells in tumours regulate pericyte differentiation and vascular survival. *Nat Cell Biol* **7**, 870-879 (2005).
266. Morikawa, S., *et al*. Abnormalities in pericytes on blood vessels and endothelial sprouts in tumors. *Am J Pathol* **160**, 985-1000 (2002).
267. Ozerdem, U., Monosov, E. & Stallcup, W.B. NG2 proteoglycan expression by pericytes in pathological microvasculature. *Microvasc Res* **63**, 129-134 (2002).
268. Winkler, E.A., Bell, R.D. & Zlokovic, B.V. Pericyte-specific expression of PDGF beta receptor in mouse models with normal and deficient PDGF beta receptor signaling. *Molecular neurodegeneration* **5**, 32 (2010).
269. Ozerdem, U. & Stallcup, W.B. Early contribution of pericytes to angiogenic sprouting and tube formation. *Angiogenesis* **6**, 241-249 (2003).
270. Gerhardt, H. & Betsholtz, C. Endothelial-pericyte interactions in angiogenesis. *Cell Tissue Res* **314**, 15-23 (2003).
271. Juchem, G., *et al*. Pericytes in the macrovascular intima: possible physiological and pathogenetic impact. *American journal of physiology*. *Heart and circulatory physiology* **298**, H754-770 (2010).
272. Nayak, R.C., Berman, A.B., George, K.L., Eisenbarth, G.S. & King, G.L. A monoclonal antibody (3G5)-defined ganglioside antigen is expressed on the cell surface of microvascular pericytes. *The Journal of experimental medicine* **167**, 1003-1015 (1988).
273. Harris, J.D., *et al*. Inhibition of atherosclerosis in apolipoprotein-E-deficient mice following muscle transduction with adeno-associated virus vectors encoding human apolipoprotein-E. *Gene Ther* **9**, 21-29 (2002).

274. Hartley, C.J., *et al*. Hemodynamic changes in apolipoprotein E-knockout mice. *Am J Physiol Heart Circ Physiol* **279**, H2326-2334 (2000).
275. Piedrahita, J.A., Zhang, S.H., Hagaman, J.R., Oliver, P.M. & Maeda, N. Generation of mice carrying a mutant apolipoprotein E gene inactivated by gene targeting in embryonic stem cells. *Proc Natl Acad Sci U S A* **89**, 4471-4475 (1992).
276. Qiao, J.H., Mertens, R.B., Fishbein, M.C. & Geller, S.A. Cartilaginous metaplasia in calcified diabetic peripheral vascular disease: morphologic evidence of enchondral ossification. *Human pathology* **34**, 402-407 (2003).
277. Bobryshev, Y.V. Transdifferentiation of smooth muscle cells into chondrocytes in atherosclerotic arteries in situ: implications for diffuse intimal calcification. *J Pathol* **205**, 641-650 (2005).
278. Rattazzi, M., *et al*. Calcification of advanced atherosclerotic lesions in the innominate arteries of ApoE-deficient mice: potential role of chondrocyte-like cells. *Arterioscler Thromb Vasc Biol* **25**, 1420-1425 (2005).
279. Greenow, K., Pearce, N.J. & Ramji, D.P. The key role of apolipoprotein E in atherosclerosis. *J Mol Med* **83**, 329-342 (2005).
280. Signori, E., *et al*. ApoE gene delivery inhibits severe hypercholesterolemia in newborn ApoE-KO mice. *Biochem Biophys Res Commun* **361**, 543-548 (2007).
281. Jongstra-Bilen, J., *et al*. Low-grade chronic inflammation in regions of the normal mouse arterial intima predisposed to atherosclerosis. *The Journal of experimental medicine* **203**, 2073-2083 (2006).
282. Wagenseil, J.E. & Mecham, R.P. Vascular extracellular matrix and arterial mechanics. *Physiological reviews* **89**, 957-989 (2009).
283. Stary, H.C., *et al*. A definition of the intima of human arteries and of its atherosclerosis-prone regions. A report from the Committee on Vascular Lesions of the Council on Arteriosclerosis, American Heart Association. *Arteriosclerosis and thrombosis : a journal of vascular biology / American Heart Association* **12**, 120-134 (1992).
284. Fazio, S., Lee, Y.L., Ji, Z.S. & Rall, S.C., Jr. Type III hyperlipoproteinemic phenotype in transgenic mice expressing dysfunctional apolipoprotein E. *The Journal of clinical investigation* **92**, 1497-1503 (1993).
285. van den Maagdenberg, A.M., *et al*. Transgenic mice carrying the apolipoprotein E3-Leiden gene exhibit hyperlipoproteinemia. *The Journal of biological chemistry* **268**, 10540-10545 (1993).
286. Fazio, S., *et al*. Susceptibility to diet-induced atherosclerosis in transgenic mice expressing a dysfunctional human apolipoprotein E(Arg 112,Cys142). *Arteriosclerosis and thrombosis : a journal of vascular biology / American Heart Association* **14**, 1873-1879 (1994).
287. Leppanen, P., Luoma, J.S., Hofker, M.H., Havekes, L.M. & Yla-Herttuala, S. Characterization of atherosclerotic lesions in apo E3-leiden transgenic mice. *Atherosclerosis* **136**, 147-152 (1998).
288. Linton, M.F., *et al*. Transgenic mice expressing high plasma concentrations of human apolipoprotein B100 and lipoprotein(a). *The Journal of clinical investigation* **92**, 3029-3037 (1993).

289. Voyiaziakis, E., *et al*. ApoA-I deficiency causes both hypertriglyceridemia and increased atherosclerosis in human apoB transgenic mice. *J Lipid Res* **39**, 313-321 (1998).
290. Purcell-Huynh, D.A., *et al*. Transgenic mice expressing high levels of human apolipoprotein B develop severe atherosclerotic lesions in response to a high-fat diet. *The Journal of clinical investigation* **95**, 2246-2257 (1995).
291. Stewart-Phillips, J.L. & Lough, J. Pathology of atherosclerosis in cholesterol-fed, susceptible mice. *Atherosclerosis* **90**, 211-218 (1991).
292. Paigen, B., Holmes, P.A., Mitchell, D. & Albee, D. Comparison of atherosclerotic lesions and HDL-lipid levels in male, female, and testosterone-treated female mice from strains C57BL/6, BALB/c, and C3H. *Atherosclerosis* **64**, 215-221 (1987).
293. Ishibashi, S., *et al*. Hypercholesterolemia in low density lipoprotein receptor knockout mice and its reversal by adenovirus-mediated gene delivery. *The Journal of clinical investigation* **92**, 883-893 (1993).
294. Ishibashi, S., Herz, J., Maeda, N., Goldstein, J.L. & Brown, M.S. The two-receptor model of lipoprotein clearance: tests of the hypothesis in "knockout" mice lacking the low density lipoprotein receptor, apolipoprotein E, or both proteins. *Proc Natl Acad Sci U S A* **91**, 4431-4435 (1994).
295. Ma, Y., *et al*. Hyperlipidemia and atherosclerotic lesion development in Ldlr-deficient mice on a long-term high-fat diet. *PLoS One* **7**, e35835 (2012).
296. Roselaar, S.E., Kakkanathu, P.X. & Daugherty, A. Lymphocyte populations in atherosclerotic lesions of apoE -/- and LDL receptor -/- mice. Decreasing density with disease progression. *Arteriosclerosis, thrombosis, and vascular biology* **16**, 1013-1018 (1996).
297. Bonthu, S., Heistad, D.D., Chappell, D.A., Lamping, K.G. & Faraci, F.M. Atherosclerosis, vascular remodeling, and impairment of endothelium-dependent relaxation in genetically altered hyperlipidemic mice. *Arteriosclerosis, thrombosis, and vascular biology* **17**, 2333-2340 (1997).
298. Witting, P.K., *et al*. Inhibition by a coantioxidant of aortic lipoprotein lipid peroxidation and atherosclerosis in apolipoprotein E and low density lipoprotein receptor gene double knockout mice. *FASEB J* **13**, 667-675 (1999).
299. Kuhlencordt, P.J., *et al*. Accelerated atherosclerosis, aortic aneurysm formation, and ischemic heart disease in apolipoprotein E/endothelial nitric oxide synthase double-knockout mice. *Circulation* **104**, 448-454 (2001).
300. Sanan, D.A., *et al*. Low density lipoprotein receptor-negative mice expressing human apolipoprotein B-100 develop complex atherosclerotic lesions on a chow diet: no accentuation by apolipoprotein(a). *Proc Natl Acad Sci U S A* **95**, 4544-4549 (1998).
301. Veniant, M.M., Withycombe, S. & Young, S.G. Lipoprotein size and atherosclerosis susceptibility in Apoe(-/-) and Ldlr(-/-) mice. *Arteriosclerosis, thrombosis, and vascular biology* **21**, 1567-1570 (2001).
302. Plump, A.S., Scott, C.J. & Breslow, J.L. Human apolipoprotein A-I gene expression increases high density lipoprotein and suppresses atherosclerosis in

the apolipoprotein E-deficient mouse. *Proc Natl Acad Sci U S A* **91**, 9607-9611 (1994).
303. Paszty, C., Maeda, N., Verstuyft, J. & Rubin, E.M. Apolipoprotein AI transgene corrects apolipoprotein E deficiency-induced atherosclerosis in mice. *The Journal of clinical investigation* **94**, 899-903 (1994).
304. Bocan, T.M., *et al*. The relationship between the degree of dietary-induced hypercholesterolemia in the rabbit and atherosclerotic lesion formation. *Atherosclerosis* **102**, 9-22 (1993).
305. Yanni, A.E. The laboratory rabbit: an animal model of atherosclerosis research. *Laboratory animals* **38**, 246-256 (2004).
306. Phinikaridou, A., Hallock, K.J., Qiao, Y. & Hamilton, J.A. A robust rabbit model of human atherosclerosis and atherothrombosis. *J Lipid Res* **50**, 787-797 (2009).
307. Brousseau, M.E. & Hoeg, J.M. Transgenic rabbits as models for atherosclerosis research. *J Lipid Res* **40**, 365-375 (1999).
308. Cos, E., *et al*. Soluble fiber and soybean protein reduce atherosclerotic lesions in guinea pigs. Sex and hormonal status determine lesion extension. *Lipids* **36**, 1209-1216 (2001).
309. Fernandez, M.L. & McNamar, D.J. Dietary fat-mediated changes in hepatic apoprotein B/E receptor in the guinea pig: effect of polyunsaturated, monounsaturated, and saturated fat. *Metabolism: clinical and experimental* **38**, 1094-1102 (1989).
310. Nistor, A., Bulla, A., Filip, D.A. & Radu, A. The hyperlipidemic hamster as a model of experimental atherosclerosis. *Atherosclerosis* **68**, 159-173 (1987).
311. Sima, A., Bulla, A. & Simionescu, N. Experimental obstructive coronary atherosclerosis in the hyperlipidemic hamster. *J Submicrosc Cytol Pathol* **22**, 1-16 (1990).
312. Chung, C. & Burdick, J.A. Influence of three-dimensional hyaluronic acid microenvironments on mesenchymal stem cell chondrogenesis. *Tissue Eng Part A* **15**, 243-254 (2009).
313. Barry, F., Boynton, R.E., Liu, B. & Murphy, J.M. Chondrogenic differentiation of mesenchymal stem cells from bone marrow: differentiation-dependent gene expression of matrix components. *Exp Cell Res* **268**, 189-200 (2001).
314. Rich, J.T., *et al*. Upregulation of Runx2 and Osterix during in vitro chondrogenesis of human adipose-derived stromal cells. *Biochem Biophys Res Commun* **372**, 230-235 (2008).
315. Johnstone, B., Hering, T.M., Caplan, A.I., Goldberg, V.M. & Yoo, J.U. In vitro chondrogenesis of bone marrow-derived mesenchymal progenitor cells. *Exp Cell Res* **238**, 265-272 (1998).

Chapter 2

Materials and Methods

All materials were supplied by Sigma-Aldrich unless otherwise stated. All the animal work was approved by the Animal Research and Ethics Committee of the National University of Ireland Galway, and was conducted under a license granted by the Department of Health and Children, Dublin, Ireland.

2.1 Mesenchymal stem cell isolation and expansion

2.1.1 Isolation of MSCs from bone marrow of ApoE$^{-/-}$ mice

Mouse MSCs (mMSCs) were isolated by the method described by da Silva Meirelles and Nardi with modifications[1]. Briefly, (BM) was obtained from femur and tibia of 8 to 12 week old ApoE$^{-/-}$ mice; animals were euthanized by inhalation of CO_2 or cervical dislocation and the dissected bones were cleaned of muscle and placed in a sterile 50ml tube containing phosphate buffered saline (PBS) and 1% (100U/ml penicillin and 100µg/ml streptomycin (P/S)). Samples were transferred to a petridish containing fresh PBS with antibiotics and the ends were removed using a scissors. Marrow plugs were obtained using PBS containing 1% P/S, which was injected into the bone cavities using a 27G needle. The plugs were transferred to Dulbecco's modified Eagle's medium (DMEM) supplemented with 0.01M HEPES (4-(2-hydroxyethyl)-1-piperazineethanesulfonic acid), 1% P/S and 10% foetal bovine serum (FBS) and dispersed by repeated pipetting.

The BM mononuclear cell (BMMNC) suspension was centrifuged at 400 x g for 10min at room temperature (RT). The supernatant was removed and the cells resuspended in 10ml culture medium and centrifuged once again at 400 x g for 10min at RT. Following this washing step, supernatant was discarded and viable cells were counted with trypan blue in a hemocytometer. Cells were then resuspended and plated at a density of 2 x 10^6 BMMNC/cm^2 and cultured in a humidified 5% CO_2 incubator at 37°C for 72h. The medium was then changed to remove non-adherent cells. Cells were fed every 3-4 days. Cells grew as colonies and once established (generally between 22 to 25 days) were passaged to avoid overgrowth. Cultures were washed once with Ca^{++} Mg^{++}-free Hank's balanced salt solution (HBSS).

A 0.25% trypsin solution with 0.01% ethylenediaminetetraacetic acid (EDTA) (trypsin/EDTA) was added and cells detached by incubation for 10min at 37°C followed by gentle tapping. Trypsin was neutralized by cell culture medium and cells were centrifuged at 400 x g for 5min at RT. The supernatant was removed and viable cells were counted with trypan blue in a hemocytometer. Cells were resuspended and replated at 5 x 10^3 cells/cm^2. Subsequent passages were plated at 2.8 x 10^3 cells/cm^2 and passaged when cultures reached about 70-80% confluence. Culture medium was changed every 3–4 days.

2.1.2 Isolation of MSCs from bone marrow of C57BL/6 and C57BL/6-GFP$^+$ mice

The protocol for isolation of mMSCs from ApoE$^{-/-}$ mouse marrow as described in Section 2.1.1 was unsuccessful for C57BL/6 mice. However, successful cultures were ultimately established using modifications of the procedure described by Sudres *et al*.[2].

Briefly, BM was obtained from femur and tibia of 8 to 12 week old C57BL/6 or C57BL/6-GFP$^+$ mice; animals were euthanized and marrow plugs obtained as described in section 2.1.1 above. The plugs were transferred to alpha minimum essential medium (α-MEM; Gibco), 1% P/S and 10% FBS and dispersed by repeated pipetting. BMMNC were then filtered through a 70mm mesh and washed twice by centrifugation at 400 x g for 6min in α-MEM supplemented with 1% P/S prior to resuspension in complete medium (α-MEM with 10% FBS and 1% P/S). Following this washing step, the supernatant was discarded and viable cells counted.

Cells were plated at 5 x 10^6 cells/cm^2 and incubated in a humidified atmosphere at 33°C and 5% CO_2. After 48h, non-adherent cells were removed by washing with PBS and fresh medium was added. The temperature of the incubation was raised by one degree every 3-4 days until it reached 37ºC. Medium was changed weekly until cultures were near confluence. At this stage, cells were washed with PBS and detached using trypsin/ EDTA for 2-3min at 37°C. Cells were expanded by plating at 4 x 10^3 cells/cm^2 and passaged at 70-80% confluence in subsequent passages at 2.8 x 10^3 cells/cm^2.

Also, C57BL/6 mMSCs isolated in Dr. Karen English's laboratory at the Institute of Immunology, Maynooth University as described previously [3] were received as a gift. These cells were expanded in the same manner as described above.

2.1.3 Cumulative population doubling

Growth characteristics of all the isolated cell populations were assessed by plotting growth curves. Cumulative population doublings over time were calculated. Following every passage, population doublings were determined based on the number of cells plated and harvested versus the duration of culture time in days. Cumulative population doublings were calculated with respect to the cell numbers at passage 1. To maintain the same conditions across different cell preparations, medium changes were done at a set interval of 3 to 4 days and cells were harvested at 80% of confluence.

2.2 Vascular stem cells (VSCs) isolation and expansion

2.2.1 Isolation of VSCs from the aortas of ApoE$^{-/-}$ mice.

Isolation of VSC from ApoE$^{-/-}$ was adopted from the protocol described by da Silva Meirelles and Nardi[4]. Briefly, the ascending aorta was dissected, cleaned and placed in DMEM/HEPES without FBS but containing Antibiotic/Antimycotic (100U/mL penicillin, 100µg/ml streptomycin and 0.25µg/ml amphotericin B), transferred to a Petri dish and cut into small pieces. The dissected pieces (around 0.2-0.8cm^3) were washed with DMEM/HEPES, cut into smaller fragments, and subsequently digested with 10ml of collagenase type I (0.5mg/ml in DMEM/HEPES) for 30min-1h at 37°C. The aorta was digested for around 30min and subjected to vigorous agitation, yielding a first cell fraction. The remnant of the vessel was then washed in 20ml DMEM/HEPES, and transferred to a new tube for a second collagenase digestion yielding a second cell fraction. Both the cell fractions were used to establish separate primary cultures. For early cultures (passage 0 to 2), (RPMI) supplemented with 10% FBS, 10% Horse Serum (HS), 1% L-glutamine and 1% P/S was used. Whereas for long term culture, DMEM supplemented with 0.01M HEPES (DMEM/HEPES), 10% FBS and 1% P/S was used.

2.2.2 Isolation of VSCs from the aortas of C57BL/6 mice.

The method described above (section 2.2.1) was initially followed to isolate VSCs from the aortas of C57BL/6 mice. Although, isolation was ultimately successful, it was difficult to obtain VSCs using this protocol. Hence, another method adopted from that described by Dellavalle *et al*. was used [5]. Aortas were dissected and cleaned and then rinsed in PBS with $Ca^{++}Mg^{++}$ and then cut into 1–2mm diameter pieces with a scalpel. Fragments of aortas were transferred to a Petri dish coated with type I collagen (1mg/ml in 0.1M acetic acid). The fragments were cultured for 7–8 days. After the initial outgrowth of fibroblast-like cells, small round cells were observed. These cells were poorly adherent and many of the cells were seen to float. Thus, this cell population was easily collected by gently tapping the petridish and pipetting out of the original culture. These cells were then plated at a density of 5 x 10^4 cells per well in a collagen-coated 6-well plate. Culture medium - DMEM supplemented with 5% FBS, 5ng/ml basic fibroblast growth factor (FGF2), 2mM glutamine, 0.1mM β-mercaptoethanol, 1% non-essential amino acids, 1% P/S was used for the first three passages; for subsequent passages, α-MEM supplemented with 10% FBS, 1% P/S was used. Cells were transferred to uncoated cell culture flasks at passage 4.

2.2.3. Cumulative population doubling

Growth curves were carried out to investigate growth characteristics and calculate cumulative population doublings of isolated VSC preparations in a similar fashion as described in section 2.1.3.

2.3 Isolation of 3G5 antibody

A hybridoma cell line was purchased from the American Type Culture collection (ATCC, CRL-1814). Cells produce IgM antibody specific to the acetylated ganglioside 3G5, a pericyte surface antigen[6]. Hybridoma cells were grown in DMEM supplemented with 10% FBS and grown in an incubator for 2 weeks to get optimum proliferation of the cells. The deprivation of FBS from the medium was achieved by reducing content of FBS by 1% every 5-7 days until 0.5% FBS in the culture was obtained. The final culture

was left for 5 days in incubator until medium became acidic and cells died. Culture was then poured into sterile 50ml tubes. Supernatant was harvested by centrifuging for 20min at 1,500 x g at RT. Supernatant was collected to fresh tubes and stored at -80 and -20ºC. The presence of IgM antibody in the supernatant was confirmed by mouse IgM specific IsoQuick strips and western blotting.

2.4 Immunocytochemical detection of the 3G5 antigen

Optimisation of conditions to detect 3G5 was performed using differentiated RIN5F cells previously shown to express the antigen[7]. VSCs and MSCs were plated at 3 x 10^3 cells per chamber in a 4-well chamber slide and cultured for 3 days. Live cells were blocked with 10% normal goat serum (NGS) and 1% BSA in PBS for 1h. Cells were then incubated overnight with non-diluted primary 3G5 antibody at 4°C. Following the incubation, cells were washed twice with 1% BSA for 3-5min. Then, cells were incubated with FITC conjugated goat anti mouse secondary antibody for 1h at 4°C at a 1:400 dilution. Again, washings were done twice with 1% BSA for 3-5min. Cells were then fixed with 4% parafomaldehyde (PFA) for 15min and washed twice with PBS for 3-5min. Hoechst solution was prepared by diluting 50µl of 10mg/mL (16.2mM) Hoechst aqueous solution in 950µl of PBS. Cells were incubated with this diluted Hoechst solution for 30s to 1min. Two washings with PBS for 5min were performed and the slides were mounted using Vectashield mounting medium H-1000 (Vector Laboratories).

2.5 Cell surface characterization by flow cytometry

For cell surface marker analysis, all isolated cells at passage 6 and 80% confluence were trypsinised and resuspended in fluorescence-activated cell sorting (FACS) buffer. Cells were centrifuged at 400 x g for 4min, supernatant was aspirated off and cells were washed twice in FACS buffer. Cells were then resuspended in FACS buffer containing 5% NGS for 30min on ice spun down and plated at 200,000 per well in 50ul FACS buffer. Afterwards, the cells were incubated with the respective primary antibodies to CD3, CD9, CD19, CD31, CD34, CD44, CD45, CD90.2, CD105, CD117, CD146, Sca-1, NK.1 and Gr-1 at concentrations of 1µl in 50µl of FACS buffer for 30min on ice

(Table 2.1). Medium was carefully aspirated off and when required, a secondary antibody (1:250) (Abcam) was added for 30min on ice (Table 2.1). Controls included cells alone (no antibody), cells incubated with secondary alone and cells incubated with an isotype control at the same concentration as primary antibodies. The cells were washed and resuspended in FACS buffer and analyzed on the FACSCanto (Becton Dickinson). Histograms of the cell number versus fluorescence intensity were recorded with 5 x 10^4 cells per sample and analyzed using FlowJo (Tree Star Inc.) software. Expression of each marker was presented as percentage of total population calculated from number of cell expressing the marker verses control unstained cells.

Table 2.1: Cell surface markers antibodies

Antibody	Isotype	Label	Supplier
primary antibodies			
Hematopoietic associated antigens			
Gr-1	IgG2b	PE	BD (553128)
CD3	IgG1,κ	Bio	BD (553060)
CD9	IgG2a,κ	Bio	BD (558749)
CD19	IgG2a,κ	Bio	BD (553784)
CD34	IgG2a,κ	Bio	BD (551387)
CD45	IgG2b,κ	PE	BD (553081)
NK-1.1	IgG2a,κ	Bio	BD (553163)
Endothelial associated antigens			
CD31	IgG2a,κ	PE	BD (553373)
MSC associated antigens			
Sca-1	IgG2a,κ	PE	BD (561076)
CD44	IgG2b,κ	PE	BD (561860)
CD90.2	IgG2a,κ	PE	BD (553014)
CD105	IgG2a,κ	PE	eBioscience (12-1051)
CD117	IgG2b,κ	PE	BD (553869)
Pericyte associated antigens			
3G5	IgM,κ	Supernatant	hybridoma
Tie-2	IgG1,κ	PE	eBioscence (124007)
CD146	IgG2a,κ	PE	BioLegend (134703)

Table 2.1: Cell surface markers antibodies (contd.)

secondary antibodies/reagents			
SA	-	PE	BD (554160)
Anti-IgM,μ	-	FITC	Sigma (F9259)
isotype controls			
Rat IgG2a,κ	-	PE	BD (553930)
Rat IgG2b,κ	-	PE	BD (553989)
Rat IgG1,κ	-	PE	BD (554685)
Mouse IgG2a,κ	-	Bio	BD (553457)
Hamster IgG1,κ	-	Bio	BD (553970)
Mouse IgM	-	Purified IgM	Sigma (M5909)

2.5.1 Fluorescence activated cell sorting of the 3G5-expressing cell subpopulation from ApoE$^{-/-}$ VSCs

ApoE$^{-/-}$ VSC were sorted using the FACSAariaII (BD). Passage 8 cultures were trypsinized at 80% confluency and resuspended in PBS with 10% FBS and 5% NGS for 30min on ice. The 3G5 hybridoma supernatant was added with 10% FBS for incubation overnight. The cells were washed and the secondary antibody (goat FITC Anti- mouse IgM) at 1:100 dilution in 10% FBS added for 45min. The cells were washed twice in FACS buffer, resuspended in the required volume of FACS buffer and filtered via a 70µm cell strainer. The dead cells were excluded by 7-amino-actinomycin D (7-AAD) (22µl of viability dye per 1ml per 1 x 10^6 cells). The 3G5$^+$ and 3G5$^-$ cell fractions were gated or analyzed based on fluorescence minus one (FMO) and isotype controls for 3G5 expression (Table 2.1). The single cell gate was set to remove any doublets and the scatter gate to ensure the any debris or dead cells were excluded. Sorted cells were re-analysed to ensure high purity. Immunohistochemistry for 3G5 antigen was performed to ensure that all cells were 3G5 positive prior to further analysis.

2.6 Differentiation assays

2.6.1 Chondrogenesis

To induce chondrogenic differentiation, harvested MSCs and VSCs were washed with PBS once by centrifugation, resuspended in chondrogenic medium, and finally centrifuged for 5min at 100 x g in sterile polypropylene round-bottom 96-well plates to form a pellet. Chondrogenic medium constituted of DMEM high glucose (HG), 100nM dexamethasone, 1mM sodium pyruvate, 50µg/ml 2-phosphate ascorbic acid, 40µg/ml L-proline, ITS+supplement (BD Biosciences) and 100U/ml penicillin/ 100µg/ml streptomysin/ 0.25µg/ml amphotericin B (antibiotic/antimycotic). This medium was further supplemented with 100ng/ml BMP-2 and 10ng/ml TGFβ-3. Medium was changed every 2 days for 3 weeks when the pellets were harvested for analysis by histology and immunohistochemistry for collagen type II and X, and quantitative assessment of glycosaminoglycan (GAG) and DNA.

2.6.1.1 Toluidine blue staining

Toluidine blue is a basic dye that stains sulphated proteoglycans red-purple (metachromasia). Pellets were washed in PBS and fixed in 10% neutral buffered formalin for 1h. Samples were wraped in Whatman filter paper placed, in a tissue cassettes and soaked in 10% neutral buffered formalin. Tissue were placed in tissue processor, Leica ASP300S overnight. Samples were removed from the processor and placed in a Leica EG1150 H heated paraffin embedding system. The samples were then removed from the cassettes and filter paper and placed in plastic tissue moulds and filed with paraffin wax. Samples were left to cool on Leica EG1150 C cold plate. Samples were cut at thickness of 5µm using the Leica RM2235 microtom. Before staining the sections were heated in oven at 60ºC for 2h. The sections were deparaffinised and hydrated (xylene twice for 5min, 100%, 95% and 70% ethanol twice for 2min) followed by water for 5min. Slides were blotted with tissue paper to dry prior to staining in the 60°C pre-heated Toluidine blue solution (0.5%) for 5min. Sections were then rinsed in running tap water until water ran clear before air-drying. Slides were cleared in xylene for 2min followed by mounting using DPX mounting medium.

2.6.1.2 Type II and X collagen immunohistochemistry

After deparaffinization by xylene (twice for 10min each), sections were hydrated through a graded series of ethanols (100%, 95% and 70% for 5min). To enhance antigen retrieval, sections were washed with PBS and digested for 40min at RT with 0.1% pepsin in 0.2M HCl and/or 25mg/ml hyaluronidase in PBS for collagen type II and only 0.1% of pepsin in 0.5M acetic acid for collagen type X. After several washings with PBS, sections were treated with 1% hydrogen peroxide in methanol for 30min to block endogenous peroxidase activity. Nonspecific binding was blocked using 10% NGS and 5% BSA for 1h in a humidity chamber followed by overnight incubation with collagen II or X antibody (Gentaur; LSL LB -1297 at 1:1000; LSL LB-0092 at 1:1000) at 4°C. The sections were treated with biotin-labeled anti-rabbit goat IgG (Dako E0432 at 1:200) for 35min at RT followed by peroxidase labeled streptavidin (Dako) for 30min at 1:200 and RT. A diaminobenzidine (DAB) tablet was dissolved in 15ml of PBS, filtered

and was activated prior to use by 12µl of H_2O_2. DAB was added to sections for 30s for color development, after which hematoxylin counterstaining was done for 30s. Slides were rinsed with water followed by dehydration through graded ethanols (95% and 100% twice for 2min) and xylene (twice for 5min). Slides were coverslipped using the mountant DPX and imaged using an upright brightfield microscope (Olympus BX51 Upright Fluorescent Microscope with Improvision Optigrid System). Negative controls were subjected to the same protocol with omission of the primary antibody.

2.6.1.3 Glycosaminoglycan quantification assay

GAG concentration in chondrogenic pellets was quantified after 21 days in chondrogenic culture using the DMMB assay. This assay is based on the ability of sulphated GAG to bind to DMMB[8-10]. Chondroitin sulphate standards, required for the assay were prepared by dilution in order to create a known concentration gradient from 0 to 2µg. The measurement of standards and samples was performed in a 96-well microtiter plate. These measurements were done in technical triplicates. To digest the pellets, 1mg of papain was dissolved in 9.75ml dilution buffer (50mM Sodium Phosphate, 2mM N-acetyl cysteine, 2mM EDTA at pH 6.5) and 250µl diluted papain solution was added to 10ml dilution buffer. Two hundred µl was added to each pellet and digested overnight at 60^{o}C. Following the digestion, DMMB stock solution was added. DMMB stock solution was prepared by dissolving 16mg of DMMB (1,9 dimethylene blue) in 5ml histology grade 100% ethanol combined with 2.73g NaCl, 3.04g glycine and 0.69ml of concentrated HCl (11.6M) in distilled water. The pH of the solution was adjusted to 3 and total volume made up to 1litre. Within 5min of incubation of the digested pellets with DMMB at RT, readings were performed on Wallac Victor^{3TM} 1420 Multilabel counter fluorescent plate reader at 595nm.

2.6.1.4 DNA quantification assay

The amount of DNA per pellet was calculated using the quanti-iT ™ PicoGreen double stranded DNA assay following the manufacturer's protocol (Molecular Probes). Briefly, standards (prepared by dilution) and samples were added to the 96-well plate in triplicate. Picogreen reaction buffer was added to the samples and standards and

incubated at RT for 3min. Readings were performed at 538nm with excitation at 485nm on a Wallac Victor^{3TM} 1420 Multilabel counter fluorescent plate reader. Following DMMB and DNA assays, GAG/pellet and DNA/pellet were calculated and GAG concentration expressed as GAG/DNA (μg/μg).

2.6.2 Osteogenesis

To induce osteogenic differentiation, MSCs and VSCs were seeded in triplicate into 6-well plates at 1.3 x 10^4 cells/well and cultured for 24h. Cells were then placed in osteoblastic differentiation medium for 14 days in complete medium supplemented with 100nM dexamethasone, 10mM beta-glycerophosphate, and 50μM ascorbic acid, with 1% antibiotic/antimycotic. Cells were maintained in inducing medium for 14 days with media changes every 2 days. Cells in complete MSC/VSC growth medium acted as a control. From the triplicate samples, the calcium concentration was quantified in duplicate; The remaining wells, one each from control and treated samples were fixed for 15min in 10% formalin for Van Kossa staining.

Quantification of calcium deposition was performed using a colorimetric calcium assay versus a standard curve using manufacturer's instructions (Calcium CPC Liquicolour, Stanbio Inc.). Briefly, standards ranging from 0.05μg to 1.5μg were prepared in 0.5M HCl and deionized water. After washing the samples twice with PBS (Gibco), 0.5M HCl was added to each well. Contents of the wells were removed by scraping and placed in separate eppendorf tubes. These eppendorf tubes containing samples were shaken overnight at 4ºC. Following the shaking, the samples were centrifuged at 1,000 x g for 5min. Two hundred μl of Stanbio Calcium (CPC) Liquicolor working solution (1:1 working dye to binding reagent) was added to standards and samples in a 96-well plate and incubated at RT for 15min. The incubation was done in the dark. Absorbance readings were performed in duplicate at 550nm on a Wallac Victor3™ 1420 Multilabel Counter spectrophotometer and standard curve was used to quantify the levels.

Von Kossa staining was carried out for calcium deposition in the osteogenic cultures. Briefly, cultures were washed twice with PBS and fixed with 4% PFA for 20min.

Subsequently, 1ml of 3% silver nitrate solution (300mg silver nitrate in 10ml deionized water (dH_2O)) was added to each well and incubated in darkness at RT for 10min. Cells were rinsed three times with dH_2O, the last rinse was left on the cells and they were exposed to bright warm light for 15min. Cells were rinsed again and photographed on an Olympus IX71 inverted microscope camera utilising Cell IP imaging software (Olympus). A silver black color confirmed the presence of calcium deposits.

2.6.3 Adipogenesis

To induce adipogenic differentiation, cultured MSCs and VSCs were seeded into 6-well plates at 2 x 10^5 cells/well and until they became confluent in complete MSC/VSC growth medium. Cells were then placed in adipogenic induction medium DMEM-HG, 10% FBS, 5% rabbit serum, 1µM dexamethasone, 10µg/ml insulin, 200µM Indomethacin, 500µM isobutylmethylxanthine (IBMX), and antibiotic/antimycotic for 3 days followed by exposure to adipogenic maintenance medium (DMEM-HG, 10% FBS, insulin 10µg/ml and P/S) for a further 3 days. After 3 cycles of induction and maintenance exposure, cell cultures were rinsed with PBS and fixed in 10% formalin for 20min at RT. Fixative was removed and wells were rinsed in distilled water. The Oil Red O stock solution (0.3% of Oil Red O powder in 99% isopropanol) was diluted to a working solution by mixing 6 parts of Oil Red O stock solution with 4 parts of distilled water. After 10min the solution was filtered using Whatman no.1 filter paper (Whatman). Cells were covered with 2ml of working Oil Red O for lipid droplet staining. After 5min incubation, Oil Red O stain was discarded. To remove excess stain, 60% isopropanol was used. Wells were then rinsed thoroughly with tap water. To counterstain, Harris Hematoxylin was added for 1min and slides were washed in warm water for 5min. During microscopy, the cells were kept covered with water. After imaging, Oil Red O extraction was performed. For the extraction, water was removed from wells and cells were incubated with 100% isopropanol (1ml/well). The assessment was done in 96-well plate. 100% isopropanol without samples was used as a blank. Absorbance readings were taken at 490nm to quantify the extracted Oil Red O using a Wallac Vistor^{3TM} 1420 Multilabel Counter

spectrophotometer. Cells exposed to in complete culture media without any induction medium were used as a control.

2.6.4 Myogenesis

To induce myogenic differentiation, harvested MSCs and VSCs were seeded into 4-chamber slides at 6 x 10^3 cells/chamber or T-25 cultured flask and cultured for 24h in complete culture medium. Myogenesis was induced by 5ng/ml TGF-β1 added every second day to the culture medium[11]. Cells were cultured for 7 days, with medium changes every 2 days. Cells in complete culture medium acted as controls. Cells were rinsed with PBS and fixed in 3.8% formaldehyde for 15min at RT. Fixative was removed and the chambers rinsed in distilled water. Fixed cells were used for alpha smooth muscle actin (α-SMA) staining.

2.6.4.1 Staining for alpha smooth muscle actin

Before immunostaining, slides were kept in ethanol and concentrated acetic acid solution (19:1) for 10min at RT. Endogenous peroxidase activity was blocked using a 3% solution of hydrogen peroxide (H_2O_2) in methanol for 15min. Sections were permeabilized by 0.01% Triton-100 with blocking solution (5% BSA for 30min). The primary antibody was a monoclonal mouse anti-human smooth muscle actin clone 1A4 ((Dako) 1:200 in 5% BSA) and the secondary antibody was a biotinylated polyclonal swine anti-goat, mouse, rabbit immunoglobulins/(Multi-Link) (1:1000 in 5% BSA). Incubation with the primary antibody was done for 1h at RT, followed by washing with PBS. The sections were then incubated for 1.5h with the secondary antibody. Sections were rinsed with PBS and incubated with streptavidin-horseradish peroxidase (streptavidin-HRP) for 30min. The peroxidase activity was visualized by applying DAB for 10min. After rinsing in PBS and counterstaining in Harris hematoxylin, the slides were dehydrated and mounted. Appropriate tissue sections as positive and negative controls for primary antibodies were also assessed.

2.6.4.2 Western blotting

After 7 days of myogenic induction by 5ng/ml TGF-β1, cells were washed with PBS. Whole lysis buffer contained: 20mM HEPES pH7.5, 350mM NaCl, 1mM $MgCl_2$, 0.5mM EDTA, 0.1mM EGTA, 1% NP40 and H_2O. Protease Inhibitor Cocktail was added to the lysis buffer just before use. Lysis buffer (100µl/T-25 culture flask) was dispensed and allowed to spread over the surface of the flask which was placed on ice. Lysate was then collected into an eppendorf tube. Samples were spun at 16,000 x g at 4ºC in a microcentrifuge for 10min. The supernatant was removed into a fresh eppendorf and stored at -70ºC. Protein concentration was quantified using a Coomassie Bradford protein assay (Thermo Scientific). Briefly, 5µl of standard and lysate were diluted with 250µl of the Coomassie Reagent and mixed for 30s on the plate shaker. The plate was then incubated for 10min at RT and readings were performed at 595nm on a Wallac Victor^{3TM} 1420 Multilabel counter fluorescent plate reader. BSA was used to prepare a standard curve and lysis buffer was used as a blank. A standard curve was used to calculate the protein concentrations; The absorbance was plotted *vs*. different concentrations of the BSA protein. Total protein (15-30µg) was resolved by sodium dodecyl sulphate-polyacrylamide gel electrophoresis 10% (w/v) (SDS-PAGE). Each sample was boiled at 95ºC for 3min in 1x *Laemmli* sample buffer (5% SDS, 20% glycerol, 0.004% bromphenol blue, 125mM Tris-HCl pH 8.0, 10% β- mercaptoethanol) before loading the sample onto a gel.

2.6.4.2.1 SDS-Polyacrylamide gel electrophoresis

The Mini-Protean® Cell System Bio-Rad (Hercules, USA) was used for 10x10 cm gels. They were run at 25mA for about 60-90min in 1 x running buffer (25mM Tris-HCl, 250mM glycine, 0.1% SDS). The 10% SDS-PAGE gels were prepared as follows: resolving gel mix: 375mM Tris-HCl pH 8.8, 10% acrylamide/bis, 0.1% SDS, 0.05% APS, 0.05% TEMED; and stacking gel mix: 125mM Tris-HCl pH 6.8, 4% acrylamide/bis, 0.1% SDS, 0.05% APS, 0.1% TEMED.

2.6.4.2.2 Immunobloting

SDS-PAGE was used to separate the proteins. Proteins were transferred to nitrocellulose membrane (Whatman GmbH). The Mini Trans-Blot Cell transfer system (Bio-Rad, Hercules) was used to perform wet transfer for 90min at 250mA in 1 x transfer buffer (72mM Tris-HCl, 58.5mM glycine, 15% methanol) at 4ºC. Gel and membrane were sandwiched between sponge pads and filter papers (Whatman GmbH). Care was taken to remove any air bubbles between the gel and the membrane. The assembly of the cassettes was performed so as to have the nitrocellulose membrane on the cathode side and the gel on the anode side. On each side of the membrane and gel, two filter papers were placed. Outside the filter papers, sponge was placed. An ice-pack was placed in the tank and 1 x transfer buffer was filled in the transfer apparatus. Confirmation of the protein transfer quality was assessed either by presence of the pre-stained protein marker on the membrane or by staining with 1% Ponceau S (0.5g Ponceau S in 5% acetic acid) solution for 5min. The membrane then was washed 3 times (10min each) under agitation with PBS containing 0.05% (v/v) Tween 20 (PBS-T) to remove the Ponceau S solution. The membrane was blocked with 5% nonfat milk in PBS-T for 1h at RT under agitation and then washed once with PBS-T to remove the excess milk. The membrane was probed with primary antibodies for α-SMA (1:500) for 1h or calponin (Dako) (1:1000) overnight at 4ºC, diluted in 5% nonfat milk in PBS-T. After washing 3 times (with agitation, each wash for 10min) with PBS-T to remove the residual primary antibody, the membrane was incubated with HRP (horseradish peroxidase)-conjugated anti-mouse and anti-rabbit IgG (H+L) secondary antibodies for ECL goat polyclonal (Jackson Labs) (1:10,000) in 5% nonfat milk in PBS-T for 1h. The membrane was washed three times in PBS-T. This was followed by incubation with the Western Blotting Detection Reagents (GE Healthcare) or Immobilon Western-Chemiluminescent HRP substrate detection system (Millipore) for 1min. Densitometric analysis was performed using the AlphaInnotech FluorChem Chemiluminescent Imaging System.

Incubation with polyclonal anti-Cu/Zn superoxide dismutase (CuZnSOD) (Millipore) (1:1000 in 5% nonfat milk in PBS-T) for 1h at 4ºC or anti-human rabbit polyclonal

β-actin (Sigma) (1:10,000 in 5% nonfat milk in PBS-T) overnight at 4ºC was used as a loading control. The BenchMark pre-stained protein ladder (Invitrogen) or SuperSignal molecular weight protein ladder (Thermo Scientific) was used. The membrane was stripped, if required, with the Restore Western Blot Stripping buffer (Thermo Scientific) for 30min at 37ºC. Incubation with primary antibody was then performed as described earlier.

2.7 Effect of pro-inflammatory cytokines on *in vitro* chondrogenesis of VSCs

The effect of pro-inflammatory cytokines on the chondrogenic differentiation of VSCs from ApoE$^{-/-}$ and C57BL/6 mice was assessed. Pellet cultures of these cells were established in chondrogenic medium with or without treatment with IL-6 (200ng/ml)[12], IL-1β (1ng/ml)[13] or TNF-α (10ng/ml)[13] (Peprotech) for 48h, 7 days, 14 days and 21 days. In this study, lineage factors such as Sox9, fibromodulin and aggrecan (early chondrogenesis), collagen type II (chondrogenic commitment) runt-related transcription factor 2 (Runx2) (pre-hypertrophy in endochondral ossification), and collagen type X and alkaline phosphatase (Alp) (hypertrophy) were assessed by real-time PCR.

2.7.1 RNA isolation and reverse transcription

2.7.1.1 RNA isolation

For 48h cultures, five chondrogenic pellets per sample were homogenized with 1ml Trizol reagent (Invitrogen) incubating at RT for 1min and then pipetting. Pellets which were in culture for 7 days or more were snap frozen in liquid nitrogen and pulverized in a cell crusher (Cellcrusher Limited, http://cellcrusher.com/). The pulverized pellets were transferred into 1ml Trizol and incubated at RT for 5min to complete dissociation. Samples were stored at -80°C until required. Frozen samples were thawed and 200µl chloroform was added per 1ml homogenate in Trizol. Samples were shaken vigorously with inversion several times. This mixture was then incubated at RT for 15min following which centrifugation was done at 12,000 x g for 15min at 4°C.

Following centrifugation, phase separation resulted in 3 distinct layers: the lower phenol chloroform layer, the middle interphase and the upper translucent aqueous phase. The

translucent aqueous phase (~650µl) was removed and added to a fresh tube. Following phase separation, RNA isolation was performed according to manufacturer's instructions (RNA isolation kit, Qiagen). One volume (~700µl) of 70% ethanol was added slowly and carefully mixed by inversion. The sample (700µl at a time) was then applied to a RNeasy® mini spin column (Qiagen), centrifuged for 15s at 8,000 x g and flow through was discarded. 350µl of RW1 buffer was added to center of column, centrifuged for 15s at 8,000 x g and flow through was discarded. 10µl DNase stock solution was added to 70µl Buffer RDD and the DNase incubation mix was added directly onto the RNeasy column and incubated at RT for 15min. Then 350µl of RW1 buffer was added to center of column, centrifuged for 15s at 8,000 x and flow through was discarded. Column was then transferred to a new 2ml collection tube. 500µl RPE was added to the center of column, centrifuged for 15s at 8,000 x g and flow through was discarded. A second wash with 500µl of RPE buffer was performed and a final centrifugation performed for 2min at 8,000 x g.

The column was transferred to new 1.5ml tube, 10µl RNase-free water added onto the column, incubated at RT for 1min and centrifuged for 1min at 8,000 x g. A second elution step with 10µl RNase-free water was performed and finally a wash with 10µl of eluate. The concentration of RNA in the final eluate was determined using NanoDrop and samples were frozen at -80°C until required.

2.7.1.2 RNA integrity

The integrity of the isolated RNA was checked using Agilent 2100 Bioanalyzer and Agilent RNA 6000 Nano kit according to the protocol given in the Agilent RNA 6000 Nano Kit Guide.

A new syringe at the chip priming station on Agilent 2100 Bioanalyzer was used each time. The base plate and the syringe clip at the chip priming station were adjusted. The electrodes were decontaminated using RNase decontamination protocol with RNase AWAY in electrode cleaner. Bioanalyzer's chip selector was adjusted. The vortex mixer was set up. All reagents, except RNA and ladder were brought to RT for 30min

before use with the dye concentrate protected from light. Finally, the software was started before loading the chip.

550µl of Agilent RNA 6000 Nano gel matrix was placed into the top receptacle of the spin filter and centrifuged for 10min at 800 x g. 65µl filtered gel was aliquoted into 0.5ml RNase-free microfuge tubes. The aliquots were stored at 4°C and used within one month of preparation.

The gel-dye mix was prepared as follows. RNA 6000 Nano dye concentrate was vortexed for 10s and spun down. 1µl of RNA 6000 Nano dye concentrate was added to a 65µl aliquot of filtered gel. The tube was capped, vortexed thoroughly and visually inspected for proper mixing of gel and dye. The dye concentrate was stored at 4°C in the dark again. Finally, the tube was spun for 10min at RT at 16,000 x g. Prepared gel-dye mix was used within one day.

A new RNA nano chip was placed on the chip priming station. 9µl gel-dye mix was pipetted at the bottom of the well marked "G" for the gel dye mix and pressurized using the plunger for 30s. 9µl gel-dye mix was pipetted in each of the marked wells. 5µl RNA 6000 Nano marker was pipetted into the well marked with the ladder symbol and each of the 12 sample wells. No well was left empty. To minimize secondary structure, the samples were heat denatured (70°C, 2min) before loading on the chip. The ladder was heat denatured and aliquoted upon arrival. 1µl of the RNA ladder was pipetted into the well marked with the ladder symbol. 1µl of each sample was pipetted into each of the 12 sample wells. 1µl of buffer in which samples were diluted was pipetted in each of the unused wells if any. The chip was placed horizontally in the adapter of the IKA vortex mixer and vortexed at 448 x g for 60s, taking care to avoid liquid spills.
The lid of Agilent 2100 Bioanalyser was opened and correct insertion of electrode cartridge and the chip selector position was checked. Electrodes on the Agilent 2100 Bioanalyser were cleaned using RNAzap for 1min and RNAse free water for 1min. The chip was placed carefully into the receptacle. The lid was closed carefully, and the electrodes in the cartridge fit into the wells of the chip. At this stage the software should

indicate that chip was inserted and lid closed. After selecting the proper assay (eukaryotic RNA program), the run was started. After the run was finished, the chip was removed and discarded according to good laboratory practice. Data was saved automatically. The RNA integrity number (RIN) was checked. To clean the electrode, the electrode cleaner was placed in the Bioanalyser, the lid closed and kept closed for 10s. Then the lid was opened for water to evaporate.

2.7.1.3 cDNA synthesis

RNA was reverse transcribed to cDNA for analysis of gene expression by real-time PCR. Sterile nuclease free tubes, pre-chilled on ice were used at all times with 1µg of RNA template and 0.5µg of oligo(dT) primers and random primers. The target RNA and primers were denatured by incubation at 70°C for 5min and quick-chilled on ice for 5min.

The reaction mix was prepared as described in Table 2.2 and maintained on ice until incubation. After combining all components, the mix was subjected to gentle vortexing. After mixing, the tube with the reaction mix was placed into the reverse transcription machine and the program was run as detailed in Table 2.3. After the reaction was completed, cDNA was used immediately for real-time PCR analysis or stored at -20°C until required.

Table 2.2: Reaction components and quantities required for a single reverse transcriptase reaction

Component	Volume per Reaction (in μl)	Final Concentration
Nuclease free water	5.6	
ImProm-II™ 5X reaction buffer	4	1X
MgCl2, 25mM	2.4	3mM
dNTP mix (10mMeach dNTP)	1	0.5mM
Recombinant Rnasin ribonuclease inhibitor	1	1U/µl
ImProm-II™ reverse transcriptase	1	
Final volume reaction mix	15	

Table 2.3: Example of typical PCR reaction conditions

Step	Temperature	Time
Annealing	25°C	5 min
Extension	42°C	60 min
Heat inactivation reverse transcriptase	70°C	15 min
End	4°C	+ ∞

2.7.2 Real-time PCR

Relative transcript levels for the various genes of interest were assessed using real-time PCR with GAPDH transcript as internal control for normalization. The cDNA template was diluted to obtain a minimum final concentration of 20ng per well. The master mix was then prepared by mixing the Quantifast® SYBR® Green RT-PCR master mix, primers, nuclease free water and cDNA template as listed in Table 2.4. The conditions used for amplification are listed in Table 2.5. To confirm that there were no contaminating products, a dissociation (melt) curve was run each time.

The $2^{-\Delta\Delta Ct}$ method[14,15] was used to analyze the relative gene expression. For the genes of interest and for the normalizing gene, the average Ct was calculated. The ΔCT (Ct gene of interest–Ct normaliser) and $2^{-\Delta\Delta ct}$ were calculated. The levels of gene expression in comparison to controls were then calculated. Primers were selected from Roche molecular probes (Table 2.6) and ordered from Eurofins Operon.

Table 2.4: Polymerase chain reaction components

Component	Volume per Reaction (in μl)	Final Concentration
2X Quantifast SYBR Green PCR master mix	5	1.5mM
Forward, pmol	1	1 µM
Reverse, pmol	1	1 µM
Template DNA	2	≤100ng/reaction
Nuclease free water (to bring volume to 25 μl)	1	1U/µl
Final volume	10	

Table 2.5: Typical real-time PCR program

Step	Temperature	Time	Ramp Rate	No. of Cycles
Initial step	50°C	2 min	Maximal/fast mode	1
PCR initial activation step	95°C	5 min		1
Two step cycling				
Denaturation	95°C	10 sec	Maximal/fast mode	35
Annealing/Extension	60°C	30 sec		
Final step				
Denaturation	95°C	15 sec	Maximal/fast mode	1
Annealing/Extension	60°C	20 sec		
Final denaturation	95°C	15 sec		

Table 2.6: Primer sequences and product sizes, for real-time PCR

Gene	Real-time PCR primer sequence (5'-3')	Amplicon size base pair (bp)	Accession number
Chondrogenic markers			
Type II Collagen	5'gccatcgccatagctgaa'3	107nt	NM_001113515
	5'cgactgtccctcggaaaa'3		
Aggrecan	5'ccagcctacaccccagtg'3	66 nt	NM_007424.2
	5'gagggtgggaagccatgt'3		
Fibromodulin	5'cagggcaacaggatcaatg'3	78nt	NM_021355.3
	5'ctgcagcttggagaagttcat'3		
Sox9	5'tatcttcaaggcgctgcaa'3	126nt	NM_011448.2
	5'tcggttttgggagtggtg'3		
Hypertrophy and osteogenic markers			
Type X Collagen	5'gcatctcccagcaccaga'3	85nt	NM_009925.4
	5'ccatgaaccagggtcaagaa'3		
Alkaline Phosphatase	5'cggatcctgaccaaaaaacct'3	74nt	NM_007431
	5'tcatgatgtccgtggtcaat'3		
Runx2	5'gcccaggcgtatttcaga'3	82nt	NM_001145920.1
	5'tgcctggctcttcttactgag'3		
Internal control			
GAPDH	5'atgtgtccgttgtggatctg'3	123nt	NM_008084.2
	5'ggtcctcagtgtagcccaag'3		

2.8 *In-vivo* assessment of VSC and MSC osteogenic potential

The *in vivo* study aimed at assessment of bone formation by VSC and MSC. The objective asses the intrinsic capacity of VSC and MSC to form bone, the effect of atherosclerotic environment and *in vitro* chondrogenic priming. Towards this, *in vitro* chondrogenically primed and unprimed VSC or MSC from atherosclerotic and non-atherosclerotic mice were implanted subcutaneously in atherosclerotic or background mice. ApoE$^{-/-}$ mice were used as atherosclerotic model[16-18] while C57BL/6 mice acted as background control. In order to improve in vivo cell viability, cells were seeded onto collagen chondroitin sulphate scaffolds. The choice of scaffold was dictated by previous finding of improved cell viability using this scaffold[19]. Histomorphometric assessment of bone or cartilage formation was performed at 8 weeks post-implantation.

2.8.1 Scaffold seeding

At 70-80% confluence, passage 8 VSCs and MSCs were detached and counted as described in Section 2.1.1. Suspensions at 5 x 10^6 cells/ml were seeded onto collagen GAG scaffolds as described previously[19]. Briefly, each scaffold around 5-5-3mm was placed in a single well of a six-well plate, seeded with 100µl of cell suspension and incubated for 30min. Scaffolds were overturned onto agar-coated wells (2ml of 2% autoclaved agarose gel per well; Promega) and another 100µl of suspension was placed onto the samples. After 30min, 3ml of appropriate cell culture medium was added.

2.8.2 Chondrogenic priming

To induce chondrogenesis, chondrogenic medium was supplemented with BMP-2 100ng/ml and TGF-β3 10ng/ml. Primed scaffolds were fed every 3 to 4 days by changing half of the media. Samples were maintained in culture for 5 weeks following seeding. Control scaffolds were loaded in the same manner and fed with complete culture medium.

2.8.3 Subcutaneous implantation of chondrogenically primed constructs

The pre-differentiated constructs were implanted subcutaneously into 8 week old C57BL/6 control mice and 8 week old atherosclerotic ApoE$^{-/-}$ mice that were fed a Western diet and had fully developed atherosclerotic plaques. For direct comparison, chondrogenically primed and control constructs, either MSC or VSC, from each mouse strain, were implanted in both C57BL/6 and ApoE$^{-/-}$ mice (Table 2.7). Empty scaffold controls were also implanted. Constructs were randomly assigned to implantation position. Since two different mice strains were used in the in vivo experiment, the possibility of immune clearance of implanted cells especially mismatched host cannot be ruled out. Keeping this in mind, time point of 8 weeks was long enough to let the initial acute inflammatory reaction to die down and give the cells enough time to differentiate. The use of control treatments in the mismatched host provided a good baseline to eliminate the effect of immune mediated cell loss.

Table 2.7: Treatment groups for subcutaneous implantation

		Host mouse	
Cell type		$ApoE^{-/-}$	C57BL/6
	$ApoE^{-/-}$ MSCs	8	8
	$ApoE^{-/-}$ VSCs	8	8
	C57BL/6 MSCs	8	8
	C57BL/6 VSCs	8	8

2.8.4 Surgical procedure

Anesthesia

Animals were anesthetized by subcutaneous injection with ketamine 80-125mg/kg and xylazine 5-10mg/kg. The pre-procedural antibiotic eurofloxacin 5mg/kg was also injected.

Subcutaneous Implantation

MSCs or VSCs from ApoE$^{-/-}$ or C57BL/6 mice were loaded on to the collagen-chondroitin sulphate constructs as detailed in section 2.8.1. Chondrogenically primed collagen-chondroitin sulphate constructs were implanted subcutaneously as described in section 2.8.3. Five implantations were carried out per mouse on the back in predetermined locations. Implantation sites were marked with a non-absorbable suture for identification at the experimental time point. Following implantations, mice were monitored closely for first 2h in recovery room. For recovery from anesthesia, mice were transferred carefully into a clean recovery cage. This recovery cage was kept on a heating pad, lined with paper towels and covered with non-transparent drapes. Once mice started to exhibit their normal in behavior, they were transferred from the recovery cage. Post-operative care was involved close observation of the group housed mice (three per unit, tagged by identification tail marks) for signs of pain, infection or distress, with special attention for the first 48h. All animals were monitored daily and analgesia (0.05-2mg/kg butorphanol or 4mg/kg carprofen) was administered by subcutaneous injections if necessary. General signs of activity such as overall movement, posture and coat condition were noted. Signs of general wellbeing such as nest formation were noted. Sites of surgical incisions were inspected regularly for any swelling or discharge. Mice were weighed weekly.

At 8 weeks post implantation, mice were euthanized by CO_2 asphyxiation. Mice were kept in a CO_2 chamber which was fitted with a valve for rapid filling with CO_2. Within 1 to 2min, mice were dead.

2.8.5 Sample retrieval

At 8 weeks post-implantation, all mice were sacrificed by CO_2 inhalation. Inserted constructs were retrieved with the use of a dissecting microscope where necessary. The outcome measures used were histological staining (hematoxylin and eosin (H&E) and Safranin O/fast green), and immunohistochemistry for collagen type X.

Explants were washed twice in PBS and fixed in 10% neutral buffered formalin for 1h. The explanted samples were decalcified in 10% EDTA at pH 8 for 24h. To determine if all calcium salts were removed, samples were checked by bending and inserting a needle in the explants. EDTA was changed every 3 days until samples were ready to process at day 7. Samples were enveloped in pieces of Whatman filer paper that were pre-soaked in PBS and placed in tissue cassettes. Tissue cassettes were placed in the Leica ASP300 S automated tissue processor and the protocol from Section 2.6.1.1 was fallowed.

2.8.6 H&E staining

Slides were placed in an oven for 2h at 60ºC and subsequently hydrated (xylene twice for 10-5min, 100%, 95% and 70% ethanol 3min each) followed by exposure to water for 5min. After hydration slides were stained in Harris hematoxylin for 10min following which slides were dipped in running tap water for 5min. Then slides were dipped in acid alcohol for 3-10s. Slides were soaked in running tap water for 3min and stained in eosin (Eosin-y solution aqueous) for 5-10min. Slides were then soaked in tap water for 3min. Slides were dehydrated in alcohol (70%, 90%, 100% ethanol for 1-5min), cleared in xylene and mounted using DPX and a coverslip.

2.8.7 Safranin O/fast green staining

The 5µm thick sections were deparaffinised and hydrated (xylene twice for 5min, 100%, 95% and 70% ethanol twice for 2min) followed by water for 5min. Slides were stained with hematoxylin for 3min, counterstained with fast green for 8min and decolorized in 1% acetic acid briefly. Following this, the sections were stained for 10min in 0.1% Safranin O, dehydrated in alcohol (95%, 100% ethanol for 2min) and

cleared in xylene for 20min followed by mounting using DPX mounting medium and coverslip.

2.8.8 Histomorphometric analysis for bone formation

The constructs were explanted for microscopic examination and histomorphological evaluation. They were cut into 3 equal parts (smaller explants were left intact) which were fixed in 10% phosphate buffered formalin, decalcified with 10% EDTA for 7 days and embedded in paraffin. Four serial sections (5μm) were cut at 4-8 levels through constructs at least 100μm apart. All the sections were stained with H&E and Safranin O/fast green and examined using a histomorphological grading system.

This system (Table 2.8) was developed to take in to account the appearance, quality and volume of bone, cartilage, bone marrow, fat, fibrous matrix and blood vessels formation. This grading provided a robust qualitative aspect to the interpretation of the results. Each retrieved sample was evaluated by 3 individual blinded reviewers and the scores were averaged. Overall bone score was determined by adding the scores for calcified cartilage, bone and bone marrow. The overall bone formation in each sample was then calculated as percentage of the overall bone score for that sample with a score of 4 as 100% (Table 2.8).

2.9 Statistical analysis

All data are shown as mean ± standard deviation (SD). Unless otherwise stated, statistical significance was tested using One-Way ANOVA and Tukey's test. P value of ≤ 0.05 was set as cut off for statistical significance.

Table 2.8: Histological grading scale for subcutaneous retrieved samples The grading score took in to account the appearance of bone, cartilage, bone marrow, fat, fibrous matrix and blood vessel formation as well as surrounding host tissue.

Percent volume (%) of the total retrieved sample	Score
76-100%	4
51-75%	3
26-50%	2
1-25%	1
0%	0

2.10 References

1. Meirelles Lda, S. & Nardi, N.B. Murine marrow-derived mesenchymal stem cell: isolation, in vitro expansion, and characterization. *British journal of haematology* **123**, 702-711 (2003).
2. Sudres, M., *et al*. Bone marrow mesenchymal stem cells suppress lymphocyte proliferation in vitro but fail to prevent graft-versus-host disease in mice. *J Immunol* **176**, 7761-7767 (2006).
3. English, K., Barry, F.P. & Mahon, B.P. Murine mesenchymal stem cells suppress dendritic cell migration, maturation and antigen presentation. *Immunology letters* **115**, 50-58 (2008).
4. da Silva Meirelles, L., Chagastelles, P.C. & Nardi, N.B. Mesenchymal stem cells reside in virtually all post-natal organs and tissues. *J Cell Sci* **119**, 2204-2213 (2006).
5. Dellavalle, A., *et al*. Pericytes of human skeletal muscle are myogenic precursors distinct from satellite cells. *Nat Cell Biol* **9**, 255-267 (2007).
6. Nayak, R.C., Berman, A.B., George, K.L., Eisenbarth, G.S. & King, G.L. A monoclonal antibody (3G5)-defined ganglioside antigen is expressed on the cell surface of microvascular pericytes. *The Journal of experimental medicine* **167**, 1003-1015 (1988).
7. Powers, A.C., Rabizadeh, A., Akeson, R. & Eisenbarth, G.S. Characterization of monoclonal antibody 3G5 and utilization of this antibody to immobilize pancreatic islet cell gangliosides in a solid phase radioassay. *Endocrinology* **114**, 1338-1343 (1984).
8. Barbosa, I., *et al*. Improved and simple micro assay for sulfated glycosaminoglycans quantification in biological extracts and its use in skin and muscle tissue studies. *Glycobiology* **13**, 647-653 (2003).
9. Panin, G., *et al*. Simple spectrophotometric quantification of urinary excretion of glycosaminoglycan sulfates. *Clinical chemistry* **32**, 2073-2076 (1986).
10. Farndale, R.W., Buttle, D.J. & Barrett, A.J. Improved quantitation and discrimination of sulphated glycosaminoglycans by use of dimethylmethylene blue. *Biochim Biophys Acta* **883**, 173-177 (1986).
11. Ross, J.J., *et al*. Cytokine-induced differentiation of multipotent adult progenitor cells into functional smooth muscle cells. *The Journal of clinical investigation* **116**, 3139-3149 (2006).
12. Parhami, F., Basseri, B., Hwang, J., Tintut, Y. & Demer, L.L. High-density lipoprotein regulates calcification of vascular cells. *Circulation research* **91**, 570-576 (2002).
13. Lacey, D.C., Simmons, P.J., Graves, S.E. & Hamilton, J.A. Proinflammatory cytokines inhibit osteogenic differentiation from stem cells: implications for bone repair during inflammation. *Osteoarthritis Cartilage* **17**, 735-742 (2009).
14. Livak, K.J. & Schmittgen, T.D. Analysis of relative gene expression data using real-time quantitative PCR and the 2(-Delta Delta C(T)) Method. *Methods* **25**, 402-408 (2001).
15. Pfaffl, M.W. A new mathematical model for relative quantification in real-time RT-PCR. *Nucleic acids research* **29**, e45 (2001).

16. Coleman, R., Hayek, T., Keidar, S. & Aviram, M. A mouse model for human atherosclerosis: long-term histopathological study of lesion development in the aortic arch of apolipoprotein E-deficient (E0) mice. *Acta histochemica* **108**, 415-424 (2006).
17. Meir, K.S. & Leitersdorf, E. Atherosclerosis in the apolipoprotein-E-deficient mouse: a decade of progress. *Arteriosclerosis, thrombosis, and vascular biology* **24**, 1006-1014 (2004).
18. Nakashima, Y., Plump, A.S., Raines, E.W., Breslow, J.L. & Ross, R. ApoE-deficient mice develop lesions of all phases of atherosclerosis throughout the arterial tree. *Arteriosclerosis and thrombosis : a journal of vascular biology / American Heart Association* **14**, 133-140 (1994).
19. Tierney, E.G., Duffy, G.P., Hibbitts, A.J., Cryan, S.A. & O'Brien, F.J. The development of non-viral gene-activated matrices for bone regeneration using polyethyleneimine (PEI) and collagen-based scaffolds. *Journal of controlled release : official journal of the Controlled Release Society* **158**, 304-311 (2012).

Chapter 3

Isolation and Characterization of Murine Mesenchymal and Vascular Stem Cells

3.1 Introduction

In general, the vessel wall is considered to be composed of very limited number of cells of mesodermal origin organized in the orderly fashion to form three layers of the wall, each layer with a specific function and characteristics. The intimal layer is composed of endothelial cells (ECs) creating the interface with blood. Apart from a permeability barrier function, ECs act to regulate hemostasis, recruit leukocytes and control vascular tone. Several layers of SMCs form the media of the vessel wall. SMCs mainly act as contractile moieties with synthetic abilities. The outermost layer called the adventitia is composed of dense fibrous and adipose tissue. Apart from the normal structural and synthetic function in physiology, the contribution of ECs and SMCs to vascular remodeling in disease states has been studied in connection with the response to injury model. The notion that the progenitor cells which give rise to cells of the vessel wall in the embryo remain in the niche and are activated to repair/regenerate the vascular wall in adults has become quite popular in the recent past. While the embryological origins of these cells are being studied, the existence of bone marrow derived and resident stem progenitor cells in the vessel wall is increasingly being examined.

In this study, the presence of stem progenitors in the vessel wall was investigated to unravel their role, if any, in the pathogenesis of atherosclerosis, a major vascular debilitating disease. To that end, the presence of resident progenitor cells was investigated in aortae of normal background C57BL/6 mice and ApoE$^{-/-}$ mice. The latter strain is established as a model of atherosclerosis[1,2]. The characterization, in terms of surface signature and differentiation potential of cells from both aortae and bone marrow of the normal and diseased animal models, was performed to assess potential differences that might be of relevance in the pathology of atherosclerosis. Additionally, the pericyte nature of the isolated cells was explored.

CD146 and 3G5 were of particular interest as pericyte-specific markers. CD146 expression on perivascular cells around small vessels was assessed in a previous study[3] by CD146 and NG2 double staining. This along with other markers have been used as an indicator of pericyte/perivascular cell identity. CD146 and NG2 expression has also

been shown on larger blood vessels[3]. However, another finding suggests that $CD146^+$ cells in the subendothelial layer in bone marrow in humans comprises osteogenic progenitors, similar to ones at the origin of stromal cells involved in maintenance of hematopoiesis[4]. The 3G5 antigen is a cell surface ganglioside typically found on vascular pericytes which have multidifferentiation potential[5-7]. Pericytes have been accounted as stem niches[8-10] and 3G5 has been utilized to identify pericyte-like cells in various human tissues[11]. A study has shown that a small population of bone marrow derived MSCs is 3G5 positive[12].

3.2 Results

3.2.1 MSC Isolation from $ApoE^{-/-}$, C57BL/6 mice and C57BL/6 GFP^+ mice

Mesenchymal stem cells were isolated from bone morrow with BMMNC harvested from femur and tibias of $ApoE^{-/-}$, C57BL/6 and C57BL/6 GFP^+ mice. Different protocols were assessed for each strain of mice. The protocol modified from that described by da Silva Meirelles and Nardi in 2003[13] was successful for $ApoE^{-/-}$ MSC isolation (Section 2.1.1). MSCs from C57BL/6 and C57BL/6 GFP^+ mice were isolated by a protocol modified from the one described by Sudres *et al*.[14] (Section 2.1.2). After 2-3 weeks of culture, a heterogeneous population was seen, generally referred to as bone marrow stroma (Fig. 3.1). Further maintenance of culture with thrice weekly medium changes and removal of non-adherent cells resulted in a relatively homogeneous culture of cells morphologically similar to MSCs after 3 weeks. The mean yield from $175cm^2$ flasks varied between 2×10^6 to 4×10^6 cells. Cell lines were stable by passage 5, thereafter monolayer cultures were confluent for passaging every 3-4 days while seeding at 2.8×10^3 cells/cm^2. Cultures were maintained for variable period by subculturing as described in section 2.1.1.Culture media varied between the strains. Although C57BL/6 is the background strain for $ApoE^{-/-}$ mice, the isolation of MSCs following the same methods was not successful. For establishment of long term cultures (LTC), various media were tested. DMEM-HEPES containing 10% FBS did not support C57BL/6 MSCs growth. However, α-MEM as the basal medium was found to maintain LTC in presence of serum.

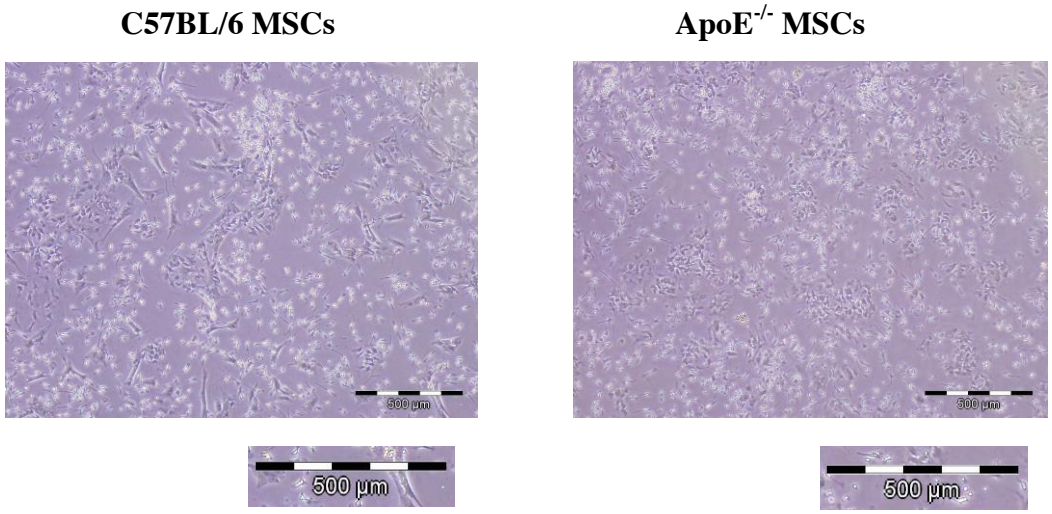

Figure 3.1 Cultures of isolated MSCs. Representative image of bone marrow stroma-like appearance after 10 days post plating of C57BL/6 and ApoE$^{-/-}$ MSCs at passage 0. Scale bars represent 500µm.

Growth curves illustrating culture kinetics were created as described previously[13]. Representative growth curves and morphology (right panels) from different preparations of MSC cultures from ApoE$^{-/-}$, C57BL/6, C57BL/6 GFP^{+} are shown in figures 3.2, 3.3 and 3.4, respectively. The growth characteristics varied slightly with different strains. All cultures demonstrated a very low growth rate during early passages, as suggested by the lower slope of the curves. However, with serial subcultures, growth rate increased consistently until stable cultures were established. The time point where contaminating hematopoietic cells failed to detach during subculture or underwent apoptosis varied between strains.

For ApoE$^{-/-}$ mesenchymal outgrowth was apparent from passage 1 or 2 and increased consistently until stable cultures were established after approximately 60 days in culture (Fig. 3.2). The mMSCs were generally observed to be morphologically highly heterogeneous before passage 5 and comprised round, spindle-shaped, and flattened cells (Fig. 3.2 A & B ii). After passage 5, most cells were spindle shaped and few round cells were observed. The morphology was not altered and the cells continued to proliferate after passage 22. Under the conditions described above, cell confluency was usually reached between 20-22 days in passage 0. The interval between passages varied greatly until passage 5 thereafter, a passage interval approximately 4 days was set. In LTC, continuous cell growth was observed in all cell cultures. In ApoE$^{-/-}$ MSCs, an increasing growth rate was observed that was constant till passage 16. The doubling time was analyzed at each passage over the extended cell culture. There were no significant changes observed between passages with regard to the time required for population doubling.

A) Pooled cell preparation 1

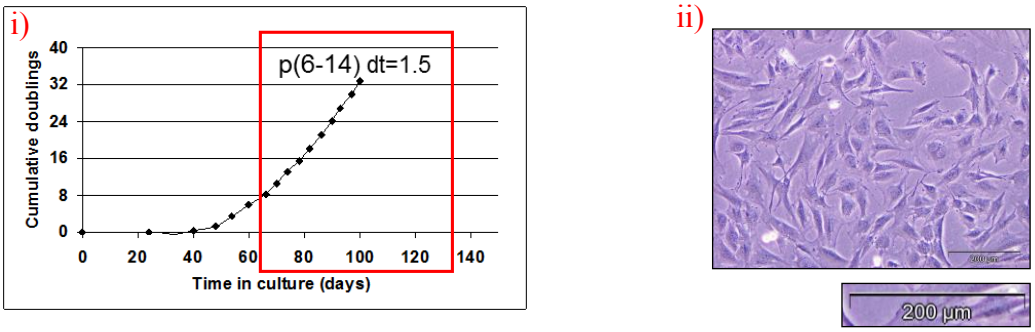

B) Pooled cell preparation 2

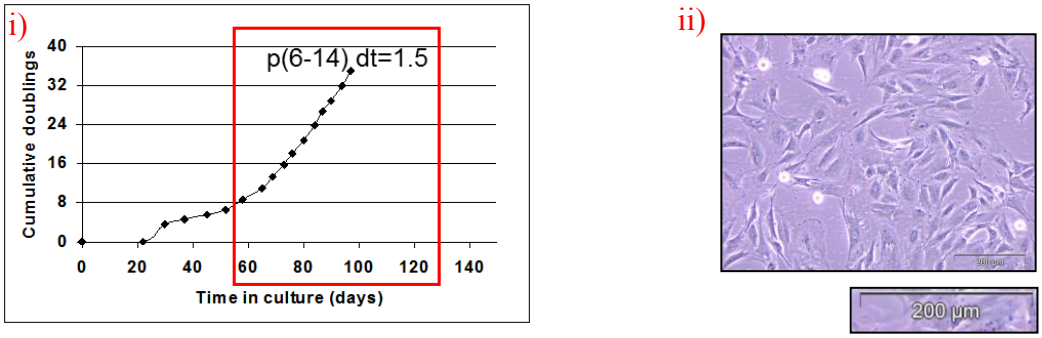

C) Pooled cell preparation 3

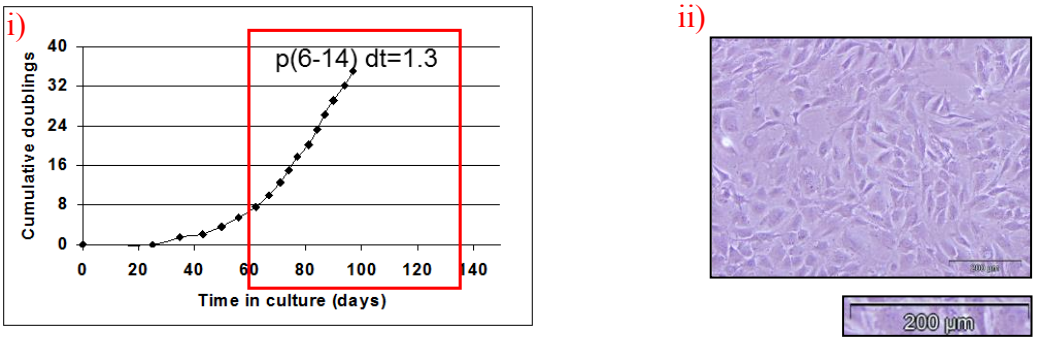

Figure 3.2: Growth and morphology of different preparations of MSCs isolated from ApoE$^{-/-}$ mice. Cumulative population doublings over time were determined for 3 different MSC preparations established from pooled marrow from 3 ApoE$^{-/-}$ mice. Doubling time for established cultures from passage 6-14 varied from 1.3 days (C i) to 1.5 days for preparations 1 and 2 (A & B i). Representative images from each preparation at passage 7 showed characteristic fibroblast morphology for all (A, B & C ii). Scale bars represent 200µm.

For C57BL/6 MSC preparations, compared to ApoE$^{-/-}$, the growth was slower until passage 6.

For C57BL/6 mesenchymal outgrowth was apparent from passage 1 - 3 and increased consistently until stable cultures were established between 75-100 days in culture (Fig. 3.3). Morphologically, highly heterogeneous cultures were observed before passage 5 and comprised of spindle-shaped and flattened cells (Fig. 3.3 A, B & C ii). After passage 5, most cells were spindle shaped and very few round cells were observed. The morphology was not altered and the cells continued to proliferate after passage 20. Under the conditions described above, cell confluency was usually reached between 15-22 days in passage 0. The interval between passages varied greatly until passage 7; thereafter, a passage interval of approximately 4-5 days was set. In LTC, continuous cell growth was observed in all cell cultures. The doubling time was analyzed at each passage over the extended cell culture. There were no significant changes observed between passages with regard to the time required for population doubling.

A) Pooled cell preparation 1

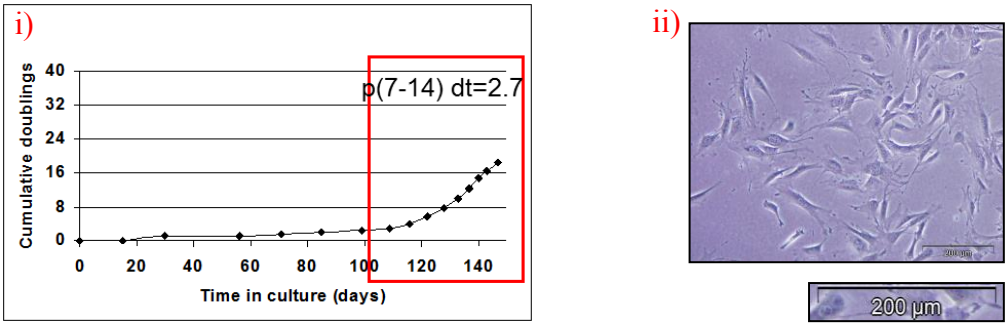

B) Pooled cell preparation 2

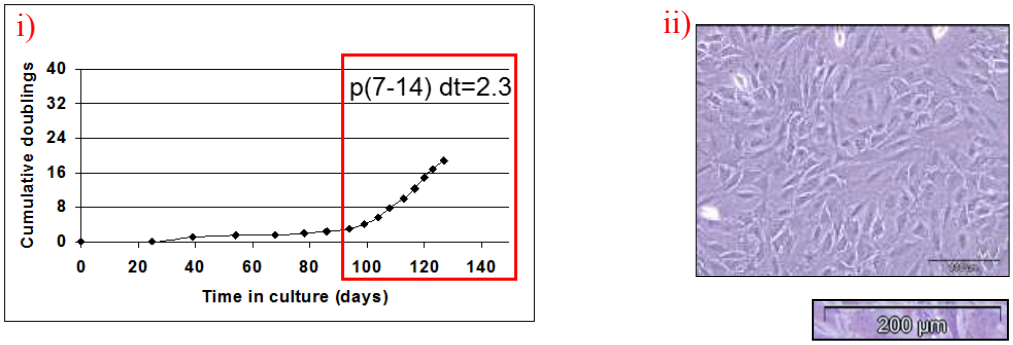

C) Pooled cell preparation 3

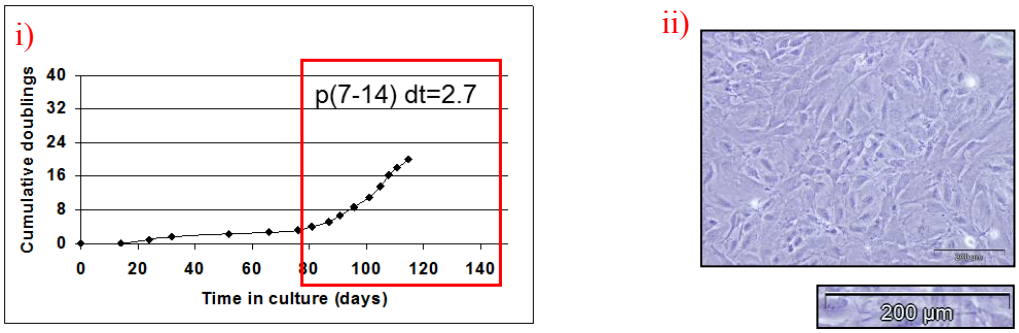

Figure 3.3: Growth and morphology of MSCs isolated from C57BL/6 mice. Cumulative population doublings over time were determined for 3 different MSC preparations established from pooled marrow from 3 C57BL/6 mice. Doubling time for established cultures from passage 7-14 varied from 2.3 days (B i) to 2.7 days for preparations 1 and 2 (A & C i). Representative images from each preparation at passage 7 showed characteristic fibroblast morphology for all (A, B & C ii). Scale bars represent 200µm.

For C57BL/6 GFP^+ mice, mesenchymal outgrowth was apparent from passage 1 - 3 and increased consistently until stable cultures were established between 45-90 days in culture (Fig. 3.4). Morphologically highly heterogeneous cultures were observed before passage 4 and comprised of spindle-shaped and flattened cells (Fig. 3.4 A, B ii). After passage 4, most cells were spindle shaped and very few round cells were observed. The morphology was not altered and the cells continued to proliferate to passage 15. Under the conditions described above, cell confluency was usually reached between 25-30 days in passage 0. The interval between passages varied greatly until passage 7; thereafter, a passage interval of approximately 3-5 days was set. In LTC, continuous cell growth was observed in all cell cultures. The doubling time was analyzed at each passage over the extended cell culture. There were no significant changes observed between passages with regard to the time required for population doubling.

A) Pooled cell preparation 1

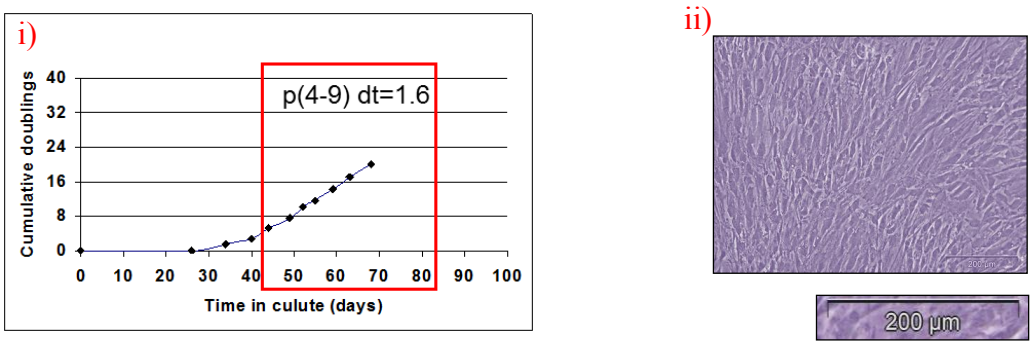

B) Pooled cell preparation 2

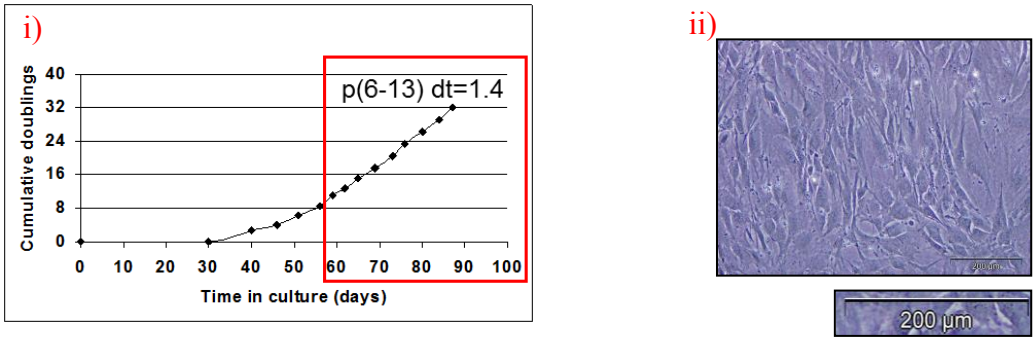

Figure 3.4: Growth and morphology of MSCs isolated from C57BL/6 GFP$^+$ mice. Cumulative population doublings over time were determined for 3 different MSC preparations established from pooled marrow from 3 C57BL/6 GFP$^+$ mice. Doubling time for established cultures from passage 4-13 varied from 1.4 days (B i) to 1.6 days (A i). Representative images from each preparation at passage 7 showed characteristic fibroblast morphology for all (A & B ii). Scale bars represent 200µm.

3.2.2 VSC Isolation form ApoE$^{-/-}$ and C57BL/6 mice

3.2.2.1 ApoE$^{-/-}$ VSC culture and isolation

VSC cultures were established as described in section 2.2.1. Aortas were dissected from euthanized mice and cut into small pieces prior to digestion in 0.5mg/ml collagenase solution in DMEM-HEPES using the two-step method. The first cell fraction was obtained after 30 min of digestion. After a further 30min digestion, the second cell fraction was obtained as described (section 2.2.1). Both cell fractions were used to establish separate primary cultures. Initially, the cells were seeded into six-well plates. After 24h seeding, it was observed that both cell fractions demonstrated a similar morphology to MSCs. After three days of culture, isolated cells formed small colonies (Fig. 3.5). At this stage, cultures were washed and the culture medium was replaced with fresh medium containing no antibiotics or antimycotics. The adherent layer was re-fed every 3 or 4 days. Since the time required for confluence was dependent on the starting amount of aorta, aortas from three ApoE$^{-/-}$ mice were combined to enable subculture within 14 days. Cultures were split at confluence. The ratios of splitting were determined empirically to ensure adequate growth for 7 days in subcultures. Thus, initial ratios were typically 1:2 or 1:3. However, as growth kinetics changed to faster rates at later passages, ratios were 1:6 or 1:8 until the cultures stabilized. At initial passages, P1 to P4, adherent cells demonstrated a heterogeneous morphology. This heterogeneity was attributed to contamination from either hematopoietic cells or surrounding tissue remaining from the collagenase digestion.

Homogeneous cultures started to predominate gradually with flat cells having large nuclei present primarily in the cultures, irrespective of the cell fraction. However, cells from the early first fraction appeared senescent after passage 4. Hence, in further experiments, cells from the second fraction, with potentially less contaminants such as debris, fat, endothelial basement membrane and/or adventitia containing smooth muscle cells, were used. Thus, long term cultures were established only using the second cell fraction.

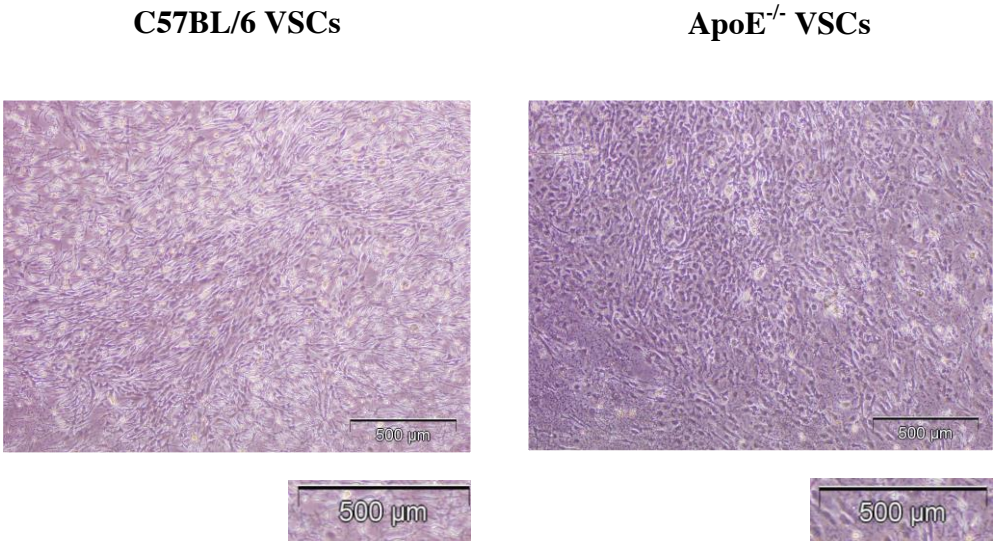

Figure 3.5: Cultures of isolated VSCs. Representative image of the pericyte-like appearance after 7 days post plating of C57BL/6 and ApoE$^{-/-}$ VSCs at passage 0. Scale bars represent 500µm.

Growth curves describing the culture kinetics were generated based on the population doublings. The population doublings were calculated as described in Sections 2.1.3 and 2.2.3. Examples of growth curves (left panels) and morphology (right panels) of 3 preparations of VSCs from ApoE$^{-/-}$ mice are shown in Figure 3.6. For ApoE$^{-/-}$ VSCs, outgrowth in the form of dense colonies was apparent until passage 1 or 2 and then more stable cultures with homogenous growth in monolayer were established after approximately 55 days in culture (Fig. 3.6). VSCs were generally observed to be morphologically highly heterogeneous before passage 6 and comprised elongated and flattened cells. After passage 6, most cells were morphologically similar to MSCs. The morphology was not altered and the cells continued to proliferate after passage 15. Under the culture conditions described in section 2.2.1, cell confluency was usually reached between 15-22 days in passage 0. The interval between passages varied greatly until passage 6; thereafter, a passage interval of approximately 4 days was set. In LTC, continuous cell growth was observed in all cell cultures. In ApoE$^{-/-}$ VSCs, an increasing growth rate was observed that was constant till passage 15. The doubling time was analyzed at each passage over the extended cell culture. There were no significant changes observed between passages with regard to the time required for population doubling.

A) Pooled cell preparation 1

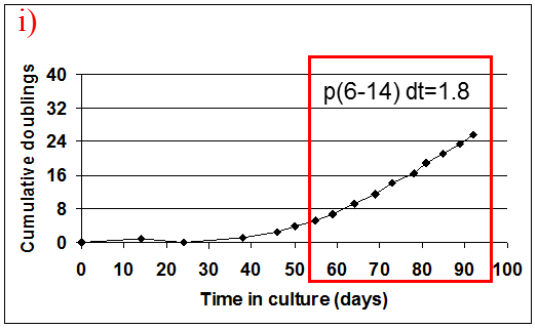

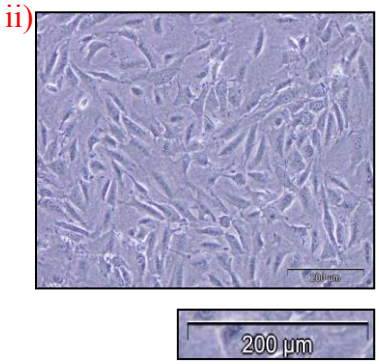

B) Pooled cell preparation 2

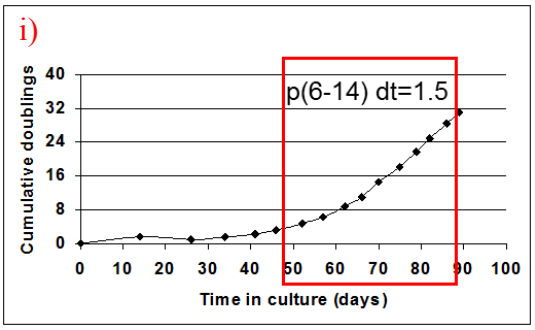

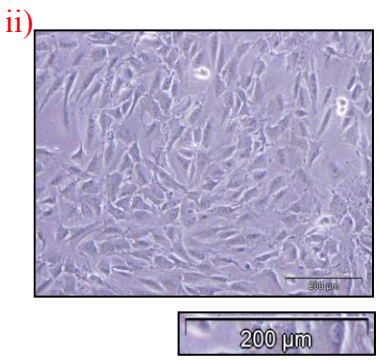

C) Pooled cell preparation 3

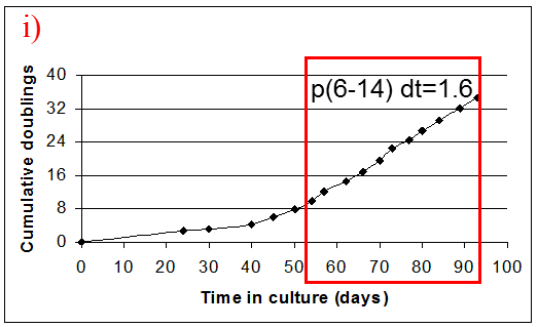

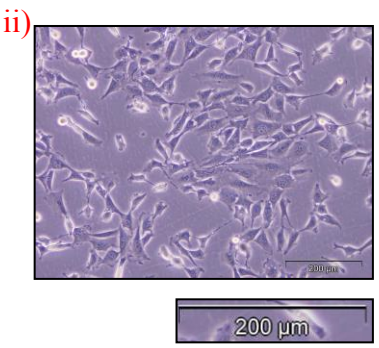

Figure 3.6: Growth and morphology of VSCs isolated from ApoE$^{-/-}$ mice. Cumulative population doublings over time were determined for 3 different VSC preparations established from pooled aortas from 3 ApoE$^{-/-}$ mice. Doubling time for established cultures from passage 6-14 varied from 1.5 days (B i) to 1.8 days (A i). Representative images from each preparation at passage 7 showed morphology similar to MSCs for all (A, B & C ii). Scale bars represent 200µm.

3.2.2.2 C57BL/6 VSC culture and isolation

For establishing the VSC cultures form C57BL/6 mice, the same protocol as described for VSCs from ApoE$^{-/-}$ mice was followed (section 2.2.1). Although, ultimately successful cultures were established, it was difficult to obtain VSCs using this protocol. Hence, additionally the protocol described by A. Dellavalle[15] where dissected fragments of aortas plated on collagen coated plates were utilized to establish VSCs cultures as described in section 2.2.2 was used. For all further analyses, VSCs isolated by the first protocol were used.

Growth kinetics were studied by generating growth curves based on population doublings in a similar fashion as for ApoE$^{-/-}$ VSCs. Population doublings were calculated as described in Sections 2.1.3 and 2.2.3. Representative examples of growth curves (left panel) and morphology (right panels) from different preparations of VSCs from C57BL/6 mice are shown in figure 3.7. Similar to ApoE$^{-/-}$ VSCs, initial outgrowth in the form of dense colonies was apparent until passage 1 or 2 and then more stable cultures with homogenous growth in monolayer were established after approximately 45 and 72 days in culture (Fig. 3.7). VSCs were generally observed to be morphologically highly heterogeneous before passage 6 and comprised elongated and flattened cells. After passage 6, most cells were morphologically similar to MSCs. The morphology was not altered and the cells continued to proliferate after passage 15. Under the culture conditions described in section 2.2.2, cell confluency was usually reached between 7-22 days in passage 0. The interval between passages varied greatly until passage 6; thereafter, a passage interval of approximately 3-5 days was set. In LTC, continuous cell growth was observed in all cell cultures. In C57BL/6 VSCs, an increasing growth rate was observed that was constant till passage 15. The doubling time was analyzed at each passage over the extended cell culture. There were no significant changes observed between passages with regard to the time required for population doubling.

A) Pooled cell preparation 1

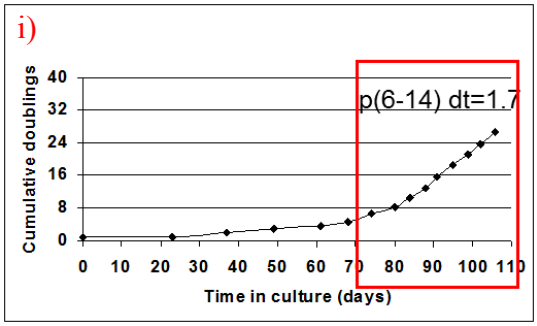

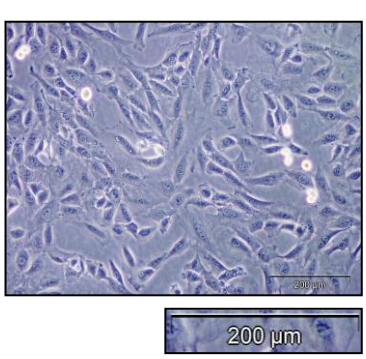

B) Pooled cell preparation 2

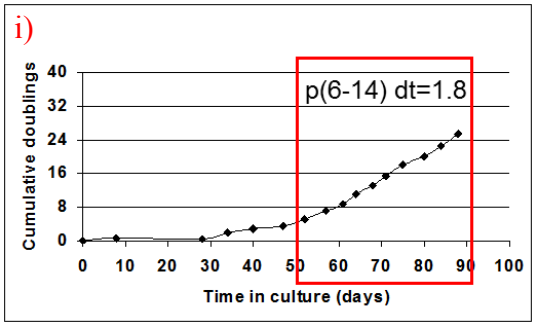

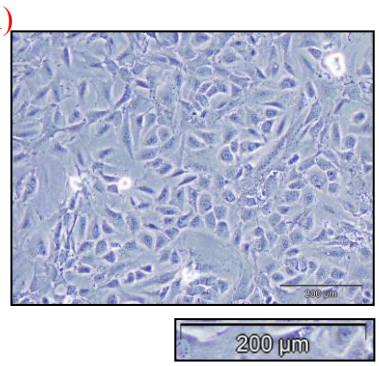

C) Pooled cell preparation 3

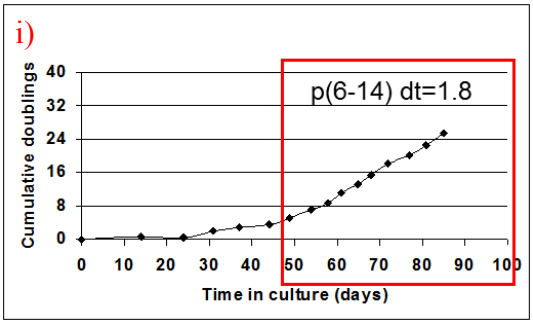

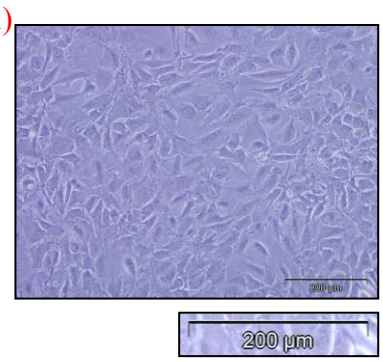

Figure 3.7: Growth and morphology of VSCs isolated from C57BL/6 mice. Cumulative population doublings over time were determined for 3 different VSC preparations established from pooled aortas from 3 C57BL/6 mice. Doubling time for established cultures from passage 6-14 varied from 1.7 days (A i) to 1.8 days (B & C i). Representative images from each preparation at passage 7 showed morphology similar to MSCs for all (A, B & C ii). Scale bars represent 200µm.

3.2.3 Cell surface characterization of MSCs and VSCs.

Antigen expression profiles of the MSCs and VSCs were investigated by flow cytometry. To determine whether VSCs and MSCs express putative stem cell, hematopoietic, endothelial or pericyte/perivascular cell surface markers, flow cytometry was performed on cell cultures with mouse specific antibodies to CD antigens 3, 9, 19, 31, 34, 44, 45, 90.2, 105, 146, Gr-1, Sca-1, Tie-2 and Nk1.1 as described in section 2.5.

Table 3.1 Surface characteristic of isolated cells by flow cytometry. Values are presented as the mean ±SD of 3 preparations and represent percentage positive cells

Surface marker expression	C57BL/6 MSCs	C57BL/6 VSCs	ApoE$^{-/-}$ MSCs	ApoE$^{-/-}$ VSCs
Hematopoietic associated antigens				
Gr-1	0.048±0.01	1.03±0.65	0.693±0.11	0.482±0.32
CD3	0.273±0.15	0.21±0.1	0.633±0.39	0.156±0.17
CD9	91.033±9.46	97.43±2.25	97.53±1.42	87.63±8.83
CD19	0.095±0.92	1.45±1.54	1.68±0.42	1.65±1.47
CD34	0.111±0.08	2.57±1.38	1.68±0.97	1.76±0.90
CD45	0.099±0.12	0.78±0.72	1.1±0.42	0.973±1.23
NK-1.1	0.036±0.02	0.661±0.67	0.67±0.25	0.413±0.25
CD105	0.21±0.27	4.95±3.28	1.04±0.21	4.4±4.9
CD117	0.06±0.01	1.53±1.13	2.67±2.16	0.83±0.81
Endothelial associated antigens				
CD31	0.09±0.12	0.89±0.80	0.76±0.17	1.02±1.24
MSC associated antigens				
Sca-1	86.5±4.84	91.73±4.12	91.46±1.7	95.16±2.8
CD44	59.05±1.34	70.2±11.59	66.26±2.05	77.93±9.71
CD90.2	16.6±2.26	97.86±2.23	6.54±0.13	81.35±0.91
Pericyte associated antigens				
3G5	0.72±0.92	9.29±2.14	1.44±0.34	41±1.43
Tie-2	1.02±0.43	0.57±0.83	0.28±0.37	0.54±0.31
CD146	2.29±2.25	43.66±5.51	1.03±1.4	47.6±3.41

3.2.3.1 Cell surface analysis of mesenchymal stem cell markers in MSCs and VSCs

It was necessary to assess the expression of the typical MSC markers considering the heterogeneity of the populations Sca-1, CD44 and CD90.2 were analysed as stem cell markers. The data indicated that all the cell preparations expressed these markers suggesting their stemness. CD90 expression is strong in MSCs from many species including mice; however, different strains of mice express either CD90.1 or CD90.2[16] Hence, in this study we used CD90.2 was used. VSCs from both C57BL/6 and ApoE$^{-/-}$ mice were strongly positive (97.86% and 81.35%, respectively) while MSCs were weakly positive (16.6% and 6.54%, respectively) (Fig. 3.8).

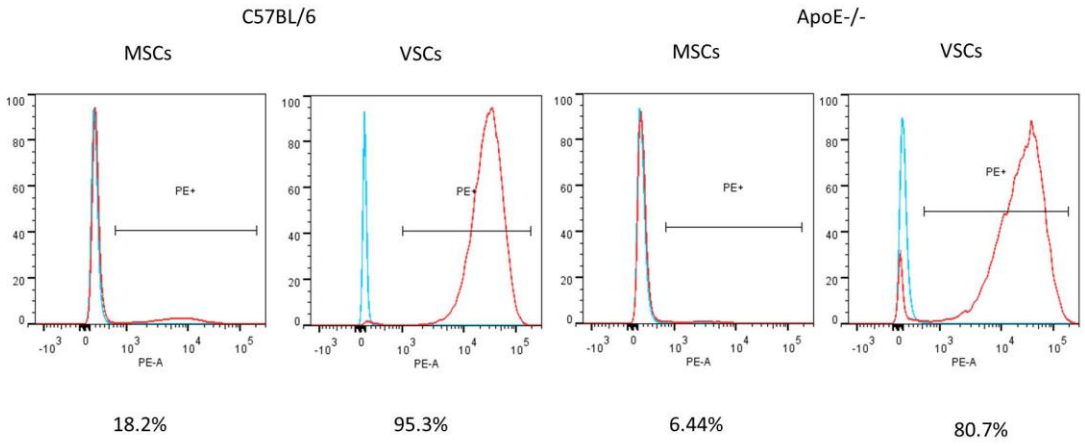

Figure 3.8 Representative flow cytometry histogram of CD90.2 expression in ApoE$^{-/-}$ and C57BL/6 MSC and VSC. Cells were stained at passage 6 with a specific monoclonal antibody against CD90.2 (red line). Blue lines indicate isotype-matched mouse immunoglobulin G antibody control staining. Both MSCs were weakly positive while the VSCs were strongly positive.

Sca-1 is murine hematopoietic and mesenchymal stem/progenitor cell marker[17]. Recently, in combination with platelet-derived growth factor receptor α (PDGF-α), Sca-1 was successfully used as selective mouse MSC marker[18]. VSCs from both C57BL/6 and ApoE$^{-/-}$ mice were strongly positive (91.73% and 95.16%, respectively). Similarly, MSCs were also strongly positive (85.5% and 91.46%, respectively) (Fig. 3.9).

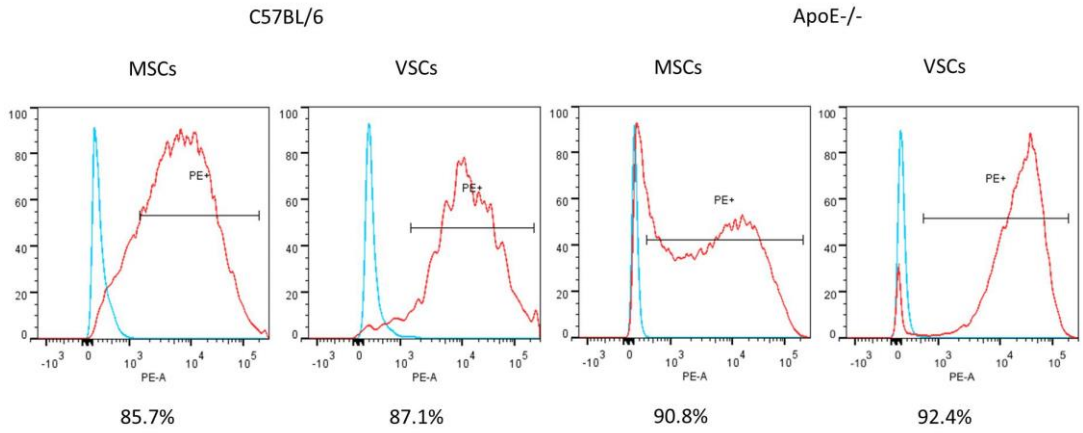

Figure 3.9 Representative flow cytometry histogram of Sca-1 expression in ApoE$^{-/-}$ and C57BL/6 MSC and VSC. Cells were stained at passage 6 with a specific monoclonal antibody against Sca-1 (red line). Blue lines indicate isotype-matched mouse immunoglobulin G antibody control staining. Both MSCs and VSCs were strongly positive.

CD44 is one of the markers consistently expressed on MSCs across species. However, many different cell types including MSCs express CD44 leading to lack of specificity[19]. A recent proposition is that CD44 is involved in stem cell pluripotency[20]. Again, due to a significant role of CD44 in cell-matrix interaction, adhesion and resistance to apoptosis, CD44 is on its own is not considered as a robust marker of MSCs. Nevertheless, along with other MSCs markers, CD44 can be considered to be a complementary marker. VSCs from both C57BL/6 and ApoE$^{-/-}$ mice were positive (70.2% and 77.93%, respectively). Similarly, MSCs were also positive (59.05% and 66.26%, respectively) (Fig. 3.10).

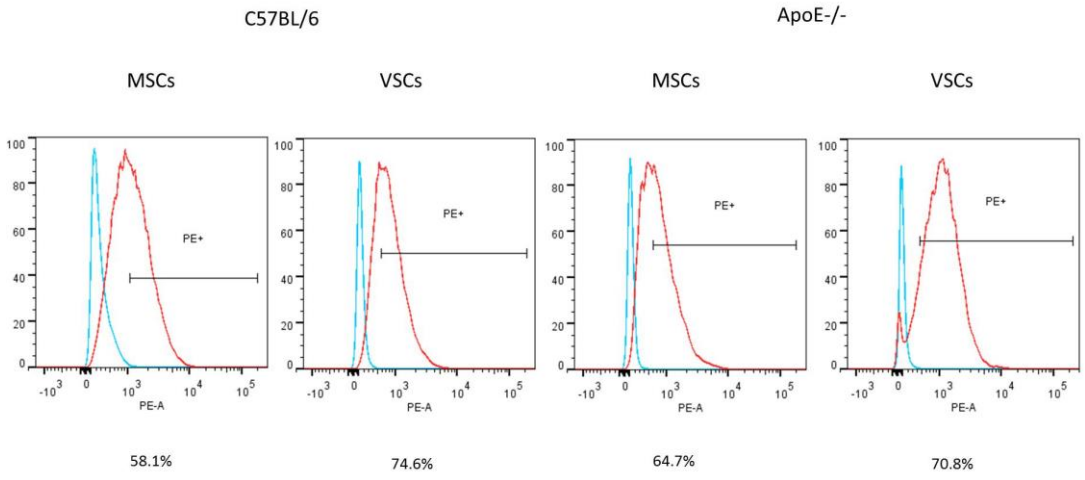

Figure 3.10 Representative flow cytometry histogram of CD44 expression in ApoE$^{-/-}$ and C57BL/6 MSC and VSC. Cells were stained at passage 6 with a specific monoclonal antibody against CD44 (red line). Blue lines indicate isotype-matched mouse immunoglobulin G antibody control staining. Both MSCs and VSCs were positive.

3.2.3.2 Cell surface analysis of hematopoietic markers

CD34 is a cell surface marker that is expressed in early stages in both hematopoietic and angioblastic lineages[21]; however, its expression is retained in the angioblastic lineage but lost in the hematopoietic lineage[22]. Although CD34-deficient mice do not show an obvious developmental phenotype, CD34 deficiency presents with unique hematopoietic defects compatible with its expression by hemangioblastic stem cells[23,24]. CD34 is a pan-endothelial marker of endothelial cells in microvasculature however most of the large blood vessels do not express it[25,26]. Recently it has been that lymphatic endothelial cells in human tumors also express CD34[27].

CD34 is considered to be hallmark of murine as well as human hematopoietic stem cells[28]. Studies have observed CD34 expression on vascular endothelial cells, basement membrane structures and dendritic and perifollicular cells in human skin[29,30]. CD34 expression has been utilized to separate human bone marrow cells[30]. However, following in vivo culture of these stromal cells, there is no reaction with CD34 antibodies[31]. In a similar fashion, endothelial cells of human umbilical vein have a disputable expression of CD34 as it is not found in vitro[26]. VSCs from both C57BL/6 and ApoE$^{-/-}$ mice were negative (2.57% and 1.76%, respectively). Similarly, MSCs were also negative (0.11% and 1.68%, respectively) (Fig. 3.11).

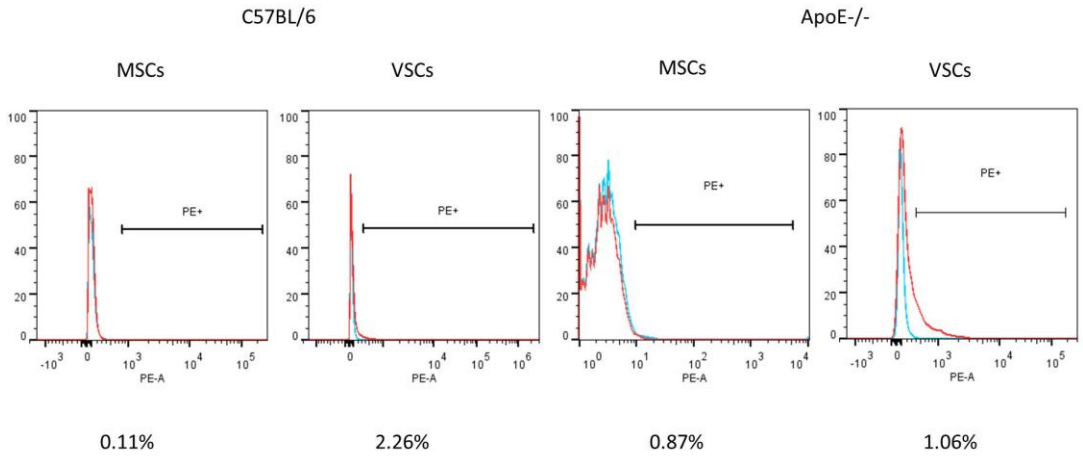

Figure 3.11 Representative flow cytometry histogram of CD34 expression in ApoE$^{-/-}$ and C57BL/6 MSC and VSC. Cells were stained at passage 6 with a specific monoclonal antibody against CD34 (red line). Blue lines indicate isotype-matched mouse immunoglobulin G antibody control staining. Both MSCs and VSCs were negative.

All mature T-cells have CD3 antigen bound to their membranes. This expression is almost exclusive to T-cells with the exception of purkinje cells where CD3 is present in small amounts. VSCs from both C57BL/6 and ApoE$^{-/-}$ mice were negative (0.21% and 0.15%, respectively). Similarly, MSCs were also negative (0.27% and 0.63%, respectively) (Fig. 3.12).

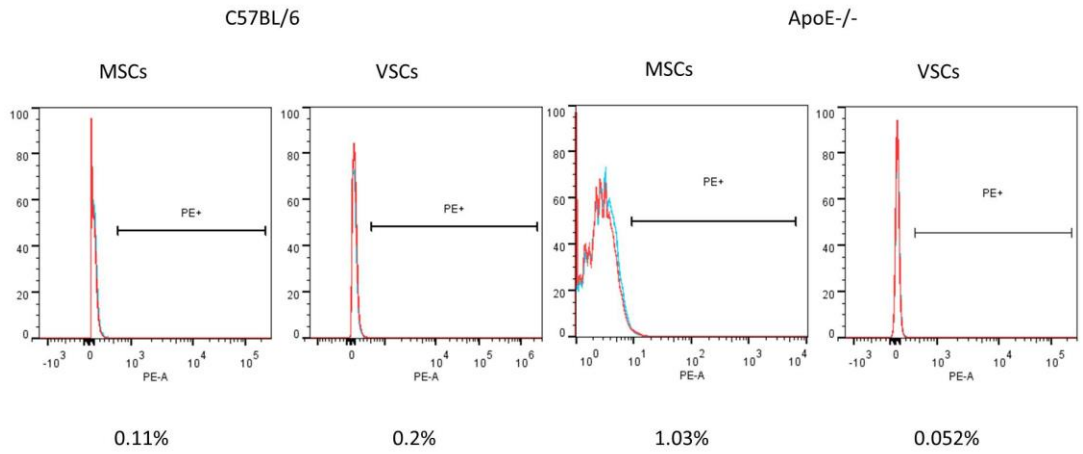

Figure 3.12 Representative flow cytometry histogram of CD3 expression in ApoE$^{-/-}$ and C57BL/6 MSC and VSC. Cells were stained at passage 6 with a specific monoclonal antibody against CD3 (red line). Blue lines indicate isotype-matched mouse immunoglobulin G antibody control staining. Both MSCs and VSCs were negative.

Neutrophils have a high level of expression of Gr-1[32]. VSCs from both C57BL/6 and ApoE$^{-/-}$ mice were negative (1.03% and 0.48%, respectively). Similarly, MSCs were also negative (0.04% and 0.69%, respectively) (Fig. 3.13).

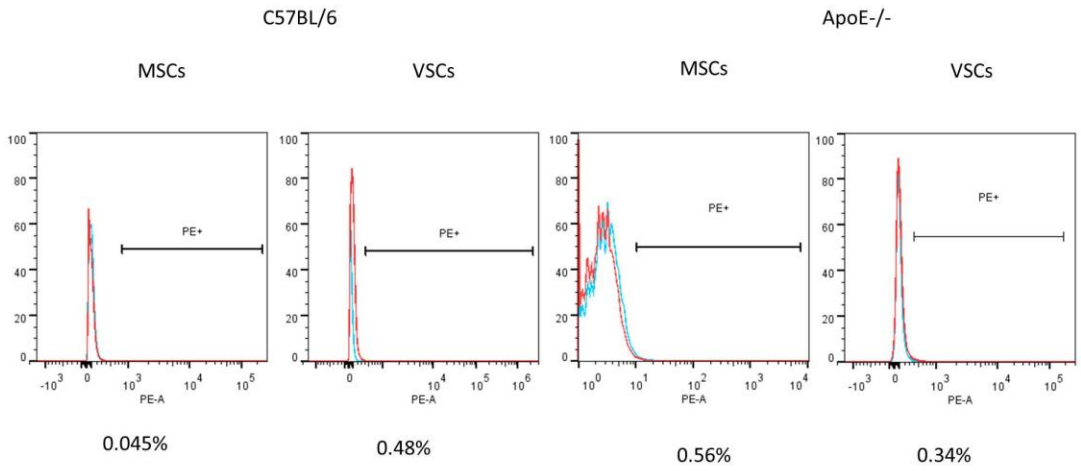

Figure 3.13 Representative flow cytometry histogram of Gr-1 expression in ApoE$^{-/-}$ and C57BL/6 MSC and VSC. Cells were stained at passage 6 with a specific monoclonal antibody against Gr-1 (red line). Blue lines indicate isotype-matched mouse immunoglobulin G antibody control staining. Both MSCs and VSCs were negative.

CD9 belongs to the tetraspanin family and has been found to be expressed in human mesenchymal stem cells to different degrees[33]. CD9 has been shown to influence cell proliferation, motility, and adhesion.

For example, in human adipose derived stem cells, clonal expansion has been directly related to CD9 expression, where cells with high expression showed increased ability to proliferate and adhere, tube formation in vitro, and higher ICAM-1 and eNOS expression compared cells with low expression[34,35]. CD9 expression has been linked with efficacy of human adipose derived stem cells[35]. It is one of the markers currently used to define MSCs[36]. It has been shown that hematopoiesis can be controlled by treatment of stromal cells with CD9 antibody[33]. VSCs from both C57BL/6 and ApoE$^{-/-}$ mice were strongly positive (97.43% and 87.63%, respectively). Similarly, MSCs were also strongly positive (91.03% and 97.53%, respectively) (Fig. 3.14).

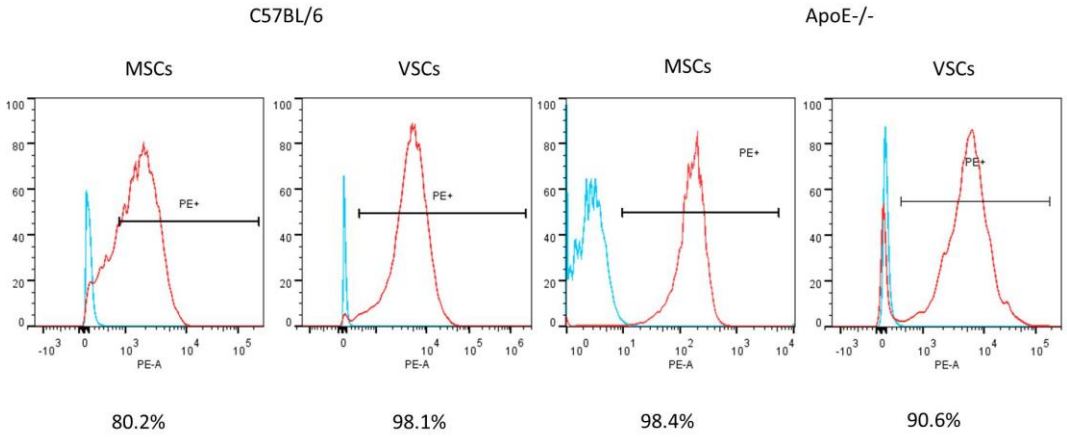

Figure 3.14 Representative flow cytometry histogram of CD9 expression in ApoE$^{-/-}$ and C57BL/6 MSC and VSC. Cells were stained at passage 6 with a specific monoclonal antibody against CD9 (red line). Blue lines indicate isotype-matched mouse immunoglobulin G antibody control staining. Both MSCs and VSCs were strongly positive.

Expression of CD19 has been shown to be good distinguishing factor between $CD34^{+}CD19^{+}$ and $CD34^{+}CD19^{-}$ progenitor/stem cells where the later represents a more immature phenotype in newly diagnosed B-cell precursor acute lymphoblastic leukemia[37]. VSCs from both C57BL/6 and $ApoE^{-/-}$ mice were negative (1.45% and 1.65%, respectively). Similarly, MSCs were also negative (0.09% and 1.68%, respectively) (Fig. 3.15).

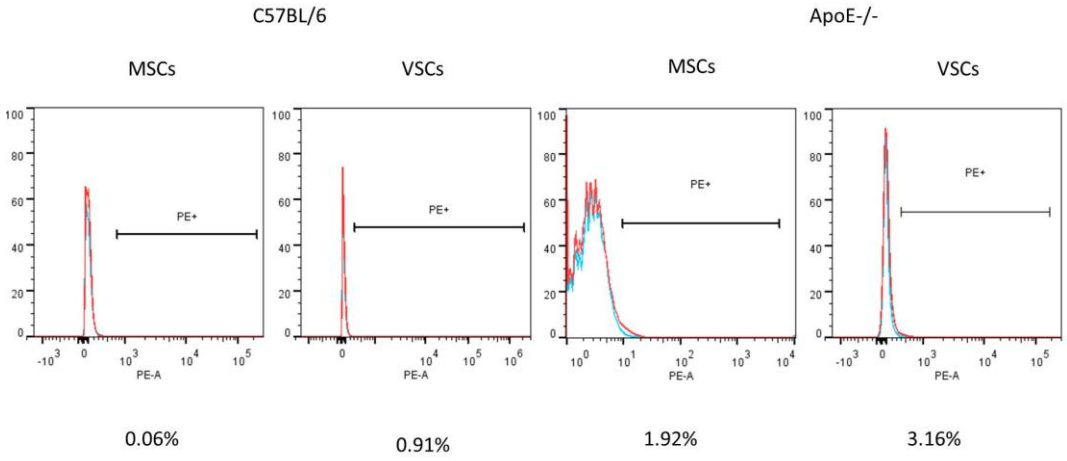

Figure 3.15 Representative flow cytometry histogram of CD19 expression in $ApoE^{-/-}$ and C57BL/6 MSC and VSC. Cells were stained at passage 6 with a specific monoclonal antibody against CD19 (red line). Blue lines indicate isotype-matched mouse immunoglobulin G antibody control staining. Both MSCs and VSCs were negative.

CD45 is most profusely expressed on leukocytes and usually considered to be exclusive to the hematopoietic system. However, in patients with hematological malignancies in some instances CD45 expression can be found on bone marrow derived MSCs[38].

It has been shown that CD45 is a hematopoietic marker with an expression pattern that changes to negative with increasing passages of MSC[39]. On the contrary, CD106 expression pattern shifts positively[39]. VSCs from both C57BL/6 and ApoE$^{-/-}$ mice were negative (0.78% and 0.97%, respectively). Similarly, MSCs were also negative (0.09% and 1.1%, respectively) (Fig. 3.16).

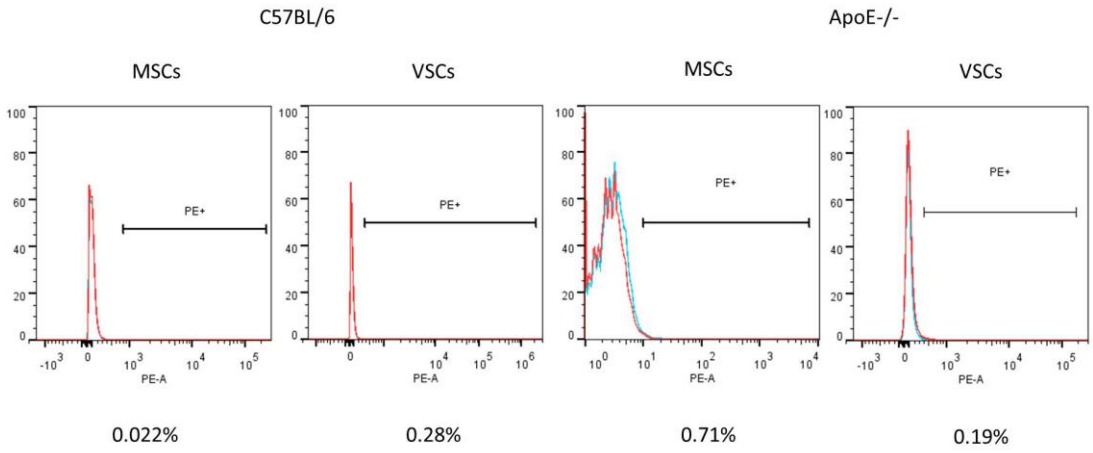

Figure 3.16 Representative flow cytometry histogram of CD45 expression in ApoE$^{-/-}$ and C57BL/6 MSC and VSC. Cells were stained at passage 6 with a specific monoclonal antibody against CD45 (red line). Blue lines indicate isotype-matched mouse immunoglobulin G antibody control staining. Both MSCs and VSCs were negative.

Natural killer (NK) cells are components of innate immunity. NK1.1 is one of the identifying markers for NK cells. Since NK cells acquire these markers through their development from hematopoietic stem cells[40], we investigated this marker for all cells we isolated. VSCs from both C57BL/6 and ApoE$^{-/-}$ mice were negative (0.66% and 0.41%, respectively). Similarly, MSCs were also negative (0.03% and 0.67%, respectively) (Fig. 3.17).

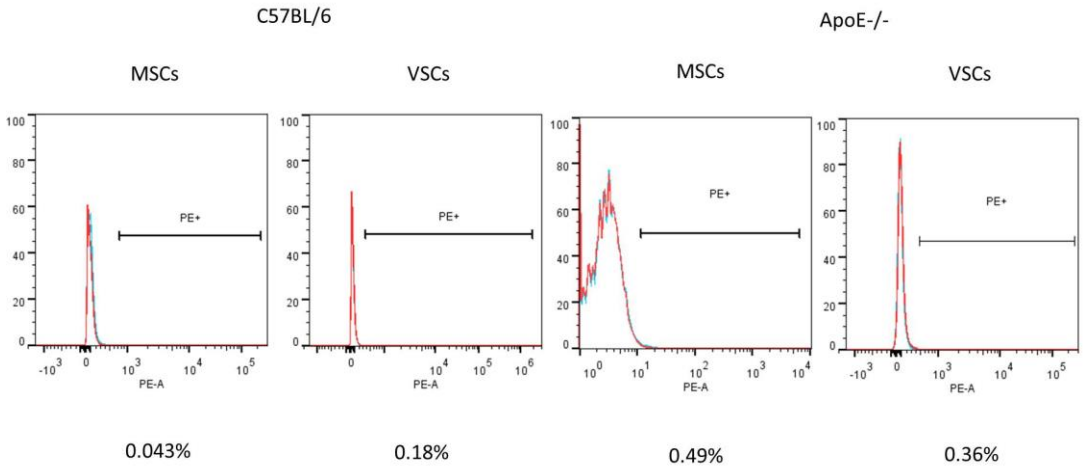

Figure 3.17 Representative flow cytometry histogram of NK 1.1 expression in ApoE$^{-/-}$ and C57BL/6 MSC and VSC. Cells were stained at passage 6 with a specific monoclonal antibody against NK 1.1 (red line). Blue lines indicate isotype-matched mouse immunoglobulin G antibody control staining. Both MSCs and VSCs were negative.

CD117, also known as stem cell growth factor receptor, has been shown to play a critical role in survival and proliferation of adult HSCs[41]. CD117 expression is altered by Sca-1[42]. CD117 expression has also been noted in some differentiated cells such as mast cells and melanocytes[43,44]. EC, in the lung, do not express CD117 as frequently as Sca-1 or CD105. A study has shown that when CD117-enriched fractions of ECs are assayed for CFCs, they show a 10-fold frequency compared to the CD117-depleted fraction[45]. VSCs from both C57BL/6 and ApoE$^{-/-}$ mice were negative (1.53% and 0.83%, respectively). Similarly, MSCs were also negative (0.06% and 2.67%, respectively) (Fig. 3.18).

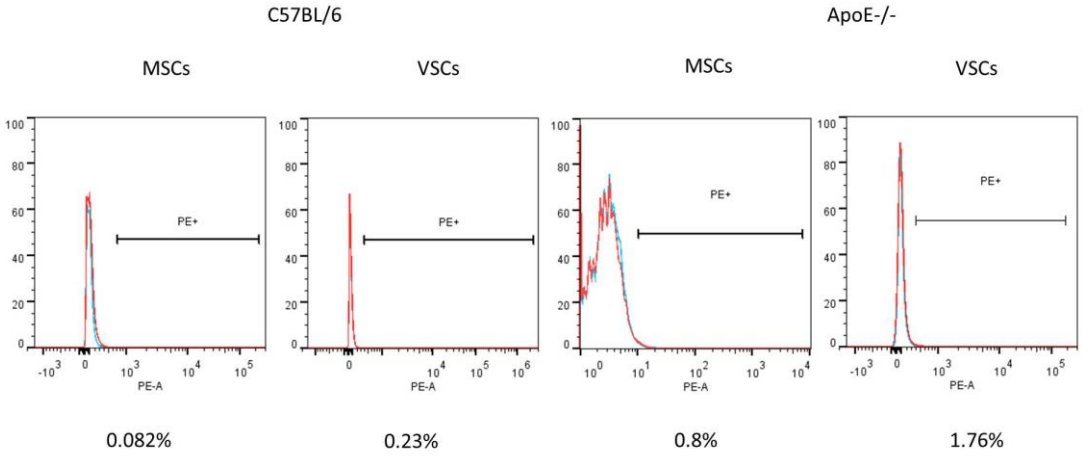

Figure 3.18 Representative flow cytometry histogram of CD117 expression in ApoE$^{-/-}$ and C57BL/6 MSC and VSC. Cells were stained at passage 6 with a specific monoclonal antibody against CD117 (red line). Blue lines indicate isotype-matched mouse immunoglobulin G antibody control staining. Both MSCs and VSCs were negative.

CD105, also known as endoglin, is a membrane glycoprotein expressed on vascular cells, particularly on proliferating endothelial cells. It is known to be involved in development of blood vessels and can be considered as a strong marker of angiogenesis. In neoplastic tissues, CD105 has a unique distribution, almost exclusively expressed on endothelial cells of blood vessels in and around the tumor, thus suggesting a potential role of CD105 in treatment or diagnosis of malignant diseases[46]. On the other hand, CD105 is also known to be a mesenchymal stem cell marker and has been shown to be involved in TGF-β signalling in chondrogenic differentiation[47]. The assessment in our study showed that VSCs from both C57BL/6 and ApoE$^{-/-}$ mice were weakly positive (4.95% and 4.4%, respectively) while MSCs were negative (0.21% and 1.04%, respectively) (Fig. 3.19).

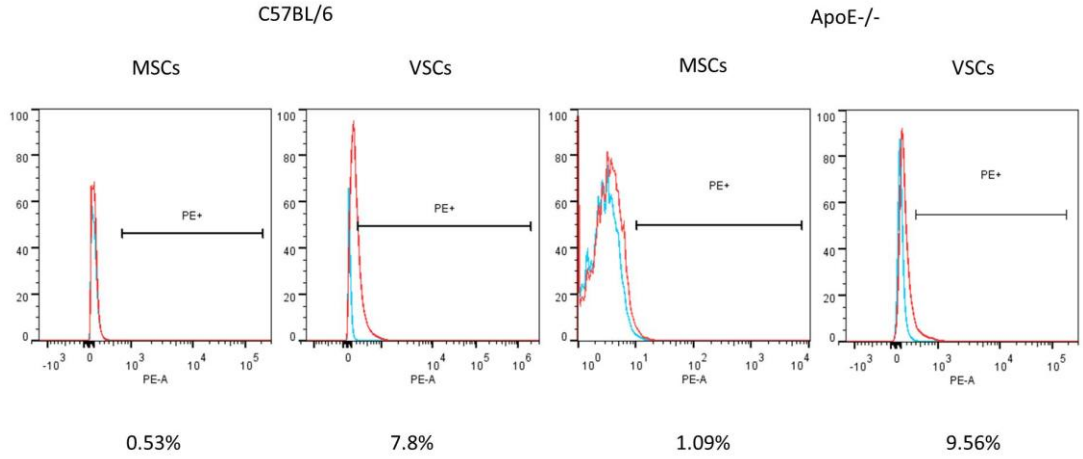

Figure 3.19 Representative flow cytometry histogram of CD105 expression in ApoE$^{-/-}$ and C57BL/6 MSC and VSC. Cells were stained at passage 6 with a specific monoclonal antibody against CD105 (red line). Blue lines indicate isotype-matched mouse immunoglobulin G antibody control staining. VSCs were weakly positive while MSCs were negative.

3.2.3.3 Cell surface analysis of endothelial markers

CD-31 is normally expressed on a number of cells including endothelial cells, platelets, macrophages and Kupffer cells, granulocytes, T/NK cells, lymphocytes, megakaryocytes, osteoclasts, neutrophils. VSCs from both C57BL/6 and ApoE$^{-/-}$ mice were negative (0.89% and 1.02%, respectively). Similarly, MSCs were also negative (0.09% and 0.76%, respectively) (Fig. 3.20).

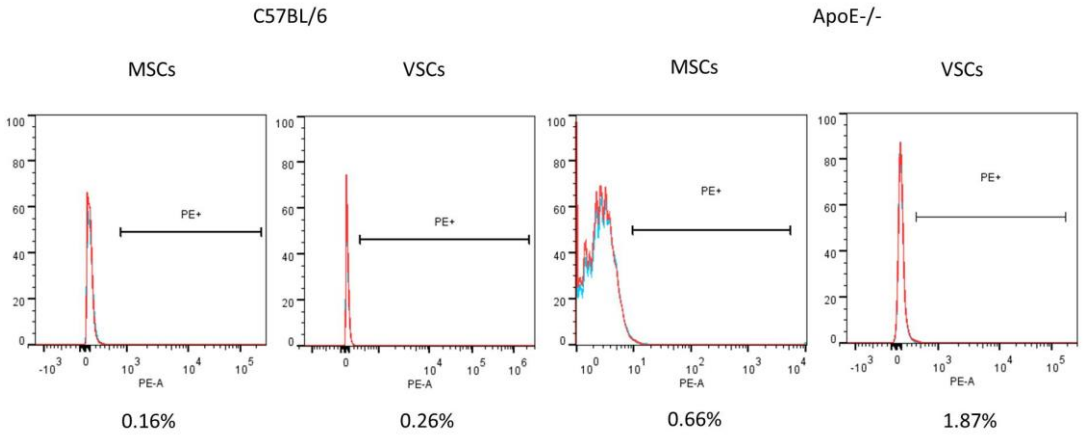

Figure 3.20 Representative flow cytometry histogram of CD31 expression in ApoE$^{-/-}$ and C57BL/6 MSC and VSC. Cells were stained at passage 6 with a specific monoclonal antibody against CD31 (red line). Blue lines indicate isotype-matched mouse immunoglobulin G antibody control staining. Both MSCs and VSCs were negative.

3.2.3.4 Cell surface analysis of pericyte/perivascular markers

Tie-2 is expressed by endothelial cells. Some monocytes which express Tie-2 are cells of the hematopoietic lineage which aid angiogenesis. Apart from these, Tie-2 expression is associated with mesenchymal progenitor cells which form the source of tumor pericytes. Thus, overall, Tie-2 expression can define three cell types including endothelial cells, proangiogenic monocytes and tumor pericytes, all of which are involved in tumor angiogenesis[48]. VSCs from both C57BL/6 and ApoE$^{-/-}$ mice were negative (0.57% and 0.54%, respectively). Similarly, MSCs were also negative (1.02% and 0.28%, respectively) (Fig. 3.21).

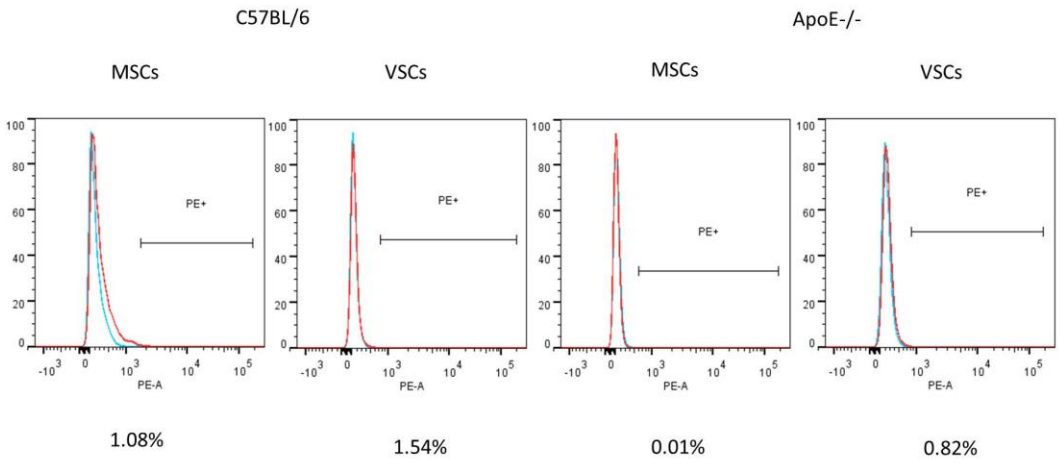

Figure 3.21 Representative flow cytometry histogram of Tie-2 expression in ApoE$^{-/-}$ and C57BL/6 MSC and VSC. Cells were stained at passage 6 with a specific monoclonal antibody against Tie-2 (red line). Blue lines indicate isotype-matched mouse immunoglobulin G antibody control staining. Both MSCs and VSCs were negative.

CD146 is a member of IgG superfamily of cell adhesion molecules and is a glycoprotein present across the membrane[49]. CD146 is ubiquitously present in all endothelial cells in humans irrespective of size or distribution of blood vessel and is localized especially at the intercellular endothelial junctions[50]. In addition to endothelial cells, CD146 expression, albeit at low levels, has been observed in melanoma cells[51], smooth muscle cells and follicular dendritic cells[52] and a subpopulation of activated T-cells[53]. Recent findings have shown that CD146 can be used as a specific pericyte marker[54,55]. Similar to humans, murine CD146 is expressed at high levels on endothelial cells and at low levels in many other organs in mice. One major difference between murine and human CD146 is in smooth muscle cells. In mice, there is no notable expression of CD146 on smooth muscle cells, T cells or follicular dendritic cells[56]. VSCs from both C57BL/6 and ApoE$^{-/-}$ mice were positive (43.66% and 47.6%, respectively) while MSCs were negative (2.29% and 1.03%, respectively) (Fig. 3.22).

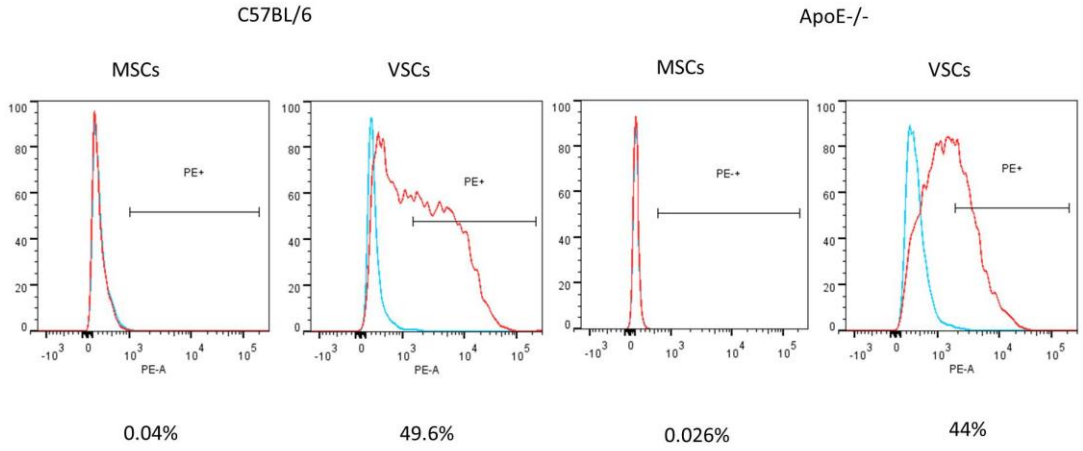

Figure 3.22 Representative flow cytometry histogram of CD146 expression in ApoE$^{-/-}$ and C57BL/6 MSC and VSC. Cells were stained at passage 6 with a specific monoclonal antibody against CD146 (red line). Blue lines indicate isotype-matched mouse immunoglobulin G antibody control staining. Both MSCs were negative while the VSCs positive.

3G5 has been considered as a specific marker for pericytes within the microvasculature in particular. A monoclonal antibody to 3G5 has been used to stain retinal capillaries and the fluorescence distribution has been shown to be consistent with pericyte staining. Despite the fact that other tissues such as brain cells, pancreatic islets peripheral blood lymphocytes do react with the 3G5 monoclonal antibody, 3G5 is a distinct and useful pericyte marker and can be used as a selective agent to enrich pericytes, particularly from microvasculature[57]. VSCs from both C57BL/6 and ApoE$^{-/-}$ mice were weakly positive (9.29% and 42%, respectively) while MSCs were negative (0.72% and 1.44%, respectively) (Fig. 3.23).

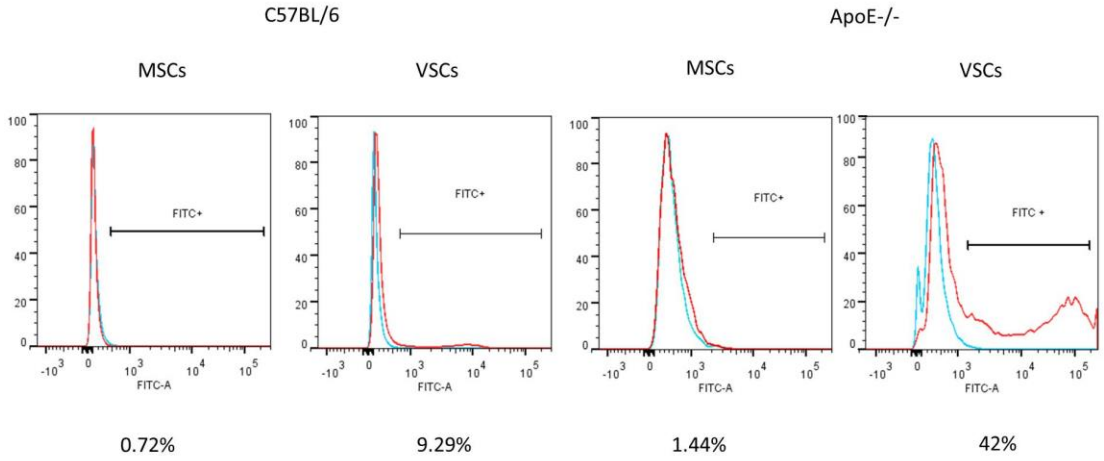

Figure 3.23 Representative flow cytometry histogram of 3G5 expression in ApoE$^{-/-}$ and C57BL/6 MSC and VSC. Cells were stained at passage 6 with a specific monoclonal antibody against 3G5 (red line). Blue lines indicate isotype-matched mouse immunoglobulin M antibody control staining. Both MSCs were negative while the VSCs weakly positive.

VSCs express a similar set of CD antigens that have been shown to be expressed by MSCs, suggesting that VSCs share same the surface marker profile with known MSCs (See Table 3.1 for details). However, only VSCs were positive for CD146 and 3G5 which is a pericyte marker (Fig. 3.22 and 3.23).

It is known that pericytes derived from blood vessels and aorta express the 3G5 antigen. Stained cells at passage 6 to 13 were observed and only VSCs stained positive for the 3G5 antigen. Upon quantification, it was evident that almost 45% of VSCs from ApoE$^{-/-}$ mice stained positive for the 3G5 marker, whereas only 25% of VSCs from C57BL/6 mice were positive (Fig. 3.24).

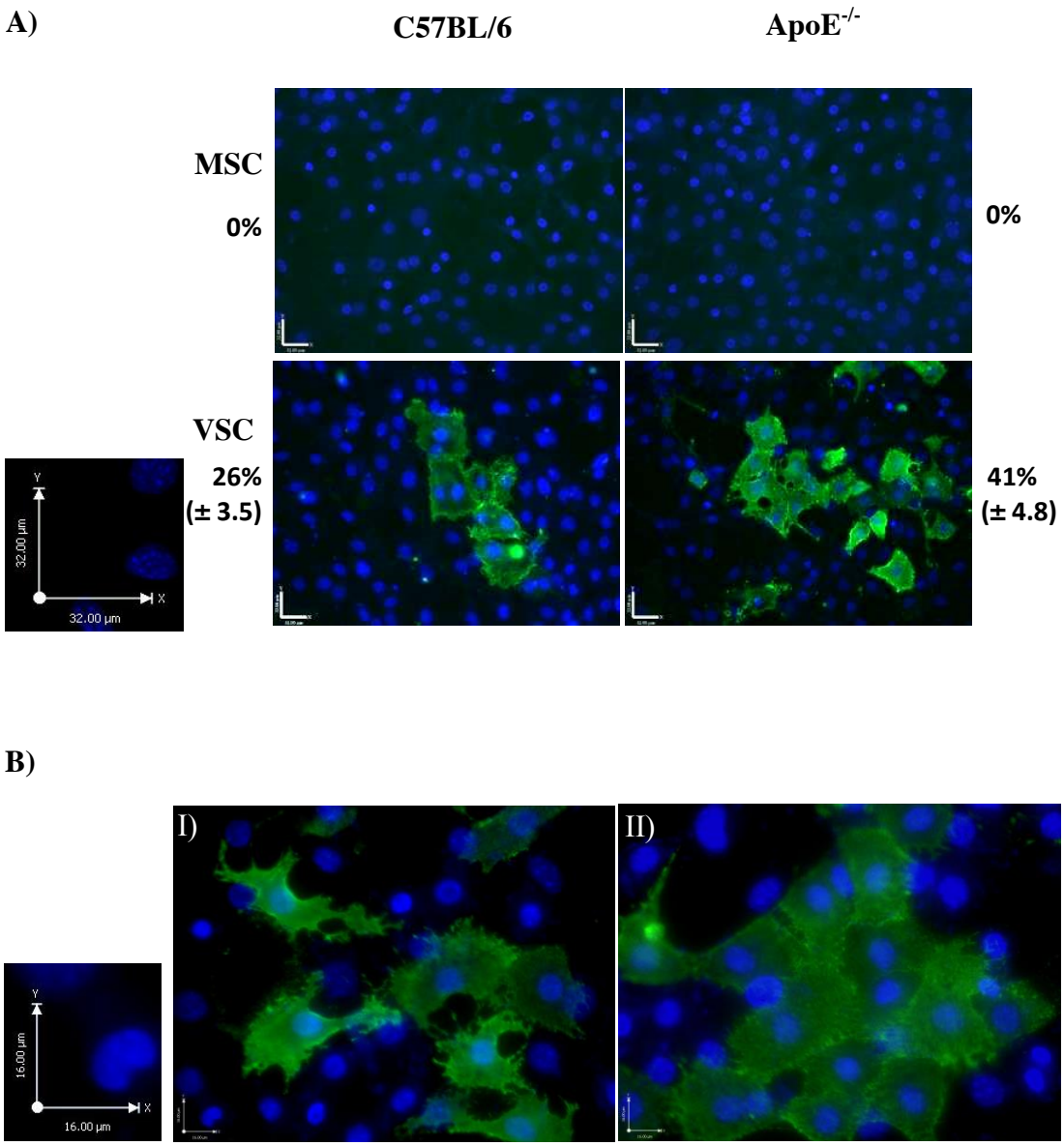

Figure 3.24: Immunocytochemistry for 3G5 antibody. a) MSCs were negative for 3G5 while a proportion of VSCs stained positive. A higher proportion of ApoE$^{-/-}$ VSCs (41%) were positive for 3G5 compared to C57BL/6 VSCs (26%). Scale bar represents 32µm. b) High magnification images of C57BL/6 (I) and ApoE$^{-/-}$ (II) VSCs. Scale bar represents 16µm.

3.2.4 Differentiation Assays

To determine the multilineage potential of VSCs and MSCs, functional markers of chondrogenic, osteogenic, adipogenic and myogenic lineages were assessed. Preparations of cells between passages 6-14 were tested for their differentiation ability. Cells were incubated in osteogenic, chondrogenic, adipogenic and myogenic differentiation media to check their ability to differentiate to osteocytes, chondrocytes, adipocytes and myocytes.

3.2.4.1 Comparison of osteogenic potential between C57BL/6 and ApoE$^{-/-}$ isolated cells after induction for 14 days

MSCs and VSCs from C57BL/6 and ApoE$^{-/-}$ were subjected to osteogenic differentiation as described in section 2.6.2. VSCs were demonstrated to possess similar osteogenic differentiation potential as MSCs after induction in osteogenic medium for 14 days.

When cultured in osteogenic differentiation medium, both MSCs and VSCs from C57BL/6 and ApoE$^{-/-}$ mice showed mineralization with calcium deposition demonstrated by Van Kossa staining (Fig. 3.25). Cells grown in control medium did not stain for Van Kossa. In osteogenically induced wells, black nodule-like formation appeared and was more obvious in cells isolated from ApoE$^{-/-}$ mice. The level of calcification of the cells was assessed using the Stanbio calcium liquid colour kit as described in section 2.6.2. Osteogenically treated ApoE$^{-/-}$ MSCs showed a 100-fold increase in calcium content compared to controls and 2.3 times compared to similarly treated C57BL/6 MSCs. Similarly, osteogenically treated ApoE$^{-/-}$ VSCs showed a 43-fold increase in calcium content compared to controls and 3.2 times compared to similarly treated C57BL/6 VSCs (Fig. 3.26). Untreated cells were used as controls in the experiment.

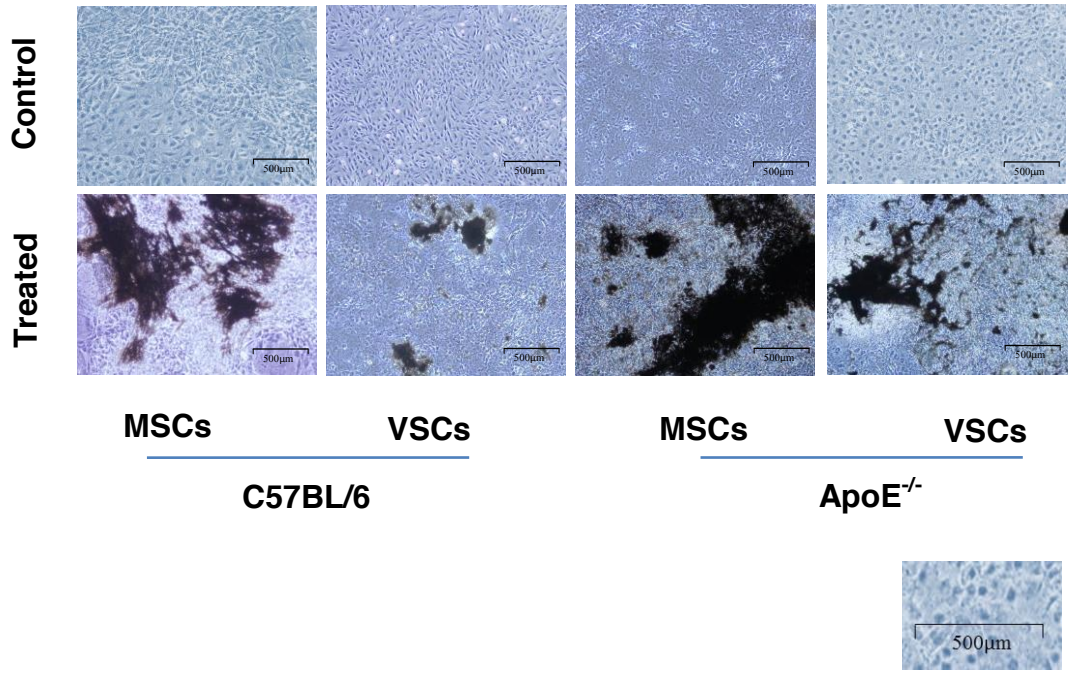

Figure 3.25: Osteogenic differentiation of MSCs and VSCs. Both MSCs and VSCs underwent osteogenesis as demonstrated macroscopically with Von Kossa staining. ApoE$^{-/-}$ MSCs and VSCs and C57BL/6 MSCs and VSCs cultured in control medium were negative. In osteogenic culture medium, ApoE$^{-/-}$ MSCs and VSCs, and C57Bl/6 MSCs and VSCs showed black calcified nodules indicating successful osteogenesis. Scale bar represents 500µm.

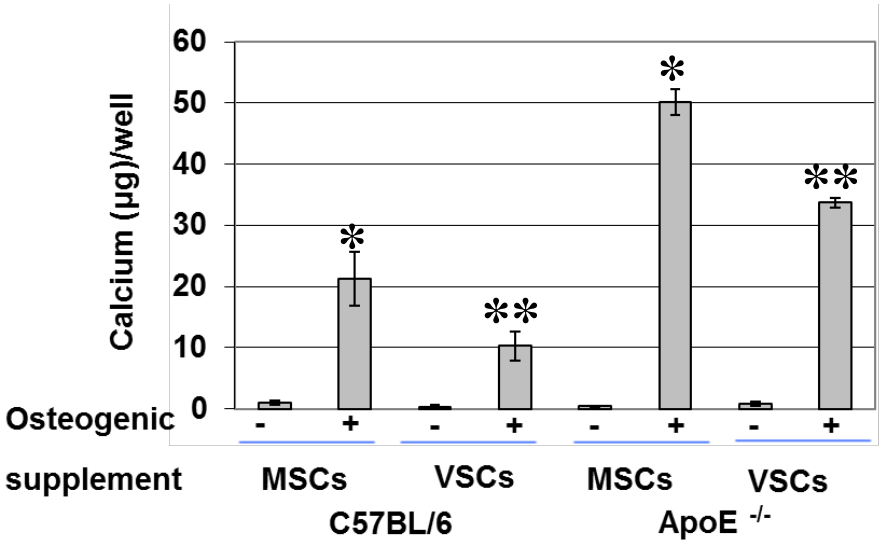

Figure 3.26: Quantification of calcium content following osteogenic differentiation of MSCs and VSCs. The graph of calcium content (µg/well) showed positive osteogenesis in all treated samples compared to respective controls following osteogenic differentiation. With osteogenic differentiation, calcium was significantly higher in ApoE$^{-/-}$ MSCs and VSCs over that in C57BL/6 MSCs and VSCs, respectively. Values are presented as the mean ± SD of data from three cell preparations; *, ** represent $p \leq 0.05$.

3.2.4.2 Comparison of chondrogenic potential between C57BL/6 and ApoE$^{-/-}$ isolated cells

MSCs and VSCs of 3 preparations were individually cultured in micromass pellet with chondrogenic induction medium as described in section 2.6.1. Pellets assumed a round, nodule like morphology after 1 day in culture. Formalin fixed and paraffin embedded C57BL/6 and ApoE$^{-/-}$ MSC and VSC pellets were sectioned. Toluidine blue staining after 21 days in culture revealed a high content of cartilage proteoglycans in induced cultures (Fig. 3.27).

Toluidine blue staining was more intense and uniform in the outer rim of the cultures and decreased irregularly towards the centre of the cultures, suggesting a higher content of cartilage proteoglycans in the outer part of the pellets (Fig. 3.28). At higher magnification, hypertrophic cells similar to chondrocytes were observed to be embedded in the matrix rich in proteoglycan. This observation is consistent with progression of endochondral ossification. In contrast to this, control cultures in cell culture medium or chondrogenic medium without TGF-β3 and BMP-2 did not undergo chondrogenesis by micromass culture.

Figure 3.27 shows sections from the centre of the pellets, immunostained for type II and X collagen. At the periphery, type II collagen staining was prominent while the central zone seemed to have remained undifferentiated. The outermost layer of the pellets showed extensive type II and type X collagen-rich matrix. ApoE$^{-/-}$ MSC and VSC pellets were bigger in size than respective C57BL/6 pellets. At 21 days, all pellet cultures showed abundant accumulation of type II and X collagen. Nonetheless, the extent of type II and X collagen staining was greater in ApoE$^{-/-}$ MSC and VSC pellets. GAG deposition was also higher in ApoE$^{-/-}$ MSC and VSC pellets than respective C57BL/6 pellets (Fig. 3.27). With the total cellular content of all the pellets being similar as shown by the DNA measurements (Fig. 3.27); the GAG/DNA ratio in ApoE$^{-/-}$ MSC and VSC pellets was significantly higher

compared to respective C57BL/6 pellets (Fig. 3.28 C), suggesting either a higher synthesis rate or low turnover per cell.

The pellets of all cell preparations of $ApoE^{-/-}$ isolated cells showed similar patterns of collagen type II and proteoglycan accumulation and exhibited chondrogenic differentiation after 21 days. They also exhibited higher chondrogenic potential than C57BL/6 preparations where cultures were performed concurrently. GAG and DNA content from MSCs and VSCs pellets was analysed for 3 individual preparations and showed significant increase as expected in accordance to the Toluidine blue staining (Fig. 3.28).

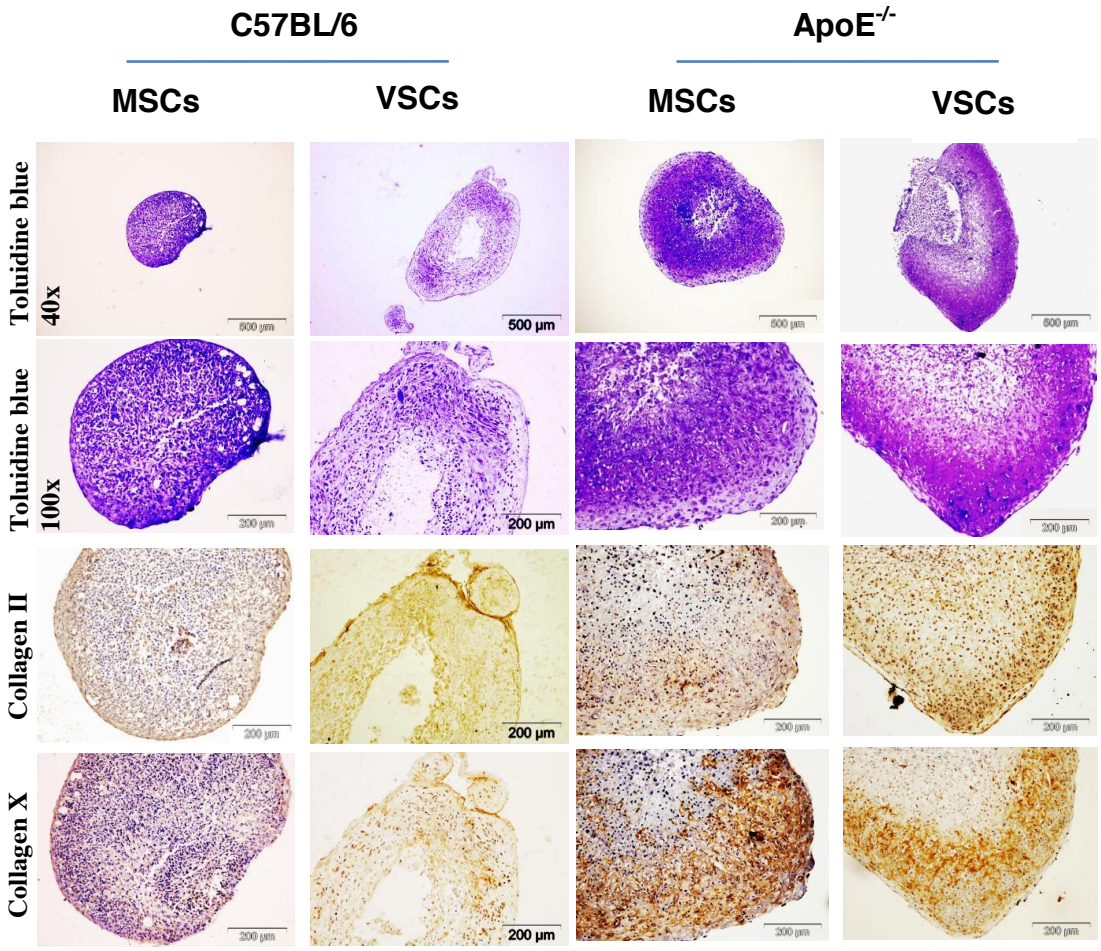

Figure 3.27: Chondrogenic differentiation of MSCs and VSCs. Following chondrogenic pellet cultures for 21 days, Toluidine blue staining showed proteoglycan deposition. Scale bars represent 500µm. At low magnification, it was evident that ApoE$^{-/-}$ MSCs and VSCs pellets were bigger in size compared to C57BL/6 MSCs and VSCs, respectively. At higher magnification, the appearance of large chondrocyte-like cells embedded in the proteoglycan rich matrix showed a hypertrophic phenotype associated with progression of endochondral ossification. Scale bars represent 200µm and 500µm. In chondrogenic medium, pellets expressed cartilage proteins. Serial cross sections of pellets were immunostained for collagen type II and collagen type X. Scale bars represent 200µm.

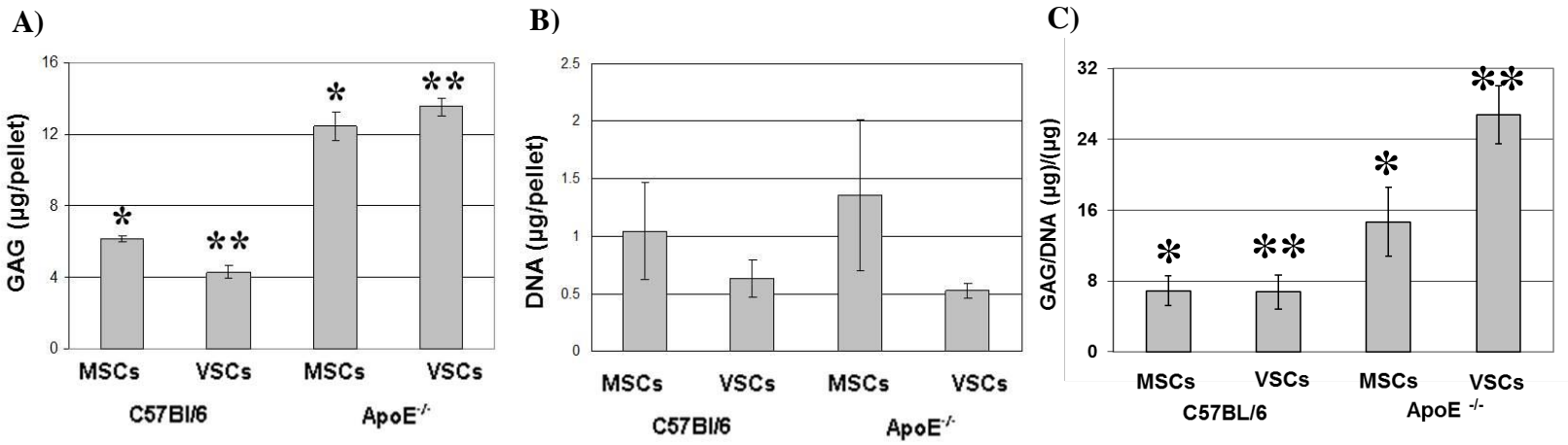

Figure 3.28: Quantification of GAG and DNA following chondrogenic differentiation of MSCs and VSCs. Graphs showing (A) GAG deposition, (B) DNA levels and (C) GAG/DNA ratios for isolated cell cultures. Results are presented as the mean ± SD of data from 3 individual cell preparations from each group. Although positive chondrogenesis was observed in all cell preparations ApoE$^{-/-}$ MSCs and VSCs had a significantly higher GAG/DNA ratio compare to respective cell preparation from C57BL/6 mice. *, ** represent $p \leq 0.05$.

3.2.4.3 Comparison of adipogenic potential between C57BL/6 MSCs and ApoE$^{-/-}$ isolated cells

Adipogenic induction was performed by following the protocol described in section 2.6.3 and analysed by Oil Red O staining. C57BL/6 MSCs grown in induction medium stained for Oil Red O with appreciable lipid accumulation (Fig. 3.29).

The extent of adipogenic differentiation was assessed by microscopic observation of lipid vacuoles in the induced cells. After 26 days of adipogenic induction, light microscopy analysis showed that MSCs from C57BL/6 mice possessed an adipogenic phenotype with a high number of accumulated lipid droplets in the cytoplasm identified by Oil Red O staining.

The amount of Oil Red O staining was quantified and measured for absorbance at 490nm. The data correlated with the microscopic evaluation with a significant 5-fold increase in the Oil Red O staining in adipogenically induced C57BL/6 MSCs compared to control MSCs. However, the increase in Oil Red O staining in C57BL/6 VSCs following adipogenic induction was not significant. Cells from ApoE$^{-/-}$ mice were negative for adipogenesis (Fig. 3.30). Different protocols were assessed to see if the cells could undergo adipogenesis. The use of higher serum content in the induction medium and different timing of exposure to induction medium was also assessed. C57BL/6 MSC cultures underwent Adipogenesis with all conditions tested. Although ApoE$^{-/-}$ cells were subjected to the various assays and different conditions were applied, Oil Red O accumulation was not evident. As a result, there was only minimal accumulation of lipids vacuoles in ApoE$^{-/-}$ cells. It has been suggested that ApoE$^{-/-}$ mice have decreased lipid accumulation which might be due to the fact that cells lack apolipoprotein-e which plays important role in lipid transports and formation[58,59]. These mice are known to utilize different pathway of fat formation[59].

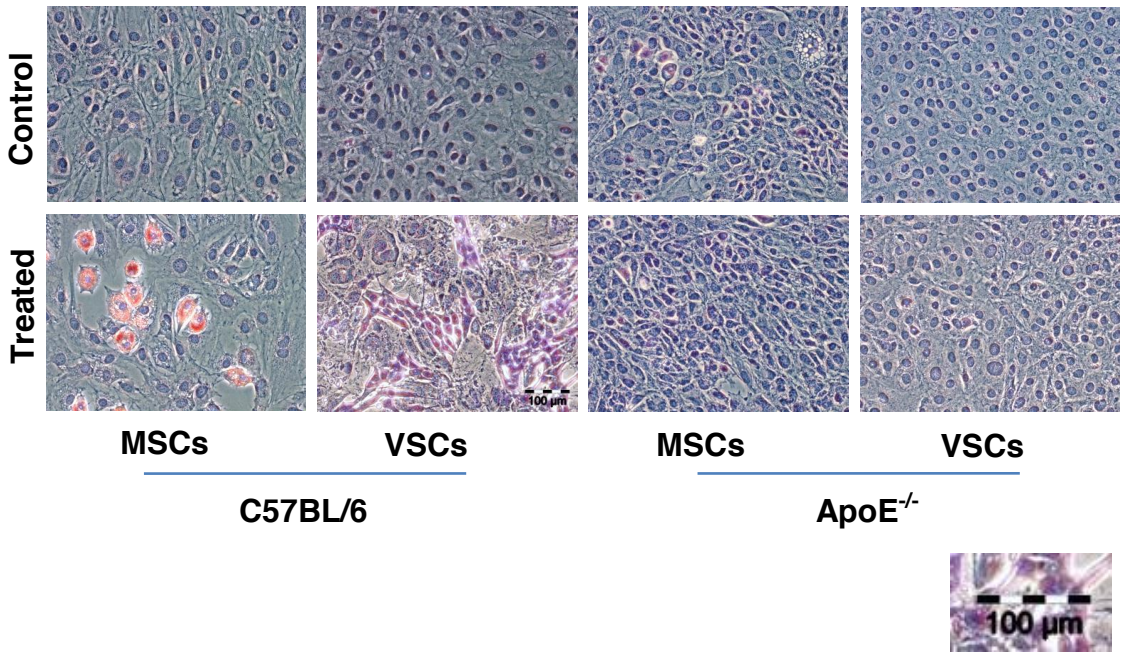

Figure 3.29: Adipogenic potential of MSCs and VSCs. MSCs and VSCs from ApoE$^{-/-}$ mice, subjected to adipogenic medium, did not show potential to form adipocytes although C57BL/6 MSCs showed lipid droplet accumulation. It is known that ApoE$^{-/-}$ cells do not differentiate into adipocytes due to lack of apolipoprotein-e, important in the formation of intracellular lipid vacuoles. VSCs from C57BL/6 mice did not show significant accumulation of Oil Red O positive lipid droplets after exposure to adipogenic induction. Scale bar represents 100µm.

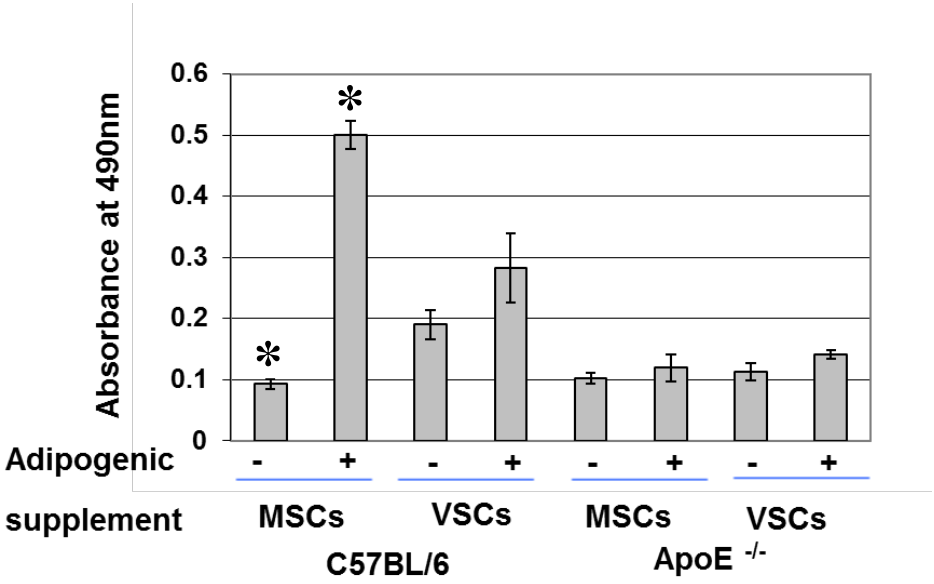

Figure 3.30: Quantification of Oil Red O following adipogenic differentiation of MSCs and VSCs. Adipocyte differentiation of MSCs was quantified after extraction of Oil Red O and absorbance at 490nm was measured. Data represents the mean ± SD of 3 individual cell preparations. Significantly higher amounts of Oil Red O was observed in adipogenically induced C57BL/6 MSCs compared to controls while C57BL/6 VSCs showed only slight increase in Oil Red O. Adipogenic induction did not result in any increase in the amount of Oil Red O in both $ApoE^{-/-}$ MSCs and VSCs. * represents $p \leq 0.05$.

3.2.4.4 Comparison of myogenic potential between C57BL/6 and ApoE$^{-/-}$ isolated cells

Cells were treated with TGF β1 (5ng/ml) every second day for 7 days. Culture medium without myogenic induction factors was used as a control. α-smooth muscle actin staining was observed under a light microscope. Although control cells showed α-SMA staining, TGF-β1 treatment increased this staining to some extent (Fig. 3.31). To further assess expression of α-SMA, western blotting was performed. Western blotting analysis showed that the MSCs and VSCs were positive for α-SMA (Fig. 3.32 A). Densitometry showed that the treated cells had higher α-SMA content (Fig. 3.32 B). However, this difference was not significant.

After TGF-β1 treatment, cells were partially induced into the SMC phenotype. This partial phenotypic switch was demonstrated by immune-histological staining for smooth muscle actin which is an early SMC marker. The distribution and level of α-SMA in western blot was similar to that of coronary artery smooth muscle cells (CASMCs), which served as a positive control (Fig. 3.32). However, there was no staining for calponin which is a mid-SMC marker (Fig. 3.33). This result may indicate a committed yet immature stage of SMC differentiation of MSCs and VSCs after 7 days of exposure to TGF-β1. The presence of α-SMA staining in the control cells may raise some confusion about the smooth muscle origin of isolated cells. But, the absence of calponin staining even in the control cells suggests that the isolated cells are not smooth muscle cells.

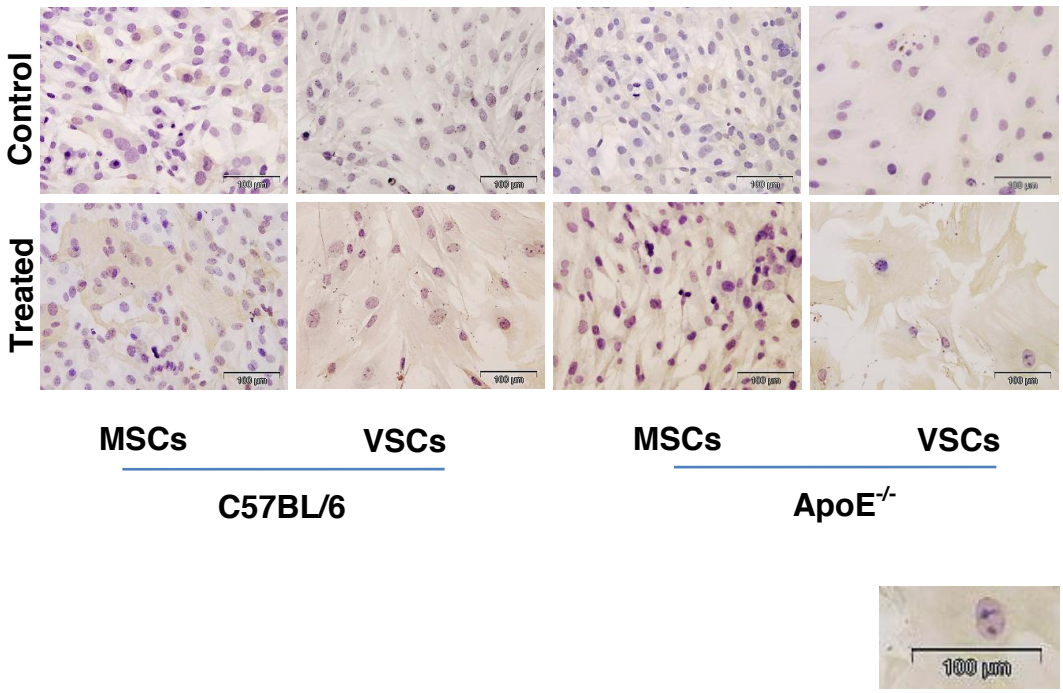

Figure 3.31: α-SMA staining for myogenesis. The myogenic induction medium (TGF-β1 (5ng/ml) added every second day) was used. Cells grown in culture medium without myogenic factor acted as controls. Both control and treated cells showed α-SMA staining with some increase following TGF-β1 treatment. Scale bars represent 100µm.

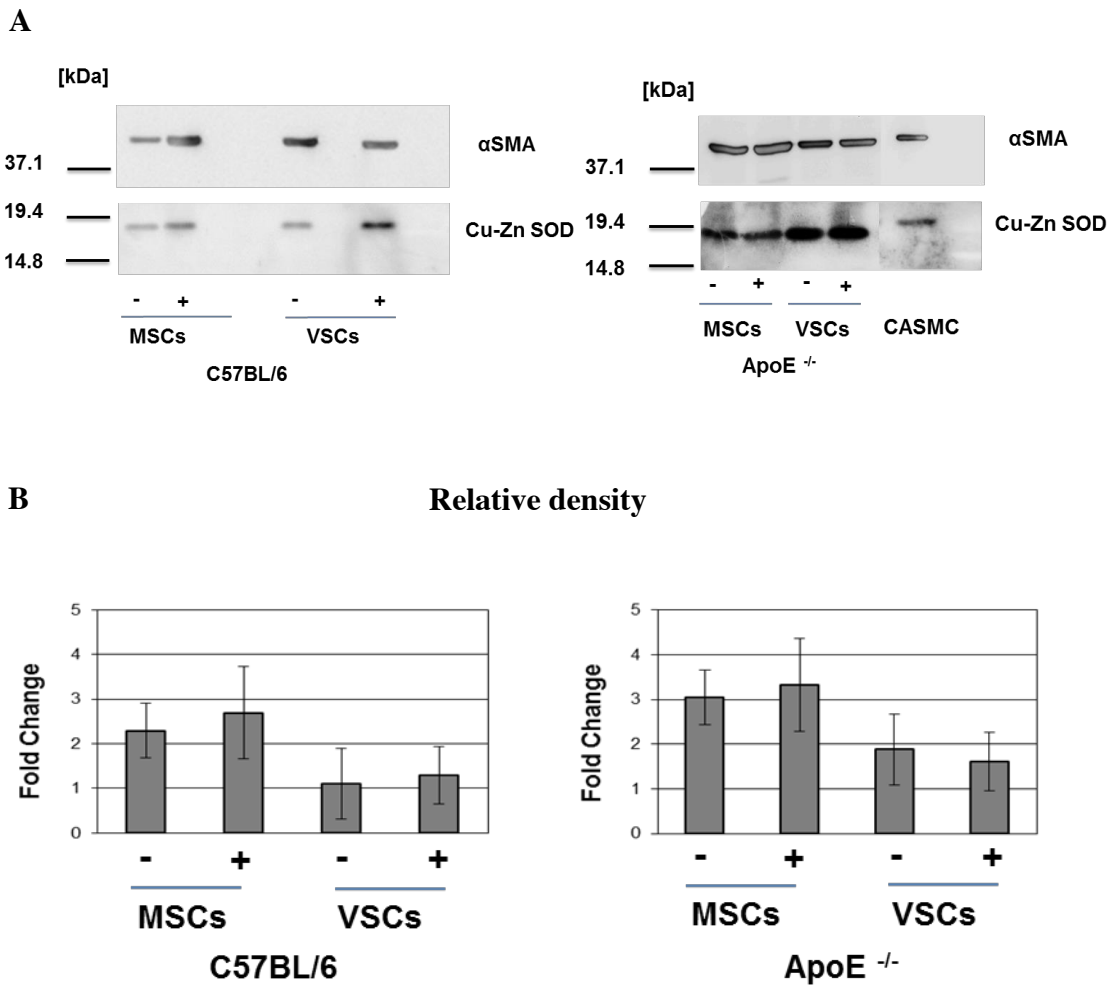

Figure 3.32: α-SMA staining for myogenesis. (A) Western blotting to assess expression of α-SMA after 7 days of treatment. (B) Relative detection of α-SMA standardized to Cu-ZnSOD levels. Western blots were performed on protein lysates from each treatment group after 7 days. The increase in band intensity following TGF-β1 treatment was not significant.

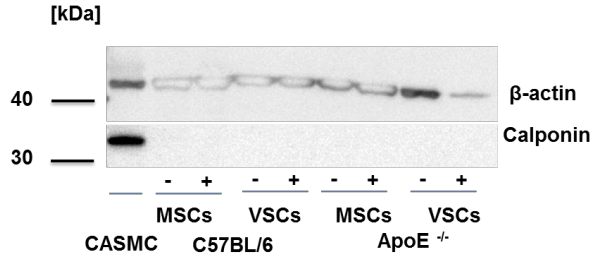

Figure 3.33: Western blotting for calponin as a mid-stage maturation SMC marker. The absence of calponin staining in treated and control cells suggests that the smooth muscle phenotypic switch following TGF-β1 treatment is only partial.

3.3 Discussion

Here, we provide evidence of a multipotent cell population isolated from the aortic vessel wall capable of differentiating into bone and cartilage. In recent years, interest in the regenerative capacity of the vascular system has increased dramatically. The dogmas of not only the repair and regeneration of the vasculature but also disease progression are changing rapidly with the discoveries of stem or progenitor cells in the vessel walls[60-63]. One target cell population has been pericytes or pericyte-like cells[64,65]. Although the current knowledge of vessel-derived stem progenitor cells is in its infancy, much attention and interest has been skewed towards their potential therapeutic application in myocardial infarction, ischemic heart disease and limb ischemia[66,67]. Our interest in investigating the presence of stem or progenitor cells in the vessel wall was to unravel their role, if any, in the pathogenesis of atherosclerosis, which is the major debilitating disease of the vasculature. Discovery of stem or progenitor cell populations have challenged the current theory of the involvement of smooth muscle proliferation and differentiation in atherosclerosis or vascular calcification[68,69].

Hemangioblasts are bipotent progenitor cells which are thought to be the common origin of hematopoietic and endothelial lineages[70-72]. Stem cells with hemangioblast-like properties have been isolated from humans[73,74]. Bone marrow-derived EPCs circulate in blood following vascular injury and have a high regenerative capacity. Apart from these circulating EPCs, mature ECs in humans have been found to contain a subpopulation of EPCs niched in the endothelial layer with distinctly different clonogenic and proliferative potential. Sprouting of structures similar to capillaries from human embryological aorta was shown using ring assays. Also, isolated cells were shown to differentiate to mature ECs confirming the presence of endothelial progenitor cells in human aorta[75]. Similarly, human fetal aortas were also shown to contain vascular progenitor cells in their walls which could differentiate to

ECs following VEGF treatment and in mural cells following treatment with PDGF-BB[76]. In adult life, a study has shown presence of EPCs in areas between media and adventitia of the human internal thoracic artery, which are capable of forming capillary-like structures *ex vivo*[77]. Apart from EPCs, arteries of healthy adult mice were shown to have smooth muscle progenitor cells. The presence of Sca-1-positive cells capable of differentiating to SMCs under PDGF-BB treatment was confirmed supporting the notion that the adult vessel wall contains these progenitors, which have a repair function replacing dead and defective smooth muscle cells[78]. Thus, the presence of bipotent precursor cells which act as EPCs or SMC progenitors has been probed[79,80]. Studies have also shown that pericyte-like cells from rat aortas express SMCs markers under serum and PDGF-BB treatment or in presence of capillary sprouts of rat aorta[81]. Also, the presence of MSCs in the adult vessel wall was demonstrated by Tintut *et al*.[82-84] The authors termed these cells as calcifying vascular cells and showed their multipotency by osteogenic and chondrogenic differentiation. In the present study we isolated a similar population of multipotent cells from aorta wall.

Based on studies which focused on capillary structures present between media and adventitia[77,85], the niche concept in the area between media and adventitia evolved potentially explaining the isolation and in vitro expansion of populations of cells akin to bone marrow-derived mesenchymal stem cells from a number of locations such as thoracic aorta, pulmonary artery, and the saphenous vein[86-88]. Cells isolated in this study could also be from peri-endothelial layer where pericytes reside. Pericytes are periendothelial cells of the microvasluature. Despite their recognized importance in both vasculogenesis and angiogenesis, pericytes have received less attention than ECs, and their functions are only now beginning to be understood. Since the VSCs isolated in this study expressed pericyte-specific markers and shared MSCs markers as well, these VSCs can be considered as pericyte-like cells. The different batches of fetal bovine serum used to cultivate these cells may introduce

some phenotypic variations, showing the influence of unknown factors on the selection and expansion of the cells. In this study, there was no special addition of growth factors which may increase the heterogeneity observed in some MSC cultures described in literature.

Thus, a number of researchers have isolated and characterized stem cell populations in vessel walls[3,61,77,81,89-91] and based on the multipotency of these cells, there have been some postulations regarding their possible role in formation of ectopic bone or cartilage in vascular diseases such as atherosclerosis. This postulation formed the hypothesis for the present study. Our approach was to compare the vessel-derived stem cells and bone marrow-derived stem cells from diseased and healthy animals. The significantly higher osteogenic and chondrogenic potential of $ApoE^{-/-}$ VSCs points to their possible role in the pathogenesis of atherosclerosis. The difference also suggests that there are certain factors in disease state which trigger the activation of these cells to differentiate and contribute to vascular calcification.

3.4 References

1. O'Neill, T.P. Apolipoprotein E-deficient mouse model of human atherosclerosis. *Toxicol Pathol* **25**, 20-21 (1997).
2. Meir, K.S. & Leitersdorf, E. Atherosclerosis in the apolipoprotein-E-deficient mouse: a decade of progress. *Arteriosclerosis, thrombosis, and vascular biology* **24**, 1006-1014 (2004).
3. Crisan, M., *et al*. A perivascular origin for mesenchymal stem cells in multiple human organs. *Cell Stem Cell* **3**, 301-313 (2008).
4. Sacchetti, B., *et al*. Self-renewing osteoprogenitors in bone marrow sinusoids can organize a hematopoietic microenvironment. *Cell* **131**, 324-336 (2007).
5. Brighton, C.T., *et al*. The pericyte as a possible osteoblast progenitor cell. *Clinical orthopaedics and related research*, 287-299 (1992).
6. Farrington-Rock, C., *et al*. Chondrogenic and adipogenic potential of microvascular pericytes. *Circulation* **110**, 2226-2232 (2004).
7. Doherty, M.J., *et al*. Vascular pericytes express osteogenic potential in vitro and in vivo. *J Bone Miner Res* **13**, 828-838 (1998).
8. Gronthos, S., *et al*. Surface protein characterization of human adipose tissue-derived stromal cells. *J Cell Physiol* **189**, 54-63 (2001).
9. Chiou, M., Xu, Y. & Longaker, M.T. Mitogenic and chondrogenic effects of fibroblast growth factor-2 in adipose-derived mesenchymal cells. *Biochem Biophys Res Commun* **343**, 644-652 (2006).
10. Tare, R.S., Babister, J.C., Kanczler, J. & Oreffo, R.O. Skeletal stem cells: phenotype, biology and environmental niches informing tissue regeneration. *Mol Cell Endocrinol* **288**, 11-21 (2008).
11. Andreeva, E.R., Pugach, I.M., Gordon, D. & Orekhov, A.N. Continuous subendothelial network formed by pericyte-like cells in human vascular bed. *Tissue & cell* **30**, 127-135 (1998).
12. Shi, S. & Gronthos, S. Perivascular niche of postnatal mesenchymal stem cells in human bone marrow and dental pulp. *J Bone Miner Res* **18**, 696-704 (2003).
13. Meirelles Lda, S. & Nardi, N.B. Murine marrow-derived mesenchymal stem cell: isolation, in vitro expansion, and characterization. *British journal of haematology* **123**, 702-711 (2003).
14. Sudres, M., *et al*. Bone marrow mesenchymal stem cells suppress lymphocyte proliferation in vitro but fail to prevent graft-versus-host disease in mice. *J Immunol* **176**, 7761-7767 (2006).
15. Dellavalle, A., *et al*. Pericytes of human skeletal muscle are myogenic precursors distinct from satellite cells. *Nat Cell Biol* **9**, 255-267 (2007).
16. Rege, T.A. & Hagood, J.S. Thy-1 as a regulator of cell-cell and cell-matrix interactions in axon regeneration, apoptosis, adhesion, migration, cancer, and fibrosis. *FASEB J* **20**, 1045-1054 (2006).

17. Sung, J.H., *et al*. Isolation and characterization of mouse mesenchymal stem cells. *Transplant Proc* **40**, 2649-2654 (2008).
18. Houlihan, D.D., *et al*. Isolation of mouse mesenchymal stem cells on the basis of expression of Sca-1 and PDGFR-alpha. *Nat Protoc* **7**, 2103-2111 (2012).
19. Boxall, S.A. & Jones, E. Markers for characterization of bone marrow multipotential stromal cells. *Stem Cells Int* **2012**, 975871 (2012).
20. Zoller, M. CD44: can a cancer-initiating cell profit from an abundantly expressed molecule? *Nature reviews*. *Cancer* **11**, 254-267 (2011).
21. Choi, K., Kennedy, M., Kazarov, A., Papadimitriou, J.C. & Keller, G. A common precursor for hematopoietic and endothelial cells. *Development* **125**, 725-732 (1998).
22. Ito, A., *et al*. Enhanced expression of CD34 messenger RNA by developing endothelial cells of mice. *Lab Invest* **72**, 532-538 (1995).
23. Cheng, J., *et al*. Hematopoietic defects in mice lacking the sialomucin CD34. *Blood* **87**, 479-490 (1996).
24. Suzuki, A., *et al*. CD34-deficient mice have reduced eosinophil accumulation after allergen exposure and show a novel crossreactive 90-kD protein. *Blood* **87**, 3550-3562 (1996).
25. Baumhueter, S., Dybdal, N., Kyle, C. & Lasky, L.A. Global vascular expression of murine CD34, a sialomucin-like endothelial ligand for L-selectin. *Blood* **84**, 2554-2565 (1994).
26. Fina, L., *et al*. Expression of the CD34 gene in vascular endothelial cells. *Blood* **75**, 2417-2426 (1990).
27. Fiedler, U., *et al*. The sialomucin CD34 is a marker of lymphatic endothelial cells in human tumors. *Am J Pathol* **168**, 1045-1053 (2006).
28. Sato, T., Laver, J.H. & Ogawa, M. Reversible expression of CD34 by murine hematopoietic stem cells. *Blood* **94**, 2548-2554 (1999).
29. Nickoloff, B.J. The human progenitor cell antigen (CD34) is localized on endothelial cells, dermal dendritic cells, and perifollicular cells in formalin-fixed normal skin, and on proliferating endothelial cells and stromal spindle-shaped cells in Kaposi's sarcoma. *Arch Dermatol* **127**, 523-529 (1991).
30. Brown, J., Greaves, M.F. & Molgaard, H.V. The gene encoding the stem cell antigen, CD34, is conserved in mouse and expressed in haemopoietic progenitor cell lines, brain, and embryonic fibroblasts. *Int Immunol* **3**, 175-184 (1991).
31. Simmons, P.J. & Torok-Storb, B. CD34 expression by stromal precursors in normal human adult bone marrow. *Blood* **78**, 2848-2853 (1991).
32. Egan, C.E., Sukhumavasi, W., Bierly, A.L. & Denkers, E.Y. Understanding the multiple functions of Gr-1(+) cell subpopulations during microbial infection. *Immunologic research* **40**, 35-48 (2008).

33. Aoyama, K., *et al*. Stromal cell CD9 regulates differentiation of hematopoietic stem/progenitor cells. *Blood* **93**, 2586-2594 (1999).
34. Ying, L. & Hofseth, L.J. An emerging role for endothelial nitric oxide synthase in chronic inflammation and cancer. *Cancer Res* **67**, 1407-1410 (2007).
35. Kim, Y.J., *et al*. Role of CD9 in proliferation and proangiogenic action of human adipose-derived mesenchymal stem cells. *Pflugers Archiv : European journal of physiology* **455**, 283-296 (2007).
36. Halfon, S., Abramov, N., Grinblat, B. & Ginis, I. Markers distinguishing mesenchymal stem cells from fibroblasts are downregulated with passaging. *Stem Cells Dev* **20**, 53-66 (2011).
37. Hotfilder, M., *et al*. Immature CD34+CD19- progenitor/stem cells in TEL/AML1-positive acute lymphoblastic leukemia are genetically and functionally normal. *Blood* **100**, 640-646 (2002).
38. Yeh, S.P., *et al*. Induction of CD45 expression on bone marrow-derived mesenchymal stem cells. *Leukemia* **20**, 894-896 (2006).
39. Ooi, Y.Y., Ramasamy, R. & Vidyadaran, S. Mouse bone marrow mesenchymal stem cells acquire CD45-CD106+ immunophenotype only at later passages. *The Medical journal of Malaysia* **63 Suppl A**, 65-66 (2008).
40. Luther, C., Warner, K. & Takei, F. Unique progenitors in mouse lymph node develop into CD127+ NK cells: thymus-dependent and thymus-independent pathways. *Blood* **117**, 4012-4021 (2011).
41. Ikuta, K. & Weissman, I.L. Evidence that hematopoietic stem cells express mouse c-kit but do not depend on steel factor for their generation. *Proc Natl Acad Sci U S A* **89**, 1502-1506 (1992).
42. Uchida, N. & Weissman, I.L. Searching for hematopoietic stem cells: evidence that Thy-1.1lo Lin- Sca-1+ cells are the only stem cells in C57BL/Ka-Thy-1.1 bone marrow. *The Journal of experimental medicine* **175**, 175-184 (1992).
43. Drew, E., Merkens, H., Chelliah, S., Doyonnas, R. & McNagny, K.M. CD34 is a specific marker of mature murine mast cells. *Exp Hematol* **30**, 1211-1218 (2002).
44. Miettinen, M. & Lasota, J. KIT (CD117): a review on expression in normal and neoplastic tissues, and mutations and their clinicopathologic correlation. *Applied immunohistochemistry & molecular morphology : AIMM / official publication of the Society for Applied Immunohistochemistry* **13**, 205-220 (2005).
45. Fang, S., Wei, J., Pentinmikko, N., Leinonen, H. & Salven, P. Generation of functional blood vessels from a single c-kit+ adult vascular endothelial stem cell. *PLoS biology* **10**, e1001407 (2012).

46. Fonsatti, E., Sigalotti, L., Arslan, P., Altomonte, M. & Maio, M. Emerging role of endoglin (CD105) as a marker of angiogenesis with clinical potential in human malignancies. *Current cancer drug targets* **3**, 427-432 (2003).
47. Barry, F.P., Boynton, R.E., Haynesworth, S., Murphy, J.M. & Zaia, J. The monoclonal antibody SH-2, raised against human mesenchymal stem cells, recognizes an epitope on endoglin (CD105). *Biochem Biophys Res Commun* **265**, 134-139 (1999).
48. De Palma, M., *et al*. Tie2 identifies a hematopoietic lineage of proangiogenic monocytes required for tumor vessel formation and a mesenchymal population of pericyte progenitors. *Cancer Cell* **8**, 211-226 (2005).
49. Sers, C., Kirsch, K., Rothbacher, U., Riethmuller, G. & Johnson, J.P. Genomic organization of the melanoma-associated glycoprotein MUC18: implications for the evolution of the immunoglobulin domains. *Proc Natl Acad Sci U S A* **90**, 8514-8518 (1993).
50. Bardin, N., *et al*. Identification of CD146 as a component of the endothelial junction involved in the control of cell-cell cohesion. *Blood* **98**, 3677-3684 (2001).
51. Shih, I.M. The role of CD146 (Mel-CAM) in biology and pathology. *J Pathol* **189**, 4-11 (1999).
52. Bardin, N., *et al*. S-Endo 1, a pan-endothelial monoclonal antibody recognizing a novel human endothelial antigen. *Tissue antigens* **48**, 531-539 (1996).
53. Pickl, W.F., *et al*. MUC18/MCAM (CD146), an activation antigen of human T lymphocytes. *J Immunol* **158**, 2107-2115 (1997).
54. Covas, D.T., *et al*. Multipotent mesenchymal stromal cells obtained from diverse human tissues share functional properties and gene-expression profile with CD146+ perivascular cells and fibroblasts. *Exp Hematol* **36**, 642-654 (2008).
55. Li, Q., Yu, Y., Bischoff, J., Mulliken, J.B. & Olsen, B.R. Differential expression of CD146 in tissues and endothelial cells derived from infantile haemangioma and normal human skin. *J Pathol* **201**, 296-302 (2003).
56. Yokoyama, W.M. & Seaman, W.E. The Ly-49 and NKR-P1 gene families encoding lectin-like receptors on natural killer cells: the NK gene complex. *Annual review of immunology* **11**, 613-635 (1993).
57. Nayak, R.C., Berman, A.B., George, K.L., Eisenbarth, G.S. & King, G.L. A monoclonal antibody (3G5)-defined ganglioside antigen is expressed on the cell surface of microvascular pericytes. *The Journal of experimental medicine* **167**, 1003-1015 (1988).
58. Georgiadou, D., Chroni, A., Vezeridis, A., Zannis, V.I. & Stratikos, E. Biophysical analysis of apolipoprotein E3 variants linked with development of type III hyperlipoproteinemia. *PLoS One* **6**, e27037 (2011).

59. Huang, Z.H., Reardon, C.A. & Mazzone, T. Endogenous ApoE expression modulates adipocyte triglyceride content and turnover. *Diabetes* **55**, 3394-3402 (2006).
60. Majesky, M.W., Dong, X.R., Hoglund, V., Daum, G. & Mahoney, W.M., Jr. The adventitia: a progenitor cell niche for the vessel wall. *Cells Tissues Organs* **195**, 73-81 (2012).
61. Klein, D., *et al*. Vascular wall-resident CD44+ multipotent stem cells give rise to pericytes and smooth muscle cells and contribute to new vessel maturation. *PLoS One* **6**, e20540 (2011).
62. Urbich, C. & Dimmeler, S. Endothelial progenitor cells: characterization and role in vascular biology. *Circulation research* **95**, 343-353 (2004).
63. Chen, C.W., Corselli, M., Peault, B. & Huard, J. Human blood-vessel-derived stem cells for tissue repair and regeneration. *J Biomed Biotechnol* **2012**, 597439 (2012).
64. Bergers, G. & Song, S. The role of pericytes in blood-vessel formation and maintenance. *Neuro-oncology* **7**, 452-464 (2005).
65. Juchem, G., *et al*. Pericytes in the macrovascular intima: possible physiological and pathogenetic impact. *American journal of physiology. Heart and circulatory physiology* **298**, H754-770 (2010).
66. Dar, A., *et al*. Multipotent vasculogenic pericytes from human pluripotent stem cells promote recovery of murine ischemic limb. *Circulation* **125**, 87-99 (2012).
67. Chen, C.W., *et al*. Human pericytes for ischemic heart repair. *Stem Cells* **31**, 305-316 (2013).
68. Canfield, A.E., *et al*. Role of pericytes in vascular calcification: a review. *Z Kardiol* **89 Suppl 2**, 20-27 (2000).
69. Collett, G.D. & Canfield, A.E. Angiogenesis and pericytes in the initiation of ectopic calcification. *Circulation research* **96**, 930-938 (2005).
70. Jaffredo, T., *et al*. From hemangioblast to hematopoietic stem cell: an endothelial connection? *Exp Hematol* **33**, 1029-1040 (2005).
71. Peault, B. Hemangioblasts: back to the future? *Blood* **116**, 2864-2865 (2010).
72. Schatteman, G.C. & Awad, O. Hemangioblasts, angioblasts, and adult endothelial cell progenitors. *The anatomical record. Part A, Discoveries in molecular, cellular, and evolutionary biology* **276**, 13-21 (2004).
73. Forrai, A. & Robb, L. The hemangioblast--between blood and vessels. *Cell cycle* **2**, 86-90 (2003).
74. Wang, L., *et al*. Endothelial and hematopoietic cell fate of human embryonic stem cells originates from primitive endothelium with hemangioblastic properties. *Immunity* **21**, 31-41 (2004).
75. Alessandri, G., *et al*. Human vasculogenesis ex vivo: embryonal aorta as a tool for isolation of endothelial cell progenitors. *Lab Invest* **81**, 875-885 (2001).

76. Invernici, G., *et al*. Human fetal aorta contains vascular progenitor cells capable of inducing vasculogenesis, angiogenesis, and myogenesis in vitro and in a murine model of peripheral ischemia. *Am J Pathol* **170**, 1879-1892 (2007).
77. Zengin, E., *et al*. Vascular wall resident progenitor cells: a source for postnatal vasculogenesis. *Development* **133**, 1543-1551 (2006).
78. Hu, Y., *et al*. Abundant progenitor cells in the adventitia contribute to atherosclerosis of vein grafts in ApoE-deficient mice. *The Journal of clinical investigation* **113**, 1258-1265 (2004).
79. Yamashita, J., *et al*. Flk1-positive cells derived from embryonic stem cells serve as vascular progenitors. *Nature* **408**, 92-96 (2000).
80. Ferreira, L.S., *et al*. Vascular progenitor cells isolated from human embryonic stem cells give rise to endothelial and smooth muscle like cells and form vascular networks in vivo. *Circulation research* **101**, 286-294 (2007).
81. Howson, K.M., *et al*. The postnatal rat aorta contains pericyte progenitor cells that form spheroidal colonies in suspension culture. *Am J Physiol Cell Physiol* **289**, C1396-1407 (2005).
82. Tintut, Y., *et al*. Multilineage potential of cells from the artery wall. *Circulation* **108**, 2505-2510 (2003).
83. Parhami, F., Basseri, B., Hwang, J., Tintut, Y. & Demer, L.L. High-density lipoprotein regulates calcification of vascular cells. *Circulation research* **91**, 570-576 (2002).
84. Ting, T.C., *et al*. Increased lipogenesis and stearate accelerate vascular calcification in calcifying vascular cells. *The Journal of biological chemistry* **286**, 23938-23949 (2011).
85. Pasquinelli, G., *et al*. Smooth muscle cell injury after cryopreservation of human thoracic aortas. *Cryobiology* **52**, 309-316 (2006).
86. Pasquinelli, G., *et al*. Thoracic aortas from multiorgan donors are suitable for obtaining resident angiogenic mesenchymal stromal cells. *Stem Cells* **25**, 1627-1634 (2007).
87. Hoshino, A., Chiba, H., Nagai, K., Ishii, G. & Ochiai, A. Human vascular adventitial fibroblasts contain mesenchymal stem/progenitor cells. *Biochem Biophys Res Commun* **368**, 305-310 (2008).
88. Covas, D.T., *et al*. Mesenchymal stem cells can be obtained from the human saphena vein. *Exp Cell Res* **309**, 340-344 (2005).
89. Crisan, M., *et al*. Perivascular multipotent progenitor cells in human organs. *Annals of the New York Academy of Sciences* **1176**, 118-123 (2009).
90. Tonlorenzi, R., Dellavalle, A., Schnapp, E., Cossu, G. & Sampaolesi, M. Isolation and characterization of mesoangioblasts from mouse, dog, and human tissues. *Curr Protoc Stem Cell Biol* **Chapter 2**, Unit 2B 1 (2007).

91. da Silva Meirelles, L., Chagastelles, P.C. & Nardi, N.B. Mesenchymal stem cells reside in virtually all post-natal organs and tissues. *J Cell Sci* **119**, 2204-2213 (2006).

Chapter 4

Effect of the atherosclerotic niche on resident progenitor cells: *In-vitro* assessment

4.1 Introduction

One of the most common complications of atherosclerosis is vascular calcification[1]. The atherosclerotic microenvironment may act as an accelerator to promote certain changes and making the body susceptible to the factors involved in hypertrophy of tissue and calcification. A number of factors regulate the process of calcification. Among the most important ones are the TGF-βs, which are critical for the induction of in vitro chondrogenesis. TGF-β^2 is not only detected in plaque but is actively secreted [2,3]. BMP-2 is another important factor involved in chondrogenic development of bone. However, the mechanism of vascular calcification is not fully understood. Apart from EC and SMCs, pericytes are being understood as major players in this process. Interactions between these cells are involved in crucial physiological processes such as maintenance of vascular tone and hemodynamics of the vessel, as well as the pathology of calcification. From the standpoint of contributing factors in the pathogenesis of a number of inflammatory disorders including atherosclerotic vascular calcification, immune cells such as T cells and macrophages are crucial.

As described in detail in section 1.3, the regulation of inflammation and involvement of the immune system in atherosclerosis is central. The interactions between soluble factors and the response to immune injuries, infections, post-ischemic injuries are involved at all stages of the disease. Atherosclerotic lesion development is initiated when reactions, protective to begin with, develop into chronic inflammation. Lesion progression occurs by interactions between monocyte-derived macrophages, T lymphocytes and arterial wall constituents through modified lipoproteins and pro-inflammatory factors. Briefly, accumulation of lipoproteins and increased endothelial cell permeability is followed by increased monocyte adhesion. This is then followed by their migration in intima and differentiation to macrophages. With the expression of scavenger receptors and production of a variety of enzymes and cytokines, macrophages internalize oxidized lipoproteins and ultimately form foam cells[4]. This process involves release of pro-inflammatory cytokines from activated platelets, macrophages and vessel wall cells. SMC recruitment to the surface of the plaque is induced and their

proliferation leads to ECM production and further release of pro-inflammatory cytokines. Along with macrophages, activated ECs also produce factors that attract leucocytes.

In some studies on the inflammatory response in advanced human atherosclerotic lesions a Th1-type T cell response was mostly found[5]. Macrophages also produce pro-inflammatory cytokines such as IL-1β and TNF-α (Fig 4.1), which are detected in the atherosclerotic plaques[6]. TNF-α is involved in virtually every stage of inflammation as the lesion progresses[7]. Studies have implicated TNF-α in both early stages of intimal thickening and also subsequent vessel occlusion[8]. The pro-inflammatory mediators enhance atherogenesis by promoting the pro-inflammatory environment through facilitating the interactions between ECs, leucocytes and platelets[9]. Inflammation has also been shown to be involved in altering plaque morphology, probably through stimulation of secretion of proteases such as MMP-1, 9, 11 and 13 from ECs, SMCs and/or macrophages[10,11] and is thus implicated in plaque rupture[9]. IL-1 is another important pro-inflammatory cytokine detected in the atherosclerotic plaque[6]. IL-1β has been shown by recent studies to play a crucial and causal role in atherothrombosis in coronary artery disease[12]. The role of IL-1β is well known in all the phases of atherosclerosis. For example, during the initial stages of plaque formation, IL-1β stimulates expression of adhesion molecules by ECs, thus helping the extravasation of macrophages[13]. However, some studies have suggested a possible protective role for IL-1β in advanced stages of atherosclerosis and vascular remodeling revealing the complexity of IL-1 signaling in the disease[12].

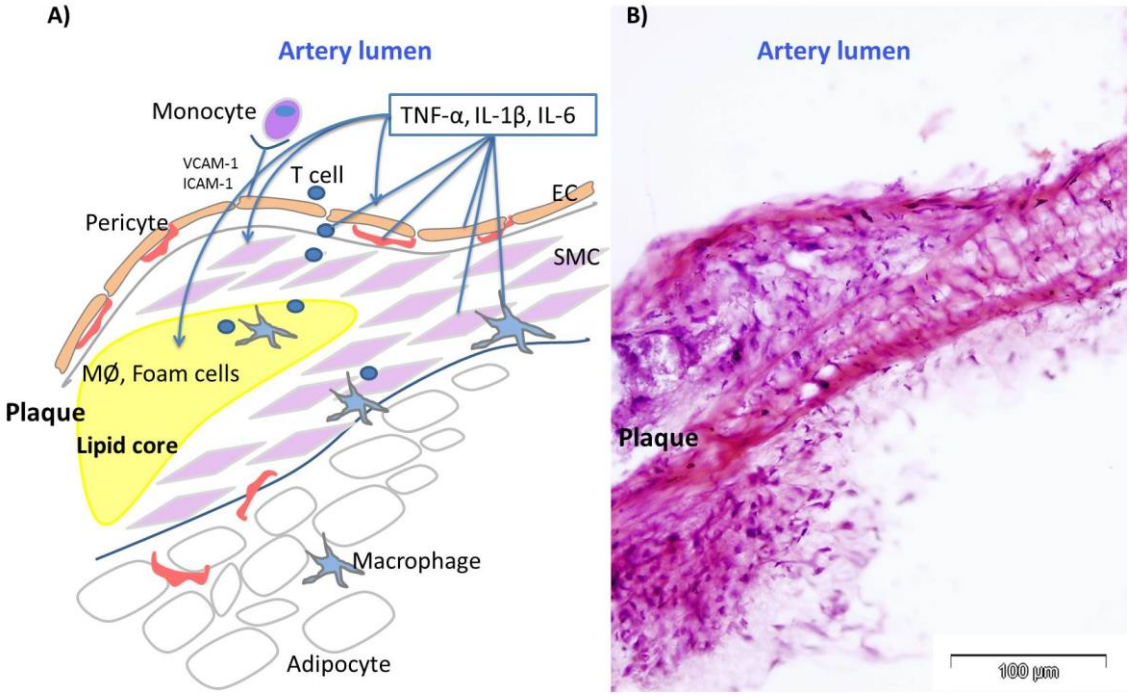

Figure 4.1 Perivascular and immune cell involvement in atherogenesis. (A) Model of arterial wall and perivascular cells in atherosclerotic plaque formation. The process involves complex interactions between different cell types like macrophages, T cells EC, SMC and pericytes producing IL-6, IL-1-β and TNF-α. Activation leads to differentiation of naïve T-cells into pro-atherogenic Th1 cells as well as regulation of smooth muscle, endothelial and pericyte functions. (B) Histologic H&E staining of aorta form ApoE$^{-/-}$ mice showing a fibrous cap and pathological intimal thickening. Scale bar at 100 µm.

The role of IL-6 in atherosclerosis is complex and manifold. In general, IL-6 has been shown to upregulate expression of cell adhesion molecules by ECs and SMCs as well as to stimulate production of C-reactive protein and TNF-α, at least by hepatocytes[9,14]. Interestingly, IL-6 can stimulate its own production by positive feedback mechanism with macrophages and intimal cells (Fig. 4.1)[9]. It also stimulates production of other factors such as IL-8 and MCP-1[9]. IL-6 is involved in immune cell recruitment in the plaque through events such as enhancement of I-CAM-1 expression by SMCs and chemokine release by endothelium[15]. It is also postulated that IL-6 affects the plaque morphology by stimulating formation of foam cells[16].

In this chapter, the effect of various pro-inflammatory cytokines was assessed at the molecular level. VSC preparations from C57BL/6 and ApoE$^{-/-}$ mice were induced to undergo chondrogenesis in pellet format in the presence of the growth factors: TGF-β and BMP-2. To assess the effect of pro-inflammatory cytokines, chondrogenesis was performed either in the presence or absence of IL-6, IL-1β or TNF-α. In order to determine temporal patterns of expression of the matrix components during different stages of differentiation under the effect of these pro-inflammatory cytokines, gene expression by pellets at 0, 2, 7, 14 and 21 days was quantified. At each time point 5 pellets were pooled and analyzed. This assessment was carried out using real-time PCR and analyzed using the ΔΔCt method[17,18], where GAPDH acted as the endogenous control. Chondrogenic pellets in the absence of the pro-inflammatory cytokines served as controls.

4.2 Results

4.2.1 Effect of IL-6, IL-1β or TNF-α on chondrogenesis of VSCs

After 21 days of pellet culture in the presence of pro-inflammatory cytokines, ApoE$^{-/-}$ VSCs had a distinct chondrogenic appearance/morphology (Fig. 4.2) and pellets were increased in size with strong toluidine blue staining. Figure 4.2 shows toluidine blue stained sections from the centers of the pellets treated with optimal concentrations of IL-6 (200ng/ml), TNF-α (10ng/ml) or IL-1β (1ng/ml) for 21 days every 2-3 days when pellets were fed as described in section 2.7.

Notably, the IL-6 treated pellets of C57BL/6 mice were much smaller and showed no evidence of matrix accumulation or chondrogenesis, while ApoE$^{-/-}$ VSCs in the presence of IL-6 had glycosaminoglycan deposition, especially in the cells close to the periphery.

Treatment with IL-1β of C57BL/6 and ApoE$^{-/-}$ VSCs resulted in the formation of smaller pellets with less differentiated cells and an undifferentiated central zone. For the C57BL/6 pellets, positive staining was observed only close to the periphery (Fig. 4.2). In the case of C57BL/6 VSCs, TNF-α treated pellets formed a dense cellular structure with no sign of differentiation. ApoE$^{-/-}$ VSCs pellets treated with TNF-α for 21 days were bigger in size with some positive toluidine blue staining (Fig. 4.2).

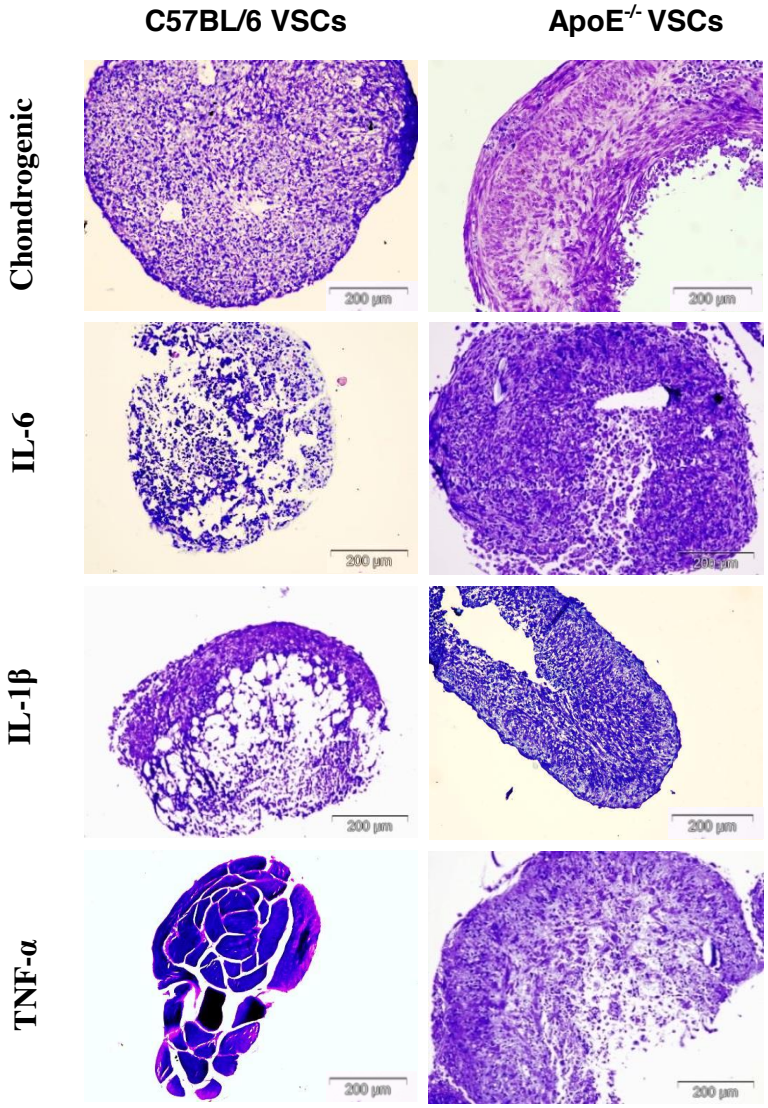

Figure 4.2 ApoE$^{-/-}$ and C57BL/6 VSCs subjected to chondrogenesis in the presence of pro-inflammatory cytokines. The effect of IL-6, IL-1β or TNF-α on chondrogenic differentiation of C57BL/6 and ApoE$^{-/-}$ VSCs is shown with toluidine blue-stained sections. Control cultures, grown in chondrogenic medium with BMP-2 and TGF-β3 for 21 days in the absence of pro-inflammatory cytokines showed a chondrogenic morphology and pellets were increased in size with strong toluidine blue staining. Although TNF-α treatment of ApoE$^{-/-}$ VSCs showed some positive staining IL-6 treatment promoted a chondrogenic phenotype in ApoE$^{-/-}$ VSCs compared to other pro-inflammatory cytokine treated pellets. Scale bars represent 200µm.

Glycosaminoglycan deposition in the pellets was quantified at 21 days in independent experiments as described in section 2.6.13 and DNA quantification was performed as described in section 2.6.1.4. In the case of C57BL/6 VSCs, there were distinct differences in GAG levels at 21 days after treatment with IL-1β (1ng/ml) and TNF-α (10ng/ml). The pellets cultured in the presence of IL-1β and TNF-α showed less glycosaminoglycan compared to those cultured with IL-6 (200ng/ml) added (Fig. 4.3). All treated C57BL/6 VSCs pellets showed a significantly lower GAG/DNA ratio compared to controls suggesting that the lower GAG accumulation in pellets treated with IL-6, IL-1β and TNF-α is a reflection of either low synthesis or higher turnover per cell.

In contrast to C57BL/6 VSCs, GAG accumulation in $ApoE^{-/-}$ VSCs pellets cultured in the presence of IL-1β, TNF-α and IL-6 showed no significant difference at 21 days (Fig. 4.4). However, the GAG/DNA ratio, in case of IL-6 treated $ApoE^{-/-}$ VSCs, was significantly higher compared to IL-1β treated $ApoE^{-/-}$ VSCs, TNF-α treated $ApoE^{-/-}$ VSCs and controls at 21 days suggesting a higher synthesis rate or low turnover per cell (Fig. 4.4). GAG/DNA in TNF-α treated cultures was lower, although not significantly, than untreated cultures.

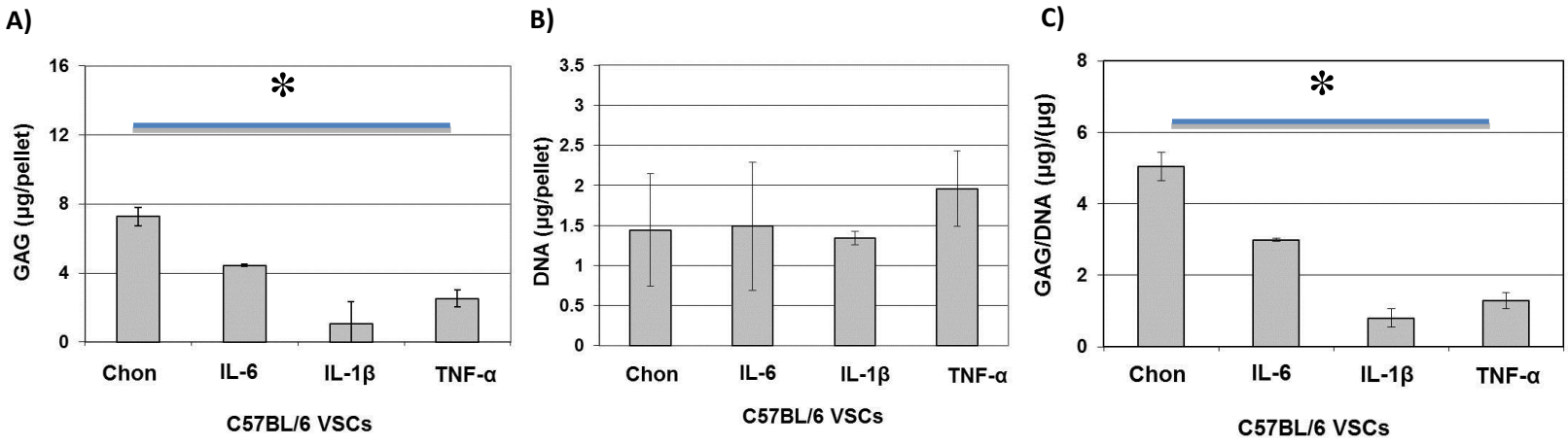

Figure 4.3: Quantification of GAG and DNA following chondrogenic differentiation C57BL/6 VSCs in the presence of pro-inflammatory cytokines. (A) GAG per pellet was assessed following extraction and reaction with DMMB. (B) Total DNA per pellet was also calculated. (C) Based on these calculations GAG synthesis per cell was determined and presented as the ratio of GAG and DNA content in each pellet. There was significant difference in GAG concentration between untreated and IL-6 treated pellets. The IL-1β and TNF-α also had significantly lower levels of GAG compared to IL-6 treated pellets. Results are presented as the mean ± SD of data at 21 days from 3 individual cell preparations from each group. * represents $p \leq 0.05$.

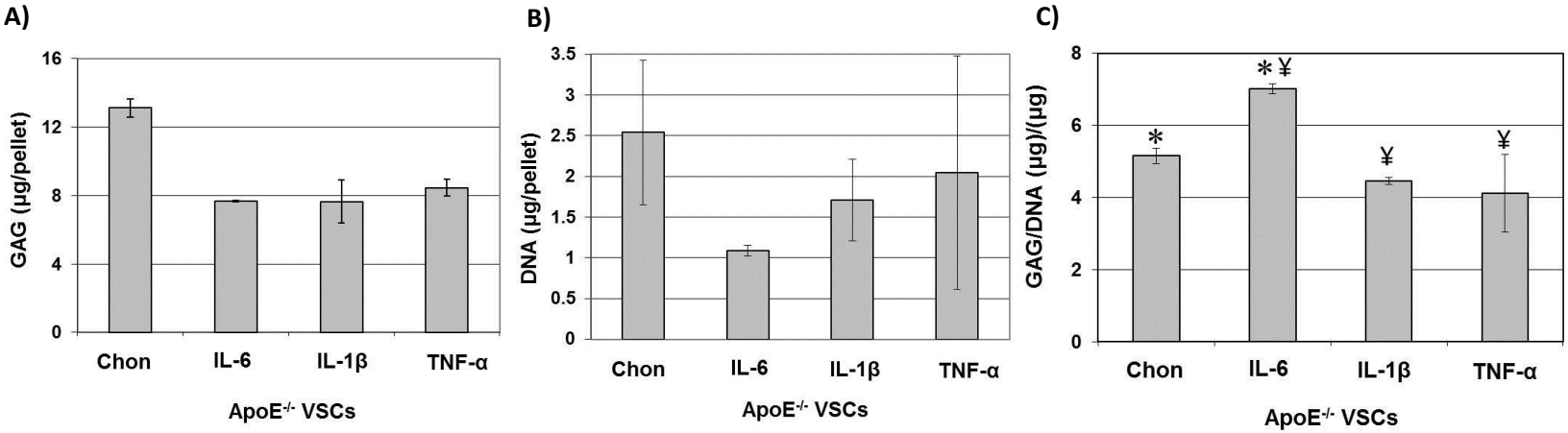

Figure 4.4: Quantification of GAG and DNA following chondrogenic differentiation ApoE$^{-/-}$ VSCs in the presence of pro-inflammatory cytokines. (A) GAG per pellet was calculated following extraction and reaction with DMMB. (B) Total DNA per pellet was also calculated. (C) Based on these calculations GAG synthesis per cell was determined and presented as a ratio of GAG and DNA content in each pellet. Results are presented as the mean ± SD of data at 21 days from 3 individual cell preparations from each group. GAG: DNA ratio was significantly higher in IL-6 treated pellets as compared to IL-1β ted and TNF-α treated pellets as well as control pellets. *, ¥ represent $p \leq 0.05$.

For all the gene expression studies, RNA was isolated from the pellets at 0, 2, 7, 14 and 21 days and real time PCR was performed. Analysis was performed using ΔΔCt method, where GAPDH acted as endogenous control and chondrogenic pellets in absence of pro-inflammatory cytokines as the calibrator.

4.2.2 Effect of IL-6 on gene expression of early chondrogenic markers

4.2.2.1 Real-time PCR analysis of Sox9

Sox9 is considered the master transcription factor for initiation of chondrogenesis which usually peaks between 24-48h after chondrogenic induction[19]. The effect of IL-6 (200ng/ml) on the expression of Sox9 varied substantially between C57BL/6 and ApoE$^{-/-}$ VSCs at different time points (Fig. 4.5 A). At 48 hours, Sox9 was upregulated in ApoE$^{-/-}$ VSCs whereas in C57BL/6 VSCs, the Sox9 expression was rapidly suppressed. During follow up at 7 and 14 days after exposure to 200 ng/ml of IL-6 treatment, the Sox9 expression dropped in ApoE$^{-/-}$ VSCs while C57BL/6 VSCs did not show any significant changes. The difference in Sox9 expression was most evident at 21 days post IL-6 induction. The ApoE$^{-/-}$ VSCs were shown to have significantly higher levels of Sox9 compared to the C57BL/6 VSC treatment group. There was a suppressive effect of IL-6 on C57BL/6 VSC on Sox9 gene expression.

4.2.2.2 Real-time PCR analysis of fibromodulin

Fibromodulin is usually undetected in undifferentiated MSCs and increases with exposure to chondrogenic inducers in a 3D format to peak at day 7 during chondrogenesis[20]. The presence of IL-6 in the culture medium for C57BL/6 VSCs pellets resulted in down regulation of fibromodulin RNA levels at 48h and day 7 whereas ApoE$^{-/-}$ VSCs showed an up-regulation but not significantly so (Fig 4.5 B). At day 14, a suppressive effect of IL-6 was observed on fibromodulin expression in both ApoE$^{-/-}$ and C57BL/6 VSCs. However, at day 21, the ApoE$^{-/-}$ VSCs showed upregulation of the fibromodulin message while C57BL/6 VSCs maintained reduced expression throughout the culture period. Thus, IL-6 treatment could not prevent fibromodulin gene expression during differentiation at day 21 in ApoE$^{-/-}$ VSCs but did suppress fibromodulin expression in C57BL/6 VSCs (Fig 4.5 B).

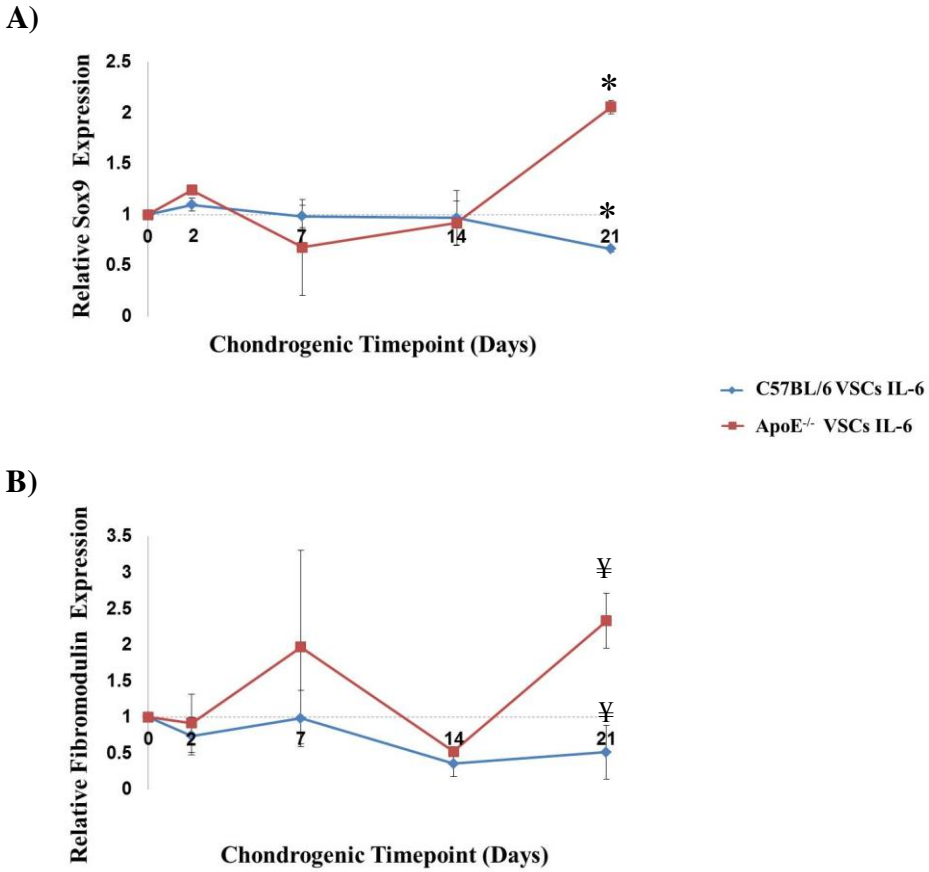

Figure 4.5: Effect of IL-6 on Sox9 and fibromodulin gene expression in chondrogenically differentiating ApoE$^{-/-}$ and C57BL/6 VSCs. Isolated cells were differentiated in chondrogenic conditions in the presence or absence of IL-6 (200ng/ml) and cultured in pellet format for 21 days. To analyse Sox9 and fibromodulin expression cells at 0 hours in normal culture media and 48 hours, 7 days, 14 days and 21 day pellets (n=5) in chondrogenic medium in presence and absence of IL-6 were harvested. RNA was extracted and the expression of Sox9 (A) and fibromodulin (B) measured by real-time PCR. Expression levels were normalized to those for GAPDH. 2 technical replicates from 3 preparations were analyzed and data presented as mean ± SD. *, ¥ represent $p \leq 0.05$.

4.2.3 Effect of IL-6 on gene expression of chondrogenic markers.

4.2.3.1 Real-time analysis of type II collagen.

There have been conflicting reports on the effect of IL-6 on type II collagen expression. A report has shown that the presence of IL-6 increases type II collagen expression in human chondrocytes[21], whereas another report on chondrogenic progenitors showed that IL-6 decreases both type II along with type X collagen expression[22]. The effect of IL-6 on the expression of type II collagen during chondrogenesis of C57BL/6 and ApoE$^{-/-}$ VSCs was analysed. At 48h, 7 and 14 days, the expression of type II collagen in C57BL/6 and ApoE$^{-/-}$ VSCs was maintained at low and almost uniform levels, equivalent to that measured in control chondrogenic pellets. However, at 21 days post IL-6 induction, type II collagen expression was evidently different. While C57BL/6 VSCs still maintained equivalent expression levels to controls, ApoE$^{-/-}$ VSCs were shown to have significant upregulation of up to 28-fold in type II collagen expression (Fig. 4.6 A).

4.2.3.2 Real-time analysis of aggrecan.

In chondrogenically-treated MSC pellets, aggrecan expression usually remains upregulated until 21 days appearing at 4-5 days after induction[20]. Figure 4.6 B clearly indicates that exposure to IL-6 during chondrogenesis maintained aggrecan at a level equivalent to that of control chondrogenic pellets cultured with 10ng/ml TGF-β3 and 100ng/ml BMP throughout differentiation. However, between 14 and 21 days aggrecan expression was downregulated in C57BL/6 VSCs. Similarly, aggrecan message was decreased in IL-6-exposed compared to control pellets generated from ApoE$^{-/-}$ VSCs; however, at day 21, a 3.9-fold upregulation of mRNA levels was observed (Fig. 4.6 B).

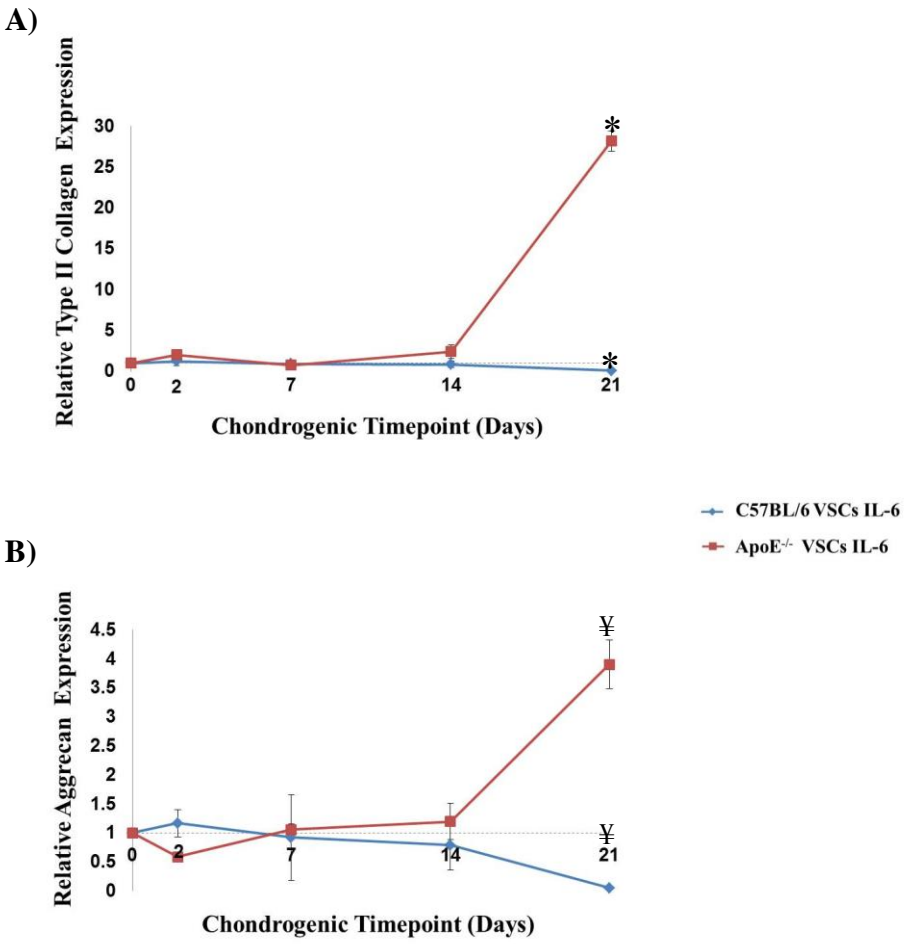

Figure 4.6: Effect of IL-6 on type II collagen and aggrecan gene expression in chondrogenically differentiating ApoE$^{-/-}$ and C57BL/6 VSCs. Isolated cells were differentiated in chondrogenic conditions in the presence or absence of IL-6 (200ng/ml) and cultured in pellet format for 21 days. Pellets were harvested at 0 hours, 48 hours, 7 days, 14 days and 21 days and RNA was extracted and the expression of type II collagen (A) and aggrecan (B) measured by real-time PCR. Expression levels were normalized to those for GAPDH. 2 technical replicates from 3 preparations were analyzed and data presented as mean ± SD. *, ¥ represent $p \leq 0.05$.

4.2.4 Effect of IL-6 on gene expression of hypertrophic chondrogenic markers.

4.2.3.2 Real-time analysis of Runx2.

The expression pattern of Runx2 in the presence of IL-6 was analysed. The activity of IL-6 suppressed expression of Runx2 in C57BL/6 VSC generally; however, there was a slight increase over control values at day 7. Chondrogenically treated ApoE$^{-/-}$ VSCs on the other hand exhibited increased levels of Runx2 mRNA transcript level throughout the culture period in the presence of IL-6 (Fig. 4.7 A). The increase in Runx2 expression induced by IL-6 at 48h and day 21 in ApoE$^{-/-}$ VSCs during chondrogenesis was notable in contrast to the decrease seen in C57BL/6 VSCs at this time point.

4.2.3.2 Real-time analysis of alkaline phosphatase.

In order to analyze alkaline phosphatase (ALP) expression in chondrogenically primed pellets in the presence of IL-6, real time PCR was carried out (Fig. 4.7 B). ALP message was detected at 48h after IL-6 induction with a robust increase in ApoE$^{-/-}$ VSCs. At day 7, the upregulation was much more pronounced in ApoE$^{-/-}$ VSCs while at day 14 the expression of ALP was decreased. However, at day 21 the presence of IL-6 resulted in significantly elevated ALP mRNA expression in ApoE$^{-/-}$ VSCs. In contrast, C57BL/6 VSCs had consistent levels of expression throughout differentiation in pellet culture indicating that the pro-inflammatory cytokine had no additional effect on levels of ALP compared to that in control untreated chondrogenic pellets.

4.2.3.2 Real-time analysis of type X collagen.

Chondrogenic differentiation in the presence of IL-6 exhibited a significant trend toward decreased type X collagen expression throughout differentiation in both ApoE$^{-/-}$ and C57BL/6 VSCs (Fig. 4.7 C). The continuing decrease in type X collagen expression resulted in lowest levels of expression at 21 days post IL-6 induction. Thus, downregulation was observed in both ApoE$^{-/-}$ and C57BL/6 VSCs.

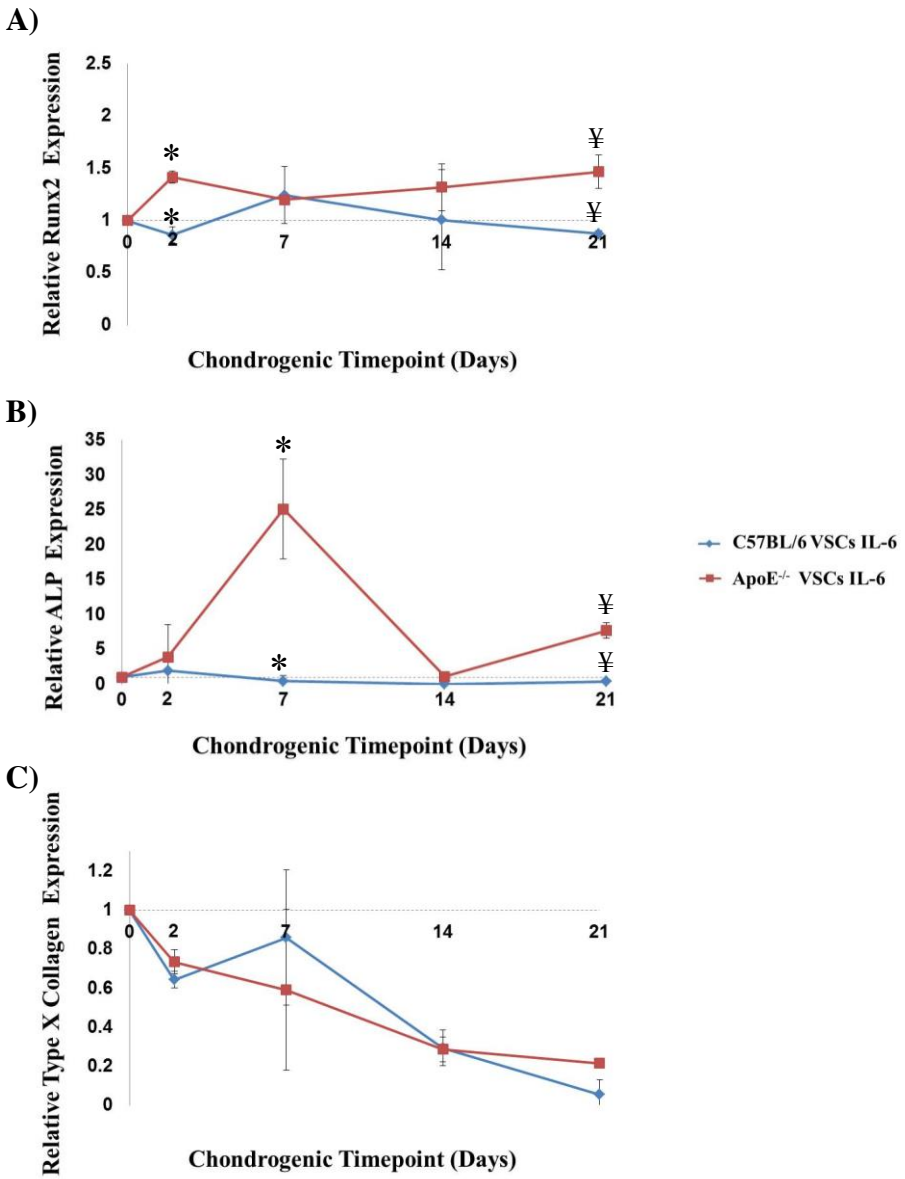

Figure 4.7: Effect of IL-6 on Runx2, ALP and type X collagen gene expression in chondrogenically differentiating ApoE$^{-/-}$ and C57BL/6 VSCs. Isolated cells were differentiated in chondrogenic conditions in the presence or absence of IL-6 (200ng/ml) and cultured in pellet format for 21 days. Pellets were harvested at 0 hours, 48 hours, 7 days, 14 days and 21 days and RNA was extracted and the expression of Runx2 (A), ALP (B) and type X collagen (C) measured by real-time PCR. Expression levels were normalized to those for GAPDH. 2 technical replicates from 3 preparations were analyzed and data presented as mean ± SD. *, ¥ represent $p \leq 0.05$.

4.2.5 Effect of IL-1β and TNF-α on gene expression of early chondrogenic markers.

4.2.5.1 Real-time PCR analysis of Sox9.

The expression of Sox9 in response to 1ng/ml IL-1β and 10ng/ml TNF-α varied between ApoE$^{-/-}$ and C57BL/6 VSCs at different time points. Ultimately, both cytokines suppressed chondrogenic differentiation in ApoE$^{-/-}$ and C57BL/6 VSCs (Fig. 4.8 A). At 48h, Sox9 message was a little bit increased but not significantly in ApoE$^{-/-}$ VSCs in response to IL-1β. Similarly, treatment with TNF-α could not prevent Sox9 gene expression in ApoE$^{-/-}$ VSCs. In contrast, at 48 hours the expression of Sox9 in C57BL/6 VSCs showed negative effect in response to both IL-1β and TNF-α treatment. At all further time points in chondrogenic differentiation, with IL-1β or TNF-α added to the chondrogenic medium, the Sox9 expression pattern indicated a robust inhibitory effect on both ApoE$^{-/-}$ and C57BL/6 VSCs (Fig. 4.8 A).

4.2.5.2 Real-time PCR analysis of fibromodulin.

IL-1β or TNF-α exposure during chondrogenesis also resulted in decreased fibromodulin RNA levels in ApoE$^{-/-}$ VSCs (Fig. 4.8 B). The fibromodulin message was downregulated within 48h after exposure to IL-1β or TNF-α in ApoE$^{-/-}$ and C57BL/6 VSCs. This effect was least pronounced in C57BL/6 VSCs treated with IL-1β and most evident in ApoE$^{-/-}$ VSCs treated with TNF-α. A similar inhibitory pattern was observed at day 7 with a more pronounced effect compared to 48h. The IL-1β treatment resulted in strong downregulated fibromodulin expression in the ApoE$^{-/-}$ VSCs at day 7 with a much more pronounced effect of TNF-α. Also at day 7, a similar effect on the expression pattern of fibromodulin in C57BL/6 VSCs was observed with more robust downregulation in the presence of TNF-α. Again, a less pronounced effect was observed in C57BL/6 VSCs treated with IL-1β. At day 14 and 21, the overall inhibitory effect continued with some differences in IL-1β treated C57BL/6 VSCs. The presence of IL-1β did not suppress fibromodulin RNA expression during C57BL/6 VSCs pellet culture (Fig. 4.8 B).

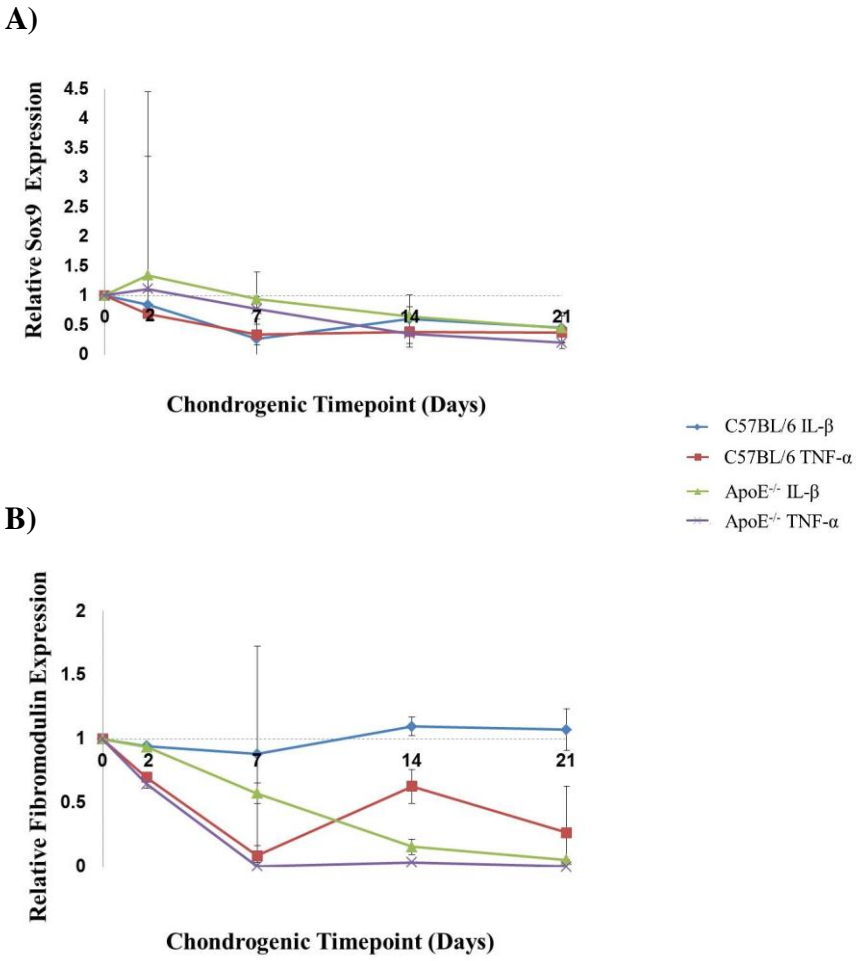

Figure 4.8: Effect of IL-1β and TNF-α on Sox9 and fibromodulin gene expression in chondrogenically differentiating ApoE$^{-/-}$ and C57BL/6 VSCs. Isolated cells were differentiated in chondrogenic conditions in the presence or absence of IL-1β (1ng/ml) and TNF-α (10ng/ml) and cultured in pellet format for 21 days. Pellets were harvested at 0 hours, 48 hours, 7 days, 14 days and 21 days and RNA was extracted and the expression of Sox9 (A) and fibromodulin (B) measured by real-time PCR. Expression levels were normalized to those for GAPDH. 2 technical replicates from 3 preparations were analyzed and data presented as mean ± SD.

4.2.6 Effect of IL-1β and TNF-α on gene expression of chondrogenic markers.

4.2.6.1 Real-time analysis of type II collagen.

Treatment of ApoE$^{-/-}$ and C57BL/6 VSCs with either IL-1β or TNF-α inhibited type II collagen expression. After 48h of exposure to the cytokine treatment, both ApoE$^{-/-}$ and C57BL/6 VSCs showed a decrease in type II collagen mRNA expression compared to control levels (Fig 4.9 A). At day 7, all cell preparations showed a robust inhibitory effect in the presence of either IL-1β or TNF-α. The ApoE$^{-/-}$ VSCs maintained this effect up to day 14 in the presence of cytokines. However, at day 21, IL-1β treatment showed a significant elevation in expression of type II collagen in ApoE$^{-/-}$ VSCs whereas TNF-α maintained uniform levels. However, the effect was still inhibitory compared to control cultures.

4.2.6.2 Real-time analysis of aggrecan.

Expression of aggrecan appeared to be downregulated at all stages of chondrogenic differentiation in the presence of 1ng/ml IL-1β or 10ng/ml TNF-α in both ApoE$^{-/-}$ and C57BL/6 VSCs (Fig 4.9 B). The effect of TNF-α was more pronounced compared to IL-1β at day 7 in ApoE$^{-/-}$ VSCs. A decrease in aggrecan RNA levels was observed at 7 and 14 days in C57BL/6 VSCs. The effect on the expression of aggrecan in presence of IL-1β on ApoE$^{-/-}$ VSCs at day 14 clearly indicated a continued and more robust inhibitory effect of IL-1β exposure. Also, in C57BL/6 VSCs, there was continuous down regulation in the presence of TNF-α; however, at 48h, treatment with IL-1β could not prevent a slight increase in expression of aggrecan (Fig 4.9 B).

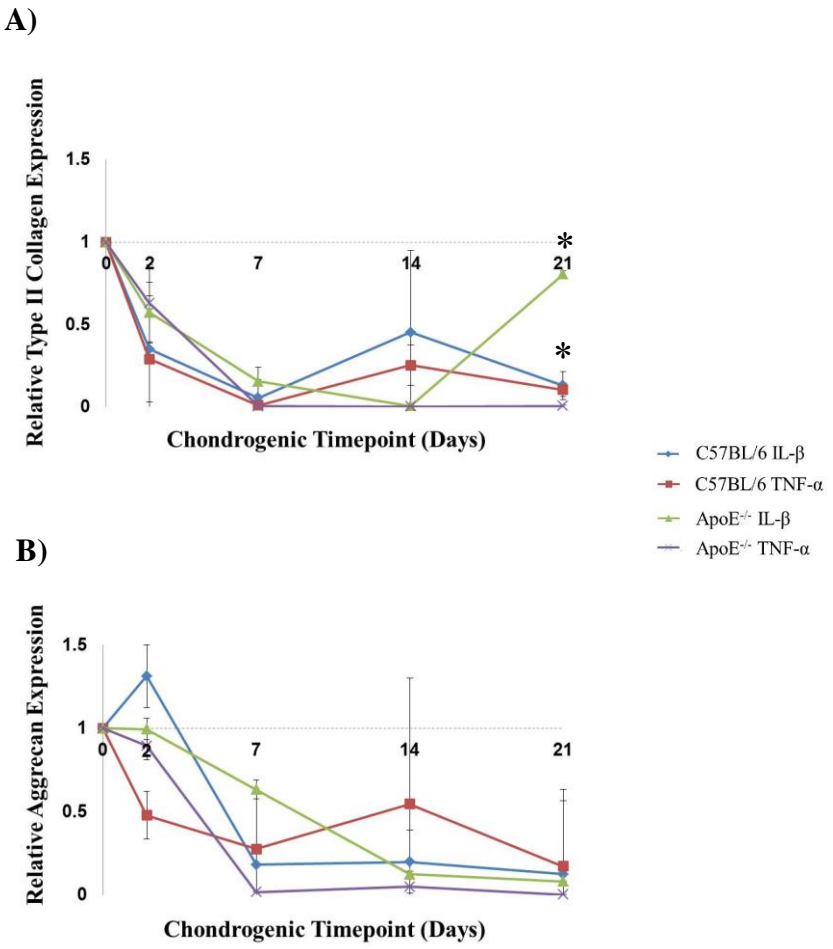

Figure 4.8: Effect of IL-1β and TNF-α on type II collagen and aggrecan gene expression in chondrogenically differentiating ApoE$^{-/-}$ and C57BL/6 VSCs. Isolated cells were differentiated in chondrogenic conditions in the presence or absence of IL-1β (1ng/ml) and TNF-α (10ng/ml) and cultured in pellet format for 21 days. Pellets were harvested at 0 hours, 48 hours, 7 days, 14 days and 21 days and RNA was extracted and the expression of type II collagen (A) and aggrecan (B) measured by real-time PCR. Expression levels were normalized to those for GAPDH. 2 technical replicates from 3 preparations were analyzed and data presented as mean ± SD. * represents $p \leq 0.05$.

4.2.7 Effect of IL-1β and TNF-α on gene expression of hypertrophic chondrogenic markers.

4.2.7.1 Real-time analysis of Runx2.

Data analysed for Runx2 expression indicated that the effect of IL-1β or TNF-α varied between the mice strains (Fig. 4.10 A). At 48 hours, Runx2 was upregulated in $ApoE^{-/-}$ VSCs whereas in C57BL/6 VSCs, Runx2 expression was suppressed. During follow up at 7 and 14 days after IL-1β or TNF-α treatment, Runx2 expression dropped in $ApoE^{-/-}$ VSCs. $ApoE^{-/-}$ VSCs were shown to have significantly lower Runx2 mRNA levels at day 7 upon IL-1β and TNF-α treatment. Upon treatment of $ApoE^{-/-}$ VSCs with IL-1β, Runx2 expression was decreased and a higher inhibition effect was observed at 14 and 21 days. In the case of C57BL/6 VSCs, Runx2 message was rapidly downregulated as reported previously[23], and then maintained at uniform level in presence of cytokines in pellet culture.

4.2.7.2 Real-time analysis of alkaline phosphatase.

Both cytokines suppressed mineralization. ALP mRNA expression with IL-1β or TNF-α added to the chondrogenic medium was rapidly downregulated within 48h in C57BL/6 VSCs. Figure 4.10 B clearly indicates that both cytokines decrease ALP mRNA levels with a much more pronounced effect at day 7 and 14 in C57BL/6 VSCs. However, we found that IL-1β treated C57BL/6 could elevate ALP expression at day 21 in comparison to 7 and 14 day whereas TNF-α treated C57BL/6 maintained a uniform level. The analysis of $ApoE^{-/-}$ VSCs ALP expression levels in the presence of cytokines showed some increase after 48h. However, TNF-α, unlike IL-1β, could inhibit the ALP mRNA expression to a greater degree at day 7 and maintained consistent downregulation throughout differentiation. The IL-1β showed an abrogated effect at day 14 which was maintained until day 21 in pellet culture (Fig. 4.10 B).

4.2.7.3 Real-time analysis of type X collagen.

Type X collagen message was decreased at 48h post treatment with IL-1β and TNF-α (Fig. 4.10 C). However, IL-1β in pellet culture showed lesser inhibition at this time

point in C57BL/6 VSCs. At day 7, the expression pattern showed a decrease with continuing negative effect of both cytokines in all preparations (Fig. 4.10 C). The downregulation was maintained throughout differentiation in ApoE$^{-/-}$ VSCs in the presence of TNF-α in culture; in contrast IL-1β elevated type X collagen expression at day 14. Nonetheless, at day 21 IL-1β had inhibitory effect on type X collagen expression.

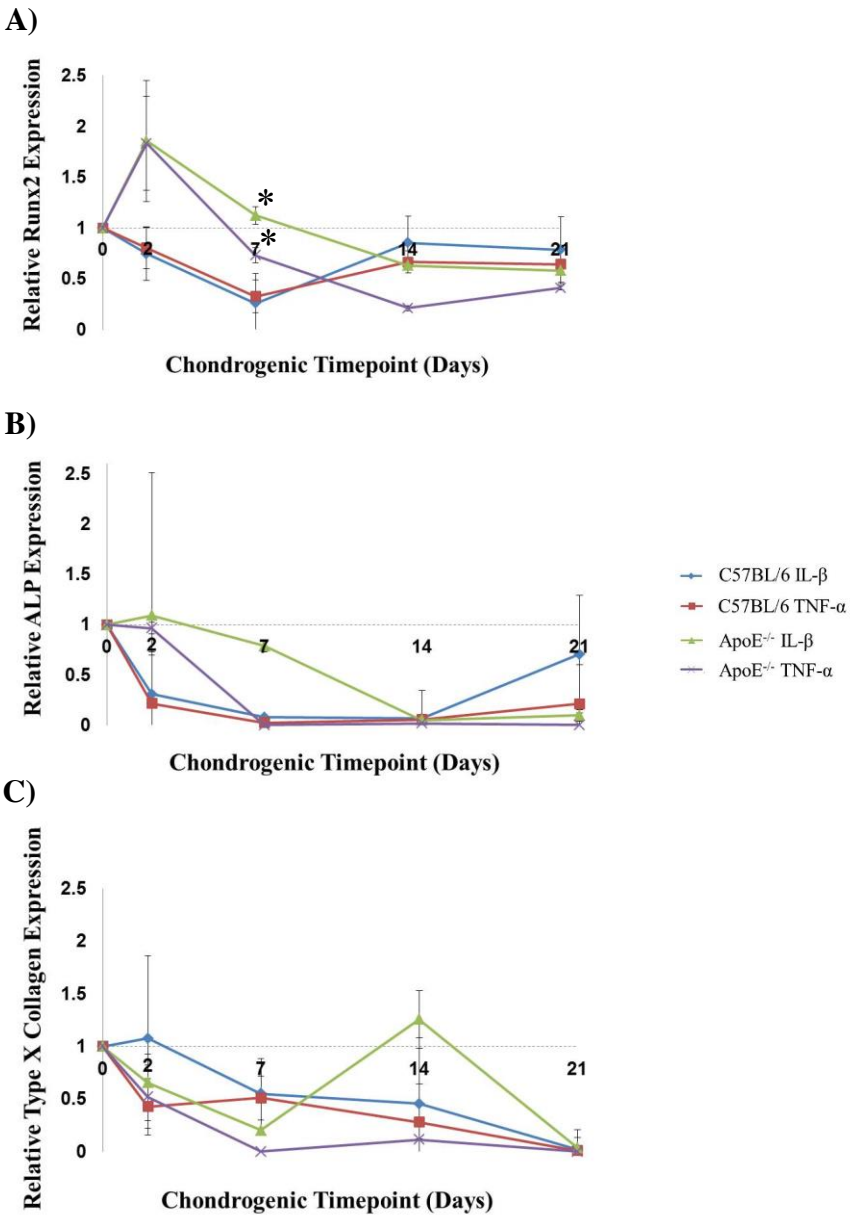

Figure 4.10: Effect of IL-1β and TNF-α on Runx2, ALP and type X collagen gene expression in chondrogenically differentiating ApoE$^{-/-}$ and C57BL/6 VSCs. Isolated cells were differentiated in chondrogenic conditions in the presence or absence of IL-1β (1ng/ml) and TNF-α (10ng/ml) and cultured in pellet format for 21 days. Pellets were harvested at 0 hours, 48 hours, 7 days, 14 days and 21 days, RNA was extracted and the expression of Runx2 (A), ALP (B) and type X collagen (C) measured by real-time PCR. Expression levels were normalized to those for GAPDH. 2 technical replicates from 3 preparations were analyzed and data presented as mean ± SD. * represents $p \leq 0.05$.

4.3 Discussion

Since Ross revisited his response to injury theory and presented atherosclerosis as a chronic inflammatory disease[24], a number of reports have supported the role in inflammation and immunity in pathogenesis of atherosclerosis as against SMC proliferation[25]. Thus, it is conceived that atherosclerosis may be initiated by monocyte/lymphocyte adhesion to activated EC. However, we are proposing here that the inflammatory environment activates vessel derived stem cells which leads to their differentiation to bone and cartilage. Thus, our approach was to investigate the effect of pro-inflammatory cytokines, seen routinely in the atherosclerotic environment, on the differentiation of VSCs from ApoE$^{-/-}$ mice and C57BL/6. In the atherosclerotic environment, a number pro-inflammatory cytokines such as TNF-α, IL-6, IL-1β are increased. TNF-α and IL-1β are major cytokines that lead to cartilage resorption in osteoarthritis and other inflammatory diseases. In contrast to their effect on cartilage loss, inflammatory cytokines are strongly suspected to induce ectopic bone formation[26,27].

What triggers this inflammatory reaction is not completely understood. However, numerous triggering factors such as oxidized LDL, free oxygen radicals and to some extent, MMPs, heat shock proteins and advanced glycation end products have been implicated. Activation of Toll like receptors via pathogen-associated molecular patterns (PAMPs) is one the important pathways involved in atherogenesis known to induce macrophages and vascular cells to produce pro-inflammatory cytokines. Much of the initial evidence of cytokine expression in atherosclerosis came from the work done by Hansson and colleagues[3,6,28]. TNF-α, generally considered as a prerequisite for induction of many other pro-inflammatory cytokines[24], has been shown to be expressed in the atherosclerotic plaque by a number of reports[6,24]. ApoE$^{-/-}$ mice deficient in TNF-α has been shown to have significantly decreased expression of other pro-inflammatory cytokines compared to ApoE$^{-/-}$ mice[29]

Potentially, all cells present in the atherosclerotic plaque can produce a set of cytokines contributing to the inflammatory milieu of the plaque. IL-1α and IL-1β are produced by

SMC and EC[30] while SMC can be induced to produce TNF-α in the presence of TNF-α[31]. IL-6 production is quite high in activated SMCs[32] and IFN-γ induces EC to produce IL-15 which has been implicated in T-cell migration[33]. However, macrophages, with their huge repository of pro-inflammatory cytokines such as TNF-α, IL-1, IL-6, IL-12 are by far the most important source of cytokines in the atherosclerotic plaque. Platelets may also participate in inflammatory action as they are rich source of chemokines and cytokines. IL-1β is secreted by platelets in activated state[34]. Mast cells present in the arterial wall form a part of inflammatory cell infiltrate in atherosclerosis[35]. Mast cells, both in the resting and stimulated state, can secrete exuberant amounts of TNF-α[36].

It has been reported that brain pericytes also produce immunoregulatory cytokines like IL-1β and IL-6[37]. It has be suggested that TGF-β produced by pericytes might act also as an immunomodulator at the BBB[38,39]. Pericytes are associated with blood vessels and proinflammatory cytokines and vasoactive substances secreted by them and other cells, could differentiate them to the chondrogenic lineage during the increased tension and oxidative stress associated with atherosclerotic plaque formation.

The vessel-resident progenitor cells or VSCs could possibly act as uncontrolled cells during ectopic bone formation. In conjunction with growth factors and cytokines released from EC and SMC and localized inflammatory cells, they seem to either commit to an endochondral ossification path and form bone or inhibit bone formation as shown by this study.

The overall research goal of this chapter was to seek the reason behind the abnormal vascular calcification in atherosclerosis. Data presented here help to better understand the regulatory mechanisms that links pericytes/VSCs and ectopic calcification. In this context the aims of the chapter were to determine effects of IL-6, IL-1β and TNF-α on chondrogenic differentiation and mineralization shown here for the first time with VSCs and to determine how VSCs, a heterogeneous stem cell population, might behave in an inflammatory environment; thereby to determine the feasibility of using different

inflammatory modulators to control the process occurring in the aortic plaque formation.

As shown in the previous chapter, the isolated MSCs from BM and VSCs from an aorta have abilities to differentiate to osteo- and chondro-genic lineage. The MSC and VSC populations were positive for stem cell markers but the pericyte markers were expressed only by VSCs. The fact that ApoE$^{-/-}$ VSCs that had significantly increased chondrogenic activity as described in Chapter 3, additional investigation to assess their ability to respond to pro-inflammatory cytokines during the course of chondrogenesis was required. Furthermore, whether the intrinsic capacity of the ApoE$^{-/-}$ VSCs that are prone to calcification resulted in a higher GAG/DNA ratio or whether this is seen due to alternative effects of inflammatory mediators, remained to be investigated.

To expand the current understanding of the behaviour of VSC niche in the atherogenic environment, this present study looked at the ability of VSCs to form bone in presence of proinflammatory cytokines via the endochondral ossification pathway. This was achieved through a series of real time PCR experiments investigating the effects on genes relevant at different time points during chondrogenesis. It was obvious that this process is impacted by numerous factors, which included the presence of chondrogenic growth factors and pro-inflammatory cytokines.

Differentiation of the cells in the presence of each of the tested cytokines showed lower levels of GAG at 21 days compared to the pellets cultured in absence of the cytokines. The work in this chapter highlights the potential inhibitory effect of all chosen pro-inflammatory cytokines on C57BL/6 VSCs. Similarly, in a report on MSCs, Lacey et al. demonstrated that when MSCs were differentiated down in the presence of pro-inflammatory cytokines, genes associated with chondrogenesis were downregulated[40]. Interestingly, the GAG/DNA ratio in ApoE$^{-/-}$ VSCs treated with IL-6 was significantly higher compared to the controls; in contrast to reduction in GAG production in MSCs as shown previously[41]. In this study, we have shown for the first time that the ApoE$^{-/-}$ VSCs have the ability to respond to IL-6 treatment and induce accumulation of proteoglycans. The difference between ApoE$^{-/-}$ VSCs and C57BL/6

VSCs was clear when following the pellet culture for 21 days cultured with IL-6, the ApoE$^{-/-}$ VSCs showed a chondrogenic morphology and pellets were similarly in size to the control pellets with strong toluidine blue staining; however, C57BL/6 VSC pellets were considerably smaller and showed no evidence of matrix accumulation.

The chondrogenic ability of ApoE$^{-/-}$ and C57BL/6 VSCs was significantly reduced in presence of IL-1β and TNF-α compared to chondrogenic controls. However the morphology and GAG concentration in TNF-α treated ApoE$^{-/-}$ VSCs showed accumulation of proteoglycans with positive toluidine blue staining. Nonetheless, the GAG/DNA ratio was significantly lower as there was observed or lower synthesis per cell or high turnover. The C57BL/6 VSCs had smaller pellets and did not stain with toluidine blue, except in case of IL-1β treatment where very little staining was observed.

The molecular analysis in this chapter was based on markers signifying three progressive phases of chondrogenesis. The early gene expression profile takes into account markers of chondrogenic progenitors like Sox9 and fibromodulin, followed by markers of mature chondrocytes like type II collagen and aggrecan, and by markers of hypertrophic chondrocytes defined by robust upregulation of collagen type X, alkaline phosphatase and Runx2[42]. To this purpose, the VSCs cultured in chondrogenic medium in the presence or absence of IL-6, IL-1β and TNF-α were analysed to assess these markers.

During first phase of chondrogenic differentiation with IL-6 at 48h, the Sox9 message was increased in ApoE$^{-/-}$ VSCs compared to C57BL/6 VSCs, where it was decreased. The effect of IL-1β and TNF-α showed decreased Sox9 and fibromodulin RNA levels in both ApoE$^{-/-}$ and C57BL/6 VSCs. The importance of Sox9 expression not only in encoding cartilage matrix proteins such as type II collagen but also in promoting their transcription has been reported previously[43]. This may, at least partially, explain the increase in type II collagen expression in ApoE$^{-/-}$ VSCs.

Fibromodulin message was at low levels at early stages of chondrogenesis in both ApoE$^{-/-}$ and C57BL/6 VSCs in the presence of IL-6. Fibromodulin binds to TGF-β and

maintains cartilage integrity in murine articular cartilage[44] and promotes early articular cartilage development in mice limb[20]. Our study shows a slight but not significant increase in fibromodulin expression at day 7.

The last stage of chondrogenic process, with GAG accumulation, represents mature chondrocyte formation. At 14 days Sox-9 expression remains at low levels in both IL-6 treated cell populations but at the 21 day time point there was significant upregulation (up to 1.9-fold change) over and above the normal levels in ApoE$^{-/-}$ VSCs. In C57BL/6 VSCs, Sox-9 remains inhibited at 21 days.

A similar suppressive effect of IL-1β and TNF-α on Sox-9 and fibromodulin gene expression (albeit with lesser effect of C57BL/6 VSC in presence of IL-1β) was noted in both ApoE$^{-/-}$ and C57BL/6 VSC populations.

Type II collagen, which is critically important in chondrogenesis was assessed at all stages of chondrogenesis. During the middle phase of chondrogenesis in MSCs, expression of type II collagen and aggrecan message was observed[20]. Type II collagen and aggrecan expression during the early and middle phases of chondrogenesis showed constant uniform low expression in the presence of IL-6 in ApoE$^{-/-}$ and C57BL/6 VSCs. However, at day 21, significant overexpression of type II collagen (28-fold) was observed in ApoE$^{-/-}$ VSCs in the presence of IL-6. This result suggests that the cytokine plays an important role in the fate of the resident blood vessel stem cells. In our studies Sox9 upregulation at 21 days (up to 1.9-fold) and type II collagen (up to 28-fold) could support the previous finding that upregulation of type II collagen is dependent on increased levels of Sox9 expression even in the phase of mature chondrocyte formation. Thus, late appearance of type II collagen in the matrix assembly can be linked with Sox-9 expression in IL-6-treated ApoE$^{-/-}$ VSCs. Another possible link is between type II collagen and aggrecan. Along with type II collagen upregulation after exposure to IL-6 presence in ApoE$^{-/-}$ VSCs, our studies showed that aggrecan is significantly overexpressed, up to 3.9-fold, at 21 days. It has previously been shown that type II collagen makes aggregates with other collagen types and proteoglycans to form mature chondrocytes[45,46]. Molecular analysis after IL-1β and TNF-α treatment of ApoE$^{-/-}$ and

C57BL/6 VSCs showed suppression of type II collagen and aggrecan at each time point. This finding is consistent with a previous report by Lacey *et al* where both cytokines decreased type II collagen and aggrecan expression in murine enriched C57BL/6 MSCs over 14 days in chondrogenic conditions *in vitro* [40].

Our results indicated that in presence of IL-6, Runx2 expression remained at uniform levels in ApoE$^{-/-}$ VSCs as compared to a drop in Runx2 expression in C57BL/6 VSCs at each time point. Exposure to IL-1β and TNF-α induces a slight increase in Runx2 expression at 48h in ApoE$^{-/-}$ VSC, but later time points showed suppression which is consistent with previous studies in human MSC mineralization in the presence of these cytokines[47].

The alkaline phosphatase transcript levels in ApoE$^{-/-}$ VSCs in exposed to IL-6 was shown to have a slight but not significant increase. The most obvious significant (25.1-fold) upregulation was observed at day 7. This finding suggests that the presence of Il-6 cytokine exaggerates the effect of chondrogenic induction and promotes Alp expression, as opposed to C57BL/6 VSCs where inhibition was observed at each time point. Day 14 showed robust downregulation of Alp in the presence of IL-6 in ApoE$^{-/-}$ VSCs. Surprisingly, at day 21 the Alp expression was significantly raised to 7.7-fold. The most interesting finding in the study could be that IL-6 strongly acts on the one of the mature chondrogenic genes in VSCs and is able to stimulate further mineralization. This data might indicate that progenitor cells from blood vessels provide the cellular link between calcification of atherosclerotic plaques and chondrogenesis with deposition of calcified matrix within.

Further analysis of type X collagen, known to be associated with hypertrophic cartilage[42], showed downregulation in IL-6 exposed culture of ApoE$^{-/-}$ and C57BL/6 VSCs. At 48h, there was a significant drop in expression of the type X collagen as well as at 7, 14, and 21 days in ApoE$^{-/-}$ and C57BL/6 VSCs. In general, type I, II and X collagen are expressed sequentially, type X collagen making its appearance at a later stage in differentiating cells[20]. Expression of type X collagen in IL-1β and TNF-α treated cultures showed similar inhibition patterns to IL-6 exposed cultures.

Taken together, the significant upregulation of key genes in chondrogenesis in ApoE$^{-/-}$ VSCs in the presence of IL-6 at different stages of chondrogenic differentiation reveals that this cytokine plays a central pathological role in the atherosclerotic microenvironment. VSCs possess a differentiation potential which is responsive to cytokines and makes them capable of formation of ectopic bone in non-bone tissue like aorta. The differentiation of ApoE$^{-/-}$ VSCs in the presence of IL-6 to chondrocytes characterized in this study and the temporal changes observed in the gene expression largely paralleled the pattern of extensive calcification *in vivo* occurring in atherosclerosis.

Sequential gene expression patterns which closely regulate cell-cell and cell matrix interactions leading to alterations at morphological and metabolic levels during development of cartilage[48,49] are not only mirrored during deposition of calcified matrix in the atherogenic processes but also to some extent during commitment of VSCs to the endochondral pathway.

IL-6 has multifunctional effect and changes in its level have been implicated in cause and development of chronic inflammatory diseases. So far, the effect of IL-6 has been studied more extensively in chronic joint diseases such as OA and RA. A study pointed out that IL-6 may contribute to the destructive changes in bone and cartilage accompanying joint disease[50]. The study showed that IL-6 leads to downregulation of major cartilage-specific genes through activation of STAT signaling pathways but not ERK-dependent pathways. The study also reported downregulation of Sox9 expression, concluding that IL-6 contributes to loss of chondrocyte phenotype and alteration of articular cartilage in joint diseases. In RA, the ability of IL-6 to decrease aggrecan synthesis in ECM has been shown[51]. Another pathway through which IL-6 may act in RA is by stimulation of MMPs[52]. Similar MMPs mediated mechanism of cartilage destruction by IL-6 has been observed in OA[53].

On the contrary, a recent study in 2012 indicated that increased levels of IL-6 appear to enhance anabolic activity of the chondrocytes and also formation of new cartilage during in vitro regeneration experiment[54]. It has been postulated that high levels of IL-6

produced by chondrocytes during regeneration play direct role in cartilage regeneration. Tocilizumab (monoclonal antibody against IL-6 receptor) has shown positive effects in diseases such as RA[55-57], systemic juvenile idiopathic[58,59] and many other inflammatory disorders. The postulation is that this treatment can inhibit progression of atherosclerosis and thereby decrease cardiovascular events[60,61].

A report has shown significant increase in ALP expression at day 7 in IL-6 treated MSCs during osteogenesis[41]. In chondrogenic assays, MSCs treated with IL-6 showed increase in the size of pellets although collagen type II and aggrecan were decreased at day 21[41]. However, this study didn't investigate other chondrogenic markers. In light of these range of different effects of IL-6, in our studies, it was not surprising to observe stimulatory effect of IL-6 on chondrogenic genes in atherosclerotic VSCs.

This study also revealed that in presence of pro-inflammatory cytokines, IL-6 in particular, released by surrounding or localized inflammatory cells, $ApoE^{-/-}$ VSCs become more permissive to this microenvironment and commit to chondrogenic differentiation pathway leading to endochondral ossification and create an expression pattern of cartilage specific genes. On the contrary, the constant inhibition of chondrogenic genes in C57BL/6 VSCs under the influence of the pro-inflammatory cytokines suggests that these cytokines promote their stemness and keep them at an undifferentiated stage

4.4 References

1. Tintut, Y*., et al.* Monocyte/macrophage regulation of vascular calcification in vitro. *Circulation* **105**, 650-655 (2002).
2. Hansson, G.K. Immune mechanisms in atherosclerosis. *Arteriosclerosis, thrombosis, and vascular biology* **21**, 1876-1890 (2001).
3. Hansson, G.K. & Jonasson, L. The discovery of cellular immunity in the atherosclerotic plaque. *Arteriosclerosis, thrombosis, and vascular biology* **29**, 1714-1717 (2009).
4. Frostegard, J. Immunity, atherosclerosis and cardiovascular disease. *BMC medicine* **11**, 117 (2013).
5. Frostegard, J*., et al.* Cytokine expression in advanced human atherosclerotic plaques: dominance of pro-inflammatory (Th1) and macrophage-stimulating cytokines. *Atherosclerosis* **145**, 33-43 (1999).
6. Hansson, G.K. Inflammation, atherosclerosis, and coronary artery disease. *N Engl J Med* **352**, 1685-1695 (2005).
7. Branen, L*., et al.* Inhibition of tumor necrosis factor-alpha reduces atherosclerosis in apolipoprotein E knockout mice. *Arteriosclerosis, thrombosis, and vascular biology* **24**, 2137-2142 (2004).
8. Barath, P*., et al.* Detection and localization of tumor necrosis factor in human atheroma. *Am J Cardiol* **65**, 297-302 (1990).
9. Girn, H.R., Orsi, N.M. & Homer-Vanniasinkam, S. An overview of cytokine interactions in atherosclerosis and implications for peripheral arterial disease. *Vascular medicine* **12**, 299-309 (2007).
10. Young, J.L., Libby, P. & Schonbeck, U. Cytokines in the pathogenesis of atherosclerosis. *Thromb Haemost* **88**, 554-567 (2002).
11. Galis, Z.S., Muszynski, M., Sukhova, G.K., Simon-Morrissey, E. & Libby, P. Enhanced expression of vascular matrix metalloproteinases induced in vitro by cytokines and in regions of human atherosclerotic lesions. *Annals of the New York Academy of Sciences* **748**, 501-507 (1995).
12. Qamar, A. & Rader, D.J. Effect of interleukin 1beta inhibition in cardiovascular disease. *Curr Opin Lipidol* **23**, 548-553 (2012).
13. Bhaskar, V*., et al.* Monoclonal antibodies targeting IL-1 beta reduce biomarkers of atherosclerosis in vitro and inhibit atherosclerotic plaque formation in Apolipoprotein E-deficient mice. *Atherosclerosis* **216**, 313-320 (2011).
14. Haddy, N*., et al.* IL-6, TNF-alpha and atherosclerosis risk indicators in a healthy family population: the STANISLAS cohort. *Atherosclerosis* **170**, 277-283 (2003).
15. von der Thusen, J.H., Kuiper, J., van Berkel, T.J. & Biessen, E.A. Interleukins in atherosclerosis: molecular pathways and therapeutic potential. *Pharmacological reviews* **55**, 133-166 (2003).
16. Klouche, M., Rose-John, S., Schmiedt, W. & Bhakdi, S. Enzymatically degraded, nonoxidized LDL induces human vascular smooth muscle cell activation, foam cell transformation, and proliferation. *Circulation* **101**, 1799-1805 (2000).
17. Livak, K.J. & Schmittgen, T.D. Analysis of relative gene expression data using real-time quantitative PCR and the 2(-Delta Delta C(T)) Method. *Methods* **25**, 402-408 (2001).
18. Pfaffl, M.W. A new mathematical model for relative quantification in real-time RT-PCR. *Nucleic acids research* **29**, e45 (2001).

19. Akiyama, H., Chaboissier, M.C., Martin, J.F., Schedl, A. & de Crombrugghe, B. The transcription factor Sox9 has essential roles in successive steps of the chondrocyte differentiation pathway and is required for expression of Sox5 and Sox6. *Genes & development* **16**, 2813-2828 (2002).
20. Barry, F., Boynton, R.E., Liu, B. & Murphy, J.M. Chondrogenic differentiation of mesenchymal stem cells from bone marrow: differentiation-dependent gene expression of matrix components. *Exp Cell Res* **268**, 189-200 (2001).
21. Namba, A.*, et al.* Effects of IL-6 and soluble IL-6 receptor on the expression of cartilage matrix proteins in human chondrocytes. *Connective tissue research* **48**, 263-270 (2007).
22. Nakajima, S.*, et al.* Interleukin-6 inhibits early differentiation of ATDC5 chondrogenic progenitor cells. *Cytokine* **47**, 91-97 (2009).
23. Gilbert, L.*, et al.* Expression of the osteoblast differentiation factor RUNX2 (Cbfa1/AML3/Pebp2alpha A) is inhibited by tumor necrosis factor-alpha. *The Journal of biological chemistry* **277**, 2695-2701 (2002).
24. Tedgui, A. & Mallat, Z. Cytokines in atherosclerosis: pathogenic and regulatory pathways. *Physiological reviews* **86**, 515-581 (2006).
25. Jonasson, L., Holm, J., Skalli, O., Bondjers, G. & Hansson, G.K. Regional accumulations of T cells, macrophages, and smooth muscle cells in the human atherosclerotic plaque. *Arteriosclerosis* **6**, 131-138 (1986).
26. Demer, L.L. Vascular calcification and osteoporosis: inflammatory responses to oxidized lipids. *International journal of epidemiology* **31**, 737-741 (2002).
27. Helske, S., Kupari, M., Lindstedt, K.A. & Kovanen, P.T. Aortic valve stenosis: an active atheroinflammatory process. *Curr Opin Lipidol* **18**, 483-491 (2007).
28. Hansson, G.K. & Libby, P. The immune response in atherosclerosis: a double-edged sword. *Nature reviews. Immunology* **6**, 508-519 (2006).
29. Ait-Oufella, H., Taleb, S., Mallat, Z. & Tedgui, A. Recent advances on the role of cytokines in atherosclerosis. *Arteriosclerosis, thrombosis, and vascular biology* **31**, 969-979 (2011).
30. Fearon, W.F. & Fearon, D.T. Inflammation and cardiovascular disease: role of the interleukin-1 receptor antagonist. *Circulation* **117**, 2577-2579 (2008).
31. Peppel, K.*, et al.* Activation of vascular smooth muscle cells by TNF and PDGF: overlapping and complementary signal transduction mechanisms. *Cardiovasc Res* **65**, 674-682 (2005).
32. Chen, L.*, et al.* Interaction of vascular smooth muscle cells and monocytes by soluble factors synergistically enhances IL-6 and MCP-1 production. *American journal of physiology. Heart and circulatory physiology* **296**, H987-996 (2009).
33. Oppenheimer-Marks, N., Brezinschek, R.I., Mohamadzadeh, M., Vita, R. & Lipsky, P.E. Interleukin 15 is produced by endothelial cells and increases the transendothelial migration of T cells In vitro and in the SCID mouse-human rheumatoid arthritis model In vivo. *The Journal of clinical investigation* **101**, 1261-1272 (1998).
34. Cha, J.K.*, et al.* Activated platelets induce secretion of interleukin-1beta, monocyte chemotactic protein-1, and macrophage inflammatory protein-1alpha and surface expression of intercellular adhesion molecule-1 on cultured endothelial cells. *Journal of Korean medical science* **15**, 273-278 (2000).
35. Rautou, P.E.*, et al.* Microparticles, vascular function, and atherothrombosis. *Circulation research* **109**, 593-606 (2011).

36. Gordon, J.R. & Galli, S.J. Mast cells as a source of both preformed and immunologically inducible TNF-alpha/cachectin. *Nature* **346**, 274-276 (1990).
37. Fabry, Z*., et al.* Production of the cytokines interleukin 1 and 6 by murine brain microvessel endothelium and smooth muscle pericytes. *Journal of neuroimmunology* **47**, 23-34 (1993).
38. Balabanov, R. & Dore-Duffy, P. Role of the CNS microvascular pericyte in the blood-brain barrier. *J Neurosci Res* **53**, 637-644 (1998).
39. Dore-Duffy, P., Balabanov, R., Rafols, J. & Swanborg, R.H. Recovery phase of acute experimental autoimmune encephalomyelitis in rats corresponds to development of endothelial cell unresponsiveness to interferon gamma activation. *J Neurosci Res* **44**, 223-234 (1996).
40. Lacey, D.C., Simmons, P.J., Graves, S.E. & Hamilton, J.A. Proinflammatory cytokines inhibit osteogenic differentiation from stem cells: implications for bone repair during inflammation. *Osteoarthritis Cartilage* **17**, 735-742 (2009).
41. Pricola, K.L., Kuhn, N.Z., Haleem-Smith, H., Song, Y. & Tuan, R.S. Interleukin-6 maintains bone marrow-derived mesenchymal stem cell stemness by an ERK1/2-dependent mechanism. *J Cell Biochem* **108**, 577-588 (2009).
42. Xu, J*., et al.* Chondrogenic differentiation of human mesenchymal stem cells in three-dimensional alginate gels. *Tissue Eng Part A* **14**, 667-680 (2008).
43. Bell, D.M*., et al.* SOX9 directly regulates the type-II collagen gene. *Nat Genet* **16**, 174-178 (1997).
44. Embree, M.C*., et al.* Biglycan and fibromodulin have essential roles in regulating chondrogenesis and extracellular matrix turnover in temporomandibular joint osteoarthritis. *Am J Pathol* **176**, 812-826 (2010).
45. Antipova, O. & Orgel, J.P. Non-enzymatic decomposition of collagen fibers by a biglycan antibody and a plausible mechanism for rheumatoid arthritis. *PLoS One* **7**, e32241 (2012).
46. Djouad, F., Mrugala, D., Noel, D. & Jorgensen, C. Engineered mesenchymal stem cells for cartilage repair. *Regenerative medicine* **1**, 529-537 (2006).
47. Ding, J*., et al.* TNF-alpha and IL-1beta inhibit RUNX2 and collagen expression but increase alkaline phosphatase activity and mineralization in human mesenchymal stem cells. *Life Sci* **84**, 499-504 (2009).
48. Kronenberg, H.M. Developmental regulation of the growth plate. *Nature* **423**, 332-336 (2003).
49. DeLise, A.M., Fischer, L. & Tuan, R.S. Cellular interactions and signaling in cartilage development. *Osteoarthritis Cartilage* **8**, 309-334 (2000).
50. Legendre, F., Dudhia, J., Pujol, J.P. & Bogdanowicz, P. JAK/STAT but not ERK1/ERK2 pathway mediates interleukin (IL)-6/soluble IL-6R down-regulation of Type II collagen, aggrecan core, and link protein transcription in articular chondrocytes. Association with a down-regulation of SOX9 expression. *The Journal of biological chemistry* **278**, 2903-2912 (2003).
51. Jorgensen, C., Noel, D., Apparailly, F. & Sany, J. Stem cells for repair of cartilage and bone: the next challenge in osteoarthritis and rheumatoid arthritis. *Ann Rheum Dis* **60**, 305-309 (2001).
52. Hashizume, M. & Mihara, M. The roles of interleukin-6 in the pathogenesis of rheumatoid arthritis. *Arthritis* **2011**, 765624 (2011).

53. Martel-Pelletier, J. Pathophysiology of osteoarthritis. *Osteoarthritis Cartilage* **12 Suppl A**, S31-33 (2004).
54. Tsuchida, A.I.*, et al.* Interleukin-6 is elevated in synovial fluid of patients with focal cartilage defects and stimulates cartilage matrix production in an in vitro regeneration model. *Arthritis Res Ther* **14**, R262 (2012).
55. Smolen, J.S.*, et al.* Effect of interleukin-6 receptor inhibition with tocilizumab in patients with rheumatoid arthritis (OPTION study): a double-blind, placebo-controlled, randomised trial. *Lancet* **371**, 987-997 (2008).
56. Genovese, M.C.*, et al.* Interleukin-6 receptor inhibition with tocilizumab reduces disease activity in rheumatoid arthritis with inadequate response to disease-modifying antirheumatic drugs: the tocilizumab in combination with traditional disease-modifying antirheumatic drug therapy study. *Arthritis Rheum* **58**, 2968-2980 (2008).
57. Maini, R.N.*, et al.* Double-blind randomized controlled clinical trial of the interleukin-6 receptor antagonist, tocilizumab, in European patients with rheumatoid arthritis who had an incomplete response to methotrexate. *Arthritis Rheum* **54**, 2817-2829 (2006).
58. Yokota, S.*, et al.* Efficacy and safety of tocilizumab in patients with systemic-onset juvenile idiopathic arthritis: a randomised, double-blind, placebo-controlled, withdrawal phase III trial. *Lancet* **371**, 998-1006 (2008).
59. Imagawa, T.*, et al.* Safety and efficacy of tocilizumab, an anti-IL-6-receptor monoclonal antibody, in patients with polyarticular-course juvenile idiopathic arthritis. *Modern rheumatology / the Japan Rheumatism Association* **22**, 109-115 (2012).
60. Tanaka, T. & Kishimoto, T. Targeting interleukin-6: all the way to treat autoimmune and inflammatory diseases. *International journal of biological sciences* **8**, 1227-1236 (2012).
61. Boekholdt, S.M. & Stroes, E.S. The interleukin-6 pathway and atherosclerosis. *Lancet* **379**, 1176-1178 (2012).

Chapter 5

Endochondral ossification by chondrogenically primed vessel-derived and mesenchymal stem cells in C57BL/6 (wild type) and ApoE$^{-/-}$ mice

5.1 Introduction

Atherosclerotic lesions are known to contain ectopic tissue including bone, cartilage, fat and marrow[1,2]. VC is one of the common complications of cardiovascular, renal disease and diabetes[3]. It is increasingly understood that VC is a cell-mediated process, which is controlled through both a local and systemic balance between inducers and inhibitors of calcification[3,4]. There is some evidence that resident vascular cells contribute to VC. Reports have shown that resident stem cells in the vessel wall can differentiate to bone and cartilage under certain conditions[5,6]. Mechanisms controlling VC are not fully understood; however, the resemblance to bone formation is suggested by the presence of many bone regulators in the vessel wall[7-13] and mediators of hydroxyapatite deposition in atherosclerotic plaque by chondrocyte-like cells[14,15]. One of the most important factors is BMP2 which regulates ectopic calcification in atherosclerosis as well endochondral ossification in skeletal bone formation[15-18]. Another factor which has been found in bone development and cartilage maturation as well in atherosclerotic plaque is TGF-β[18,19] which has been implicated in regulation of ossification by the endochondral pathway during skeletal development and fracture healing[20-22]. The link between bone formation and atherosclerotic plaque calcification is more complex. The growth factors expressed in both processes are similar. Atherosclerotic plaque calcification also involves expression of major transcription factors such as Runx2 and Sox9[23,24] which are key regulators of bone and cartilage differentiation during skeletal development[24,25]. Thus, the processes of endochondral bone formation and vascular calcification with deposition of bone in atherosclerotic lesions can be understood to be linked.

The process of bone formation through the endochondral pathway is complex and well regulated, and is initiated by formation of a vascular bud in the cartilaginous template[26]. Apart from ectopic bone formation, the vascularization process in the plaque is increasingly being accepted to take place *de novo* with invasion of other blood vessels. The significance of vascularization following a bone graft cannot be over emphasized. One major factor that leads to graft rejection is poor vascularization *in vivo*[27-29]. In contrast, calcification of atherosclerotic lesions, which is also a highly organized

process, was originally thought to be a passive process. The ectopic calcification in aorta can occur either in the media and/or intima[30]. The result is mineralized bone-like tissue containing marrow and cartilage. The process resembles endochondral bone formation or repair[20,31] with factors in the vessel acting as angiogenic stimuli and ultimately blood vessels invading the plaque. In this process, pericytes play an important role by modulating angiogenesis[6,32]. It is also important to note that progression of plaque in atherosclerosis is associated with intraplaque neovascularization[33].

It is hypothesized that in the response to injury, resting pericyte-like cells or VSCs in the blood vessel are activated through a number of factors and start to proliferate and differentiate into bone-forming cells and other cell lineages. In physiology, these cells are known to be required to repair and regenerate injured cells in other organs. However, they may also contribute to pathological processes. On one hand, it is believed that during atherogenesis there is attenuation of VSC development and inadequate differentiation into mature vascular cells with diminished proliferation and increased vascular cell apoptosis[34]. On the other hand, it is thought that during atherosclerotic plaque formation there are certain, not yet fully understood, mechanisms by which cells under the effect of certain factors start to form bone and cartilage. Although it is widely believed that the cells involved in differentiation are SMCs[23,35], there is evidence suggestive of differentiation of progenitor cells[23,36,37].

Here, the aim was to investigate the effect of the atherosclerotic environment on VSC and MSC differentiation in an attempt to further understand the role of resident and circulating progenitor cells in ectopic bone and cartilage formation in the atherosclerotic plaque and VC. We investigated whether bone-like structures found in atherosclerotic plaque can be formed *in vivo* via the endochondral ossification pathway under the influence of the pro-inflammatory environment in atherosclerosis. There are many soluble factors that play role an important role in promoting the cascade of ectopic calcification in forming atherosclerotic plaque, so the effect of the combined effect of this environment was assessed.

MSCs and VSCs from ApoE$^{-/-}$ and background C57BL/6 mice were loaded on a collagen-glycosaminoglycan scaffold and chondrogenically primed to form a cartilaginous template prior to subcutaneous implantation *in vivo*. The effect of the atherosclerotic environment on bone formation was interrogated by implantation of both donor cell preparations into ApoE$^{-/-}$ recipient mice (Fig. 5.1). Donor cell preparations were implanted subcutaneously in C57BL/6 mice as controls (Fig. 5.1). The incidence, extent and quality of calcified cartilage, bone and bone formation was assessed by a histological grading system.

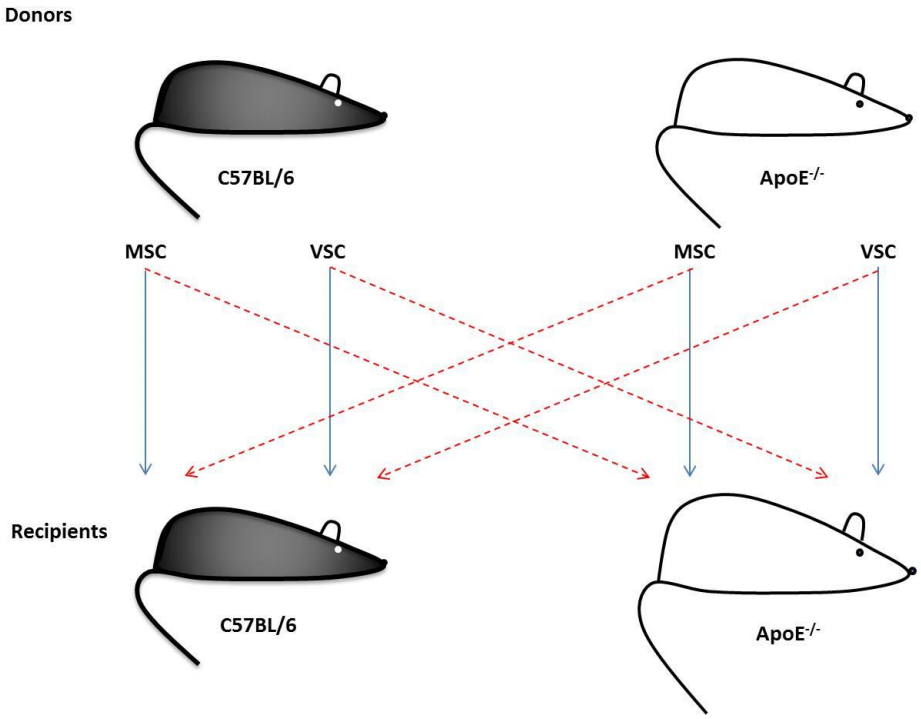

Figure 5.1 Experimental design for analysis of the role of VSCs and MSCs in atherosclerosis. To investigate the *in vivo* differentiation of ApoE$^{-/-}$ and C57BL/6 MSCs and VSCs, chondrogenically primed constructs were implanted subcutaneously in the back of control and ApoE$^{-/-}$ mice. The control constructs grown in control medium were implanted in the same fashion. After 8 weeks post-implantation, the level of bone formation, bone marrow as well as blood vessels and fat appearance in the retrieved constructs was analysed.

5.2 Results

5.2.1 Assessment of MSCs and VSCs construct seeding

5.2.1.1 Priming / pre-differentiation

The collagen-chondroitin sulphate scaffolds used in this study were kindly gifted by Prof. F. O'Brien. These scaffolds have been previously used to assess bone formation[38]. The scaffolds were non-toxic and stimulated cell growth in 3D culture[39]. The scaffolds were seeded with isolated cells, either MSCs or VSCs, from C57BL/6 or $ApoE^{-/-}$ mice. Briefly, 3 to 5mm scaffolds were placed in agarose-coated 6-well plates (LE analytical grade, Promega) (scaffold/well). The cells were seeded drop-wise on one side of the scaffold; after 30 min incubation at 37°C in 5% CO_2, scaffolds were removed from the incubator and flipped on the other side and seeded again and left for a further 30min at 37°C in 5% CO_2. This method of seeding was optimized previously[40]. Following seeding, the seeded scaffolds were incubated for 32 days with half medium changes for chondrogenic priming every 3-4 days. Seeded and unseeded scaffolds fed with control medium (section 2.8.1 and 2.8.2) were used as controls. Control and chondrogenically-primed constructs were stained with toluidine blue to assess the quality of seeding before implantation. The staining indicated distribution of cells throughout the scaffold; however, the density of cells was higher at the edges. In all the seeded and chondrogenically-primed scaffolds, except for the controls, staining for GAG was evident. Primarily, GAGs were observed at the edges of the seeding scaffold as seen in figure 5.2. The cells formed cartilage-like nodules embedded in lacunae. Toluidine blue staining confirmed the homogenous distribution of cell seeding on the scaffolds, whereas the controls showed no GAG deposition as expected. Cross-sections through the toluidine blue stained scaffolds showed that the cells penetrated the material homogenously and shrinkage of the material indicated contraction of the scaffold by the cells. Cells enclosed in the scaffolds looked healthy and a layer of cells on the top of the scaffold was evident.

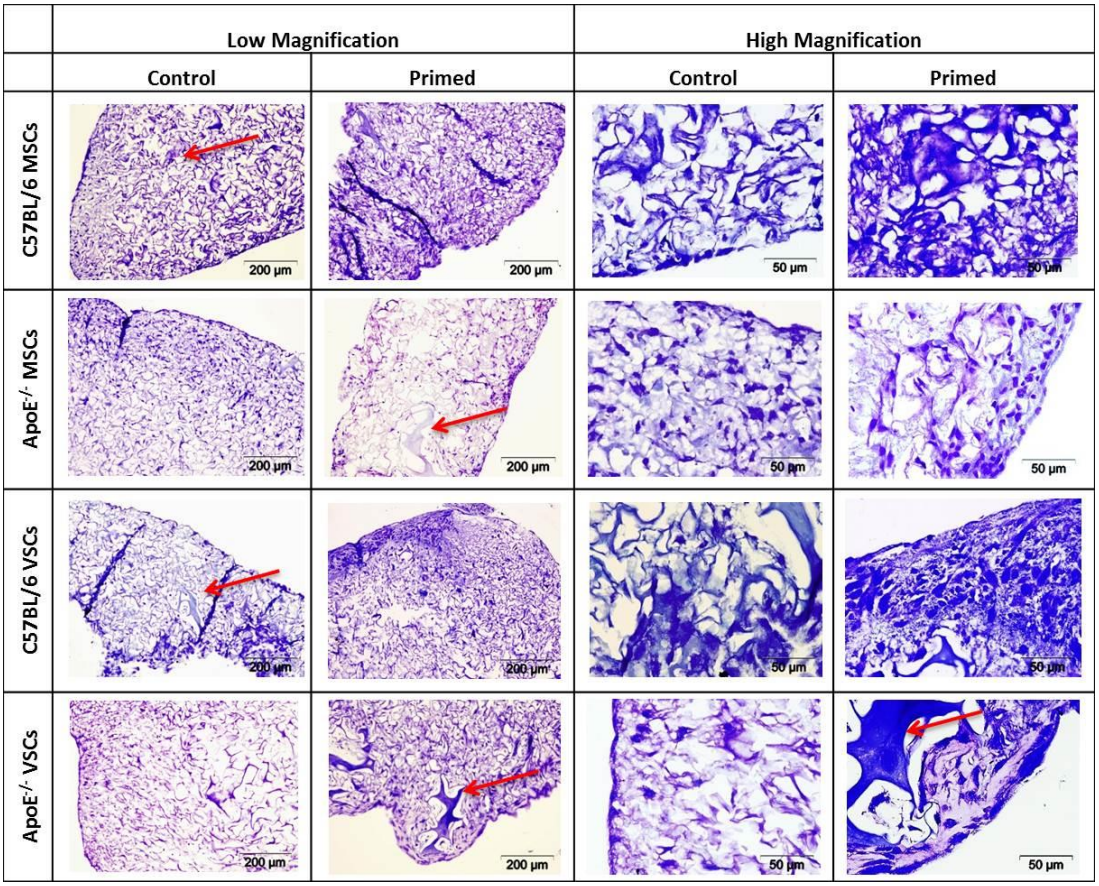

Figure 5.2 Toluidine Blue staining showing homogenous cell distribution and chondrogenic priming of constructs after 32 days in culture. Low magnification images at 200µm confirm homogenous cell seeding throughout scaffolds and accumulation of GAGs at the edges of primed constructs. Small regions of scaffolds were also present, indicated with red arrows. High magnification images at 50µm show GAG deposition and cartilage like cells in the primed samples.

5.2.1.2 Subcutaneous implantation in ApoE$^{-/-}$ and C57BL/6 control mice and sample retrieval

Following chondrogenic priming, seeded scaffolds were implanted subcutaneously in the back of C57BL/6 or ApoE$^{-/-}$ mice in a randomized manner and harvested after 8 weeks as described in section 2.8.3. The constructs were explanted, processed and sectioned for histology as described in section 2.8.4. Sections were stained with hematoxylin-eosin or safranin O/fast green (sections 2.8.5-6) for microscopic evaluation to clarify the differences of maturity level of the bone formed. Immunohistochemistry for Collagen type II and X was also performed (section 2.6.1.2) to further assess the maturity of *de novo* formed bone.

To explore whether bone can be formed *in vivo* after being induced towards to the chondrogenic lineage and if the process is enhanced by the atherosclerotic environment, constructs, both treated and untreated, were implanted in ApoE$^{-/-}$ and C57BL/6 mice (Fig. 5.1) as described previously (section 2.8.3). Empty constructs were used as internal controls to rule out *in vivo* derived bone formation driven by the infiltration of host MSC or VSC. After 8 weeks, implanted samples were retrieved. Figures 5.3 and 5.4 show the gross appearance of constructs after retrieval. All the retrieved constructs were processed and sectioned as described in section 2.8.4.

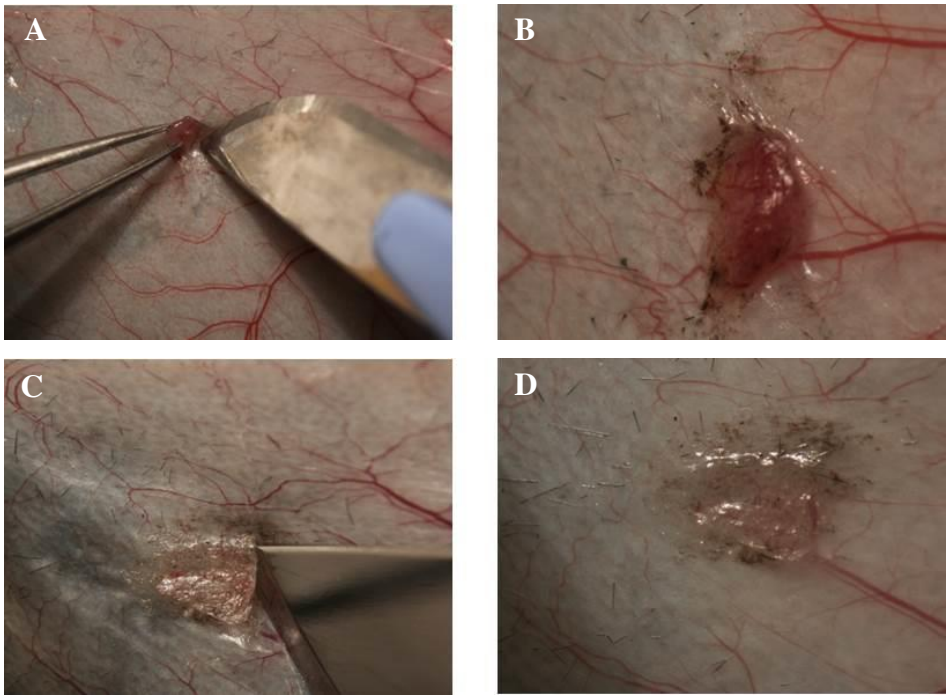

Figure 5.3 Examples of the gross appearance of retrieved samples. (A), (B) chondrogenically primed ApoE$^{-/-}$ MSC constructs retrieved from C57BL/6 mice showing the appearance of blood vessels. (C), (D) chondrogenically primed ApoE$^{-/-}$ MSC constructs retrieved from ApoE$^{-/-}$ mice showing the appearance of hard bone-like structures.

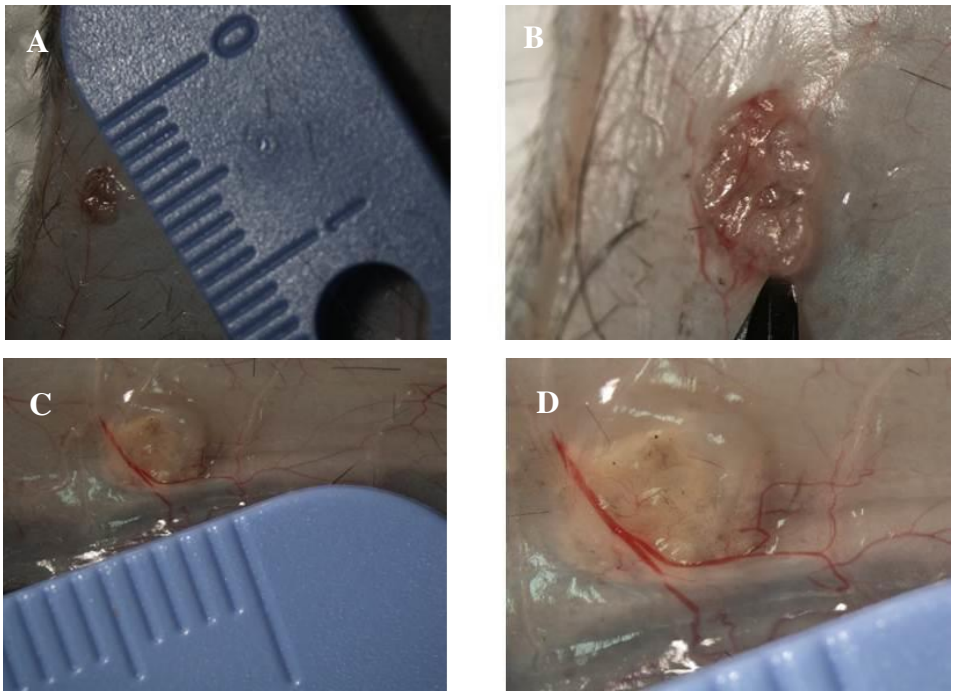

Figure 5.4 Examples of the gross appearance of retrieved samples. (A), (B) chondrogenically primed ApoE$^{-/-}$ VSC constructs retrieved from C57BL/6 mice. (C), (D) chondrogenically primed ApoE$^{-/-}$ VSC constructs retrieved from ApoE$^{-/-}$ mice. Both retrieved samples showing the appearance of hard bone-like structures and blood vessels. One division is 1mm.

5.2.1.3. Analysis of bone formation

Sections from each animal and each treatment were randomized to eliminate bias and then examined and scored by three independent, blinded researchers. The sections were graded according to the histological scale (see section 2.8.7). The grading system involves assessment of bone formation and the stage of maturity of cartilage, bone and bone marrow. It allots a total score of formed bone in correlation to the total amount of extracted sample on a scale of 0-4. Overall bone score was determined by adding the scores for calcified cartilage, bone and bone marrow. The overall bone formation in each sample was then calculated as percentage of the overall bone score for that sample with a score of 4 as 100%. The system also assesses the formation of fat in the interspaces of the explants and appearance of blood vessels and fibrous matrix. Host-derived tissue such as muscle or hair follicles was noted. The presence of a high proportion of surrounding host tissue in the retrieved samples was a confounding factor in assessment of the percentage of overall level of the bone formation in some constructs. For semi-quantitative assessment of the achieved results, the focus was on the purity and maturity of the formed bone. Results are detailed in Tables 5.1, 5.2 and 5.3.

Table 5.1 Histological analysis of MSC constructs retrieved from ApoE$^{-/-}$ and C57BL/6 mice scored for bone, calcified cartilage and bone marrow formation. The constructs were stained with H&E staining for light microscopic evaluation.

			Implanted cells			
			ApoE $^{-/-}$ MSCs		C57BL/6 MSCs	
			control	primed	control	primed
Host	ApoE $^{-/-}$	Calcified Cartilage	2/4 (0.41)	5/5 (0.94)	1/5 (0.12)	3/5 (0.37)
		Bone	2/4 (0.12)	5/5 (1.2)	2/5 (0.08)	2/5 (0.24)
		Bone Marrow	2/4 (0.19)	5/5 (0.6)	0/5 (0)	1/5 (0.14)
		Overall Bone Score	0.72	2.74	0.2	0.75
		Percentage of overall bone formation	18%	68.5%	5%	18.75%
	C57BL6	Calcified Cartilage	0/4 (0)	5/5 (1.27)	0/4 (0)	1/4 (0.23)
		Bone	0/4 (0)	5/5 (0.99)	0/4 (0)	1/4 (0.15)
		Bone Marrow	0/4 (0)	5/5 (0.84)	0/4 (0)	0/4 (0)
		Overall Bone Score	0	3.1	0	0.38
		Percentage of overall bone formation	0%	77.5%	0%	9.5%

Note: The numbers in blue represent constructs showing the presence of the particular feature out of the total retrieved constructs. The numbers in brackets represent the scores allotted by the grading system. Percentage of overall bone formation was calculated by the overall bone score based on the grading system with a score of 4 as 100%.

Table 5.2 Histological analysis of VSC constructs retrieved from ApoE$^{-/-}$ and C57BL/6 mice scored for bone, calcified cartilage and bone marrow formation. The constructs were stained with H&E staining for light microscopic evaluation.

			Implanted cells			
			ApoE $^{-/-}$ VSCs		C57BL/6 VSCs	
			control	primed	control	primed
Host	ApoE $^{-/-}$	Calcified Cartilage	3/4 (0.32)	6/6 (0.96)	0/4 (0)	0/4 (0)
		Bone	3/4 (0.27)	6/6 (1.01)	0/4 (0)	0/4 (0)
		Bone Marrow	1/4 (0.13)	6/6 (1.36)	0/4 (0)	0/4 (0)
		Overall Bone Score	0.72	3.33	0	0
		Percentage of overall bone formation	**18%**	**83.25%**	**0%**	**0%**
	C57BL/6	Calcified Cartilage	1/6 (0.023)	5/5 (1)	0/4 (0)	0/6 (0)
		Bone	0/6 (0)	5/5 (0.63)	0/4 (0)	0/6 (0)
		Bone Marrow	0/6 (0)	3/5 (0.71)	0/4 (0)	0/6 (0)
		Overall Bone Score	0.023	2.34	0	0
		Percentage of overall bone formation	**0.583%**	**58.4%**	**0%**	**0%**

Note: The numbers in blue represent constructs showing the presence of the particular feature out of the total retrieved constructs. The numbers in brackets represent the scores allotted by the grading system. Percentage of overall bone formation was calculated by the overall bone score based on the grading system with a score of 4 as 100%.

Table 5.3 Summary of overall bone formation by histological analysis of MSC and VSC constructs retrieved from ApoE$^{-/-}$ and C57BL/6 mice (extracted from tables 5.1 and 5.2)

			Implanted cells			
			ApoE $^{-/-}$ MSCs		ApoE $^{-/-}$ VSCs	
			control	primed	control	primed
Host	ApoE $^{-/-}$	Percentage of overall bone formation	18% (4.75%)	68.5% (15%)	18% (3.25%)	83.25% (34%)
	C57BL/6		0% (0%)	77.5% (21%)	0.58% (0%)	58.4% (17.75%)
			C57BL/6 MSCs		C57BL/6 VSCs	
			control	primed	control	primed
Host	ApoE $^{-/-}$	Percentage of overall bone formation	5% (0%)	18.75% (3.5%)	0% (0%)	0% (0%)
	C57BL/6		0% (0%)	9.5% (0%)	0% (0%)	0% (0%)

Note: The numbers in red represent percentage of overall bone formation. The numbers in brackets represent percentage of bone marrow scored by grading system. Percentage of overall bone formation was calculated by the overall bone score based on the grading system with a score of 4 as 100%.

5.2.2 Capacity of MSCs and VSCs from atherosclerotic mice to form bone: ApoE$^{-/-}$ cells in C57BL/6 mice

When chondrogenically primed constructs from atherosclerotic mice were transplanted into subcutaneous pouches of control mice, all constructs underwent mineralization and formed bone as shown in figure 5.5.

In the case of the primed ApoE$^{-/-}$ MSC constructs retrieved from C57BL/6 mice, 5 out of 5 retrieved constructs formed bone. The overall bone formation was 77.5% with more than 20% of bone marrow formation suggesting areas of maturity. However, the presence of 25% calcified cartilage suggested areas of less mature bone. The control ApoE$^{-/-}$ MSCs constructs which were retrieved from C57BL/6 mice did not form bone, calcified cartilage or bone marrow; all were graded as 0 as per the grading system. On the contrary, the remnants of cellular structure outside of the scaffolds were obvious in the constructs (Fig. 5.5).

The ApoE$^{-/-}$ control VSC constructs were found not to form bone but some minimal cartilage in 1 of 6 constructs retrieved from C57BL/6 mice (according to two of the three independent researchers) (Fig. 5.6). No bone marrow was seen in the sections.

The chondrogenically primed ApoE$^{-/-}$ VSC constructs retrieved from C57BL/6 mice formed bone or immature bone in 5 out of 5 retrieved samples. In 3 out of 5 constructs, bone marrow was seen (Fig. 5.6). Of the 58.4% of overall bone formation, 25% was immature bone with calcified cartilage while 17.75% of bone marrow suggesting a more mature ossicle.

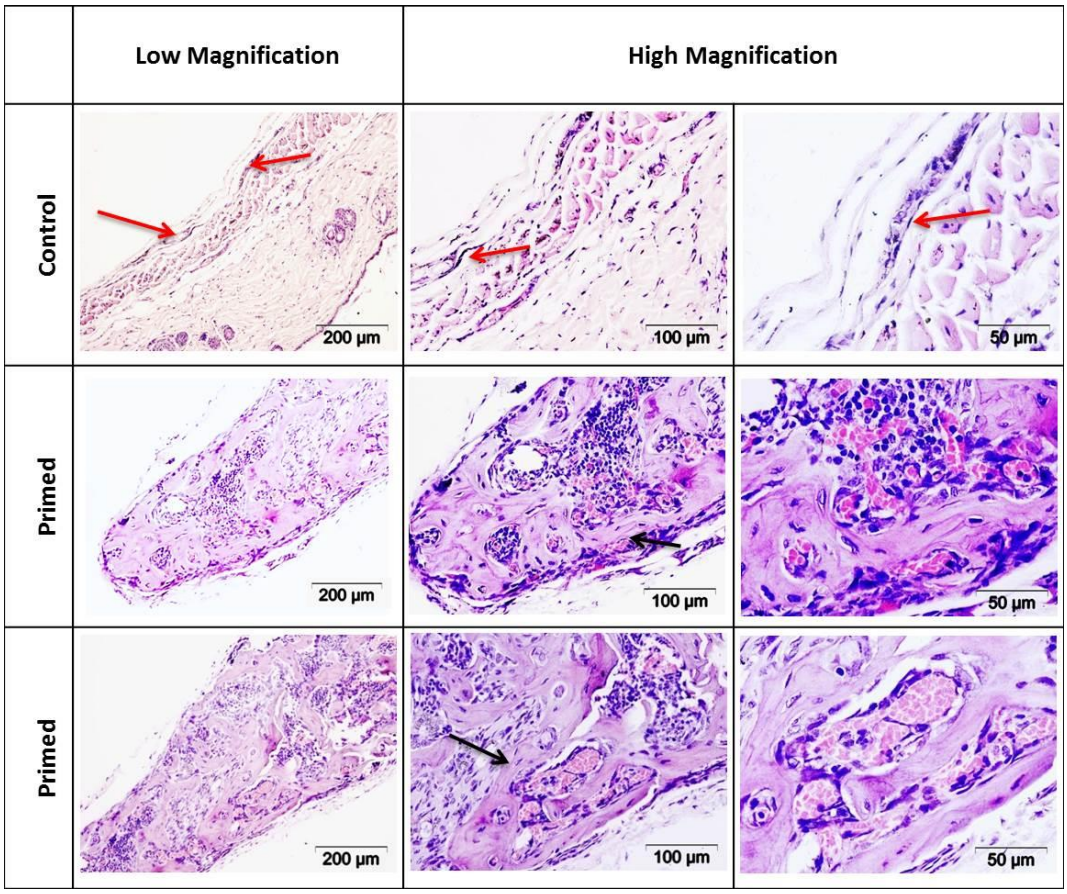

Figure 5.5: Bone formation by primed ApoE$^{-/-}$ MSCs in C57BL/6 mice. All chondrogenically primed ApoE$^{-/-}$ MSC constructs retrieved from C57BL/6 underwent mineralization and clear bone formation (black arrows). Control ApoE$^{-/-}$ MSC constructs, on the other hand, neither formed bone nor calcified cartilage nor bone marrow. The cellular structure outside of the scaffolds can be obviously seen (red arrows). Low magnification at 200µm and high magnification at 100 and 50µm.

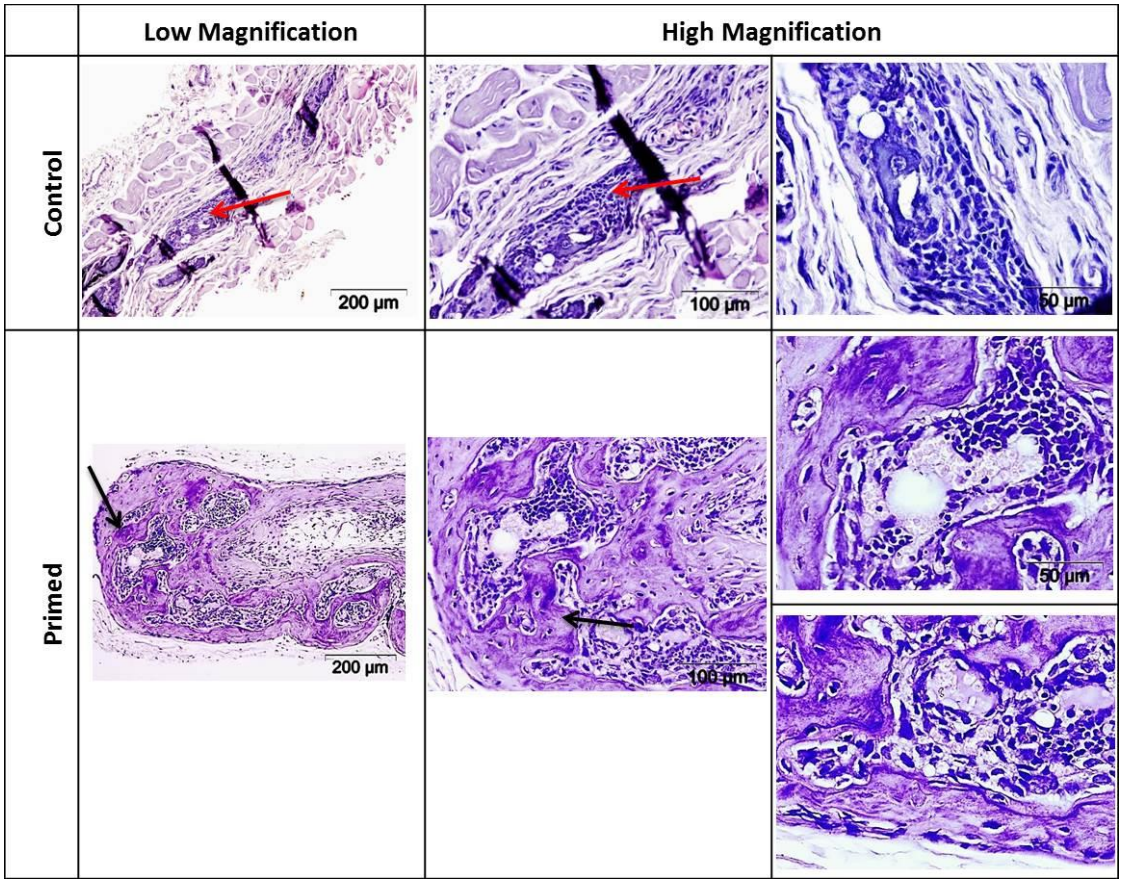

Figure 5.6: Bone formation by primed ApoE$^{-/-}$ VSCs in C57BL/6 mice. All chondrogenically primed ApoE$^{-/-}$ VSC constructs retrieved from C57BL/6 underwent mineralization and clear bone formation (black arrows) could be seen. Control ApoE$^{-/-}$ VSC constructs, on the other hand, neither formed bone nor calcified cartilage nor bone marrow. The remnants of scaffolds can be obviously seen (red arrows). Low magnification at 200µm and high magnification at 100 and 50µm.

5.2.3 The atherosclerotic environment complements the intrinsic capacity of MSCs and VSCs to form bone: ApoE$^{-/-}$ cells in ApoE$^{-/-}$ mice

To investigate how the intrinsic capacity of MSCs and VSCs from atherosclerotic mice is affected by the atherosclerotic environment, the fate of the ApoE$^{-/-}$ constructs in ApoE$^{-/-}$ mice was assessed.

All 5 of 5 constructs of primed ApoE$^{-/-}$ MSCs retrieved from atherosclerotic mice formed bone and bone marrow. With prominent dense bone appearance (30%), calcified matrix (23.5%) and areas with bone marrow (15%), the overall bone formation was rated at 68.5%. A large number of hypertrophic cells was observed surrounded by cartilage-like matrix containing bone like tissue components and permeating blood vessels (Fig. 5.7).

ApoE$^{-/-}$ MSC control constructs retrieved from atherosclerotic mice formed some bone with 18% of overall bone formation and 10.25% cartilage observed only in 2 out of 4 retrieved constructs. Total bone marrow observed was 4.75% and seen in 2 out of 4 retrieved constructs (Fig. 5.7).

The examination of 6 out of 6 primed ApoE$^{-/-}$ VSCs in the ApoE$^{-/-}$ environment showed the presence of osteoid tissue with a number of hypertrophied cells embedded in a cartilaginous matrix and notably, all constructs had invading blood vessels (Fig. 5.8). The bone appearance was dense with 83.25% of overall bone formation. The calcified matrix was prominent with 24% coverage. In all treated ApoE$^{-/-}$ constructs retrieved from ApoE$^{-/-}$ mice, substantial formation of bone marrow was observed (34%), revealing the maturity of the developed bone.

Thus, overall, these results lead to the conclusion that the atherosclerotic environment does not prevent or slow down the formation of bone but rather promotes the calcification of the constructs and bone formation, giving a hint towards solving the quest to understand ectopic bone formation in atherosclerotic plaque. Comparing these results with those of atherosclerotic cells in a non-atherosclerotic environment, it is evident that the level of maturity of bone and the overall calcifying effect is further

enhanced by the atherosclerotic environment suggesting the complimentary role of the environment on the intrinsic propensity of atherosclerotic cells to from bone.

In 3 of the 4 control constructs of $ApoE^{-/-}$ VSCs retrieved from atherosclerotic mice, a poorer bone-like formation was observed with overall new bone formation of 18%. Calcified matrix was found in 3 out of 4 retrieved constructs with 8% coverage while total bone marrow was only 3.25%. Only one of the constructs was found to have bone marrow but interestingly, without the appearance of bone (Fig. 5.8). However, when compared to controls in C57BL/6 mice, the results of VSC controls in $ApoE^{-/-}$ mice provide some evidence that even without chondrogenic priming, the atherosclerotic environment plays some role in enhancing the bone formation by atherosclerotic VSCs.

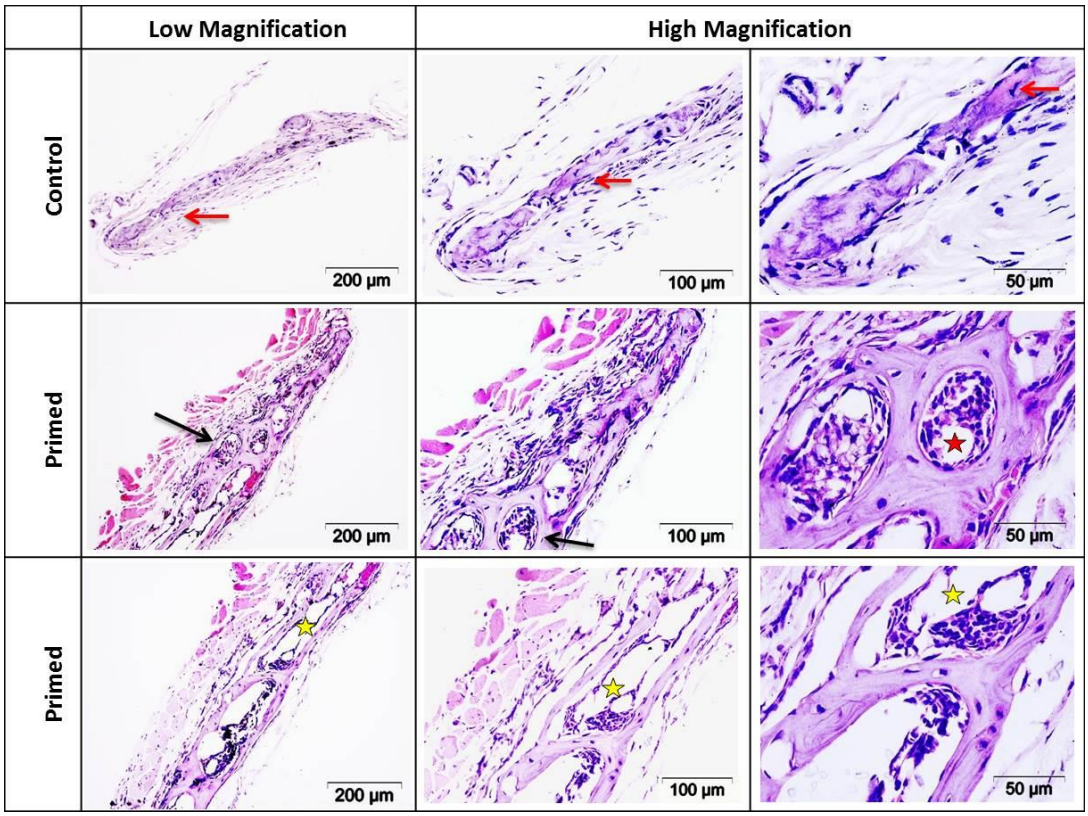

Figure 5.7: Mature bone formation in primed ApoE$^{-/-}$ MSCs in ApoE$^{-/-}$ mice. Control ApoE$^{-/-}$ MSC constructs showed the presence of calcified cartilage and some bone (red arrows). All primed ApoE$^{-/-}$ MSC constructs showed mature bone formation with bone marrow (black arrow), fat (yellow star) and blood vessels (red star). Low magnification at 200µm and high magnification at 100 and 50µm.

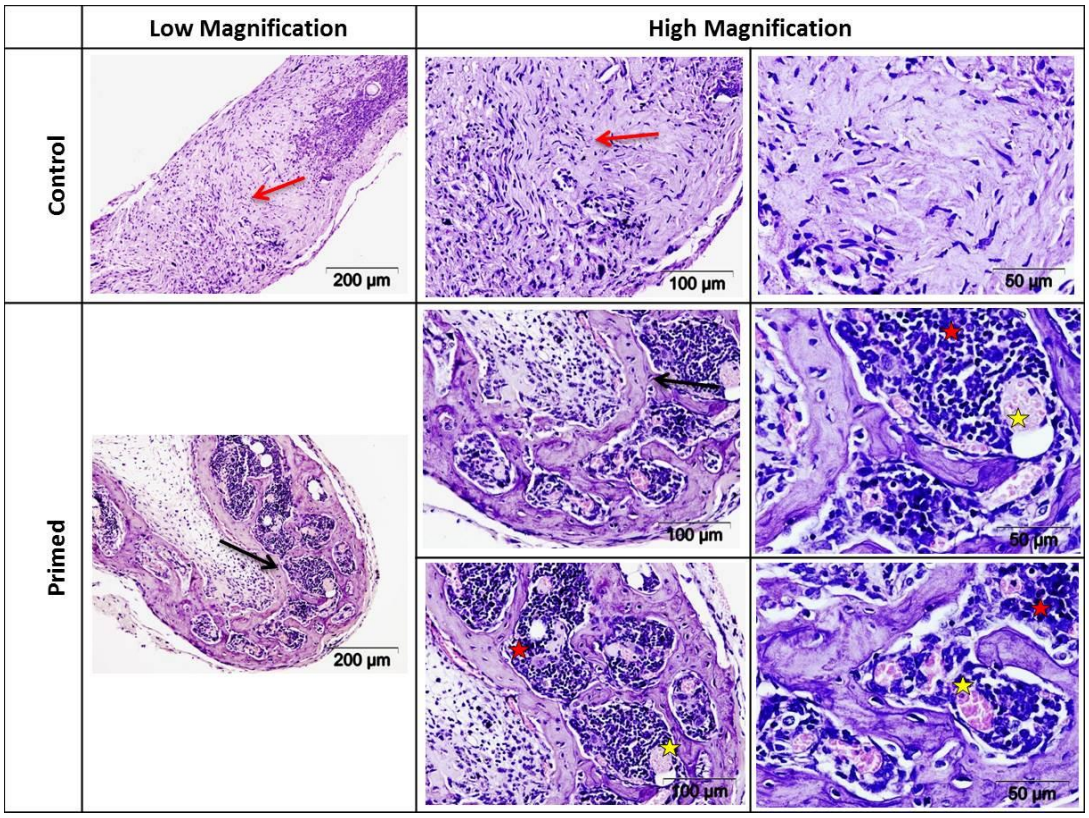

Figure 5.8: Mature bone formation in primed ApoE$^{-/-}$ VSCs in ApoE$^{-/-}$ mice. Control ApoE$^{-/-}$ VSC constructs showed the presence of calcified cartilage and some immature bone (red arrows). All primed ApoE$^{-/-}$ VSC constructs showed mature bone formation with bone marrow (red star), calcified cartilage (black arrow) and blood vessels (yellow star). Low magnification at 200µm and high magnification at 100 and 50µm.

5.2.4 Effect of the atherosclerotic environment on bone formation: C57BL/6 cells in ApoE$^{-/-}$ mice

The results obtained from analysis of non-atherosclerotic constructs retrieved from the atherosclerotic environment highlight the modest role of the atherosclerotic environment alone. Two of 5 of C57BL/6 MSCs control constructs retrieved from atherosclerotic mice formed some bone with overall bone formation of 5%. Of this, 3% was calcified cartilage while no bone marrow was observed (Fig. 5.9). For ApoE$^{-/-}$ MSC (4 out of 4) and C57BL/6 MSC (4 out of 4) control constructs retrieved from control mice, there was no bone, cartilage or bone marrow formation (Fig. 5.9).

In the case of primed C57BL/6 MSCs retrieved from atherosclerotic mice, overall new bone formation was 18.75%. Two of 5 constructs formed some bone while 3 out of 5 constructs showed an average of 9.25% calcified cartilage. One of the retrieved constructs formed 3.5% bone marrow (Fig. 5.10).

Following retrieval of control and primed constructs of C57BL/6 VSCs from atherosclerotic or control mice, no bone or calcified structures, either in primed (0 out of 4) or in control (0 out of 4) constructs, were seen (Fig. 5.10). Also, there was no evidence of bone marrow formation.

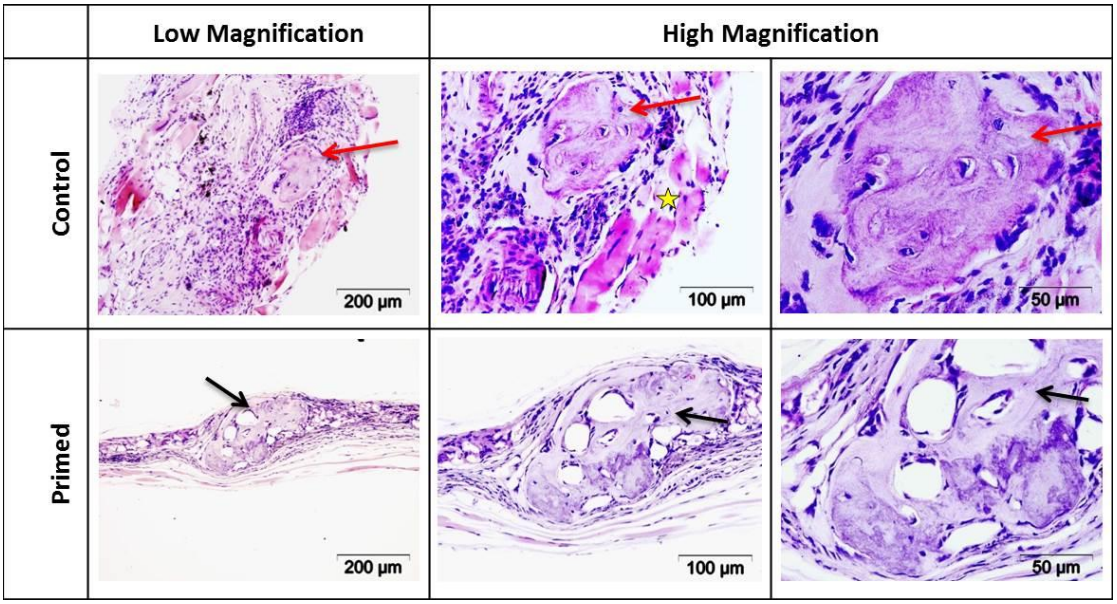

Figure 5.9: Modest bone formation by C57BL/6 MSCs in ApoE$^{-/-}$ mice. Control C57BL/6 MSC constructs showed calcified cartilage and some bone formation (red arrows). Extra tissue such as muscle (yellow star) can be seen. Comparatively, primed C57BL/6 MSC constructs showed more bone formation with marrow like spaces (black arrows). Low magnification at 200µm and high magnification at 100 and 50µm.

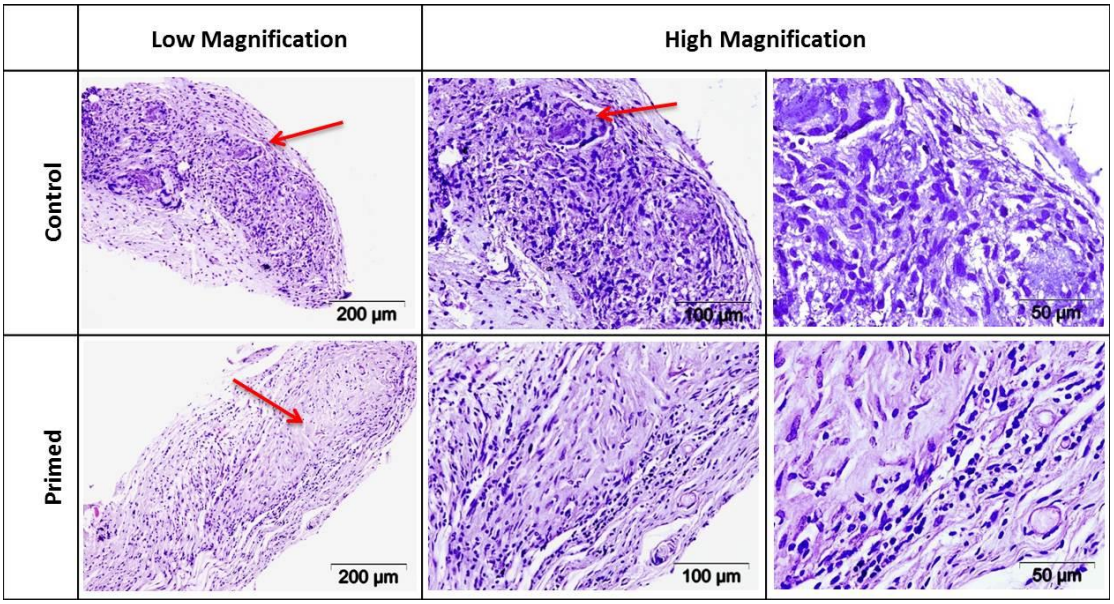

Figure 5.10: No bone formation by C57BL/6 VSCs in ApoE$^{-/-}$ mice. Control C57BL/6 VSC constructs showed no bone formation while remnants of scaffold and remnants of cellular structure (red arrows) can be seen. Primed C57BL/6 VSC constructs showed no bone formation. Low magnification at 200µm and high magnification at 100 and 50µm.

5.2.5 C57BL/6 cells in C57BL/6 mice

Control constructs of C57BL/6 MSCs retrieved from control mice, did not show bone or cartilage formation. Primed C57BL/6 MSCs implanted in C57BL/6 showed bone formation of 9.5%. This represented detection in only one of the primed constructs; 3.75% of tissue was represented by newly formed bone-like structures while 5.75% of tissue was essentially calcified cartilage with no bone marrow observed (Fig. 5.11). This makes it clear that whatever little bone formation was induced after priming, no maturation occurred. In the case of C57BL/6 VSCs retrieved from control mice, there was no bone formation either in control or primed constructs (Fig. 5.12). Thus, in case of non-atherosclerotic cells the effect of priming was minimal.

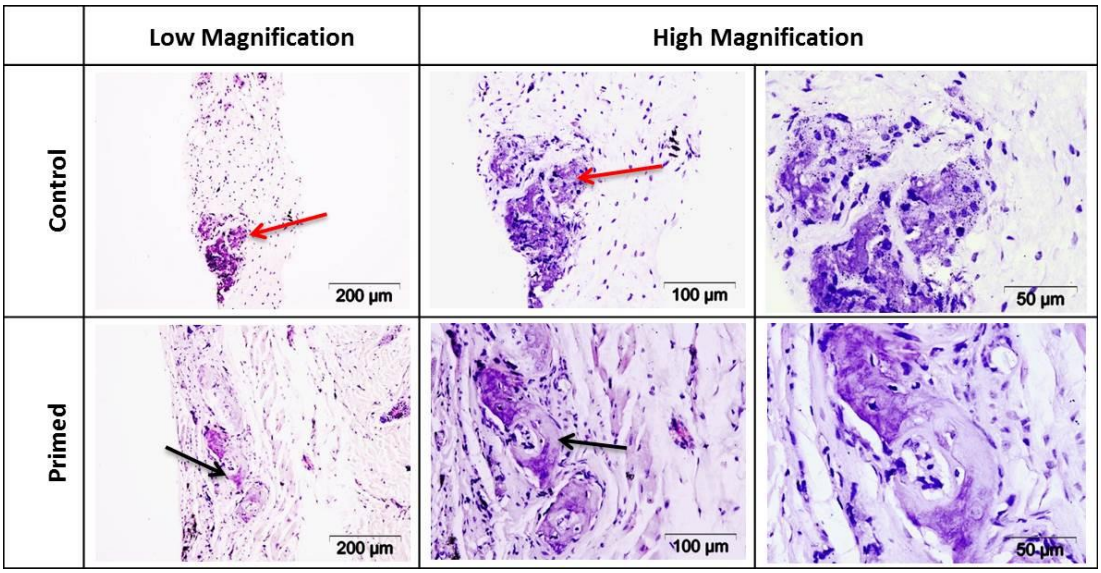

Figure 5.11: Minimal bone formation by C57BL/6 MSCs in C57BL/6 mice. Control C57BL/6 MSCs constructs showed no bone formation; however, remnants of scaffold and cellular structures outside the scaffolds were seen (red arrow). In the case of primed constructs, some bone formation was observed (black arrow) in one of the retrieved constructs only. Low magnification at 200µm and high magnification at 100 and 50µm.

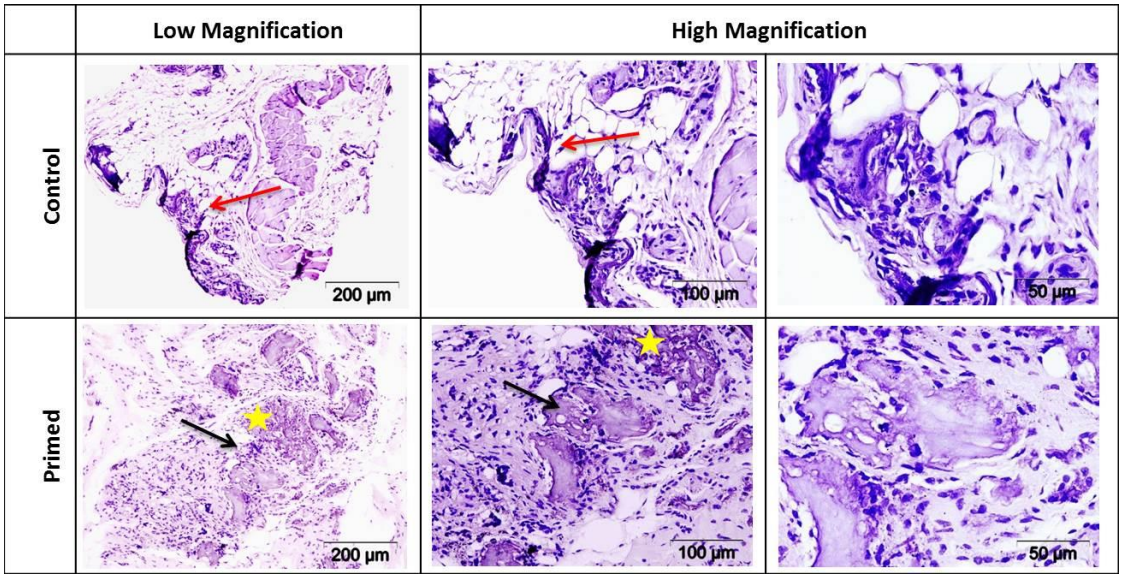

Figure 5.12: No bone formation by C57BL/6 VSCs in C57BL/6 mice. Both control (red arrows) and primed (black arrows) C57BL/6 VSC constructs showed no bone formation, however remnants of scaffold and the remnants of cellular structure outside of the scaffolds were apparent (yellow star). Low magnification at 200µm and high magnification at 100 and 50µm.

5.2.6 Priming enhances bone formation

That atherosclerotic cells have an intrinsic capacity to form bone even in a non-atherosclerotic environment has already been discussed. This capacity became more evident when the cells were chondrogenically primed. In the case of $ApoE^{-/-}$ MSC controls none of the retrieved constructs formed bone; however, when these MSCs were primed all of the retrieved constructs (5 out of 5) formed bone (Fig. 5.5). In comparison, in the case of $ApoE^{-/-}$ control VSCs there was no bone formation but the presence of immature cartilage in one of the retrieved constructs was detected. Even here priming had a significant boosting effect. Five out of five constructs formed mature or in some regions immature bone, calcified matrix and bone marrow (Fig. 5.6).

The effect of priming in the atherosclerotic environment on atherosclerotic cells was also assessed. Without priming, $ApoE^{-/-}$ MSCs formed bone and immature cartilage in 2 out of 4 retrieved constructs. However, when primed, $ApoE^{-/-}$ MSCs formed bone in all 5 out of 5 retrieved constructs (Fig. 5.7). The same boosting effect of priming was observed in the case of $ApoE^{-/-}$ VSCs. While control $ApoE^{-/-}$ VSCs showed poor bone formation in 3 of the retrieved constructs and calcified matrix in 3 out of 4 retrieved constructs, primed $ApoE^{-/-}$ VSCs showed mature bone formation in all of the 6 retrieved constructs (Fig. 5.8). Thus, from the above findings, it is clear that priming is important for the cells to exhibit their intrinsic capacity to form bone and also to reveal the complementary effect of the atherosclerotic environment on bone formation.

In the case of C57BL/6 MSCs retrieved from atherosclerotic mice, the effect of priming was not as profound. Both primed and control cells showed bone formation in 2 out of 5 retrieved constructs (Fig. 5.9). However, with priming, there was 18.75% of overall bone formation where calcified cartilage was 9.25%. This was higher as compared to the controls where overall bone formation was 5% with 3% of calcified cartilage. Also, priming induced some bone marrow formation in 3.5% of tissue in one of the constructs which was not seen in the controls. In case of C57BL/6 VSCs retrieved from atherosclerotic mice, there was no bone or calcified cartilage formation with or without priming (Fig. 5.10).

5.2.7 MSCs or VSCs in calcification associated with the atherosclerotic environment?

The process of plaque hardening and calcification appears to form in the blood vessel wall, hindering its function as an elastic perfusion tissue. Atherosclerotic metaplasia in arterial walls, although well-known as underlying phenomenon for vascular calcification, is not yet fully understood. The ectopic tissue in the artery wall is a process which occurs over decades. Monocyte infiltration is required to get rid of oxLDL. During this process, they turn into macrophages which secrete pro-inflammatory cytokines. Although not the direct cause of plaque formation, this process may lead to proliferation and differentiation of resident VSCs. We sought to assess the origin of bone and cartilage formation in the constructs to increase our understanding of aortic metaplasia. ApoE$^{-/-}$ pre-treated cell populations, either isolated from bone marrow or aortae, actively formed bone and calcified cartilage. Fat and bone marrow structures were also observed (Figs. 5.7 and 5.8). There were minor differences between the chondrogenically primed ApoE$^{-/-}$ MSC and VSC constructs. In the primed ApoE$^{-/-}$ MSC constructs (5 out of 5), the newly formed bone was mature. Calcified cartilage structures were also observed. They exhibited irregularly layered structures with regions showing rough staining with hematoxylin and eosin. The newly formed bone had clear scattered structures seen as blue in safranin-O and fast green staining (Fig. 5.13). All samples had cartilage formation with spaces between filled up with marrow and fat. In some of the samples, it was possible to pinpoint blood vessel formation with the presence of red blood cells and platelets.

Primed ApoE$^{-/-}$ VSC constructs (6 out of 6) retrieved from atherosclerotic mice showed the clear appearance of bone as seen by safranin O and fast green staining (Fig. 5.14). Invasion of the blood vessels (neovascularization) was observed in the newly formed bone structures. Also, the newly formed structures were highly enriched in bone marrow enclosed in marrow like spaces and fat dispersed in the interspaces. Notably, bone was formed throughout the scaffolds and apparently progressed inwards as the calcified cartilage was interior to the bone and marrow regions. Also, it can be noted

that osteoblasts-like cells were seen lining the newly formed bone. The level of organization and mineralization was at a much lesser degree in the control constructs.

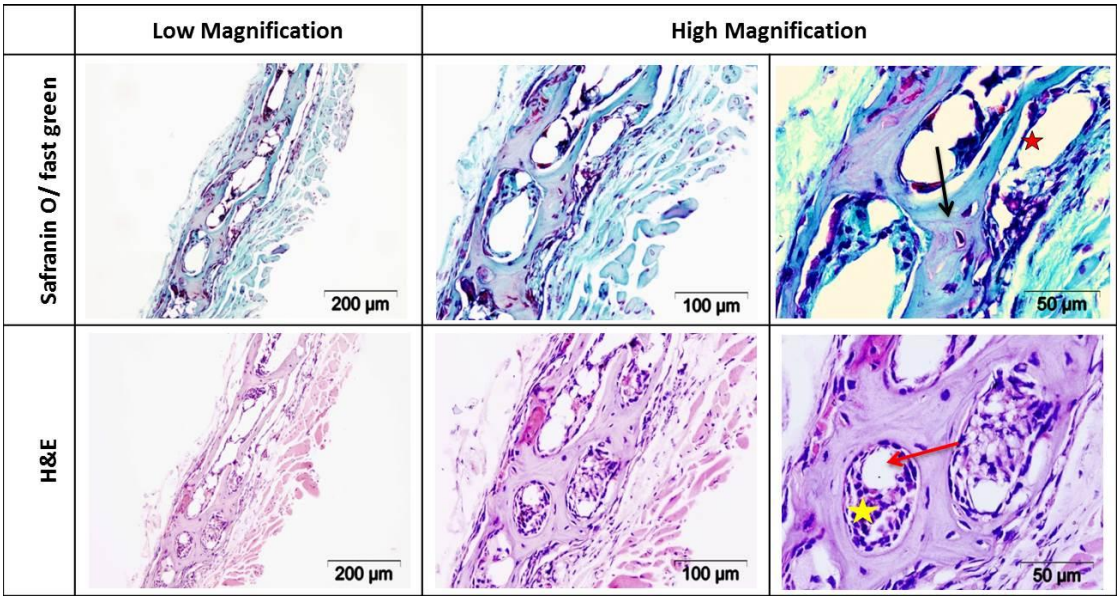

Figure 5.13: Histological staining for glycosaminoglycan with A) Safranin O/fast green and B) H&E staining of chondrogenically primed ApoE$^{-/-}$ MSCs constructs retrieved from ApoE$^{-/-}$ mice. The cellular morphology showed round and oval cells with lacunae surrounded by extracellular matrix. Also, the presence calcified cartilage and mineralizing osteoid (black arrow), fat (red star), bone marrow (yellow star) and blood vessels (red arrow) can be observed. Scale bars represent 200, 100 and 50 µm.

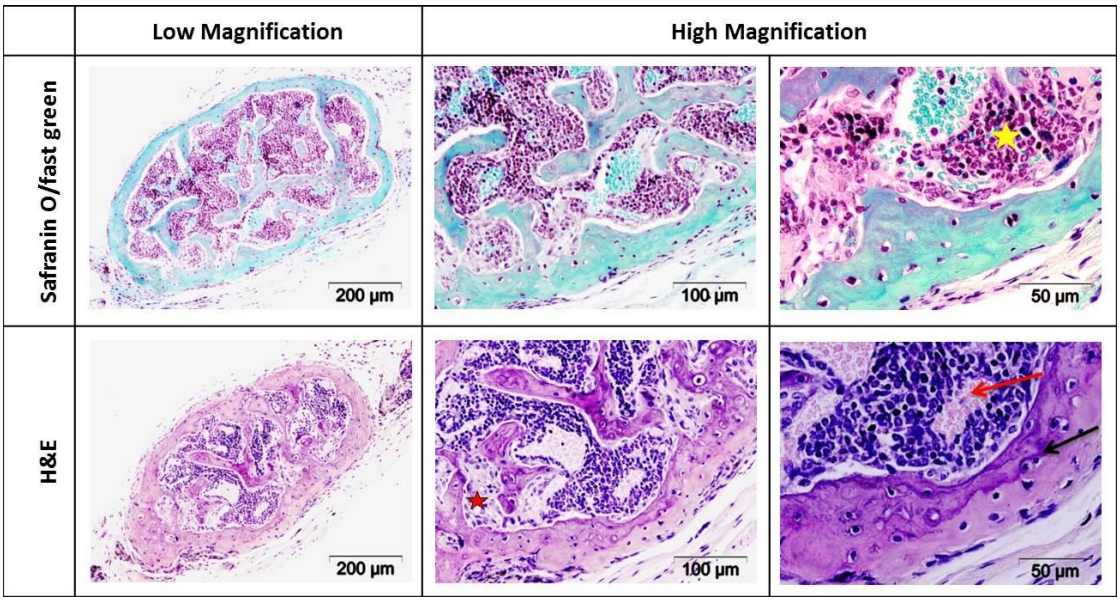

Figure 5.14: Histological staining for glycosaminoglycan with A) Safranin O/fast green and B) H&E staining of chondrogenically primed ApoE$^{-/-}$ VSCs constructs retrieved from ApoE$^{-/-}$ mice. The cellular morphology showed round and oval cells with lacunae surrounded by extracellular matrix. Also, the presence of calcified cartilage and mineralizing osteoid (black arrow), fat (red star), bone marrow (yellow star) and erythrocytes (red arrow) was observed. Scale bars represent 200, 100 and 50 µm.

5.3 Discussion

This study explored whether *in vivo* bone formation is triggered in chondrogenically primed constructs via endochondral ossification by the atherosclerotic environment. Formation of prominent and mature bone like structures in the primed ApoE$^{-/-}$ VSC and MSC constructs, even in a non-atherosclerotic environment suggested an intrinsic proclivity of these cells to form ectopic bone, which was boosted in the atherosclerotic environment. This notion was further supported by the observation that the cells from control mice, whether primed or not, were substantially less prone to form bone even in the atherosclerotic environment. In terms of mineralization, when the chondrogenically primed construct were transplanted into the subcutaneous pouches of ApoE$^{-/-}$ mice, all MSCs and VSCs derived and chondrogenically treated constructs of ApoE$^{-/-}$ cells underwent mineralization and formed calcified cartilage.

Metaplasia and calcification occurs in the aortic tunica. It is now known that this abnormality is not just a physical accumulation of calcium phosphate, but rather involves several mechanisms similar to bone formation with a number of bone related proteins expressed within the vessel wall[41].

The calcification of chondrogenically primed MSC as well as VSC constructs suggest the endochondral ossification pathway where, upon exposure to the atherosclerotic environment, mature bone starts to form. Differentiation and calcification of the constructs in the atherosclerotic environment is regulated by exposure to various factors like TNF-α, IL-6 and other pro-inflammatory cytokines, and possibly other soluble factors which may play role in formation of the plaque and atherogenesis. The hardening and instability of the plaque is the most common reason for incidence of stroke, where the unstable plaque starts to break and the cells enclosed in the atherosclerotic capsule begin to invade the atherosclerotic vessel lumen. A blood clot begins to form and may lead to a thromboembolic episode. Inflammation plays a huge role in the instability of the plaque where MMPs begin to digest collagen and start to compromise the collagen glue of the structure of plaque. The development of atherosclerotic lesions starts when the initial infiltration of macrophages for resolution

of the insult, turns into chronic inflammation and the cells start to secrete pro-inflammatory cytokines instead of preventing inflammation. The cascade of these events leads to the changes resulting in development of the plaque environment. Recent evidence has suggested that cells which usually build up the tunica media have the capacity to differentiate under factors such as TGF-β and BMPs, which direct the cells to harden and eventually become bone. The process is called ectopic metaplasia, where extra tissue like fat, bone, cartilage and marrow is formed[42].

To date, a number of researchers have reported the presence of stem cells in blood vessels including the aortae[43]. Their regenerative role in injury is well known, however our work was based on the premise that they can also be implicated in pathological processes under certain conditions. The mechanism whereby this occurs is not fully understood. The potential of these vessel wall stem cells to form bone, cartilage, muscle or fat has been reported previously[42]. More specifically, the cells which are isolated form aortic tunicae have more proclivity to differentiate to the osteogenic lineage[42,44] upon exposure to inflammatory cytokines.

The processes involved in endochondral ossification include neovascularization of avascular cartilaginous template tissue followed by calcification of cartilage, osteoclast-driven remodeling and then osteoblast-driven deposition of bone[30]. This endochondral bone formation and neovascularization heavily depend on expression of Runx2 together with Sox9[45]. Chondrogenic metaplasia of arteries occurs in models of heritable vascular calcification such as matrix Gla protein (MGP) knockout mice[46,47] and ApoE$^{-/-}$ knockout mice[14], the model used in this study.

The chondrogenically primed constructs of ApoE$^{-/-}$ MSCs, retrieved from control as well as atherosclerotic mice, formed mature bone and cartilage. It is interesting to note that ApoE$^{-/-}$ MSCs showed a similar level of bone formation in the atherosclerotic and control environments confirming their innate role in differentiation.

ApoE$^{-/-}$ MSCs had the potential to form highly developed structured bone under an inflammatory environment. They may have overcome the effect of pro-inflammatory cytokines which usually will suppress bone development[48]. When ApoE$^{-/-}$ VSCs were

subjected to a chondrogenic assay, along with IL-6 treatment (as discussed in Chapter 4), assessment over 21 days suggested that IL-6 treatment enhanced the chondrogenic potential of the cells. Cells started showing overexpression of markers of chondro-progenitors like Sox9 and fibromodulin followed by that of mature chondrocytes markers like type II collagen and aggrecan and then by hypertrophic chondrocytes defined by robust upregulation of Runx2 and Alp at 21 days in chondrogenic culture; C57BL/6 VSCs on the other hand showed inhibition of cartilage development in response to IL-6 treatment. Similarly, in this *in vivo* study where the combined effect of all proinflammatory cytokines in the atherosclerotic environment can be assessed, the chondrogenically treated ApoE$^{-/-}$ VSCs constructs formed more mature bone structures in ApoE$^{-/-}$ mice compared to those implanted in the control C57BL/6 mice.

In both environments, ApoE$^{-/-}$ cells were prone to calcify and develop bone structures; nevertheless VSCs were slightly more sensitive to environmental factors. The ApoE$^{-/-}$ environment seemed to contribute to mature bone formation in the ApoE$^{-/-}$ primed constructs but to a lesser degree in control non-primed constructs. Interestingly, the ApoE$^{-/-}$ environment also triggered bone formation in C57BL/6 control constructs, even without priming, albeit to a much lesser degree, again supporting the hypothesis that the atherosclerotic environment plays a role in differentiation and ectopic bone formation. The importance of the atherosclerotic environment in bone formation becomes even more obvious by the observation that control constructs retrieved from the control non-atherosclerotic environment did not form any bone. Nevertheless, the finding that there was some bone formation in primed C57BL/6 constructs retrieved from control mice, was similar to previous findings in Balb/C mice[49] and rats[50].

Previously, it has been shown that cells subjected to differentiation assays will usually down regulate bone and chondrogenic transcription factors under pro-inflammatory conditions[48]. In this study, it was found that the pro-inflammatory environment did not inhibit the formation of bone in subcutaneous implants but exaggerated the effect leading to more advanced calcification, particularly in the case of VSCs. Very low bone formation in C57BL/6 constructs retrieved from atherosclerotic and

non-atherosclerotic environments could be related to their resorption due to an immune response.

From this study it is clear that endochondral ossification and calcification in atherosclerosis is a complex interplay of a number of factors, each contributing differently to the process. It can be concluded that a major contributing factor is the intrinsic capacity of MSCs and VSCs derived from atherosclerotic mice to calcify. Nonetheless, this study also demonstrated that the environment in which cells are pre-differentiated and the actual host environment drive the implanted constructs to form bone or premature bone, bone marrow, calcified cartilage and promote infiltration of blood vessels as well as formation of fat.

5.4 References

1. Demer, L.L. & Tintut, Y. Mineral exploration: search for the mechanism of vascular calcification and beyond: the 2003 Jeffrey M. Hoeg Award lecture. *Arteriosclerosis, thrombosis, and vascular biology* **23**, 1739-1743 (2003).
2. Tintut, Y., *et al*. Multilineage potential of cells from the artery wall. *Circulation* **108**, 2505-2510 (2003).
3. Mikhaylova, L., Malmquist, J. & Nurminskaya, M. Regulation of in vitro vascular calcification by BMP4, VEGF and Wnt3a. *Calcified tissue international* **81**, 372-381 (2007).
4. Speer, M.Y. & Giachelli, C.M. Regulation of cardiovascular calcification. *Cardiovascular pathology : the official journal of the Society for Cardiovascular Pathology* **13**, 63-70 (2004).
5. Bianco, P., Riminucci, M., Gronthos, S. & Robey, P.G. Bone marrow stromal stem cells: nature, biology, and potential applications. *Stem Cells* **19**, 180-192 (2001).
6. Collett, G.D. & Canfield, A.E. Angiogenesis and pericytes in the initiation of ectopic calcification. *Circulation research* **96**, 930-938 (2005).
7. Giachelli, C.M. Ectopic calcification: new concepts in cellular regulation. *Z Kardiol* **90 Suppl 3**, 31-37 (2001).
8. Giachelli, C.M., *et al*. Vascular calcification and inorganic phosphate. *American journal of kidney diseases : the official journal of the National Kidney Foundation* **38**, S34-37 (2001).
9. Giachelli, C.M. Inducers and inhibitors of biomineralization: lessons from pathological calcification. *Orthodontics & craniofacial research* **8**, 229-231 (2005).
10. Shao, J.S., Cai, J. & Towler, D.A. Molecular mechanisms of vascular calcification: lessons learned from the aorta. *Arteriosclerosis, thrombosis, and vascular biology* **26**, 1423-1430 (2006).
11. Towler, D.A., Shao, J.S., Cheng, S.L., Pingsterhaus, J.M. & Loewy, A.P. Osteogenic regulation of vascular calcification. *Annals of the New York Academy of Sciences* **1068**, 327-333 (2006).
12. Abedin, M., Tintut, Y. & Demer, L.L. Vascular calcification: mechanisms and clinical ramifications. *Arteriosclerosis, thrombosis, and vascular biology* **24**, 1161-1170 (2004).
13. Li, R., *et al*. A dynamic model of calcific nodule destabilization in response to monocyte- and oxidized lipid-induced matrix metalloproteinases. *Am J Physiol Cell Physiol* **302**, C658-665 (2012).
14. Rattazzi, M., *et al*. Calcification of advanced atherosclerotic lesions in the innominate arteries of ApoE-deficient mice: potential role of chondrocyte-like cells. *Arteriosclerosis, thrombosis, and vascular biology* **25**, 1420-1425 (2005).
15. Aigner, T., Neureiter, D., Campean, V., Soder, S. & Amann, K. Expression of cartilage-specific markers in calcified and non-calcified atherosclerotic lesions. *Atherosclerosis* **196**, 37-41 (2008).

16. Bostrom, K., *et al*. Bone morphogenetic protein expression in human atherosclerotic lesions. *The Journal of clinical investigation* **91**, 1800-1809 (1993).
17. Shao, J.S., *et al*. Msx2 promotes cardiovascular calcification by activating paracrine Wnt signals. *The Journal of clinical investigation* **115**, 1210-1220 (2005).
18. Yao, Y., *et al*. Inhibition of bone morphogenetic proteins protects against atherosclerosis and vascular calcification. *Circulation research* **107**, 485-494 (2010).
19. Filvaroff, E., *et al*. Inhibition of TGF-beta receptor signaling in osteoblasts leads to decreased bone remodeling and increased trabecular bone mass. *Development* **126**, 4267-4279 (1999).
20. Hsu, J.J., Tintut, Y. & Demer, L.L. Vitamin D and osteogenic differentiation in the artery wall. *Clinical journal of the American Society of Nephrology : CJASN* **3**, 1542-1547 (2008).
21. Carrington, J.L., Roberts, A.B., Flanders, K.C., Roche, N.S. & Reddi, A.H. Accumulation, localization, and compartmentation of transforming growth factor beta during endochondral bone development. *J Cell Biol* **107**, 1969-1975 (1988).
22. Alexopoulos, N. & Raggi, P. Calcification in atherosclerosis. *Nature reviews. Cardiology* **6**, 681-688 (2009).
23. Naik, V., *et al*. Sources of cells that contribute to atherosclerotic intimal calcification: an in vivo genetic fate mapping study. *Cardiovasc Res* **94**, 545-554 (2012).
24. Tyson, K.L., *et al*. Osteo/chondrocytic transcription factors and their target genes exhibit distinct patterns of expression in human arterial calcification. *Arteriosclerosis, thrombosis, and vascular biology* **23**, 489-494 (2003).
25. Kapustin, A.N. & Shanahan, C.M. Osteocalcin: a novel vascular metabolic and osteoinductive factor? *Arteriosclerosis, thrombosis, and vascular biology* **31**, 2169-2171 (2011).
26. Venuraju, S.M., Yerramasu, A. & Lahiri, A. Abnormal myocardial perfusion in the absence of anatomically significant coronary artery disease: implications and clinical significance. *Journal of nuclear cardiology : official publication of the American Society of Nuclear Cardiology* **17**, 8-12 (2010).
27. Tsigkou, O., *et al*. Engineered vascularized bone grafts. *Proc Natl Acad Sci U S A* **107**, 3311-3316 (2010).
28. Auger, F.A., Gibot, L. & Lacroix, D. The Pivotal Role of Vascularization in Tissue Engineering. *Annual review of biomedical engineering* (2013).
29. Maraldi, T., *et al*. Human amniotic fluid- and dental pulp-derived stem cells seeded into collagen scaffold repair critical size bone defects promoting vascularization. *Stem cell research & therapy* **4**, 53 (2013).
30. Vattikuti, R. & Towler, D.A. Osteogenic regulation of vascular calcification: an early perspective. *Am J Physiol Endocrinol Metab* **286**, E686-696 (2004).
31. Canfield, A.E., *et al*. Role of pericytes in vascular calcification: a review. *Z Kardiol* **89 Suppl 2**, 20-27 (2000).

32. Gerhardt, H. & Betsholtz, C. Endothelial-pericyte interactions in angiogenesis. *Cell Tissue Res* **314**, 15-23 (2003).
33. Liu, Y., *et al*. Hepatocyte growth factor and c-Met expression in pericytes: implications for atherosclerotic plaque development. *J Pathol* **212**, 12-19 (2007).
34. Geng, Y., *et al*. Role of cellular cholesterol metabolism in vascular cell calcification. *The Journal of biological chemistry* **286**, 33701-33706 (2011).
35. Xu, S.S., Alam, S. & Margariti, A. Epigenetics in Vascular Disease - Therapeutic Potential of New Agents. *Current vascular pharmacology* (2012).
36. Ergun, S., Tilki, D. & Klein, D. Vascular wall as a reservoir for different types of stem and progenitor cells. *Antioxid Redox Signal* **15**, 981-995 (2011).
37. Juchem, G., *et al*. Pericytes in the macrovascular intima: possible physiological and pathogenetic impact. *American journal of physiology*. *Heart and circulatory physiology* **298**, H754-770 (2010).
38. Farrell, E., *et al*. A collagen-glycosaminoglycan scaffold supports adult rat mesenchymal stem cell differentiation along osteogenic and chondrogenic routes. *Tissue engineering* **12**, 459-468 (2006).
39. Tierney, C.M., *et al*. The effects of collagen concentration and crosslink density on the biological, structural and mechanical properties of collagen-GAG scaffolds for bone tissue engineering. *Journal of the mechanical behavior of biomedical materials* **2**, 202-209 (2009).
40. Farrell, E., *et al*. Chondrogenic priming of human bone marrow stromal cells: a better route to bone repair? *Tissue Eng Part C Methods* **15**, 285-295 (2009).
41. Fukagawa, M. & Kazama, J.J. The making of a bone in blood vessels: from the soft shell to the hard bone. *Kidney Int* **72**, 533-534 (2007).
42. Demer, L.L. & Tintut, Y. Vascular calcification: pathobiology of a multifaceted disease. *Circulation* **117**, 2938-2948 (2008).
43. da Silva Meirelles, L., Chagastelles, P.C. & Nardi, N.B. Mesenchymal stem cells reside in virtually all post-natal organs and tissues. *J Cell Sci* **119**, 2204-2213 (2006).
44. Abedin, M., Tintut, Y. & Demer, L.L. Mesenchymal stem cells and the artery wall. *Circulation research* **95**, 671-676 (2004).
45. Lin, L., *et al*. Synergistic inhibition of endochondral bone formation by silencing Hif1alpha and Runx2 in trauma-induced heterotopic ossification. *Mol Ther* **19**, 1426-1432 (2011).
46. Speer, M.Y., *et al*. Inactivation of the osteopontin gene enhances vascular calcification of matrix Gla protein-deficient mice: evidence for osteopontin as an inducible inhibitor of vascular calcification in vivo. *The Journal of experimental medicine* **196**, 1047-1055 (2002).
47. Luo, G., *et al*. Spontaneous calcification of arteries and cartilage in mice lacking matrix GLA protein. *Nature* **386**, 78-81 (1997).
48. Lacey, D.C., Simmons, P.J., Graves, S.E. & Hamilton, J.A. Proinflammatory cytokines inhibit osteogenic differentiation from stem cells: implications for bone repair during inflammation. *Osteoarthritis Cartilage* **17**, 735-742 (2009).

49. Farrell, E., *et al*. In-vivo generation of bone via endochondral ossification by in-vitro chondrogenic priming of adult human and rat mesenchymal stem cells. *BMC Musculoskelet Disord* **12**, 31 (2011).
50. Yang, W., Yang, F., Wang, Y., Both, S.K. & Jansen, J.A. In vivo bone generation via the endochondral pathway on three-dimensional electrospun fibers. *Acta biomaterialia* **9**, 4505-4512 (2013).

Chapter 6

Overview

6.1 Overview

The most common cause of death in the western world is atherosclerosis, which is largely attributed to chronic injury to the vasculature. There are many factors contributing to the progression of atheromatous plaques. Amongst these, the remodeling of the vascular wall that follows an assault, either acute or chronic, has been considered by many researchers as a contributing factor. However, the exact role of this remodeling and the underlying mechanisms remain largely unexplored[1]. Recent studies suggest that ectopic tissue, including bone, cartilage, fat and marrow, in the aortic wall is a common feature of pathogenesis of the plaque[2]. This ectopic calcification occurs in blood vessels, heart valves and skeletal muscles[3].

There is a growing body of evidence suggesting that pericytes are not only involved in regulating angiogenesis but can also differentiate to the osteogenic and chondrogenic lineages[3]. There have been reports showing new blood vessel formation within the intima of the atherosclerotic plaque[4-6]. It has also been hypothesized that pericytes not only can be the cause of angiogenesis occurring in the vessel wall during the pathological process, but can also differentiate to the bone phenotype where the blood supply of nutrients and oxygen is crucial. Vascular calcification is a common complication that occurs in a number of disease conditions including atherosclerosis. Calcification in atherosclerosis, has been found to spread through media and intima and affects almost all vasculature[3,7].

The identification of vascular stem cells creates the possibility of new therapeutic strategies for regenerative medicine. However, dysregulation of pericyte function in the vessel wall leads to severe problems like stroke which is a major problem. Although the formation of new vasculature is critical to regeneration and repair, the process can become pathological under the influence of certain factors leading to possible accumulation of calcium salts in the previously healthy tissues. Recent studies have emphasized the similarity between vascular calcification and endochondral bone formation[3]. Amongst many possible mechanisms for vascular calcification, it has been suggested previously that the arterial wall not only attracts circulating MSCs but also

harbors resident progenitor cells with potential to differentiate to the ectopic tissues found in the calcified vessel wall[8]. The contribution of VSCs to vascular remodeling through their proliferation and differentiation has recently been shown[9]. With a parallel comparison between background C57BL/6 and atherosclerotic ApoE$^{-/-}$ mice, this thesis aimed to investigate the role of circulating MSCs and resident VSCs in progression of atherosclerosis. Following isolation and *in vitro* characterization, these cells were investigated through a series of *in vitro* and *in vivo* experiments looking at the effect of individual potential inflammatory factors as well as the atherosclerotic environment as a whole. Therefore, this study helped to reveal the involvement of stem cells isolated from aortae in the progression of atherosclerosis.

The *in vivo* studies included in this thesis have contributed to knowledge about the role of complex interactions between aorta-derived VSCs, other resident cells, and infiltrating immune cells in atherosclerosis by filling some gaps, extending some concepts and introducing new principles. This field of research is constantly growing, and it is clear that the contribution of different cells in plaque progression is complex and can both enhance and inhibit disease.

Chondrogenic differentiation was found to be significantly increased in ApoE$^{-/-}$ -isolated cells over wild type C57BL/6 controls suggesting that ApoE$^{-/-}$-derived cells are more prone to calcification and endochondral bone formation than the control cells and implicating that their responses to specific modulators may occur in an environment-dependent fashion. The effect of pro-inflammatory cytokines in the increased chondrogenic capacity was investigated using standardized methods. Interestingly, expression of Sox9, considered the "master" chondrogenic transcription factor, was specifically upregulated in ApoE$^{-/-}$ VSCs in response to the pro-inflammatory cytokine, IL-6. Other molecules associated with chondrogenesis such as fibromodulin and type II collagen were also upregulated as were the hypertophic markers Runx2 and ALP suggesting promotion of vascular calcification. Furthermore, while analyzing the effects of other pro-inflammatory factors, TNFα and IL-1β, there was no significant change in the gene expression profile suggesting a unique, important role of IL-6 in the pathology

of atherosclerosis. However, the effect of the treatment of IL-6 can be controversial[10]. This cytokine can be secreted by MSCs[10] as well as pericytes[11]. Also, it has been published that during chondrogenic differentiation in human BM-derived MSCs, the presence of IL-6 might cause downregulation of chondrogenic genes[10]. This thesis has also shown significant effects of TNFα and IL-1β in suppressing chondrogenesis in wild type-isolated cells, whereas in $ApoE^{-/-}$ isolated cells the effect was enhanced, with further reduction in expression of some of the chondrogenic genes tested. It was important to understand how differentiated VSC populations behave in an *in vivo* inflammatory environment and therefore to determine the feasibility of their contributing to ectopic bone formation in blood vessels.

Notably, studies in this thesis have suggested the potential role of the VSC/pericyte in phenotypic changes that occur in response to inflammation in an aorta due to injury. Differentiation of the cells to the chondrogenic lineage and implantation in the pathogenic environment revealed that the cells may play a role in atherosclerotic plaque formation. Chondrogenically primed scaffolds seeded with MSC or VSC were used to explore the cellular and molecular events regulating the maturation of bone through the endochondral ossification pathway *in vivo* and provided a model to study the pathogenesis of atherosclerotic plaque formation.

It was demonstrated that the atherosclerotic environment, with interplay of a number of pro-inflammatory molecules, plays a huge role in the behavior and the response of the cells. It was revealed that the intrinsic capacity of the cells plays a role in their ability to calcify *in vivo*. Stem cells seem to be primed by the environment from which they are isolated; MSCs and VSCs seem to be more prone to calcification if they are isolated from an atherosclerotic mouse. However, the local microenvironment also plays a role with local VSCs more responsive than MSCs exposed to the same systemic environment that they were isolated from. From these insights, it can be suggested that the VSCs participate in the endochondral bone formation associated with calcified plaques.

The work described in the thesis has therefore approached a new concept of stem cell involvement in pathological processes and opens up avenues for development of potential targets for clinical application in the future. The experiments carried out in these studies have taken a step forward in our knowledge of a number of aspects and will add to the overall field; isolation of stem cells from aortae is just one example. This work also reveals that vessel-derived stem cells are chondrogenic and osteogenic. Importantly, the work also addresses possible mechanisms whereby inflammation interacts with resident cells to promote vascular calcification. *In vivo* studies have contributed to knowledge concerning the role of complex interactions between aorta-derived stem cells and other resident cells such as infiltrating immune cells in atherosclerosis. The work has added to the state-of-art in the field and introduced new concepts. This field of research is constantly growing and it is clear that the contribution of different cells in plaque progression is complex with involvement perhaps in both enhancement and inhibition of disease.

The salient findings and the implications thereby are summarized in the following sections.

6.2 Summary of key findings and implications of each chapter

6.2.1 Chapter 3: Isolation and characterization of MSCs and VSCs

It was hypothesized that a population of progenitor cells exists in aortae, that is more prone to osteogenic and chondrogenic differentiation and thereby to calcification. In addition to developing methodology to isolate VSCs, MSCs were isolated from the same mice to elucidate the involvement of bone marrow-derived stem cells in the process of ectopic bone formation and calcification. Various protocols were used to isolate the cell populations, with establishment of wild type MSCs causing the most difficulty. To determine stemness of the populations, differentiation assays and cell surface analysis was performed. Results demonstrated that all isolated populations had a defining stem cell surface signature. All VSC populations were more than 86% positive for Sca-1 and above 59% for CD44, typical MSC markers.

CD90.2 has been shown to be strongly positive in above 81% of VSC populations, where about 6.5% MSCs were positive. MSCs were negative for 3G5 whereas results for VSCs varied with the mouse strain. Around 9.2% C57BL/6 VSCs were positive for 3G5 while over 42% VSCs from ApoE-/- mice were shown to be positive. On the other hand, as deduced from immunohistochemistry MSCs were negative for 3G5 whereas over 26% VSCs were positive. We showed that over 43% cultured VSCs also expressed CD146, a molecule present at the pericyte surface. All populations had population doublings typical for MSCs while retaining the MSC phenotype. Surface markers analysis showed some variations among the cultures. This was in cohesion with previous findings[12] that their degree of the differentiation is related of site of origin as well as any gene modification they may carry.

The site of origin also had a substantial impact on the differentiation of cells, with varying degrees of differentiation seen in adipo-, chondro- and osteogenesis. For example, $ApoE^{-/-}$ and C57BL/6 VSCs showed no adipogenic ability. This may be due to the effect of interactions between the stem cells and local milieu[12,13]. However, as $ApoE^{-/-}$ cells did not show a capacity to differentiate to the adipogenic phenotype, the lack of ApoE may be a contributing factor[14]. A significant increase in chondrogenic differentiation was observed in the $ApoE^{-/-}$ isolated VSCs and MSCs compared to the wild type mice isolated cell populations.

The present study has provided robust evidence that stem/progenitor cells reside in abundance in the aortic vessel wall; these cells can differentiate to chondrogenic cells and perhaps participate in atherosclerotic lesion formation. $ApoE^{-/-}$ isolated VSCs and MSC were also shown to have significantly higher levels of GAG concentration and it was evident that pellets were bigger and more hypertrophic after morphological assessment. The immunocytochemistry for type II and X collagen showed positive staining in the chondrogenically treated pellets. These two collagens are expressed during endochondral ossification. The presence of collagen type II indicated early chondrogenesis suggesting that cells accumulated a cartilage matrix[15]. Type X collagen, on the other hand is strongly associated with hypertrophic cartilage[16]. Differentiation to

the osteogenic lineage was confirmed after culturing cells in osteogenic medium. All isolated cells treated with osteogenic medium where positive for Van Kossa staining. The ApoE$^{-/-}$ VSC and MSC showed significantly higher levels of calcium levels. It has been shown that the isolated cells possess the ability to partially differentiate to the myogenic phenotype, with some hints of a smooth muscle cell phenotype shown in this anaylsis.

The idea that stem cell populations could have a role in formation of ectopic bone or cartilage in vascular diseases such as atherosclerosis has been postulated as a result of their multipotency. This postulation formed the hypothesis for the present study. Our approach was to compare VSC and bone marrow-derived MSCs from diseased and healthy animals. The differences seen in the potential of VSCs from ApoE$^{-/-}$ mice to form aberrant tissue found in the atherosclerotic plaque points to their possible role in the pathogenesis of atherosclerosis. The differences also suggest that there are certain factors in the disease state that may trigger the activation of these cells to differentiate and contribute to vascular calcification. This chapter provides insight into the characteristics of VSCs in the vessel wall.

6.2.2 Chapter 4: Effect of the atherosclerotic niche on resident progenitor cells: *In vitro* assessment

The aim of this chapter was to determine how the isolated aorta-derived progenitor cells from ApoE$^{-/-}$ and wild type mice are affected by the factors found in calcifying atherosclerotic plaques. More precisely, this chapter was aimed to assess whether VSCs respond to candidate pro-inflammatory cytokines during chondrogenesis to regulate markers of endochondral ossification. Towards this aim, the role of IL-1β, IL-6 and TNF-α on the expression pattern of relevant molecules at different stages of chondrogenesis in VSCs was assessed. This deconstructive approach provided insights to discern the significance of external cues and identify individual factors controlling the fate of progenitor perivascular cells. The basis of the approach was the concept that inflammation is a contributing element at every stage of lesion progression in atherosclerosis. Arterial wall inflammation is a distinctive feature of atherosclerosis and

key factors in the process are the pro-inflammatory cytokines and chemokines secreted by surrounding cells. Also, the interplay between EC, PC and SMC is directly or indirectly involved in altering T cells which infiltrate the plaque. Thus the active participation of these cells in inflammation cannot be overstated. Previous studies have also shown enhancement of differentiation and mineralization of these vascular cells under the influence of inflammatory factors[17]

Since the isolated ApoE$^{-/-}$ VSCs were significantly more chondrogenic, it was thought that chondrogenesis of ApoE$^{-/-}$ VSCs might reflect an upregulation of chondrogenic markers and C57BL/6 VSCs should theoretically have less potential to respond to the stimuli. In order to assess if VSCs are involved in calcification of the plaque, the conceivable association of relevant individual mediators of inflammation was investigated. It has been shown for the first time that ApoE$^{-/-}$ VSCs treated chondrogenically for 21 days in the presence of IL-6 can exaggerate expression of chondrogenic markers such as Sox9, fibromodulin, type II collagen, aggrecan and ALP; C57BL/6 VSCs, on the contrary, show inhibition of chondrogenic markers.

Interestingly, type X collagen expression was not increased by IL-6 treatment. TGF-β has been shown to suppress chondrocyte hypertrophy in certain conditions and could inhibit the type X collagen expression[18,19]. Thus presence of TGF-β in the chondrogenic culture medium may explain the suppression of collagen type X expression.

Similar to previous findings that MSCs preserve their stemness while exposed to differentiating factors in the presence of pro-inflammatory cytokines[20], C57BL/6 VSCs treated with IL-6 during chondrogenesis generally showed suppression of the markers assessed.

In this chapter, it was shown that chondrogenic differentiation of ApoE$^{-/-}$ VSCs in the presence of IL-6 was associated with early over-expression of fibromodulin by 2.3-fold, an increase up to 3.9-fold in expression of aggrecan which appears in intermediate stage of chondrogenic differentiation, and most critically, a 28-fold increase in expression of

type II collagen, a marker definitive for chondrogenesis. Alkaline phosphatase gene expression, usually associated with hypertrophic cartilage, showed a 7.7-fold increase. As a whole, early to late chondrogenic markers were demonstrated to have significant increases in ApoE$^{-/-}$ VSCs, thus revealing a cell population that is highly prone to chondrogenesis in the presence of a pro-inflammatory cytokine seen in atherosclerotic plaques. In contrast, IL-1β and TNF-α strongly inhibited expression of all chondrogenic markers. Thus, investigation of the mechanisms whereby IL-6 potentiates chondrogenesis/endochondral ossification of ApoE$^{-/-}$ VSCs may provide a feasible tool to identify critical cues to comprehend the microenvironment that promotes the formation of ectopic bone in vasculature.

In the case of C57BL/6 VSCs, strong inhibition of expression of all chondrogenic markers tested was observed in the presence of all pro-inflammatory cytokines tested. This inhibition suggested that the presence of pro-inflammatory cytokines can compromise the ability of non-atherosclerotic cells to form bone. Thus, studying the pattern of expression of chondrogenic markers not only helped understand the pathway of controlled new bone formation but also the effect of inflammation on endochondral ossification in atherosclerotic plaque calcification.

Thus, with the objective of investigating the influence of factors in the local milieu on VSCs from atherosclerotic and control mice, this chapter attempted to map the sequence of events during chondrogenesis by studying GAG deposition and expression pattern of key matrix components. This exercise helped to define influential molecules associated with the process of plaque calcification. The experiments in this chapter revealed a novel action of IL-6 opening avenues to its further use in diagnostic and possibly therapeutic areas. Also, data on individual cues suggested that *in vivo* study would further help to investigate the effect of inflammation on bone ossicle formation in the atherosclerotic plaque environment.

6.2.3 Chapter 5: Endochondral ossification by chondrogenically primed vessel-derived and mesenchymal stem cells in wild type and ApoE$^{-/-}$ mice

Earlier in the thesis, isolation and characterization of VSCs from aorta showed that these cells can be expanded and maintained in long-term cultures and possess multilineage potential. Later in an attempt towards understanding the pathogenesis of vascular calcification and ectopic bone formation, chapter 4 focused on elucidating the effect of inflammatory factors on VSCs from both diseased and control mice. The finding that ApoE$^{-/-}$ VSCs were influenced by a pro-inflammatory cytokine to become more chondrogenic led to the design on the *in vivo* study described in chapter 5. The potential of the ApoE$^{-/-}$ VSCs to significantly upregulate early chondrogenic markers like Sox9 and fibromodulin, as well as Runx2 and ALP, which are important mature chondrocyte markers, offers a novel explanation for the mechanism that links VSCs and ectopic calcification.

To elucidate the *in vivo* bone potential of VSCs and MSCs from ApoE$^{-/-}$ and C57BL/6 mice, subcutaneous implantations were performed. Prior to implantation, cells were seeded onto collagen-chondroitin sulphate scaffolds and chondrogenically primed. The cell distribution and differentiation into the chondrogenic phenotype on the scaffold was assessed. Following 32 days, the differentiated seeded scaffolds were subjected to histological analysis and were shown to successfully differentiate to the chondrogenic phenotype. Integration of the cells into the scaffold surface and even distribution across the scaffold surface was observed. These observations imply that prior to implantation, scaffolds contained viable and differentiated cells.

Following chondrogenic priming, constructs were implanted in atherosclerotic and non-atherosclerotic environments to investigate their capability to form bone *in vivo*. Following 8 weeks, constructs were retrieved, decalcified and stained. H&E and safranin O/fast green staining provided histological evidence of mineralization in constructs with chondrogenically primed ApoE$^{-/-}$ MSCs and VSCs retrieved from both environments but to different extents. Bone formation, both in terms of extent and maturity, was highest in atherosclerotic VSCs retrieved from the atherosclerotic

environment suggesting an intrinsic capacity of atherosclerotic cells as well as a synergistic effect of the atherosclerotic environment. However, it was notable that appreciable calcified cartilage formation was observed even in control ApoE$^{-/-}$ MSCs (2/4) and VSCs (1/4), that were not chondrogenically primed and retrieved from atherosclerotic mice. This observation suggests the critical role of the atherosclerotic environment in ectopic bone formation. Bone formation in the chondrogenically primed constructs of ApoE$^{-/-}$ VSCs points towards the growing notion of looking at vascular calcification as an active process akin to endochondral bone development and repair. Another important point to note was that in the chondrogenic constructs, bone formation was observed with significant blood vessel invasion (5/5 ApoE$^{-/-}$ MSCs and 6/6 ApoE$^{-/-}$ VSCs). This finding illustrates that the compatibility of the implants to the host environment and again emphasizes the inclination towards ossification by the endochondral pathway. Blood vessels with red blood cells were observed in almost all ApoE$^{-/-}$ primed constructs.

It can be envisioned that the priming induced release of certain factors enhancing tissue vascularization[21,22]. The association of angiogenesis and ectopic calcification in atherosclerotic lesions has been made previously[5,23] and the localization of blood vessels surrounding ectopic bone in atherosclerotic plaques reported[5,6,24]. A previously published report showed that MSCs primed along the chondrogenic lineage prompted the release of angiogenic factors leading to infiltration of blood vessels in the bone formed *in vivo*. It was shown here that chondrogenically primed constructs formed vascularized bone in the atherosclerotic environment suggesting angiogenic and remodeling properties of the priming.

The evidence of induced bone formation in C57BL/6 MSC constructs in the atherosclerotic environment implicates the role of factors in atherosclerosis on the differentiation properties of the cells. Indeed this finding may explain the implication that MSCs are involved in ectopic bone forming processes in the vasculature. While circulating, MSCs could infiltrate into the subendothelial space in response to local signals, exhibit their repair properties, become stimulated to differentiate into

chondrogenic phenotype and calcify. On the contrary, in the chondrogenically primed and unprimed C57BL/6 VSCs, no bone or vascularization was visible, possibly due to lack of released inductive factors. One plausible reason for minimal bone formation may be resorption of the scaffolds. Another explanation could be the dependence of the differentiation potential of C57BL/6 VSCs on the extent of vascular assault or disease process. In other words, the intrinsic capacity of C57BL/6 VSCs and their ability to respond to the atherosclerotic environment may be substantially lower than that of ApoE$^{-/-}$ VSCs due to the difference in extent of vascular injury or disease process that the cells are exposed to in their native environment. It has been suggested previously that there are differences in differentiation potential of adult cells isolated from normal and injured vessels[9,25]. In our studies, the C57BL/6 VSCs isolated from healthy mice are different from ApoE$^{-/-}$ VSCs in that the latter have an opportunity to be exposed to the inflammatory process, which recruits more progenitor cells and acts as a priming event to redirect the cells to calcification in the atherosclerotic environment.

If we take the vascular injury theory further and apply it to VSCs, it can be proposed that VSCs can be activated by vascular injury and start to proliferate, differentiate and thus take part in remodeling. Contrary to this, the C57BL/6 environment is devoid of the instigating event of vascular injury leaving the cells dormant. Also, the heterogeneity of VSCs may contribute to conflicting observations. The novel hypothesis that vascular calcification in atherosclerosis may be a result of VSC activation and differentiation is supported by findings reported in this thesis. Experiments in this chapter suggest that under the influence of a permissive environment of cytokines and factors released by local and infiltrating cells in the plaque, VSCs are committed to a chondrogenic path to form ectopic bone. Taking this concept further, it is envisaged that VSC activation and differentiation can play an important role in pathogenesis of other vascular diseases. The work described in this chapter hinges on the role of vascular stem cells in vascular diseases and remodeling, advocating that atherosclerosis, and possibly other vascular diseases, are essentially stem cell diseases. This theory of the role of resident stem cells in vessel walls contributing to atherosclerotic plaque

formation emerging from the studies in this chapter advances the state-of-the-art in the etiopathology of atherosclerosis.

6.3 Advancing the state-of-the-art

Vascular stem or progenitor cells bring a new perspective to understanding vascular pathologies, vascular treatments and bone regeneration following damage. Stem cells from varying sources can be different with varying parameters of surface antigens. However, they show prolonged self-renewal and exhibit differentiation potential along mesenchymal cell lineages.

With lineage tracking of smooth muscle myosin heavy chain (SMMHC), a recent report has questioned the involvement of SMC de-differentiation in blood vessel remodeling. Instead, a role of multipotent VSC was suggested through differentiation and proliferation studies[9]. Many studies have described expression of similar markers on MSCs and VSCs. Since both populations are progenitors found in blood vessels, VSCs and pericytes might share a similar marker identification of a $CD146^{+}$ PDGF-$R\beta^{+}$ $CD34^{-}$ $CD31^{-}$ population. However, the ubiquitous pericyte marker accepted widely is the 3G5 antigen[26,27].

Similarity between pericytes and MSCs has been shown at various levels. For example, pericytes express MSC markers like CD44, CD90[28,29]. Also, they exhibit differentiation potential and proliferation similar to BM MSCs. The presence of pericytes in the microvasculature makes it intuitive to locate them in the BM counterparts as has been shown previously[30]. It can therefore be suggested that pericytes do play major role in the BM niche. Taking this concept further, the potential of finding the pericyte niche in other tissues is high, obviously due to the fact that blood vessels are present in most tissues to provide nutrition.

Providing insights into the characteristics of VSCs, this thesis focused on identification of progenitor cells within aorta that can differentiate into specialized cell types and contribute to ectopic calcification of the aorta in the atherosclerotic environment. It was notable that for the first time, that progenitor cells from aorta that have a greater

potential to differentiate to the chondrogenic lineage was shown in this thesis. Figure 6.1 depicts a major contribution of this study showing the involvement of IL-6 cytokine on chondrogenic differentiation of VSCs. These cells differentiate to chondrocytes under the influence of chondrogenic medium *in vitro*. However, the presence of IL-6, the proinflammatory cytokine, in the medium influences these cells to terminally differentiate and at 21 day the $ApoE^{-/-}$ VSC start to over-express mature bone phenotypic genes.

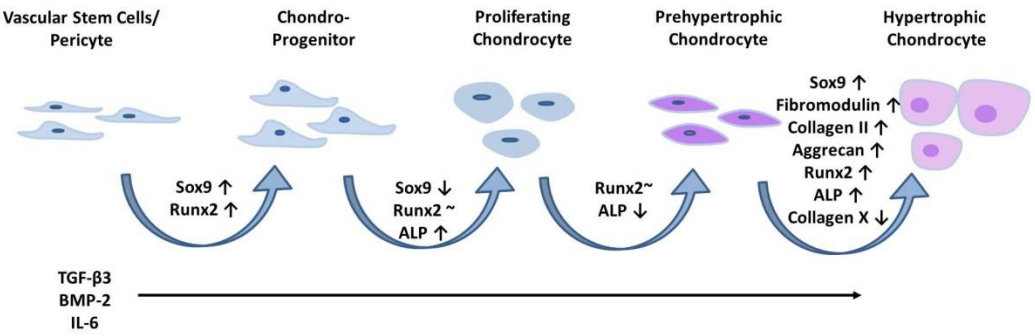

Figure 6.1 Schematic representation of the sequence of the events occurring during chondrogenesis in ApoE$^{-/-}$ VSC in the presence of IL-6. Temporal patterns of gene expression are indicated above the curved arrows on induction of the chondrogenic pathway in the presence of TGF-β3, BMP-2 and IL-6. The first 48h resulted in significant upregulation of Sox9 and Runx2 followed by upregulation of ALP at day 7. Runx2 remained at uniform levels at day 14. Further at day 21, the significant upregulation of Sox9, fibromodulin, type II collagen, aggrecan and Runx2 was reported.

Others have previously demonstrated that pro-inflammatory cytokines suppress mineralization and chondrogenic gene expression in MSCs[20]. This negatively affects regenerative capabilities of MSCs. In the pathological scenario with new bone formation, the presence of inflammatory activity of the cytokines has, more than likely, to be taken into account. Thus, the *in vitro* studies describing the differentiation of VSCs under the influence of inflammatory cytokines provided further understanding of the molecular mechanisms governing specific cytokine modulation of VSC differentiation *in vitro*. This novel insight into the mechanism of calcification was an input to the *in vivo* study. The data from this study provided a plausible pathway of vascular calcification as depicted in figure 6.2. Advancing the current state-of-the-art, this thesis, through *in vitro* and *in vivo* analysis, helped to identify a new population of progenitor cells that can overcome the suppressive effect of the pro-inflammatory state in atherosclerotic plaques and contribute to vascular calcification. Moreover, in disease states such as rheumatoid arthritis where chronic inflammation is prevalent and bone regeneration is desirable, this study made it intuitive to extrapolate that VSCs may play a therapeutic role and may be also applied to treatment of bones defects clinically. Clearly, this study hasn't answered all questions. Nonetheless, it has revealed that in midst of many perplexing issues in regards to the VSCs or pericytes and their pathophysiological functions, these cells possess many advantages and are promising new tools in the field of stem cells.

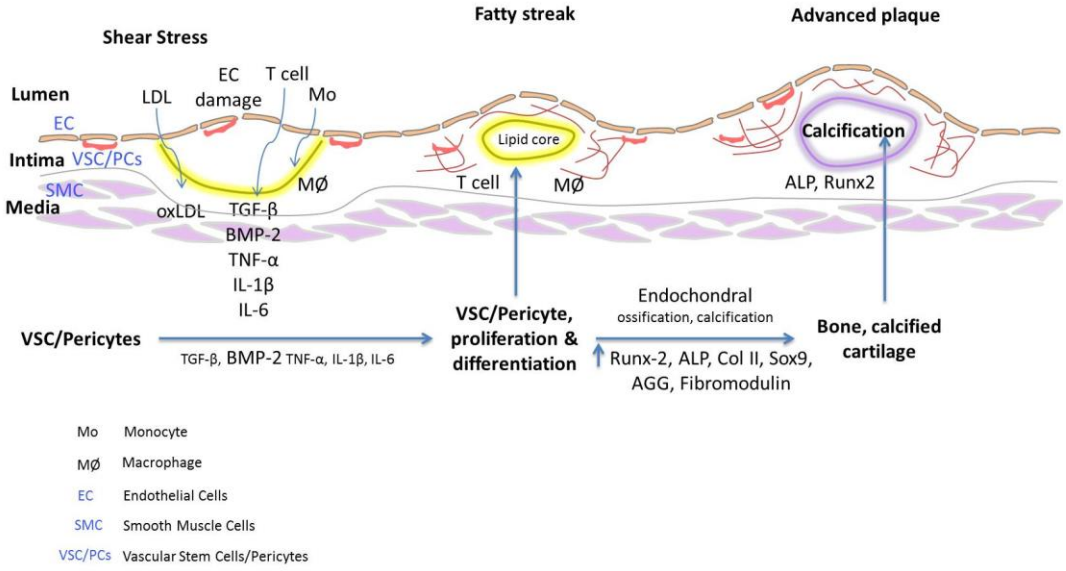

Figure 6.2 Proposed mechanism of pathologic processes occurring within the aorta during atherosclerosis. Summary of the pathological processes that may occur within the subendothelial space of the aorta involving VSC/pericytes, immune cells and other molecules produced by the cells. Lesion progression in atherosclerosis is characterized by the formation of a lipid core in the subendothelial space, which incites the recruitment of T cells and monocytes. As the atherosclerotic lesion progresses, VSCs start to differentiate to chondrocytes and upregulate hypertrophic chondrocyte markers to form ectopic bone by an endochondral mechanism.

6.4 Future plans

Many researchers are assessing MSCs populations implicated in the regeneration as well as degeneration in the body. There is no complete understanding of MSC function and the definition is changing as science progresses. As a result, an increasing number of researchers are looking for methods to select the best cell population to use for application in regenerative medicine as a therapeutic tool.

This thesis has demonstrated the versatility of VSCs. Different aspects of VSCs revealed throughout this thesis can be taken further and applied in a number of other disease processes. The studies here focused on understanding the complex mechanism of the pathologic process involved in vascular calcification. However, based on the results, an interesting direction could be the utilization of VSCs in development of better therapeutic approach not only for atherosclerosis but also bone repair.

Our finding that VSC constructs lead to better vascularization of newly formed bone *in vivo* may form the basis of their possible use in bone repair. The most important approach in bone tissue engineering is to successfully stimulate cells towards the phenotype that can induce blood vessel formation in bone grafts. Success in tissue engineering demands an environment which supports the vascularization of the grafts. Previous studied have highlighted the need to overcome formation of a necrotic core or degradation due to cell death which is a major concern. From data presented in chapter 5 it is tempting to speculate that VSCs could be the missing link to better understanding the angiogenic promotion of blood vessel formation in the engrafted constructs leading to better chondrogenic differentiation to enable mineralization to occur. This study of chondrogenically primed VSC and MSC implanted into an atherosclerotic environment showed the likelihood of bone regeneration during fracture. Further studies can be directed to specify what subpopulation of VSCs is responsible for improved vascularization. One way forward is to sort this heterogeneous population of cells based on their expression of the specific pericyte marker 3G5, especially because this may allow further insights on the vascularization potential of the cells. Towards this, a preliminary experiment was performed using FACS to sort 3G5-positive ($3G5^{+}$) cells

from parent ApoE$^{-/-}$ VSCs. Subsequently, the parent, and 3G5^{+} and 3G5^{-} cells were subjected to chondrogenic assays. As observed by immunohistochemistry, it was clear that only a fraction of VSC preparations was positive for the pericyte specific 3G5 antigen (section 3.2.3.4). Therefore, to investigate the specific role of 3G5-expressing cells in VSC preparations, their chondrogenic potential *in vitro* was determined. Surface characterization with the 3G5 antigen was optimized using flow cytometry (Beckton Dickenson, BD FACSCanto). 7-AAD staining was utilized to exclude dead cells and gates were set according to the FMO and isotype controls (Section 2.5.1). Approx. 45% viable ApoE$^{-/-}$ VSCs stained positive for the 3G5 antigen. Following this, cells were prepared for sorting as described previously (Chapter 2, section 2.3.1). Figure 6.3 (a-d) shows the appropriate cell gates and controls used to exclude doublets and dead cells. Using appropriate gates and controls, sorting was performed and resulted in 100% pure populations of 3G5^{+} and 3G5^{-} cells as shown in figure 6.3 (e-h).

Previous reports have shown that 3G5^{+} cells differentiate to bone and cartilage[31,32] and it was shown that non-sorted VSCs have differentiation potential in this study. Sorted cell fractions were subjected to chondrogenic assays with unsorted, parent cells as a control. After 21 days induction in chondrogenic medium, pellets were harvested and analysed. 3G5^{+} cells showed positive metachromatic staining of chondrogenic pellets. This pattern was similar to that seen following chondrogenic assays performed on isolated MSC and VSC preparations (section 3.2.4.2). The DMMB assay showed deposition of GAGs (Fig. 6.4). In contrast, the negative fraction did not form defined pellets and there was lower GAG deposition compared to the parent and 3G5^{+} cells. DNA quantification suggested that cell proliferation was not affected. This preliminary data indicates that the 3G5^{+} cell fraction may have a higher capacity to undergo chondrogenesis and hints at a link between the chondrogenic and angiogenic functions of the cells.

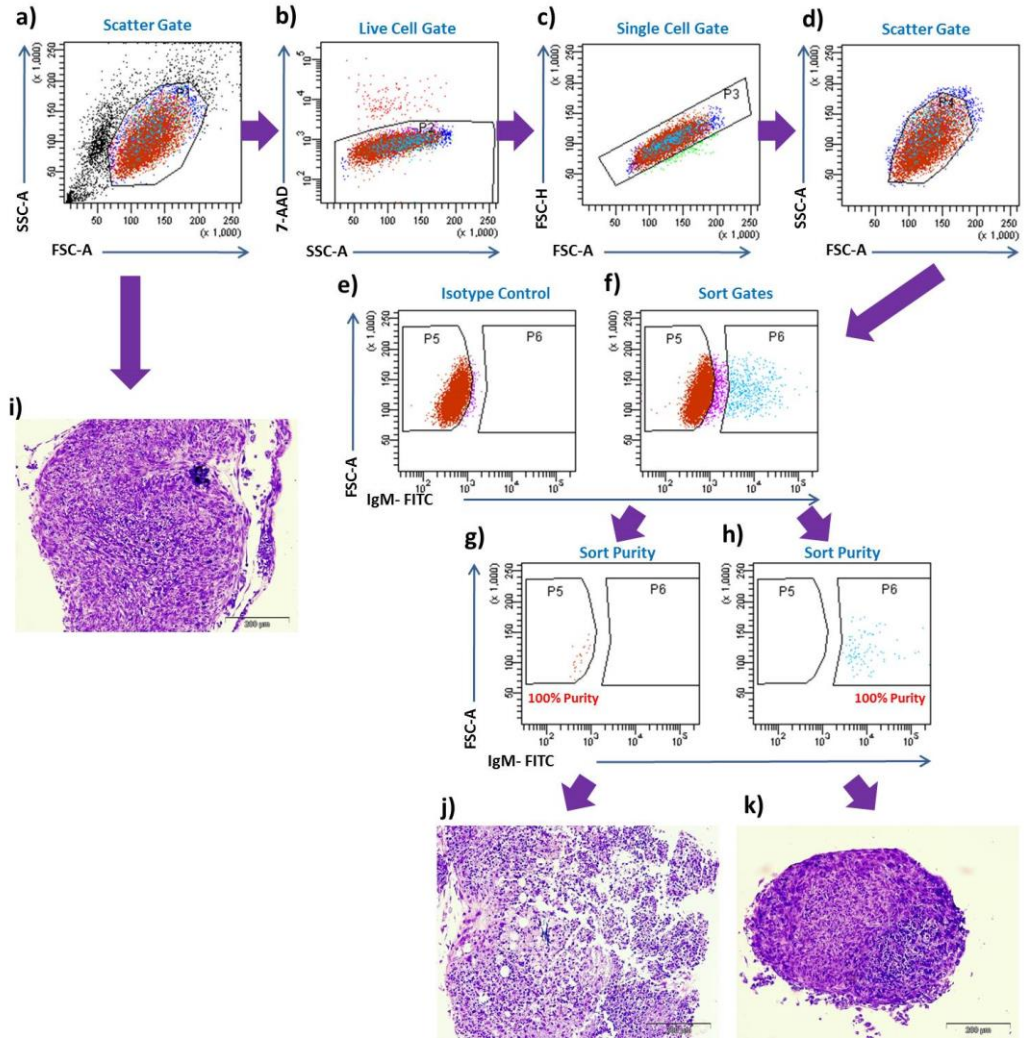

Figure 6.3 Isolated VSCs were sorted by flow cytometry for expression of 3G5. Viable cells were selected by the forward versus side scatter profile (a), with dead cells excluded by gating using 7-AAD (b) doublets by the single cell gate (c) and debris by the scatter gate (d). The isotype control and 3G5 sort gates are shown in e) and f), respectively where p5 is negative and p6 positive. Purity of each population was shown to be g) 100% negative and h) 100% positive. Sorted positive and negative 3G5 cells were subjected to chondrogenic assays. Parent VSCs (i) showed chondrogenic morphology whereas the negative fraction (j) did not form a defined pellet and the $3G5^{+}$ sorted cells (k) formed a hypertrophic pellet. Scale bar, 200µm.

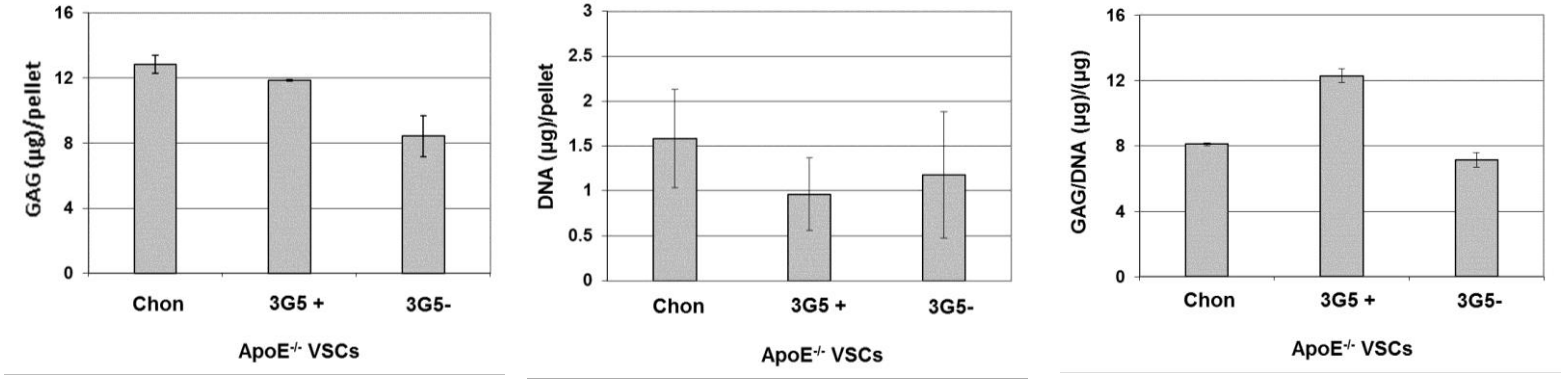

Figure 6.4 Quantification of GAG and DNA following chondrogenic differentiation of parent, 3G5 positive and 3G5 negative cell populations. Results showed parent ApoE$^{-/-}$ VSCs and 3G5^{+} cell fractions displayed similar higher GAG accumulation compared to 3G5^{-} cell fraction. The 3G5^{+} cell fraction also had higher a GAG/DNA ratio compared to parent ApoE$^{-/-}$ VSCs and 3G5^{-} sorted cells. Results are representative of the mean ± SD of data from 3 technical replicates from 1 pooled preparation.

6.4.1 Harnessing IL-6 inhibition

Successful *in vitro* differentiation and mineralization of ApoE$^{-/-}$ VSCs under inflammatory conditions is especially important since an inflammatory environment is present in most conditions where bone repair is necessary[33]. ApoE$^{-/-}$ VSCs can overcome the inhibitory effect of cytokines and IL-6, in particular, can induce their chondrogenic differentiation. It is clear that successful bone regeneration in a pro-inflammatory environment may be modulated by IL-6 and this deserves some attention in future studies.

Further, data in chapter 4 on inflammatory cytokines indicate that inhibition of IL-6 could be used as a clinically feasible approach to prevent atherosclerosis progression. This strategy is already showing results in various diseases. Trials with tocilizumab (anti-human IL-6R monoclonal antibody) have demonstrated a significant suppression of disease activity in rheumatoid arthritis and other autoimmune diseases. It has been also suggested that long term treatment may offer protection against progression of atherosclerosis[34]. Considering our finding that IL-6 promotes the calcification of ApoE$^{-/-}$ VSCs, IL-6 inhibition could indeed be an encouraging approach as an anti-inflammatory therapy to prevent the pathological process of vascular calcification in atherosclerosis. Thus, investigating this approach further and considering clinical studies of IL-6 inhibition therapy in patients with coronary artery disease could be rewarding.

6.5 References

1. Orlandi, A. & Bennett, M. Progenitor cell-derived smooth muscle cells in vascular disease. *Biochem Pharmacol* **79**, 1706-1713 (2010).
2. Tintut, Y., *et al*. Multilineage potential of cells from the artery wall. *Circulation* **108**, 2505-2510 (2003).
3. Collett, G.D. & Canfield, A.E. Angiogenesis and pericytes in the initiation of ectopic calcification. *Circulation research* **96**, 930-938 (2005).
4. Kamat, B.R., Galli, S.J., Barger, A.C., Lainey, L.L. & Silverman, K.J. Neovascularization and coronary atherosclerotic plaque: cinematographic localization and quantitative histologic analysis. *Human pathology* **18**, 1036-1042 (1987).
5. Jeziorska, M. & Woolley, D.E. Neovascularization in early atherosclerotic lesions of human carotid arteries: its potential contribution to plaque development. *Human pathology* **30**, 919-925 (1999).
6. Jeziorska, M. & Woolley, D.E. Local neovascularization and cellular composition within vulnerable regions of atherosclerotic plaques of human carotid arteries. *J Pathol* **188**, 189-196 (1999).
7. Wilkinson, F.L., *et al*. Contribution of VCAF-positive cells to neovascularization and calcification in atherosclerotic plaque development. *J Pathol* **211**, 362-369 (2007).
8. Abedin, M., Tintut, Y. & Demer, L.L. Mesenchymal stem cells and the artery wall. *Circ Res* **95**, 671-676 (2004).
9. Tang, Z., *et al*. Differentiation of multipotent vascular stem cells contributes to vascular diseases. *Nature communications* **3**, 875 (2012).
10. Pricola, K.L., Kuhn, N.Z., Haleem-Smith, H., Song, Y. & Tuan, R.S. Interleukin-6 maintains bone marrow-derived mesenchymal stem cell stemness by an ERK1/2-dependent mechanism. *J Cell Biochem* **108**, 577-588 (2009).
11. Edelman, D.A., Jiang, Y., Tyburski, J.G., Wilson, R.F. & Steffes, C.P. Cytokine production in lipopolysaccharide-exposed rat lung pericytes. *The Journal of trauma* **62**, 89-93 (2007).
12. da Silva Meirelles, L., Chagastelles, P.C. & Nardi, N.B. Mesenchymal stem cells reside in virtually all post-natal organs and tissues. *J Cell Sci* **119**, 2204-2213 (2006).
13. Fuchs, E., Tumbar, T. & Guasch, G. Socializing with the neighbors: stem cells and their niche. *Cell* **116**, 769-778 (2004).
14. Atkinson, R.D., Coenen, K.R., Plummer, M.R., Gruen, M.L. & Hasty, A.H. Macrophage-derived apolipoprotein E ameliorates dyslipidemia and atherosclerosis in obese apolipoprotein E-deficient mice. *Am J Physiol Endocrinol Metab* **294**, E284-290 (2008).

15. Perrier, E., *et al*. Analysis of collagen expression during chondrogenic induction of human bone marrow mesenchymal stem cells. *Biotechnology letters* **33**, 2091-2101 (2011).
16. Barry, F., Boynton, R.E., Liu, B. & Murphy, J.M. Chondrogenic differentiation of mesenchymal stem cells from bone marrow: differentiation-dependent gene expression of matrix components. *Exp Cell Res* **268**, 189-200 (2001).
17. Tintut, Y., Patel, J., Parhami, F. & Demer, L.L. Tumor necrosis factor-alpha promotes in vitro calcification of vascular cells via the cAMP pathway. *Circulation* **102**, 2636-2642 (2000).
18. Huang, A.H., Stein, A., Tuan, R.S. & Mauck, R.L. Transient exposure to transforming growth factor beta 3 improves the mechanical properties of mesenchymal stem cell-laden cartilage constructs in a density-dependent manner. *Tissue Eng Part A* **15**, 3461-3472 (2009).
19. Ballock, R.T., *et al*. TGF-beta 1 prevents hypertrophy of epiphyseal chondrocytes: regulation of gene expression for cartilage matrix proteins and metalloproteases. *Dev Biol* **158**, 414-429 (1993).
20. Lacey, D.C., Simmons, P.J., Graves, S.E. & Hamilton, J.A. Proinflammatory cytokines inhibit osteogenic differentiation from stem cells: implications for bone repair during inflammation. *Osteoarthritis Cartilage* **17**, 735-742 (2009).
21. Farrell, E., *et al*. Chondrogenic priming of human bone marrow stromal cells: a better route to bone repair? *Tissue engineering. Part C, Methods* **15**, 285-295 (2009).
22. Xu, J., *et al*. Chondrogenic differentiation of human mesenchymal stem cells in three-dimensional alginate gels. *Tissue Eng Part A* **14**, 667-680 (2008).
23. Jeziorska, M., McCollum, C. & Wooley, D.E. Observations on bone formation and remodelling in advanced atherosclerotic lesions of human carotid arteries. *Virchows Archiv : an international journal of pathology* **433**, 559-565 (1998).
24. Kumamoto, M., Nakashima, Y. & Sueishi, K. Intimal neovascularization in human coronary atherosclerosis: its origin and pathophysiological significance. *Human pathology* **26**, 450-456 (1995).
25. Kocher, O., *et al*. Phenotypic features of smooth muscle cells during the evolution of experimental carotid artery intimal thickening. Biochemical and morphologic studies. *Lab Invest* **65**, 459-470 (1991).
26. Nayak, R.C., Berman, A.B., George, K.L., Eisenbarth, G.S. & King, G.L. A monoclonal antibody (3G5)-defined ganglioside antigen is expressed on the cell surface of microvascular pericytes. *The Journal of experimental medicine* **167**, 1003-1015 (1988).

27. Crisan, M., Corselli, M., Chen, W.C. & Peault, B. Perivascular cells for regenerative medicine. *Journal of cellular and molecular medicine* **16**, 2851-2860 (2012).
28. Crisan, M., *et al*. A perivascular origin for mesenchymal stem cells in multiple human organs. *Cell Stem Cell* **3**, 301-313 (2008).
29. Caplan, A.I. All MSCs are pericytes? *Cell Stem Cell* **3**, 229-230 (2008).
30. Tormin, A., *et al*. CD146 expression on primary nonhematopoietic bone marrow stem cells is correlated with in situ localization. *Blood* **117**, 5067-5077 (2011).
31. Canfield, A.E., *et al*. Role of pericytes in vascular calcification: a review. *Z Kardiol* **89 Suppl 2**, 20-27 (2000).
32. Shi, S. & Gronthos, S. Perivascular niche of postnatal mesenchymal stem cells in human bone marrow and dental pulp. *J Bone Miner Res* **18**, 696-704 (2003).
33. Shanbhag, A.S., Jacobs, J.J., Black, J., Galante, J.O. & Glant, T.T. Cellular mediators secreted by interfacial membranes obtained at revision total hip arthroplasty. *The Journal of arthroplasty* **10**, 498-506 (1995).
34. Tanaka, T., Narazaki, M. & Kishimoto, T. Therapeutic targeting of the interleukin-6 receptor. *Annual review of pharmacology and toxicology* **52**, 199-219 (2012).

6.6 Achievements

Research article in preparation

Aleksandra Leszczynska, Aideen O'Doherty, Eric Farrell, Fergal O'Brien, Timothy O'Brien, Mary Murphy. Atherosclerotic Environment Accentuates Endochondral Ossification in Vessel Derived Stem Cells: *In-vitro* and *In-vivo* Assessment.

Article in local newspaper: 'Stem cells: A promising answer to the mystery of atherosclerosis' for general public was published in a local weekly newspaper under 'Science and the city' column on September 16, 2010

Selected Presentations

1. **Aleksandra Leszczynska**, Eric Farrell, Aideen O'Doherty, Fergal O'Brien, Timothy O'Brien, Mary Murphy. Enhanced endochondral ossification in vessel derived stem cells by atherosclerotic environment, poster presentation at the British Society for Cardiovascular Research, Autumn meeting, Belfast, UK, 3 - 4 September 2012

2. **Aleksandra Leszczynska**, Eric Farrell, Aideen O'Doherty, Fergal O'Brien, Timothy O'Brien, Mary Murphy. Vessel Derived Stem cells contribute to endochondral ossification of atherosclerotic plaque, poster presentation in Tissue Engineering Regenerative Medicine International Society – WC Meeting, Austria, Vienna 5 - 8 September 2012

3. **Aleksandra Leszczynska**, Eric Farrell, Aideen O'Doherty, Fergal O'Brien, Timothy O'Brien, Mary Murphy. Atherosclerotic environment accentuates endochondral ossification in vessel derived stem cells: In vitro and in vivo assessment, poster presentation in MSC Galway International Conference, Galway, Ireland, 2-3 July 2012

4. **Aleksandra Leszczynska**, Eric Farrell, Aideen O'Doherty, Fergal O'Brien, Timothy O'Brien, Mary Murphy. A comparison of endochondral ossification by vessel derived stem cells and mesenchymal stem cells in wild type and ApoE$^{-/-}$ mice, accepted for oral presentation in 2012 eECM XIII: Bone Fixation, Repair & Regeneration, Davos, Switzerland, 24 – 26 June 2012

5. **Aleksandra Leszczynska**, Eric Farrell, Aideen O'Doherty, Fergal O'Brien, Timothy O'Brien, Mary Murphy. Enhancement of endochondral ossification in vessel derived stem cells by atherosclerotic niche: *in vitro* and *in vivo* assessment in wild type and ApoE$^{-/-}$ mice, poster presentation in Royal Academy of Medicine in Ireland Biomedical Science Section Annual Meeting 2012, Galway, Ireland, 14 June 2012

6. **Aleksandra Leszczynska**, Aideen O'Doherty, Timothy O'Brien, Frank Barry, Mary Murphy, Vessel Derived Stem Cells in Pathogenesis of Atherosclerosis, oral presentation, International Atherosclerosis Research School (iARS), Prague, 21 – 26 August 2011

7. **Aleksandra Leszczynska**, Aideen O'Doherty, Timothy O'Brien, Frank Barry, Mary Murphy, Ossification of atherosclerotic plaque: the role of

vessel derived stem cells, poster presentation, British Atherosclerosis Society: Spring Meeting, Birmingham, UK, 13-14 June 2011

8. **Aleksandra Leszczynska**, Aideen O'Doherty, Timothy O'Brien, Frank Barry, Mary Murphy, Vessel derived stem cells contribute to endochondral ossification of atherosclerotic plaque, oral presentation Tissue Engineering Regenerative Medicine International Society – EU Meeting, Granada, Spain, 7-10 June, 2011

9. **Aleksandra Leszczynska**, Aideen O'Doherty, Timothy O'Brien, Frank Barry, Mary Murphy, Myogenic potential of vascular stem cells in the $ApoE^{-/-}$ mouse, poster presentation Tissue Engineering Regenerative Medicine International Society – EU Meeting, Galway, Ireland, 13-17 June, 2010

10. **Aleksandra Leszczynska**, Aideen O'Doherty, Timothy O'Brien, Frank Barry, Mary Murphy, Osteogenic and Chondrogenic Potential of Blood Vessel Derived Stem Cells, poster presentation British Society for Matrix Biology: Vascular Matrix in Health & Disease, 29-30 March, 2010

11. **Aleksandra Leszczynska**, Aideen O'Doherty, Timothy O'Brien, Frank Barry, Mary Murphy, Vascular stem cells and atherosclerosis in the $ApoE^{-/-}$ mouse, Poster presentation Stem Cells Europe, Amsterdam, Netherlands, 1-3 September, 2008